

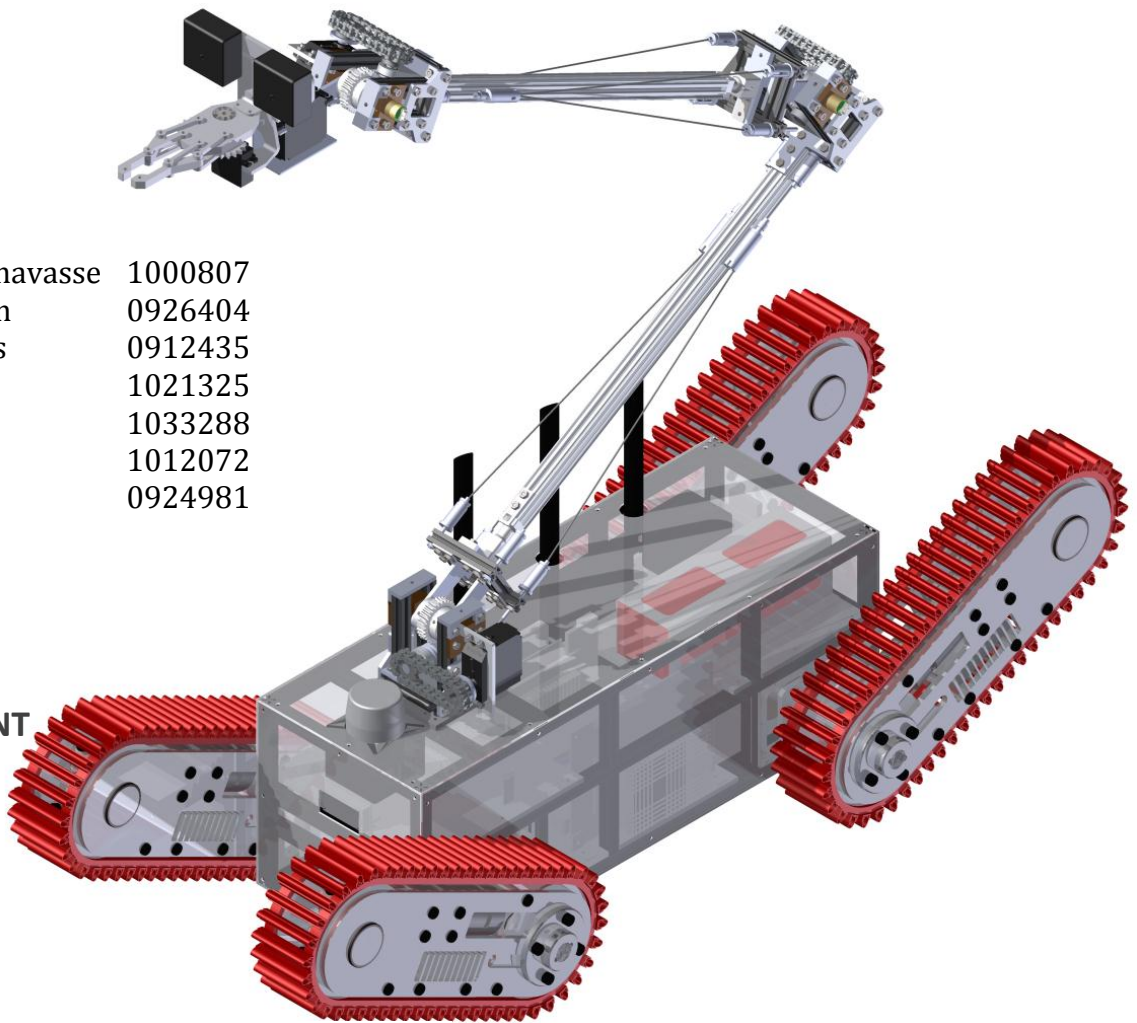


THE UNIVERSITY OF  
WARWICK

Warwick Mobile Robotics

# Urban Search and Rescue Robotics

## Technical Report



### AUTHORS

Christopher Chavasse	1000807
Andrew Parkin	0926404
Trevor Whales	0912435
Lauren Rutter	1021325
James Yardley	1033288
Vishal Dhanji	1012072
Jannah Aljafri	0924981

### PUBLISHED

1<sup>st</sup> May 2014

### WORD COUNT

9,905

### SPONSORS



School of Engineering



## Abstract

Urban Search and Rescue (USAR) robots are designed to locate survivors in hazardous environments, such as earthquake disaster zones, removing emergency service personnel from danger. A detailed analysis of current Urban Search and Rescue robotics was performed resulting in a high level specification of a small, lightweight, easily deployable modular robotic architecture. The design methodology used is explained and all calculations, equations and design decisions are detailed and discussed.

The modular design produced performs well as a research platform. However to become more commercially viable the designs need to be developed into self-contained units which end users cannot modify. Using standardised interfaces the user can configure their robotic platform to meet their requirements.

Novel methods were used in the control of a robotic arm to improve the existing Human Machine Interface using head tracking technology and 3D vision systems; however there is significant scope to explore this area further.

The robot met the target mass, 24.84kg; a reduction of 45% from the existing robot. The re-manufacture cost is much lower than the existing robot; £4,264.04 compared to £10,937.84. It also achieved a 70% volume reduction.

## i) Table of Contents

<b>Abstract</b> .....	<b>ii</b>
<b>i) Table of Contents</b> .....	<b>iii</b>
<b>ii) List of Figures</b> .....	<b>vi</b>
<b>iii) List of Tables</b> .....	<b>x</b>
<b>Chapter 1. Introduction</b> .....	<b>1</b>
1.1. Motivation of Urban Search and Rescue Robot Development.....	1
1.2. RoboCup Rescue Competition .....	1
1.3. Warwick Mobile Robotics Background .....	2
1.4. Development Strategy.....	3
1.5. USAR Platforms Review.....	4
1.6. Aims and Objectives (2013-2014).....	6
1.7. New Robot High Level Specification .....	6
1.8. New Modular Robotic Architecture .....	8
<b>Chapter 2. Chassis</b> .....	<b>9</b>
2.1. Chassis Development Strategy.....	9
2.2. Specification .....	9
2.3. Benchmarking.....	10
2.4. Development and Justification of Design.....	11
2.4.1. Size.....	11
2.4.2. Shape.....	13
2.4.3. Materials Selection .....	15
2.4.4. Mounting Systems .....	16
2.4.5. Manufacturing and Assembly .....	19
2.5. Final Design .....	19
2.6. Virtual Testing.....	20
2.6.1. Arm Mounting Plate FEA .....	20
2.6.2. Motor Mounting Plate FEA.....	21
2.7. Physical Chassis Testing.....	22
2.8. Critical Review.....	23
<b>Chapter 3. Drivetrain</b> .....	<b>26</b>
3.1. Drivetrain Development Strategy .....	26
3.2. Specification .....	26
3.3. Benchmarking.....	27
3.4. Design, Calculations and Decisions.....	28
3.4.1. Tracks vs. Wheels.....	28
3.4.2. Design Options .....	29
3.4.3. Dimensions.....	31
3.4.4. Motor Requirements .....	32
3.5. Final Design .....	33
3.5.1. Manufacture .....	34
3.6. Testing.....	35
3.6.1. Virtual Testing.....	35
3.6.2. Physical Testing.....	37
3.7. Critical Review.....	38
<b>Chapter 4. Arm System</b> .....	<b>39</b>
4.1. Development Strategy.....	40
4.2. Specification .....	41

<b>4.3.</b>	<b>Research Summary .....</b>	<b>42</b>
<b>4.4.</b>	<b>Idea Generation and Concept Selection.....</b>	<b>43</b>
4.4.1.	Gripper .....	43
4.4.2.	Arm .....	44
<b>4.5.</b>	<b>Chosen Design.....</b>	<b>45</b>
<b>4.6.</b>	<b>Arm System Package .....</b>	<b>46</b>
<b>4.7.</b>	<b>Modular Joint .....</b>	<b>48</b>
4.7.1.	Modular Architecture Strategy.....	49
4.7.2.	Mechanical & Electrical Power Transmission and Control .....	50
4.7.3.	Kinematic Analysis.....	51
4.7.4.	Joint Fine Element Analysis and Material Selection .....	55
<b>4.8.</b>	<b>Link Design and Kinematic Analysis.....</b>	<b>58</b>
4.8.1.	Cable Tension and Buckling Loads .....	59
4.8.2.	Cable Sheer Mechanism .....	62
<b>4.9.</b>	<b>Gripper Design.....</b>	<b>63</b>
4.9.1.	Manipulator Design.....	63
4.9.2.	Final Design.....	64
4.9.3.	Modified Finger Plates FEA.....	66
<b>4.10.</b>	<b>Head Design.....</b>	<b>67</b>
4.10.1.	Camera Distance Calculations .....	67
4.10.2.	Initial Design.....	68
4.10.3.	Final Design.....	69
4.10.4.	Head Plate FEA.....	70
<b>4.11.</b>	<b>Virtual Testing.....</b>	<b>73</b>
4.11.1.	Gripper Testing with Manipulation of Objects .....	73
4.11.2.	Full Arm System .....	73
<b>4.12.</b>	<b>Critical Review.....</b>	<b>75</b>
<b>Chapter 5.</b>	<b>Electronics &amp; Software.....</b>	<b>77</b>
<b>5.1.</b>	<b>Electronics and Software Development Strategy.....</b>	<b>77</b>
<b>5.2.</b>	<b>Specification .....</b>	<b>78</b>
<b>5.3.</b>	<b>Electronic Architecture Design.....</b>	<b>79</b>
<b>5.4.</b>	<b>Control Electronics.....</b>	<b>80</b>
5.4.1.	Human Machine Interface .....	80
5.4.2.	Communication.....	80
5.4.3.	On-board Computer .....	82
5.4.4.	Motor Controllers .....	83
5.4.5.	Sensors .....	83
<b>5.5.</b>	<b>Power Electronics.....</b>	<b>85</b>
5.5.1.	Research Summary .....	85
5.5.2.	Power Board Requirements .....	86
5.5.3.	Trace Widths.....	87
5.5.4.	Switchable Outputs .....	88
5.5.5.	Cables Sizing and Fuse Protection .....	89
5.5.6.	Final Designs.....	89
5.5.7.	Manufacture .....	92
<b>5.6.</b>	<b>Power Distribution .....</b>	<b>93</b>
5.6.1.	Battery Monitoring.....	93
5.6.2.	Safety System.....	94
5.6.3.	Wiring Diagrams .....	95
<b>5.7.</b>	<b>Software Design.....</b>	<b>97</b>
5.7.1.	ROS.....	97
5.7.2.	URDF .....	97
5.7.3.	Mapping.....	98

5.7.4.	3D Headset Display.....	98
<b>5.8.</b>	<b>Testing.....</b>	<b>100</b>
5.8.1.	Control Electronics.....	100
5.8.2.	Mapping Software Testing.....	100
5.8.3.	HMI Software Testing.....	103
5.8.4.	Power Board.....	104
<b>5.9.</b>	<b>Critical Review.....</b>	<b>106</b>
<b>Chapter 6.</b>	<b>Analysis, Conclusion &amp; Recommendations.....</b>	<b>108</b>
<b>6.1.</b>	<b>System Analysis.....</b>	<b>108</b>
6.1.1.	Mass and Cost Analysis.....	108
6.1.2.	Full System Virtual Testing.....	110
6.1.3.	Modular Robotic Architecture (MRA).....	111
6.1.4.	RoboCup German Open.....	112
6.1.5.	Comparison against Initial Specification and Aims and Objectives.....	115
<b>6.2.</b>	<b>Conclusion.....</b>	<b>116</b>
<b>6.3.</b>	<b>Recommendations for Further Work.....</b>	<b>117</b>
<b>Chapter 7.</b>	<b>Bibliography.....</b>	<b>I</b>
<b>Appendices.....</b>		<b>V</b>
<b>Appendix A – Acronyms.....</b>		<b>V</b>
<b>Appendix B – Chassis.....</b>		<b>VI</b>
B.1 – Analysis of Possible Chassis Materials.....		VI
B.2 – Analysis of Possible Shell Materials.....		VII
B.3 – Worm Gear Force Analysis.....		VIII
B.4 – Derivation of Load Value for Arm Chassis Mount FEA.....		X
<b>Appendix C – Drivetrain.....</b>		<b>XI</b>
C.1 – Derivation of Drivetrain Dimensions.....		XI
C.2 – Derivation of Torque and Angular Acceleration Equations.....		XIII
C.3 – Flipper Torque and Loading Scenarios.....		XVI
C.4 – Drivetrain Design Narrative.....		XX
C.5 – Drivetrain Technical Drawings.....		I
C.6 – Drivetrain FEA.....		I
<b>Appendix D – Arm, Head and Gripper.....</b>		<b>III</b>
D.1 – SWOT Analysis of 2013/14 Arm System.....		III
D.2 – Analysis of Actuation Methods.....		VI
D.3 – Maximum Door Handle Torque Calculations.....		VII
D.4 – Torque Resulting from Robot Flipping Over.....		VIII
D.5 – Base Joint Torque With Linear Joint Addition.....		IX
D.6 – Cable Termination Failure Mechanism.....		X
D.7 – Comparison of Off-the-shelf Grippers.....		XI
D.8 – Gripper Finger Design Calculations.....		XIII
D.9 – Cost Benefit Analysis of Bespoke vs. Off-the-shelf Gripper.....		XV
D.10 – Gripper Force Calculations.....		XVI
D.11 – Gripper Finger Deflection Calculations.....		XVII
D.12 – Crash Scenario Calculations for FEA.....		XVIII
<b>Appendix E – Electronics &amp; Software.....</b>		<b>XIX</b>
E.1 - New Robot ROS UDRF File.....		XIX
E.2 – SWOT Analysis of Electrical System Architecture.....		XXI
E.3 – Testing Procedure of PCB.....		XXII
<b>Appendix F – Full Testing &amp; Analysis.....</b>		<b>XXIV</b>
F.1 – Mass and Cost Distribution Analysis.....		XXIV

## ii) List of Figures

Figure 1: Existing Tele-operated Robot 2012/13 .....	2
Figure 2: 2013/14 Development Process Workflow .....	3
Figure 3: iRAP Furious .....	4
Figure 4: Stabilize.....	4
Figure 5: Quince.....	4
Figure 6: Packbot.....	5
Figure 7: Robhaz.....	5
Figure 8: Chassis Development Strategy.....	9
Figure 9: Robot maximum height and width dimensions to pass through a 600mm equilateral triangle cut in a wall by first responders.....	11
Figure 10: Final Chassis Dimensions .....	13
Figure 11: Chassis Dimensions with Approximated Components.....	14
Figure 12: Detailed CAD Models of Electronic Components within Chassis.....	14
Figure 13: MakerBeam Profile .....	15
Figure 14: MakerBeam Angle Bracket .....	15
Figure 15: Scope for Adapting the MakerBeam Chassis Platform into Larger Sizes.....	16
Figure 16: Chassis Mounting Points.....	17
Figure 17: MakerBeam Brackets.....	17
Figure 18: 3D Printed Battery Housing - CAD Image .....	18
Figure 19: Modular Arm Control Box.....	18
Figure 20: Modular Arm Control box with Power Board (Green, top) & Control Computer (Grey, bottom).....	18
Figure 21: Final MakerBeam Chassis Design - CAD Image.....	19
Figure 22: Chassis with Mounting Plates - CAD Image.....	19
Figure 23: Final Chassis Design with Internal Components - Rendered CAD Image.....	20
Figure 24: Final Chassis Design with Internal Components and Shell - Rendered CAD Image...	20
Figure 25: Von Mises Stress for Arm Mounting Plate with 24Nm moment .....	21
Figure 26: Von Mises Stress of Motor Mounting Plate with 622N force.....	22
Figure 27: Chassis Testing Rig .....	23
Figure 28: Final Chassis Assembly .....	23
Figure 29: Final Chassis Assembly with Flipper Units in the RoboCup Rescue Arena .....	24
Figure 30: Optimum Chassis Shape to Avoid Beaching.....	25
Figure 31: Drivetrain Development Strategy.....	26
Figure 32: Existing USAR Robot Drivetrain Features .....	27
Figure 33: Option 1- Simplest Drivetrain Design.....	29
Figure 34: Option 2 - Middle Drivetrain Design.....	29

Figure 35: Option 3 – Top Drivetrain Design .....	30
Figure 36: Drivetrain Cost & Complexity vs. Mobility Graph.....	30
Figure 37: Top view (top) and Side View (bottom) of Restricting Dimensions in the Drivetrain Design.....	31
Figure 38: Drivetrain Final Design .....	34
Figure 39: Manufactured & Assembled Track Unit (With Tensioning Block) .....	35
Figure 40: FEA Modelling of the Flipper Unit.....	36
Figure 41: Aluminium L Sections Bonded to Steel with Araldite .....	37
Figure 42: 20N Applied to Bonded Aluminium L Section and Withstood.....	37
Figure 43: 88.29N Applied to Bonded Aluminium L Section and Withstood .....	37
Figure 44: Arm System Overview .....	39
Figure 45: Arm System Development Strategy .....	40
Figure 46: Kinematic Chain of most Common Configuration .....	42
Figure 47: Arm Concept Selection .....	44
Figure 48: Final Arm Design and Joint Configuration.....	45
Figure 49: Arm with Single Link, Wrist, Head & Griper .....	46
Figure 50: Arm with Wrist and Head .....	46
Figure 51: Arm Development Package Constraints.....	46
Figure 52: Arm positioned to meet turning circle (Top), and 60cm triangular (bottom) .....	47
Figure 53: Arm Joint.....	48
Figure 54: Arm Joint Exploded View .....	48
Figure 55: Joint Architecture Variable Dimensions - Front View.....	49
Figure 56: Joint Architecture Fixed Dimensions –Bottom View .....	49
Figure 57: Modular Joint Transmission and Position Control.....	50
Figure 58: Manipulation of Payload at Edge of Workspace.....	52
Figure 59: Arm Configuration Base Joint Torque Comparison .....	53
Figure 60: Debris Falling on Arm at Edge of Workspace.....	54
Figure 61: Forces Generated in Worm-Gear Pairs (R.Beardmore, 2013) .....	54
Figure 62: Worm-Gear Support Optimisation Process.....	55
Figure 63: Graph Showing Different Material Density and Yield Strength Properties .....	56
Figure 64: Downstream Joint Transmission Material Optimisation .....	57
Figure 65: Arm Tension Cable Link Design.....	58
Figure 66: Changeable Link Lengths - Short (left) and Long (right) .....	58
Figure 67: Full arm and payload weight carried by two of the four cables in tension.....	59
Figure 68: Buckling Load Affected Length (TheCarTech, 2013).....	61
Figure 69: Bolt Undercut Diameter .....	62
Figure 70: Cable Termination Failure Mechanism with Ball & Socket Joint .....	62
Figure 71: Initial Gripper Concept.....	63
Figure 72: Initial Gripper Concept (Transparent).....	63

Figure 73: Initial Gripper Finger Designs .....	63
Figure 74: Dagu Gripper .....	65
Figure 75: Spring Loaded Clutch .....	65
Figure 76: Redesigned Gripper Fingers.....	65
Figure 77: Gripper Assembly with Modified Fingers (Front View) .....	65
Figure 78: Gripper Assembly with Modified Fingers (Top View) .....	65
Figure 79: FEA Loading Point on Gripper Finger .....	66
Figure 80: Finger Stress with 1kg loading.....	67
Figure 81: Finger Deflection with 1kg loading .....	67
Figure 82: Focal Area of Webcams .....	68
Figure 83: Initial Head Design.....	69
Figure 84: Evolution of Head Plate Design.....	69
Figure 85: Final Head Design Assembly .....	70
Figure 86: FEA Head Loading Scenario .....	71
Figure 87: Von Mises Stress Analysis of Final Head Plate (500N) .....	72
Figure 88: Von Mises Stress Analysis of Final Head Plate (1000N) .....	72
Figure 89: Bottle Manipulation (Original Fingers) .....	73
Figure 90: Balsawood Block Manipulation (Modified Fingers) .....	73
Figure 91: Ground Level Entombed Victim.....	74
Figure 92: Door Opening Capability .....	74
Figure 93: Valve Manipulation Tasks .....	74
Figure 94: Final Arm System Design.....	75
Figure 95: Electronics and Software Development Strategy .....	77
Figure 96: Robot Modular Electronic Architecture .....	79
Figure 97: Oculus Rift and RPY Diagram (Oculus VR, 2013).....	80
Figure 98: RoboCup 2013 Wireless Spectrum Scan (WMR, 2013).....	81
Figure 99: Existing Robot Router Placement .....	81
Figure 100: Chassis with the Router's Three Antennas Extruding Out (Black).....	81
Figure 101: pico-ITX vs. mini-ITX Space Savings.....	82
Figure 102: Axiomtek pico-ITX Computer (Mosuer, 2013).....	82
Figure 103: SyRen 25A Brushed DC Motor Driver .....	83
Figure 104: Sabertooth Dual 25A Brushed DC Motor Drive.....	83
Figure 105: 1061 - PhidgetServo Controller .....	83
Figure 106: HOKUYO URG-04LX LIDAR.....	83
Figure 107: Microsoft HD 3000 Webcam .....	84
Figure 108: Raspberry Pi Camera System.....	84
Figure 109: SEN-10724 9-Axis IMU .....	84
Figure 110: MA3 Miniature Absolute Shaft Encoders.....	84



Figure 111: SEN0159 CO2 Sensor .....	84
Figure 112: nFET and pFET switching circuit (left) and Multisim layout (right) .....	88
Figure 113: nFET and pFET transfer characteristic (Vishay Siliconix, 2010) .....	89
Figure 114: Main Power board Multisim Schematic .....	90
Figure 115: Arm Power board Multisim Schematic .....	91
Figure 116: Ultiboard Layout of Arm Powerboard.....	91
Figure 117: Ultiboard Layout of Main Power board.....	91
Figure 118: 3D Representation of the boards using Ultiboard 3D preview.....	91
Figure 119: The PCBs after component soldering.....	92
Figure 120: Battery Monitor Design 1 .....	93
Figure 121: Battery Monitor Design 2 .....	93
Figure 122: Emergency stop circuit designed using Multisim .....	95
Figure 123: Emergency Stop Electrical Drawing.....	95
Figure 124: Full System Wiring Diagram.....	96
Figure 125: USAR URDF Node Network and Model Visualisation Produced.....	98
Figure 126: Node Network Created for Mapping .....	98
Figure 127: Oculus Rift Headset Display Overview .....	99
Figure 128: Oculus Rift Displaying Two Different Video Streams & Horizon Level (1) .....	99
Figure 129: Oculus Rift Displaying Two Different Video Streams & Horizon Level (2) .....	100
Figure 130: Map 1 Created by the USAR Robot during the RoboCup German Open .....	101
Figure 131: Map 2 created by the WMR robot (Part 1/2).....	102
Figure 132: Map 2 created by the WMR robot (Part 2/2).....	102
Figure 133: Updated Node Network to Include IMU Attitude Transformation.....	103
Figure 134: Client Software Program Modified to Control Existing Robot's Head.....	103
Figure 135: Head Tracking - Looking Forward .....	104
Figure 136: Head Tracking - Looking Right.....	104
Figure 137: Head Tracking - Looking Left.....	104
Figure 138: Head Tracking - Looking Down.....	104
Figure 139: Testing of the Main Power board .....	105
Figure 140: Main Power board mounted inside the robot chassis.....	105
Figure 141: Arm Power Board Mounted to Raspberry Pi .....	105
Figure 142: Accessing High Victims and Entombed Victims.....	110
Figure 143: Accessing High 'Void Victim Boxes' .....	111
Figure 144: Modular Robotic Architecture Platform Breadth.....	112
Figure 145: New Robot Entry through First Responder Hole vs. Existing Robot through Door .....	113
Figure 146: Small Height Avoids Clearing Debris .....	114
Figure 147: Ability to Climb 45° Slope.....	114
Figure 148: Deployable by 1 Person (<25kg) .....	114

Figure 149: Inability to Clear Stepfield due to Small Robot Geometry .....	114
Figure 150: - Forces generated by worm and worm gear pair (R.Beardmore, 2013) .....	VIII
Figure 151: Diagram to Depict the Moment Calculated for the Force of the Arm on the Chassis X	
Figure 151: Drivetrain Dimensions.....	XI
Figure 152: Wheel On a Slope .....	XIII
Figure 153: Wheel Accelerating Up a Slope.....	XIII
Figure 154: Situation 1.1 .....	XVI
Figure 155: Situation 1.2.....	XVI
Figure 156: Situation 2.1 .....	XVII
Figure 157: Situation 2.2 .....	XVIII
Figure 158: Situation 3.1 .....	XIX
Figure 159: Situation 3.2 .....	XIX
Figure 161: Front Axle FEA.....	I
Figure 162: Track Side Plate FEA.....	I
Figure 163: Flipper Axle FEA.....	II
Figure 164: Flipper Axle Hat FEA .....	II
Figure 165: Previous Arm.....	III
Figure 166: Old Gripper.....	IV
Figure 167: New Gripper.....	IV
Figure 168: Old Head.....	V
Figure 169: New Head & Gripper.....	V
Figure 170: Arm Torque Opening a Door Handle.....	VII
Figure 170: Flipped Robot.....	VIII
Figure 172: Previous Arm Design Failure .....	VIII
Figure 173: Load Applied to Rod .....	X
Figure 174: Dagu Gripper Layout .....	XIII
Figure 175: Dagu Gripper Dimensions .....	XIII
Figure 176: Modified Finger Dimensions .....	XIV
Figure 176: Total Angle.....	XIV
Figure 177: Main Power Board.....	XXII

### iii) List of Tables

Table 1: Analysis of Competitor and Commercially Available USAR Robots.....	4
Table 2: Specification for the new USAR robot.....	7
Table 3: Chassis and Shell Specification.....	9
Table 4: Previous WMR USAR Robot Chassis Structures .....	10
Table 5: Maximum Chassis Dimension Parameters.....	12
Table 6: Chassis Dimensions – Maximum vs. Chosen .....	12

Table 7: Construction Methods and Justifications.....	19
Table 8: Assumption used in Chassis Stress Analysis.....	20
Table 9: Key Factors for the Stress Analysis of the Arm Mounting Plate .....	20
Table 10: Results of Stress Analysis of the Arm Mounting Plate .....	21
Table 11: Key Factors for the Stress Analysis of the Motor Mounting Plate.....	21
Table 12: Results of Stress Analysis of the Motor Mounting Plate .....	22
Table 13: Chassis Results against Specification .....	24
Table 14: Drivetrain Specification.....	26
Table 15: Tracks and Wheel Comparison against Specification .....	28
Table 16: Drivetrain Dimension .....	31
Table 17: Track Motor Requirements.....	32
Table 18: Flipper Motor Requirements .....	33
Table 19: Final Drivetrain Motor Specifications .....	33
Table 20: Impact Shock Calculations .....	35
Table 21: Comparison against Specification.....	38
Table 22: Arm Specification .....	41
Table 23: Joint Description of most Common Configuration .....	42
Table 24: Arm Design Methodology.....	45
Table 25: Arm Link Configurations .....	47
Table 26: Joint Component Index .....	48
Table 27: Arm Actuation and Transmission Cost Comparison .....	51
Table 28: Joint Worst Case Loading Scenarios .....	51
Table 29: Base Joint Torque Variables.....	52
Table 30: Forces Generated in Worm-Gear Pairs .....	54
Table 31: Transmission Weight Reduction Through Material Substitution .....	57
Table 32: Transmission Cost Reduction Through Material Substitution .....	57
Table 33: Link Loading Scenarios.....	59
Table 34: Cable Tension Parameters.....	60
Table 35: Buckling Load Parameters.....	61
Table 36: Failure Mechanism Parameters.....	62
Table 37: Gripping Forces of Various Objects.....	64
Table 38: FEA Results of Gripper Finger.....	66
Table 39: Weight Comparison of Head Plate.....	70
Table 40: Weight Comparison of Webcam Enclosures.....	70
Table 41: FEA Head Loading Scenarios .....	71
Table 42: FEA Results for Head Plate in Collision Scenarios.....	71
Table 43: Arm System Comparison against Specification.....	75
Table 44: Electrical System Specification .....	78

Table 45: Chosen Motor Controllers (Images and Data from (Active Robots, 2013)) .....	83
Table 46: Sensors Chosen & Why .....	83
Table 47: Analysis of the existing USAR power board.....	85
Table 48: Required Outputs for the main power board.....	86
Table 49: Required Outputs from the Arm Power Board.....	86
Table 50: Battery Monitoring Design .....	93
Table 51: Electronic and Software Results against Specification.....	106
Table 52: Chassis Mass & Cost Breakdown .....	108
Table 53: Drivetrain Mass & Cost Breakdown .....	109
Table 54: Arm System Mass & Cost Breakdown .....	109
Table 55: Full System Mass & Cost Breakdown .....	110
Table 56: Original Specification Objectives against Achievements .....	115
Table 57: Analysis of Possible Chassis Materials.....	VI
Table 58: Analysis of Possible Shell Materials .....	VII
Table 59: Slide Velocity- Coefficient of friction relationship (R.Beardmore, 2013) .....	VIII
Table 60: Input Parameters for Worm Gear Pairs.....	IX
Table 61: Output Forces and Efficiencies Generated by Worm Gear Pairs .....	IX
Table 62 : Drivetrain Dimensions, Calculated and Chosen .....	XII
Table 63: Situation 1 .....	XVII
Table 64: Situation 2 .....	XVIII
Table 65: Situation 3 .....	XIX
Table 66: SWOT for Previous Arm.....	III
Table 67: SWOT for Old Gripper .....	IV
Table 68: SWOT for Old Head.....	V
Table 69: Pneumatic Actuation.....	VI
Table 70: Electric Actuation.....	VI
Table 71: Base Joint Torque Variables with Linear .....	IX
Table 72: Off-the-shelf Gripper Comparison .....	XI
Table 73: Off-the-shelf Gripper Costs.....	XV
Table 74: Bespoke Gripper Costs .....	XV
Table 75: SWOT for Electrical Architecture.....	XXI
Table 76: Mass and Cost Distribution Analysis .....	XXIV

## Chapter 1. Introduction

### 1.1. Motivation of Urban Search and Rescue Robot Development

Urban populations continue to grow, global temperatures rise, and the frequency and intensity of natural disasters are predicted to continue increasing (Schneider, et al., 2007). The development of innovative Urban Search and Rescue (USAR) robotic solutions are required to save lives, and are now possible, more than ever, with the availability of affordable actuators, sensors and communication technology.

USAR robots are designed to look for survivors in buildings damaged by either natural or manmade disasters. Examples include the 2011 earthquake in New Zealand (BBC, 2011), the Fukushima Nuclear Disaster in 2011 resulting from a tsunami (Keiji Nagatani, 2013) and the terrorist attack on the World Trade Centre in 2001 (R.Murphy, 2004).

USAR operations are usually very slow, dangerous and labour intensive. The primary benefits of using USAR robots are to:

- Remove first responders from dangerous environments
- Move through confined spaces within a collapsed building
- Increase rate of victim detection; significantly improving the chances of survival as victim mortality rate increases and peaks after 48h (R.Murphy & et.al, 2008)

### 1.2. RoboCup Rescue Competition

The RoboCup is an *“international competition where USAR robots compete to find victims in a simulated earthquake environment”* (Jacoff, 2009, p. 1). Points are awarded based on the entrant’s capabilities, including manoeuvrability, victim identification, object manipulation and environment mapping. The ‘Innovative User Interface Award’ is new for 2014 to recognize the

increasing importance of the Human System Interface (HSI) in facilitating advanced manipulation and detection (Pellenz, 2014).

### 1.3. Warwick Mobile Robotics Background

Warwick Mobile Robotics (WMR) is a collection of projects in the field of mobile robotics under development at the University of Warwick ranging from rescue robots to autonomous, flying robots (Chavasse, 2013). Since 2008 WMR has been developing a USAR robot and each year choosing areas from the previous design to improve or optimise. Although the existing design (Figure 1) is very capable, it is heavy (45kg) and too large to fit through the smaller areas of the RoboCup arena, which are becoming more common.



Figure 1: Existing Tele-operated Robot 2012/13

### 1.4. Development Strategy

To aid the development process a workflow was developed (Figure 2).

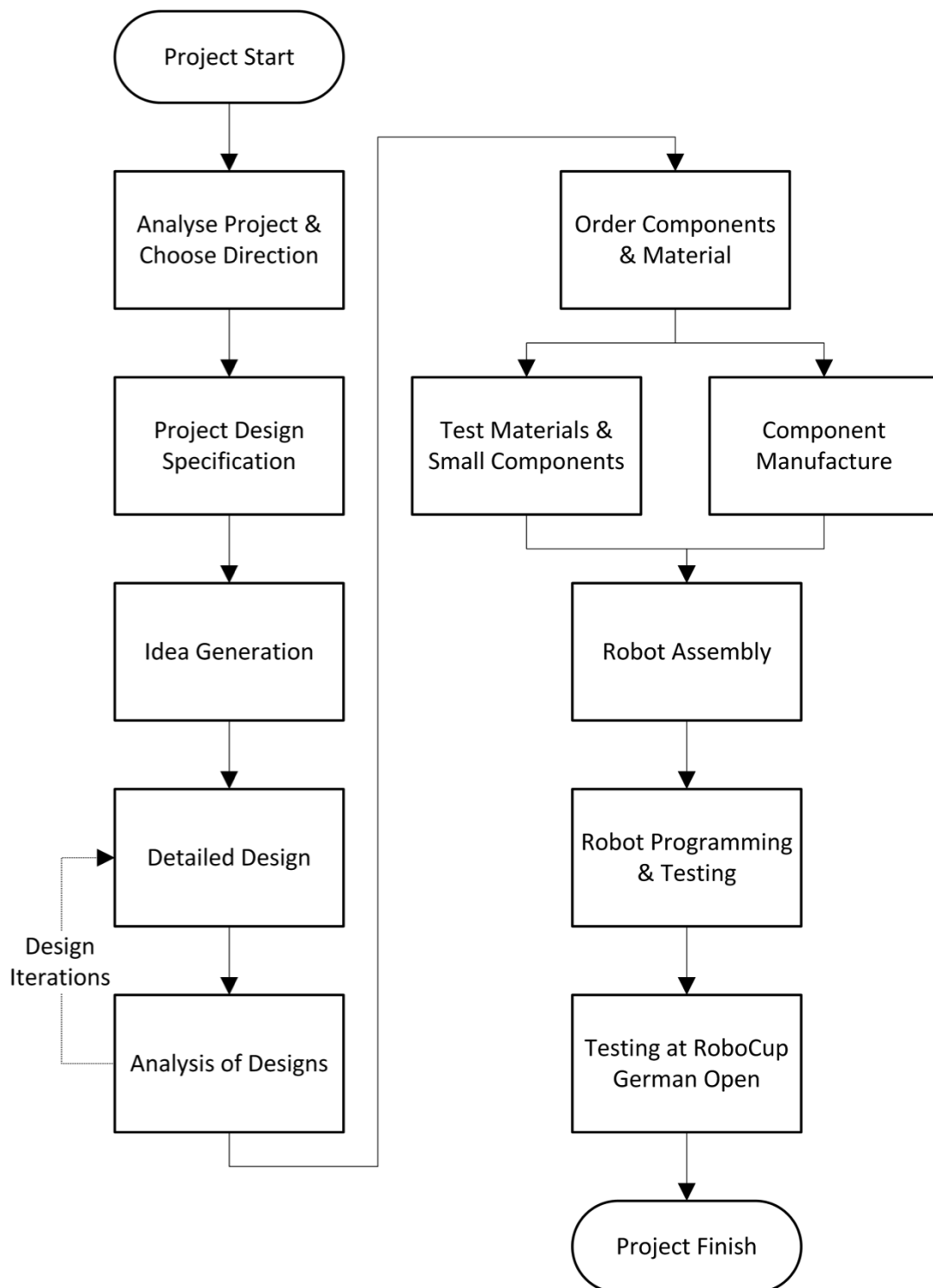


Figure 2: 2013/14 Development Process Workflow

## 1.5. USAR Platforms Review

Table 1 summarises two competitor and three commercially available USAR robots. iRAP Furious (Figure 3) won the World RoboCup in 2013 and Stabilize (Figure 4) came second.

**Table 1: Analysis of Competitor and Commercially Available USAR Robots**



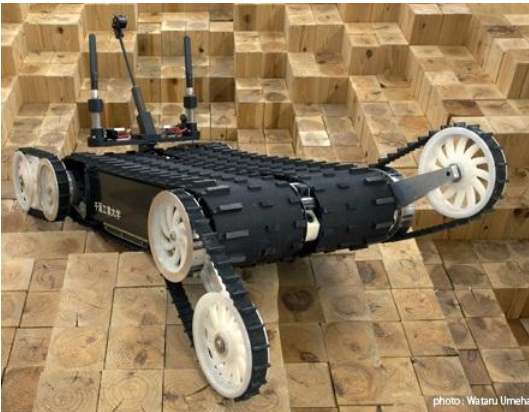
	<p><b>Name:</b> iRAP Furious</p> <p><b>Type:</b> Competitor (RoboCup)</p> <p><b>Developer:</b> King Mongkut's University of Technology, North Bangkok</p> <p><b>Real-life applications:</b> n/a</p> <p><b>Key details:</b> Team has two tele-operated robots and one autonomous robot. One USAR-T robot has industrial rubber for the tracks, the other has one with water-hose. Use flippers which can be rotated 360°. Range of sensors. Arm reach: 1.5m, max. payload: 5kg. System cost: \$14,600. (Sittiwanchai, et al., 2013)</p>
	<p><b>Name:</b> Stabilize</p> <p><b>Type:</b> Competitor (RoboCup)</p> <p><b>Developer:</b> Rajamangala University of Technology Phra Nakhon, Bangkok</p> <p><b>Real-life applications:</b> n/a</p> <p><b>Key details:</b> Caterpillar wheel design with rubber tires to enhance friction and mobility in steep terrain, CO<sub>2</sub> and temperature sensors, camera selector switch, predominantly made from aluminium, robotic arm can reach 1.5m. 65kg, 550x650x600mm. System cost: \$9,320. (Chaikanta, et al., 2013)</p>
	<p><b>Name:</b> Quince</p> <p><b>Type:</b> Commercial</p> <p><b>Developer:</b> China Institute of Technology</p> <p><b>Real-life applications:</b> Surveyed the inside of Fukushima Daiichi nuclear power plant after the earthquake in 2011.</p> <p><b>Key details:</b> 32kg, 900mm (W) x 700mm (L) x 150mm (H). The components are stored within the main tracks. (Future Robotics Technology Center, 2007)</p>





Figure 6: Packbot

**Name:** Packbot

**Type:** Commercial

**Developer:** iRobot

**Real-life applications:** Bomb disposal

**Key details:** 10.89kg, 520mm (W) x 700mm (L) x 178mm (H), modular, adaptable and expandable, aluminium chassis, components stored within tracks (iRobot, 2013)



Figure 7: Robhaz

**Name:** Robhaz

**Type:** Commercial

**Developer:** Lee et al.

**Real-life applications:** Explosives detection

**Key details:** 27kg, 425mm (W) x 732mm (L) x 140mm (H), this type has identical upper and lower parts so it can move regardless of its orientation, the shell is made from a high impact plastic. (Aving, 2006)

Comparing WMR's existing robot to the platforms in Table 1, shows it is of a similar size but much heavier at 45kg. This difference in mass and the new 2014 competition rules helped to define this year's aims and objectives.

## 1.6. Aims and Objectives (2013-2014)

1. Improve the existing robot:
  - a. Upgrade/enhance the existing USAR robot
  - b. Operator training to allow comprehensive robot control
2. Develop a smaller USAR robot capable of searching for simulated victims in a small confined disaster environment with the following core development aims:
  - a. A modular architecture that allows the platform to be easily modified
  - b. Low cost, lightweight and deployable by one person
  - c. Reliable and easily repairable
  - d. Introduce mapping capabilities to aid the robot in becoming fully autonomous
  - e. Develop HSI and support for Oculus Rift with head tracking technology
  - f. Long-term aim to allow future teams to develop this prototype into a commercially viable design
3. Enter the RoboCup German Open 2014 in the “Rescue” category utilising both robots

## 1.7. New Robot High Level Specification

The 2014 RoboCup Rescue competition rules (Pellenz, 2014) were chosen as a base specification for the new robot. The team decided to design and build a new small, modular and lightweight robot to fit through small openings in the arena rather than tackle the biggest, most challenging obstacles. Developing a small lightweight robot under 25kg would allow it to be deployed by a single operator (Warwick University, 2013). The design was split into 4 systems:

- |            |               |                         |                           |
|------------|---------------|-------------------------|---------------------------|
| 1. Chassis | 2. Drivetrain | 3. Arm System           | 4. Electronics & Software |
|            |               | a. Arm                  | a. Control Electronics    |
|            |               | b. Head and Manipulator | b. Power Electronics      |

Table 2 details the high level specification for the new design.

Table 2: Specification for the new USAR robot

ID	Objective	Description	Competition Points	Chassis	Drivetrain	Arm	Head & Manipulator	Power Electronics	Battery Monitoring	Control Electronics
1	15° Ramps	Handle continuous pitch and roll ramps of 15°	Not Directly	X	X	X				
2	Crossing 15° Ramps	These are continuous crossing roll and pitch ramps	Not Directly	X	X	X				
3	Stairs 45°	The robot should be able to climb 45° stairs	Not Directly	X	X	X				
4	Ramps 45°	Drive up/down/diagonally on 45° slopes	Not Directly	X	X	X				
5	Confined Spaces	Must be able to navigate 50-80 cm enclosed spaces and ones including 10cm "stalactites"	Not Directly	X	X	X	X			
6	Step fields	Navigate small ones, not "complex" ones	Not Directly	X	X	X	X			
7	600x600x600mm Triangle	Must be small enough to fit through this	Not Directly	X	X	X	X			
8	720mm Door Width	Drive through a door frame of 72cm	Not Directly	X	X	X	X			
9	Arm Stowing	Arm must stow well for ascents	Not Directly	X		X	X			
10	Precision Manipulation	Grasp items at 0-100cm & reach 30-60cm	20 per object per victim Max 160 (Tele-operated) Max 120 (Autonomous)				X	X		X
11	Object Grasp	Water Bottle, Walkie-Talkie, Wood Block (10cm <sup>2</sup> )	20 per object per victim				X	X		X
12	Mapping	Produce a map conforming to rules	20 per arena	X				X		X
13	QR Codes	Identify QR Codes & place on map	1 to 5	X				X		X
14	Two Way Audio	Send and receive audio messages	5/way - Max 10 per victim	X			X			X
15	CO2 Sensor	Detect CO2 emissions from simulated "life"	5 per victim	X			X			X
16	Access Victim 'Boxes'	Must access victim boxes from side/above	Yes	X	X	X	X	X		X
17	Confined Space Gripper	Must be able to deploy gripper in confined space	Yes				X			
18	30 Minutes Power	Must endure 30 minute competition rounds	Not Directly		X			X	X	
19	Wireless Range	Must have ~100m wireless range indoors	Not Directly					X		X
20	Autonomy	Implement simple "wall following"	Yes					X		X
21	Single Operator Control	Must be controlled by a single operator (intuitively)	Not Directly						X	X
22	Low Vibration in Arm	Investigate ways of minimising vibrations in the arm	Not Directly	X	X	X	X			
23	Withstand 350mm Drop	Not deform from 350mm drop and no electrical issues	Not Directly	X	X			X	X	X

<b>24</b>	Low Centre of Mass	Low centre of mass to help with inclines	Not Directly	X	X	X	X			
<b>25</b>	Protected Batteries	Must be housed so potential damage is reduced	Not Directly	X		X	X			
<b>26</b>	Easy access & Replace	Must take <60 seconds to access & swap batteries	Not Directly	X		X	X			
<b>27</b>	Battery Monitor	Must provide cell voltage level to operator	Not Directly			X	X			
<b>28</b>	Power Board	Provide all systems with correct voltage & power	Not Directly			X	X			
<b>29</b>	Emergency Stop	Have an E-Stop which cuts power to motors	Not Directly	X		X	X			
<b>30</b>	Single Connection Panel	Have a single panel for all external connectors	Not Directly	X		X	X			
<b>31</b>	Operator Awareness	Display key cameras & information	Not Directly				X			
<b>ID</b>	<b>Objective</b>	<b>Description</b>	<b>Competition Points</b>	<b>Chassis</b>	<b>Drivetrain</b>	<b>Arm</b>	<b>Head &amp; Manipulator</b>	<b>Power Electronics</b>	<b>Battery Monitoring</b>	<b>Control Electronics</b>

### 1.8. New Modular Robotic Architecture

A new Modular Robotic Architecture (MRA) was developed describing the physical layout and connections between components. The main features with this modular approach were:

- Fixed critical dimensions of the platform where the largest cost would be incurred during modification
- Flexible structure allowing non critical dimensions to be altered quickly
- A standard set of interchangeable components reducing complexity
- Future development time is reduced

The scope of this year’s project was to develop the smallest possible version of the platform with the highest capabilities.

## Chapter 2. Chassis

The primary function of the chassis is to store and protect internal components and provide a platform to mount and integrate the robot’s systems.

### 2.1. Chassis Development Strategy

Figure 8 describes the development strategy of the Chassis.

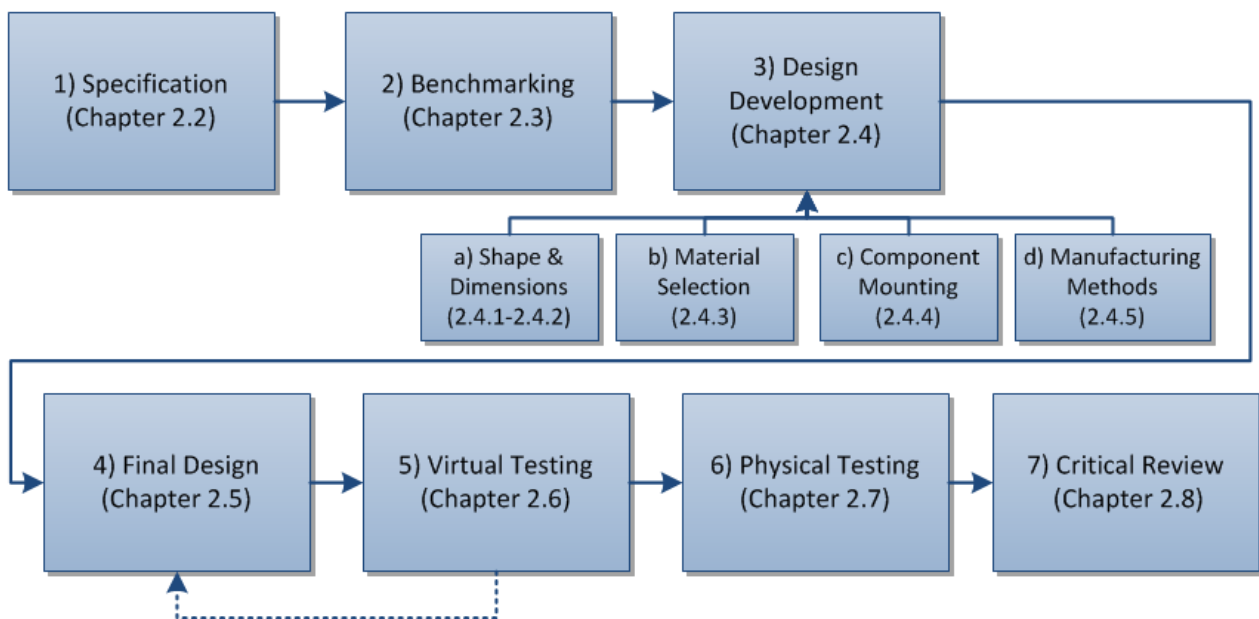


Figure 8: Chassis Development Strategy

### 2.2. Specification

Table 3 details the chassis and shell specification developed from the aims and objectives, original high-level specification (Chapter 1.6) and RoboCup Rescue rules.

Table 3: Chassis and Shell Specification


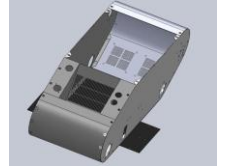

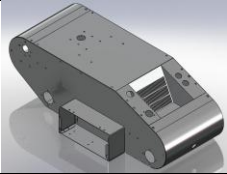
ID	Constraint	Description
1	Modular Architecture	Develop a core modular architecture that will allow the robotic platform to be easily modified or upgraded by future teams.
2	Cost	Chassis components must be low cost
3	Repair and Maintenance	Easy to repair and maintain. Design should consider ease of assembly/ disassembly and ease of access.
4	Durability	Must be able to withstand transfer of kinetic energy from collisions. Must prevent debris from getting in the chassis where possible. Must protect internal systems from damage.
5	Mass	Robot must be deployable by one person (25kg max.). There must be an even distribution of mass within the chassis. Low COG to improve mobility when ascending stairs or an inclined plane.

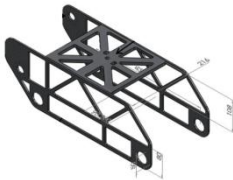
<b>6</b>	<b>Size</b>	Must fit all electronics, gearboxes, motors etc. Combined with the arm and drivetrain, must fit through small competition obstacles
<b>7</b>	<b>Systems Integration</b>	Must account for the fixed dimensions required for the drive train. Must integrate with the arm module and allow space for arm electronics. Must store and protect electronic components. Must safely store the battery and allow for easy access. Some components must be insulated from conductive materials.
<b>8</b>	<b>Load Resistance</b>	Must be able withstand a fall from 350mm. Must take the load of the arm. Must be resistant to loads generated within the drivetrain system
<b>9</b>	<b>Ease of Manufacture and Assembly</b>	Taking account of the time constraints, chosen materials and structures must be easily manufactured and assembled in the IMC workshop. Off-the-shelf parts must be used where possible. Standardise parts where possible.
<b>10</b>	<b>Material Availability</b>	Materials must be readily available from local distributors.

### 2.3. Benchmarking

Table 4 shows the design progression of WMR's chassis' over time.

**Table 4: Previous WMR USAR Robot Chassis Structures**

<b>Year</b>	<b>Photo</b>	<b>Material</b>	<b>Construction</b>	<b>Cost</b>	<b>Comments</b>
2007-08 (USAR-T)		12mm Aluminium (Al)	Plate construction (CNC milled)	£659.71	Bolted together using CAP screws, pockets removed where strength is not required saving mass.
2008-09 (USAR-T)	Same as above			n/a	n/a
2009-10 (USAR-T)		0.9mm Al	Plate construction (laser cut)	Not Available	Seven panels, could be easily replaced if damaged. Braces needed to be added to increase rigidity and reduce bending.
2009-10 (USAR-A)		0.9mm Al	Plate construction (laser cut)	Not Available	Central plate fitted across chassis to increase stiffness. Torsion bar had to be inserted after the robot landed on one of the front pulleys.
2010-11 (USAR-T)	Same as above			n/a	n/a
2010-11 (USAR-A)		0.9mm Al	Plate construction (laser cut)	£1010.58	Battery stored outside chassis (between tracks). Similar design to USAR-T 2009-10.
2011-12 (USAR-T)	Same as above			n/a	n/a

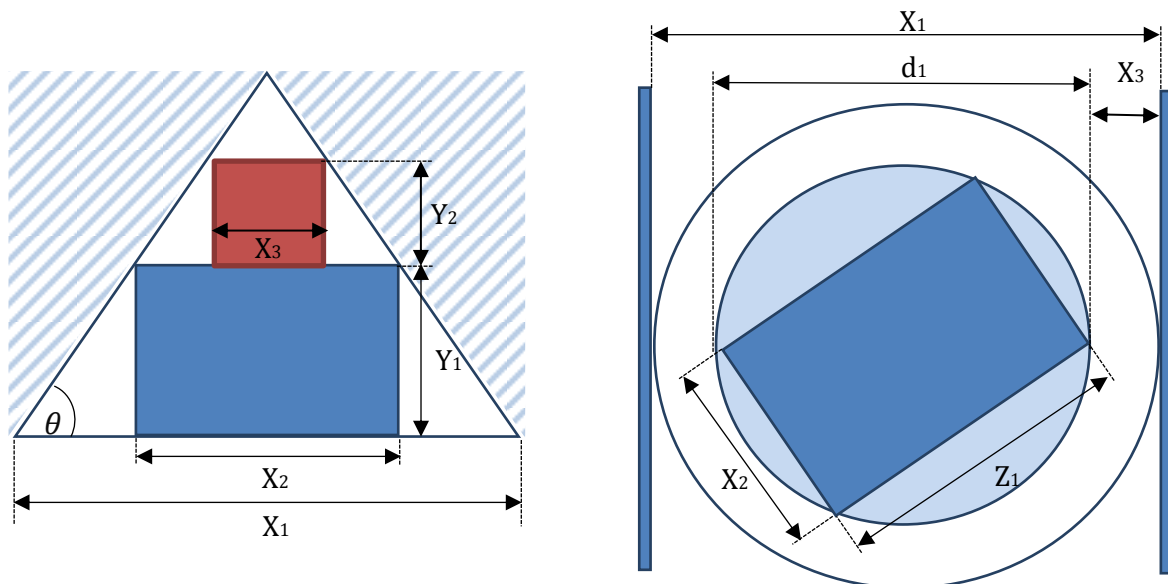
2012-13 (USAR-T)		5mm Al sides, 10mm Al base and top, 1.2mm Al internal structure	Structural space frame – plate construction (water jet cut)	£1265.98	Silver steel reinforcement rods added for rigidity. Non-load bearing shell added as a barrier to dirt and moisture. Material: 3mm ABS.
------------------	---	---	---	----------	--

USAR robots reviewed in Chapter 1.5 and previous WMR designs (Table 4) indicated that the most common factors between designs were the materials used, predominantly aluminium, and the curved shape of the chassis which aids mobility. All previous designs have been curved at the front and back to avoid catching and have control components outside of the shell. The cost has also increased over time. These factors were considered in the design process.

## 2.4. Development and Justification of Design

### 2.4.1. Size

The robot’s maximum chassis dimensions were found through geometric relationships (Equations 1, 2 and 3) derived from two specification constraints (Figure 9).



**Figure 9: Robot maximum height and width dimensions to pass through a 600mm equilateral triangle cut in a wall by first responders (Left), Robot maximum length to turn within a 600mm wide confined space (Right)**

For known triangle size ( $x_1$ ) and chosen robot width ( $x_2$ ) the maximum robot height is given by Equation 1. Turning radius ( $d_1$ ) is calculated from a chosen value of wall clearance ( $x_3$ ), Equation 2. Maximum robot length ( $z_1$ ) is calculated using Equation 3.

$$y_1 = \frac{x_1 - x_2}{2} \tan \theta \quad \text{Equation 1.}$$

$$d_1 = x_1 - 2x_3 \quad \text{Equation 2.}$$

$$z_1 = \sqrt{d_1^2 - x_2^2} \quad \text{Equation 3.}$$

Table 5 details the maximum chassis dimensions calculated.

**Table 5: Maximum Chassis Dimension Parameters**

Parameter	Symbol	Dimension (mm)
Hallway width	$x_1$	600.0
Robot width	$x_2$	320.0
Max. robot height	$y_1$	242.5
Wall clearance	$x_3$	20.0
Turning radius	$d_1$	560.0
Max. robot length	$z_1$	460.0

The final robot width and maximum length must take into account the tracks. The maximum height should account for the arm system.

Table 6 details the maximum possible chassis dimensions and the chosen dimensions illustrated by Figure 10.

**Table 6: Chassis Dimensions - Maximum vs. Chosen**

Parameter	Maximum (mm)	Chosen (mm)	Explanation
Length	460	450	10mm clearance was chosen to increase clearance whilst turning
Width	320	160	80mm for each track, plus 5mm clearance between chassis and track unit to allow space for wiring
Height	242.5	155	Minimised to reduce CoG



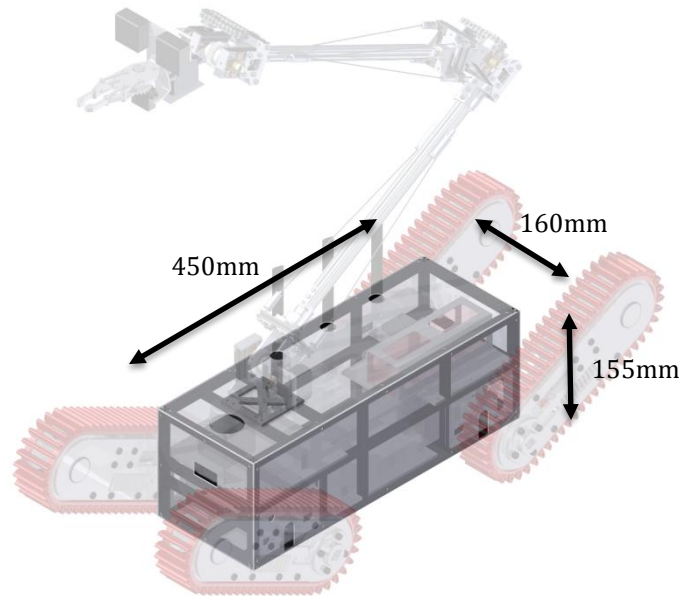


Figure 10: Final Chassis Dimensions

The arm system maximum dimensions were calculated through geometric relationships (Equations 3 and 4) derived from the specification constraints.

For known chassis width,  $x_2$ , and chosen arm system width,  $x_3$ , the maximum arm system height is given by:

$$y_2 = \frac{x_2 - x_3}{2} \tan \theta \quad \text{Equation 4.}$$

#### 2.4.2. Shape

Two critical factors were used to determine the shape of the robot:

1. Shape, size and location of internal components;
2. Collision avoidance and mobility.

Major internal components were approximated in Computer Aided Design (CAD) software and assembled into an initial chassis design to assess whether the components would fit into the available package (Figure 11). Accurate components were then created in CAD (Figure 12).

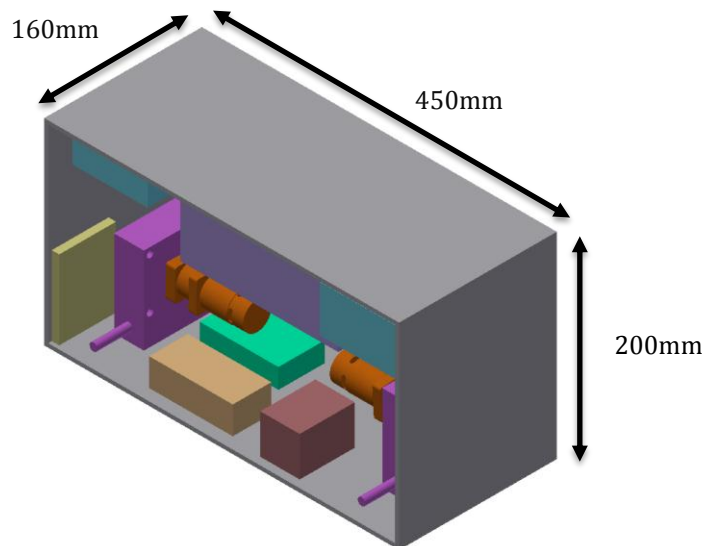


Figure 11: Chassis Dimensions with Approximated Components

The model (Figure 11) demonstrated that all of the desired components could fit inside the chassis.

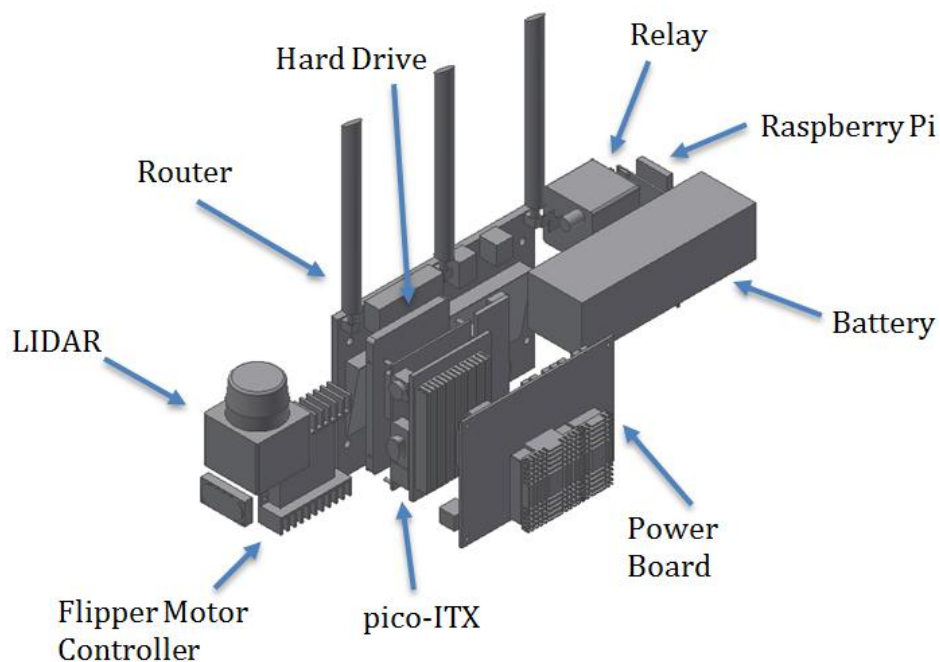


Figure 12: Detailed CAD Models of Electronic Components within Chassis

Although researched robots (Chapter 1.5) have curved front and backs to avoid collisions and improve mobility, this decreases the useable volume. This also increases manufacturing complexity and reduces the ease of modification. Due to these factors, a cuboid shaped structure was selected.

### 2.4.3. Materials Selection

The specification led to the comparison of three aluminium variants (Appendix B.1) and a lightweight, off-the-shelf aluminium beam being chosen (MakerBeam<sup>1</sup>) with a high strength to weight ratio (MakerBeam, 2013). MakerBeam has an integrated construction technique using brackets which bolt inside the T-slot of the beam (Figure 13 and Figure 14). These rigid yet non-permanent fixings allow modification and provide easy assembly.



Figure 13: MakerBeam Profile



Figure 14: MakerBeam Angle Bracket

MakerBeam's sister product, OpenBeam is larger and stronger so would allow a larger platform to be developed to meet different operational requirements. The objective is to build the smallest, highest capability model however Figure 15 shows how the size can be increased.

---

<sup>1</sup> MakerBeam is the brand name for this range of extruded aluminum beam with T-Slots used for prototyping

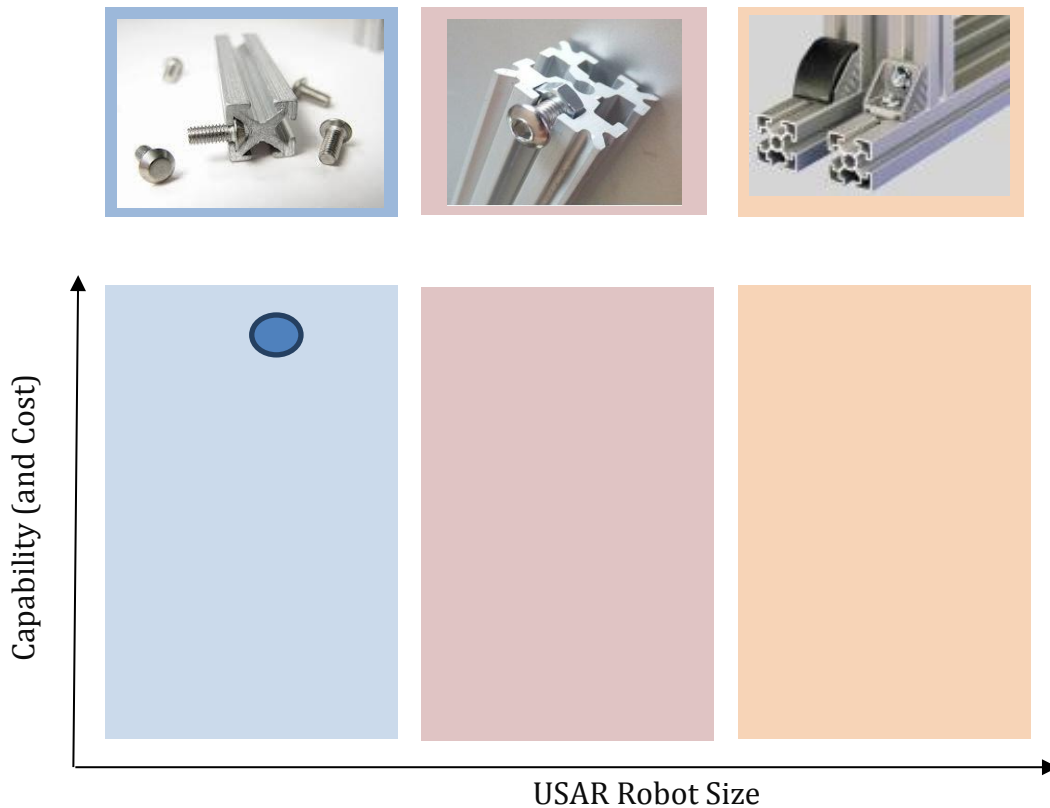


Figure 15: Scope for Adapting the MakerBeam Chassis Platform into Larger Sizes

A non-load bearing shell was required as a barrier to dirt and moisture. The shell needed to be removable and provide access to internal components, particularly the battery. Polycarbonate was chosen for the sides and top, due to its low mass and high impact resistance (Polymer Technology, 2012). Sheet aluminium was selected for the base as greater durability was required. A material analysis can be found in Appendix B.2.

#### 2.4.4. Mounting Systems

Seven load transfer points were established:

- 4 x Track Unit Axle Bearings
- 2 x Flipper Motors
- 1 x Arm-Chassis Mount

Bespoke mounting plates were designed and manufactured for these (Figure 16).

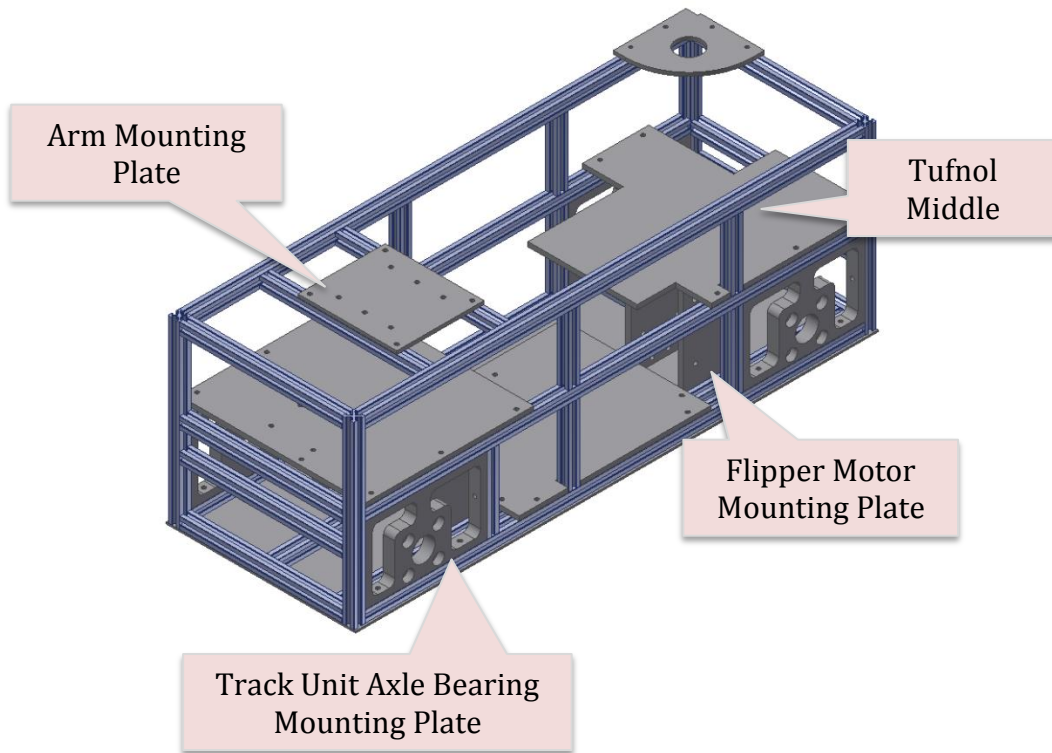


Figure 16: Chassis Mounting Points

In order to utilise off-the-shelf parts, standardise the fixings and minimise cost, MakerBeam brackets (Figure 17) were used and modified where required (82% standard vs. 18% modified).



Figure 17: MakerBeam Brackets

Some of the components were mounted directly onto MakerBeam using the brackets, and the remaining components were mounted onto Carp Brand Tufnol<sup>2</sup>.

The housing for the battery was 3D printed from ABS (Figure 18). The arm control electronics are stored in a 3D printed box (Figure 19 and Figure 20). This allows the removal of the control electronics along with the arm system if they are not required. This aligns with the modularity objectives.

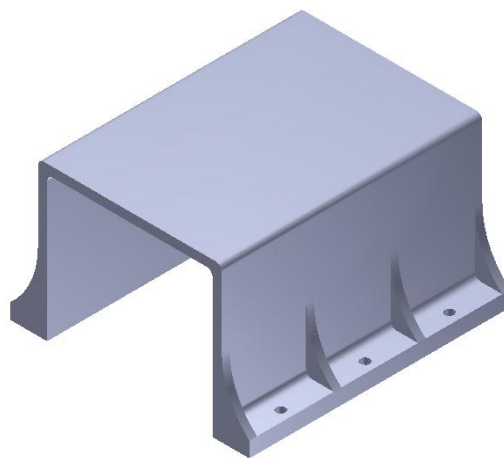


Figure 18: 3D Printed Battery Housing - CAD Image

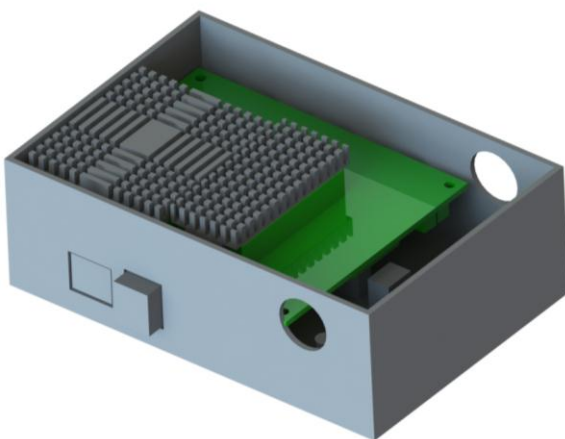


Figure 19: Modular Arm Control Box

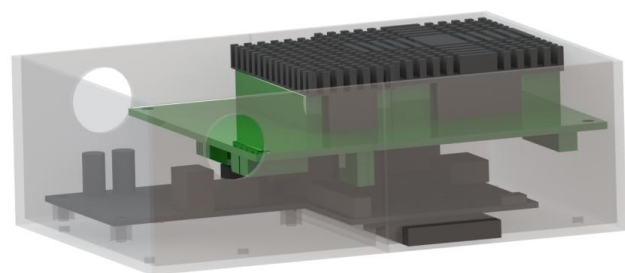


Figure 20: Modular Arm Control box with Power Board (Green, top) & Control Computer (Grey, bottom)

---

<sup>2</sup> Carp Brand Tufnol is made from a premium quality fine weave cotton fabric with high strength, wear and impact resistance, machining qualities, dimensional stability and electrical properties (Tufnol Composites Limited, 2008)

### 2.4.5. Manufacturing and Assembly

Table 7 details the manufacturing method of each part and justification.

**Table 7: Construction Methods and Justifications**

Component	Qty.	Construction Method	Comments
<b>MakerBeam</b>	53.5	Band saw and milling	Required perpendicular ends
<b>Tufnol Plates</b>	1	CNC milled and pillar drilled	Required precision
<b>Arm Chassis Mount</b>	1	Band saw and drilled	Save resources by using methods not requiring a technician
<b>Axle Mounting Plates</b>	4	Water jet cut, milled and drilled	Complex part, outsourced to save in-house resources
<b>Encoder Mounting Plate</b>	2	Milled, drilled and tapped	Off-the-shelf material procured, simple process
<b>Bottom Plate</b>	1	Band saw and folded	Simplest manufacture method
<b>Motor Mounting Plate</b>	4	Milled and drilled	Quickest method for desired shape
<b>Shell Plates</b>	5	Water jet cut	Outsourced to save in-house resources
<b>Battery Housing</b>	1	3D printed	Low cost and no structural integrity required
<b>Arm Control Box</b>	1	3D printed	Low cost and no structural integrity required
<b>Emergency Stop Plate</b>	1	Water jet cut	Outsourced to save in-house resources

### 2.5. Final Design

CAD images (Figure 21 to Figure 24) show various stages of completion of the final design.

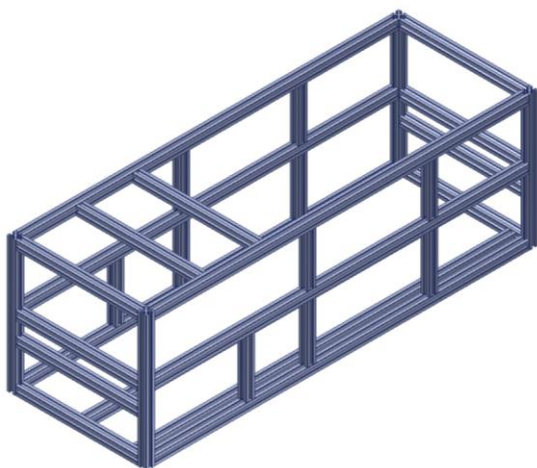


Figure 21: Final MakerBeam Chassis Design - CAD Image

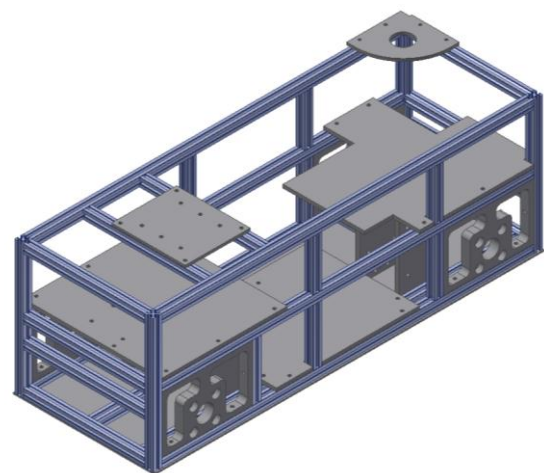


Figure 22: Chassis with Mounting Plates - CAD Image

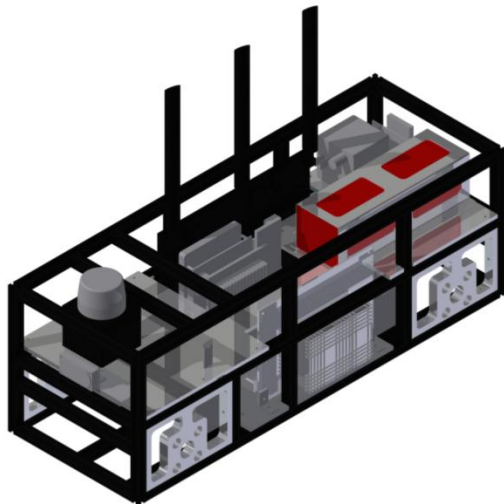


Figure 23: Final Chassis Design with Internal Components - Rendered CAD Image

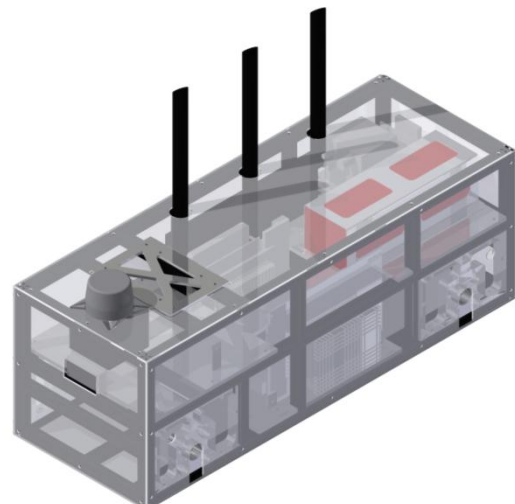


Figure 24: Final Chassis Design with Internal Components and Shell - Rendered CAD Image

## 2.6. Virtual Testing

Stress analysis was performed on two critical components with significant forces acting on them, the arm mounting plate and motor mounting plate.

### 2.6.1. Arm Mounting Plate FEA

Due to the concurrent nature of the design process, the assumptions stated in Table 8 were used. FEA was conducted using parameters specified in Table 9.

Table 8: Assumption used in Chassis Stress Analysis

Parameter	Value	Justification
Mass (kg)	3.0	Maximum arm system mass as identified in the specification (Section 2.2)
Payload (kg)	0.5	Mass of water bottle
Gravity ( $\text{ms}^{-2}$ )	10	Simplified for ease of calculations

Table 9: Key Factors for the Stress Analysis of the Arm Mounting Plate

Component	Arm mounting plate
Material	Aluminium 6082-T6
Yield Strength (MPa)	250
Load	Moment generated 24Nm (explained in Appendix B.4)
Constraint	Constrained at bolt interface



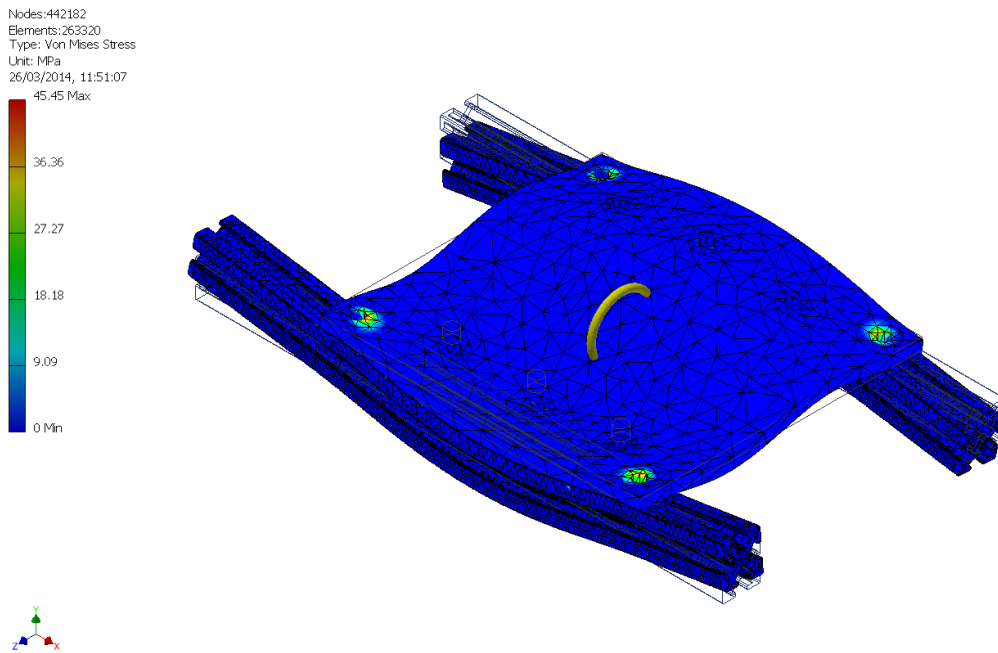


Figure 25: Von Mises Stress for Arm Mounting Plate with 24Nm moment

Figure 25 shows that the front beam negatively deflects, whereas the rear positively deflects due to the moment being created. This will not have a noticeable effect on the system.

Results are shown by Table 10.

Table 10: Results of Stress Analysis of the Arm Mounting Plate

Parameter	Value
Maximum Von Mises Stress (MPa)	45.45
Percentage of Yield Stress (%)	18.18
Maximum displacement (mm)	0.05

### 2.6.2. Motor Mounting Plate FEA

Table 11 shows the key analysis factors for the motor mounting plate.

Table 11: Key Factors for the Stress Analysis of the Motor Mounting Plate

<b>Component</b>	Motor Mounting Plate
<b>Material</b>	Aluminium 6061 (closest to required material on software)
<b>Yield Strength (MPa)</b>	250
<b>Load</b>	Force of 622N (see Appendix B.3) generated by the motor acting at the centre of the motor mounting holes on the side of the plate. The forced used is half that of the calculated force since the total force will be shared across the two plates.
<b>Constraints</b>	Constrained at the base where the plate is bolted to the MakerBeam

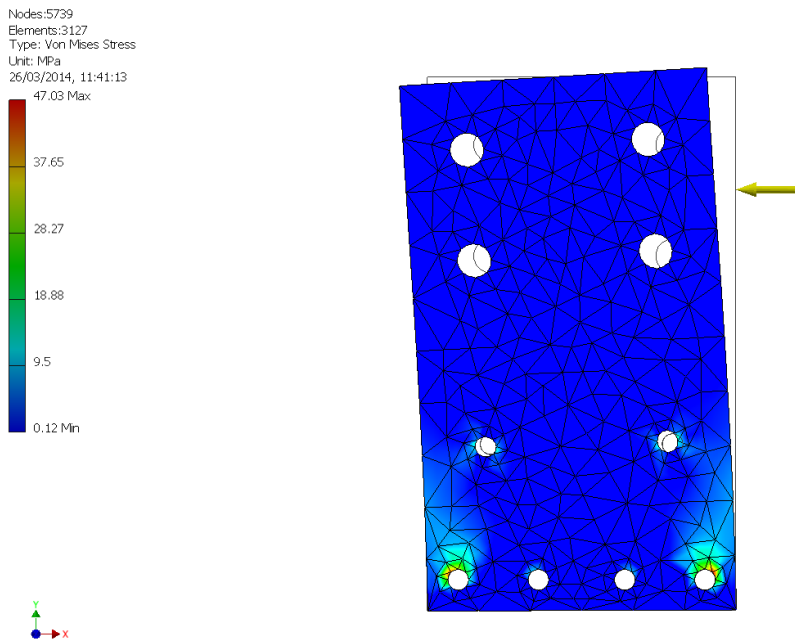


Figure 26: Von Mises Stress of Motor Mounting Plate with 622N force

Figure 26 shows that the maximum stress is concentrated around the outside two bolt holes.

Table 12: Results of Stress Analysis of the Motor Mounting Plate

Parameter	Value
Maximum Von Mises Stress (MPa)	47.03
Percentage of Yield Stress (%)	18.88
Maximum displacement (mm)	0.03

### 2.7. Physical Chassis Testing

A simplified chassis was constructed for testing purposes. A mass equivalent to the anticipated length and mass of the arm (1.2m & 3kg) was attached to the chassis to model the arm at its full extension. A 0.5kg mass was added to the end to simulate the effect of the payload (Figure 27).

Visual analysis was used to see the effect on the chassis.

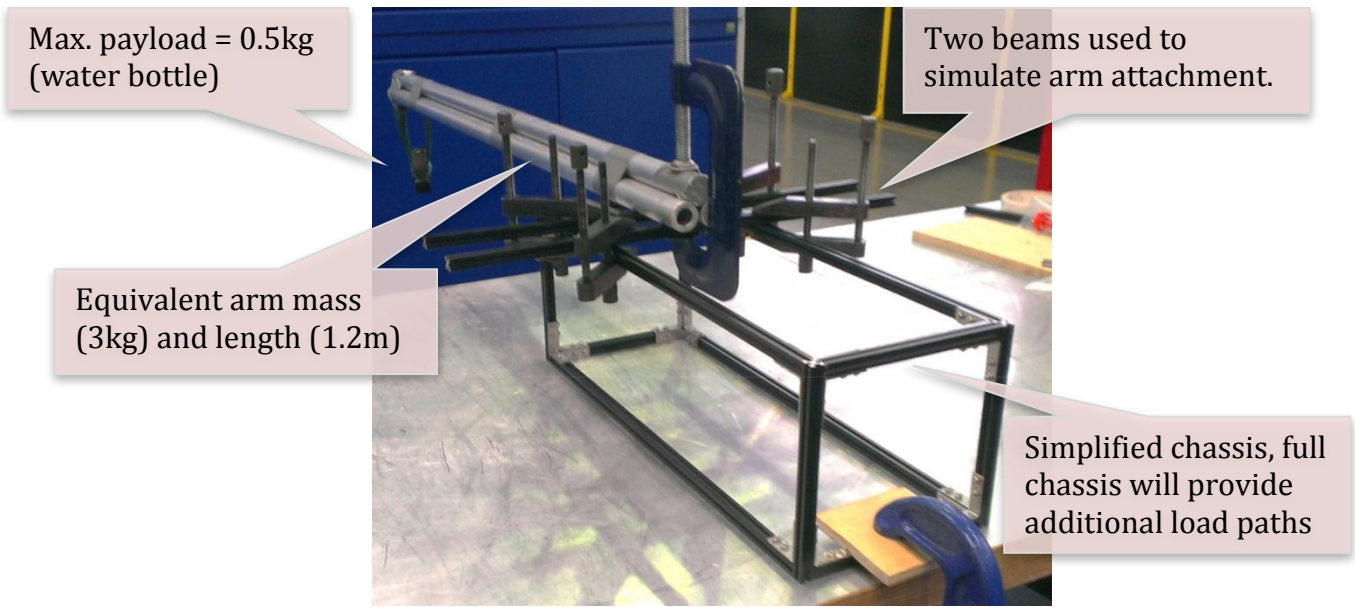


Figure 27: Chassis Testing Rig

This physical testing confirms the conclusions drawn from the FEA that the arm would produce negligible deflection on the chassis.

### 2.8. Critical Review

The design, manufacture and assembly of the chassis was completed within the timeframe (Figure 28) and taken to simulate at the RoboCup competition (Figure 29).



Figure 28: Final Chassis Assembly



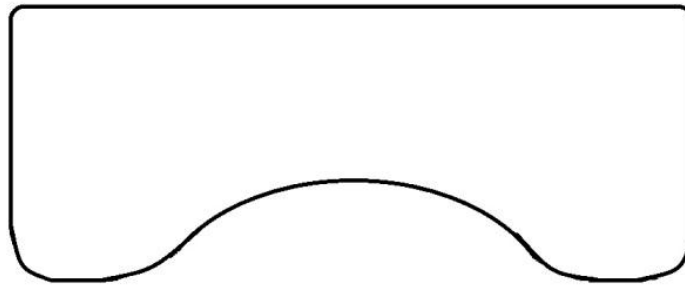
Figure 29: Final Chassis Assembly with Flipper Units in the RoboCup Rescue Arena

Table 13 shows the majority of the requirements outlined in the specification were met fully.

Table 13: Chassis Results against Specification

ID	Constraint	Met?	Explanation
1	Modular Architecture	Met	The MakerBeam is an excellent material for prototyping and modification.
2	Repair and Maintenance	Not Met	Feedback from the RoboCup Competition revealed it would not be easy to repair on the field.
3	Durability	Partially Met	Time has not allowed the full system to be tested. Debris entry into chassis will be minimal but not zero.
4	Lightweight	Met	The total mass was 24.58kg. The mass is evenly distributed in the chassis and the heaviest components are located closest to ground level.
5	Size	Met	Fits within the turning circle and triangle constraints.
6	Systems Integration	Met	Systems were fully integrated.
7	Load Resistance	Partially Met	Since the robot was not fully manufactured, this has not been tested fully. Virtual stress analysis was performed on critical components successfully.
8	Ease of Manufacture and Assembly	Met	The chassis was fully manufactured and assembled within the time.
9	Material Availability	Met	All materials selected were readily available. Many were donated by sponsors and the rest were sourced inexpensively from university suppliers.

Direct feedback from National Institute of Standards and Technology (NIST)<sup>3</sup> at the RoboCup competition suggested that the chassis may get beached on some terrain and recommended that the optimum chassis shape should resemble Figure 30. However, this makes the chassis more difficult to manufacture, assemble and modify.



**Figure 30: Optimum Chassis Shape to Avoid Beaching**

A robotics test expert from NIST (Jacoff, 2014) commented that if damage occurred in a real life situation it would take too long to repair, however the MakerBeam would allow different prototype and research models to be created quickly. Despite the MakerBeam being selected for its ease of assembly, in practice it was much more time consuming than anticipated. Furthermore the polycarbonate shell may not withstand all of the required forces in a real life situation. Future work recommendations can be found in Chapter 6.3.

---

<sup>3</sup> NIST is the organisation which defines the standard test methods for robots (and other technology) and is applied to the RoboCup Rescue competition

### Chapter 3. Drivetrain

A drivetrain is essential for a USAR robot to traverse the complex terrain common in disaster environments such as stairs, ramps and rubble.

#### 3.1. Drivetrain Development Strategy

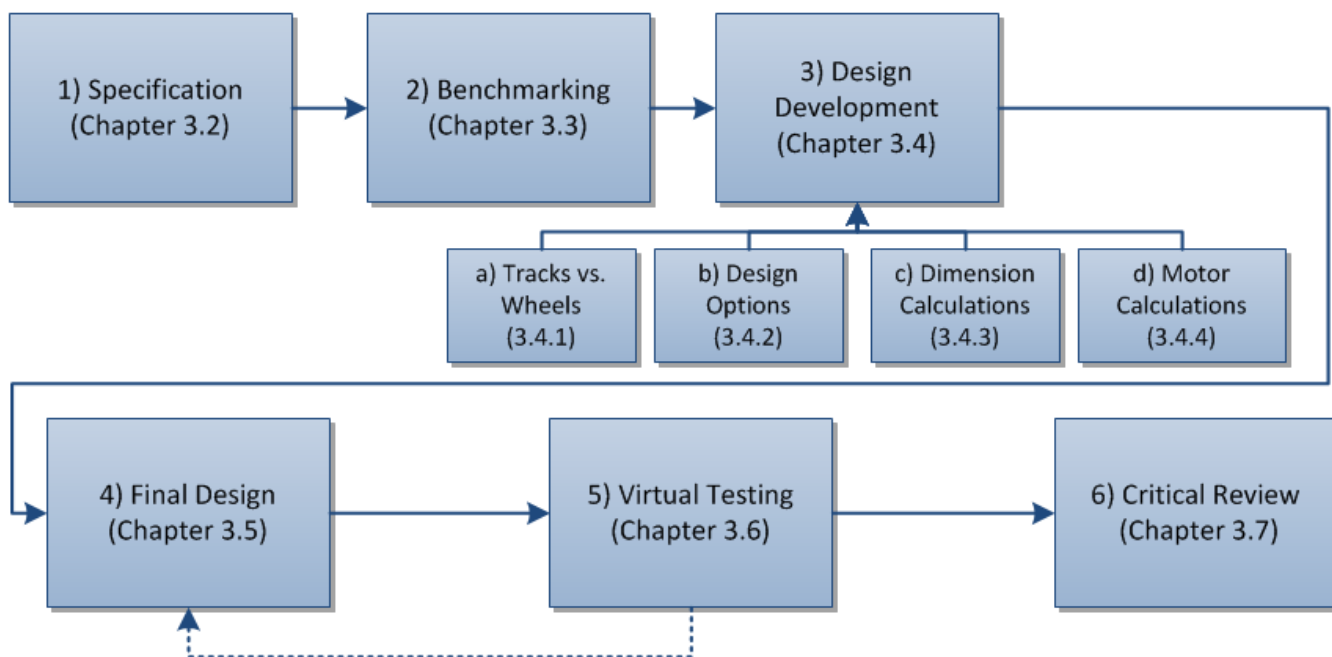


Figure 31: Drivetrain Development Strategy

#### 3.2. Specification

The new USAR robot drivetrain specification summarised in Table 14 was developed from the aims and objectives, original high-level specification (Chapter 1.6) and RoboCup Rescue rules.

Table 14: Drivetrain Specification

ID	Constraint	Description
1	Cost	Components should be sourced/ designed such to save cost
2	Mass	The robot is to be deployable by one person, limiting the mass to 25kg
3	Modular	The drivetrain must employ a modular approach allowing different designs to be interchanged
4	Size	The drivetrain must be large enough to drive the robot but small enough to fit through confined spaces
5	Repair/Maintenance	Simple to manufacture parts for easy maintenance
6	Complexity	Parts need to be simple and few
7	Durability	Be impact resistant to the expected forces from its environment

<b>8</b>	<b>Reliability</b>	Disaster environments require high levels of reliability in uncertain terrain
<b>9</b>	<b>Torque</b>	High levels of torque will be required to climb 45° slopes, and to lift the robot
<b>10</b>	<b>Traction</b>	Traction with the ground is essential for slope climbing
<b>11</b>	<b>Gap/obstacle crossing</b>	Needs to climb over 200mm high steps, and cross a 200mm wide gap
<b>12</b>	<b>Clearance</b>	As high as possible
<b>13</b>	<b>Mobility</b>	Complex terrain requires a high levels of mobility
<b>14</b>	<b>Power Source</b>	Compatible with and completely powered by an 24V battery
<b>15</b>	<b>Control</b>	Controlled remotely, requiring ease of use and information fed back to the driver
<b>16</b>	<b>Wiring</b>	Easily and simply wired to the control system
<b>17</b>	<b>Environment</b>	To be suitable for dry indoor environments

### 3.3. Benchmarking

WMR’s existing robot (Figure 32) came 10<sup>th</sup> in the world in 2013, and won ‘Best in Class Mobility’. This therefore provides a good platform to base the new drivetrain on.

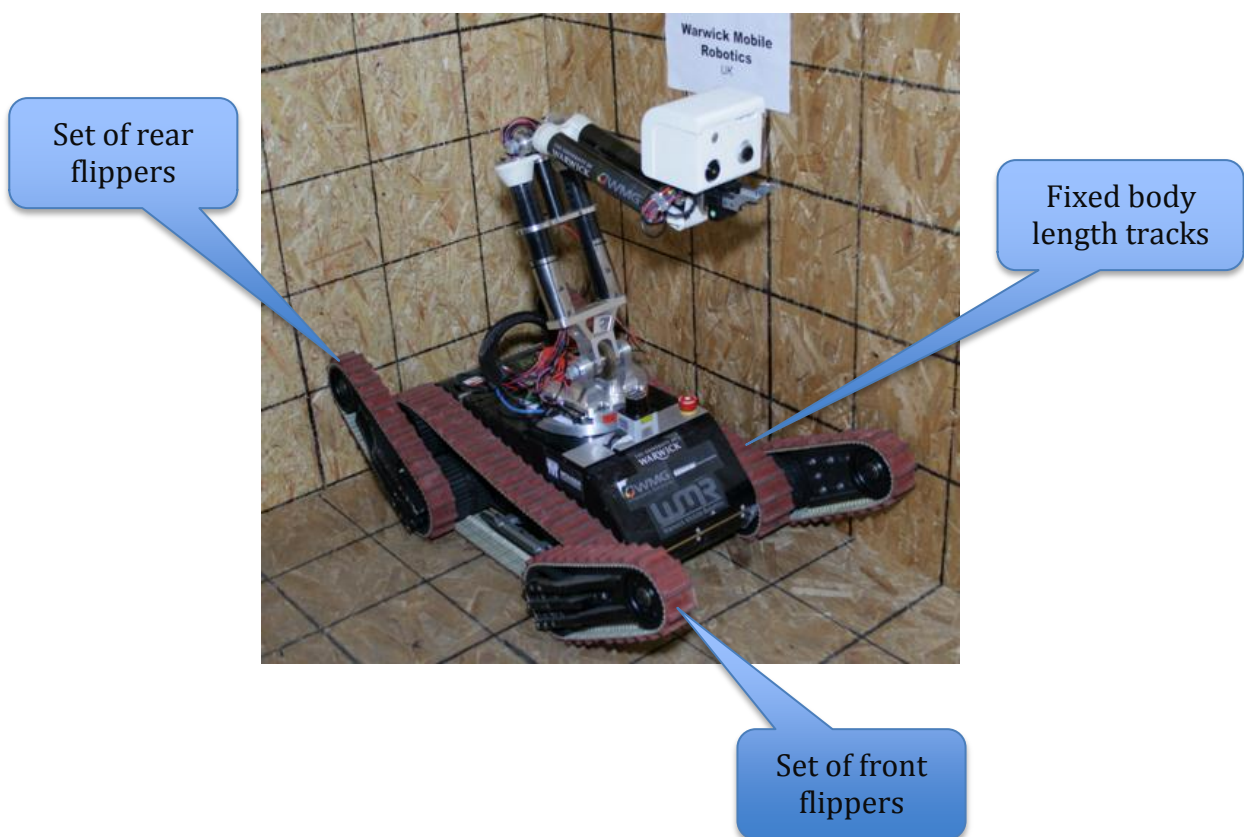


Figure 32: Existing USAR Robot Drivetrain Features

### 3.4. Design, Calculations and Decisions

#### 3.4.1. Tracks vs. Wheels

Due to cost and complexity the form of transport was limited to tracks or wheels. Table 15 compares tracks and wheels against the specification (Chapter 3.2). A 1 indicates that the option is preferable and the output is scaled depending on importance.

**Table 15: Tracks and Wheel Comparison against Specification**

ID	Constraint	Tracks	Wheels	Scale	Reason for choice
1	Cost	0	1	5	Wheels are more common and involve less parts leading to being cheaper
2	Mass	0	1	5	Tracks have more components than wheels, leading to a greater mass
3	Modular	1	0	5	Tracks can have parts mounted inside them, leading to the possibility of a self-contained unit
4	Size	1	0	4	Tracks are more flexible in shape/size of design
5	Adaptability	1	0	4	Tracks only need the tread to be changed for different levels of grip or clearance. Wheels need to be completely replaced to change these aspects
6	Repair/ Maintenance	1	0	3	If the tread breaks, the whole wheel needs replacing but the track just needs one tread element replacing
7	Complexity	0	1	3	Wheels have less components so are less complex
8	Durability	0	1	2	Generally made from thick rubber, so more durable than lots of little treads
9	Reliability	0	1	3	Tracks have more components so more can break than in a wheel
10	Torque	1	0	3	Although both have the same torque tracks can apply it more effectively
11	Traction	1	0	3	Wheels only contact the ground in a small area whereas tracks are much larger attaining better traction
12	Gap/ Obstacle crossing	1	0	5	Tracks length allows them to traverse gaps and obstacles which wheels would otherwise get stuck in/on
13	Clearance	0	1	3	Without special consideration, tracks give less clearance than wheels
14	Mobility	1	0	3	Greater gap and obstacle crossing capabilities give tracks better mobility
15	Power Source	-	-	-	As the power source will be the same for both, this will not be compared
16	Control	-	-	-	Control methods will be the same for



				both	
17	Wiring	-	-	-	Wiring to motors will not depend on wheels/tracks
18	Environment	1	0	3	Tracks have lower ground pressure and can therefore handle a wider range of environments e.g. Sand/Gravel
	<b>Total</b>	<b>33</b>	<b>21</b>		

The comparison determined that tracks were the most suitable form of motion for the new USAR robot.

### 3.4.2. Design Options

Of the concepts considered three were reviewed in detail (Figure 33, Figure 34 and Figure 35).

Cost and complexity increased with improved mobility (Figure 36).

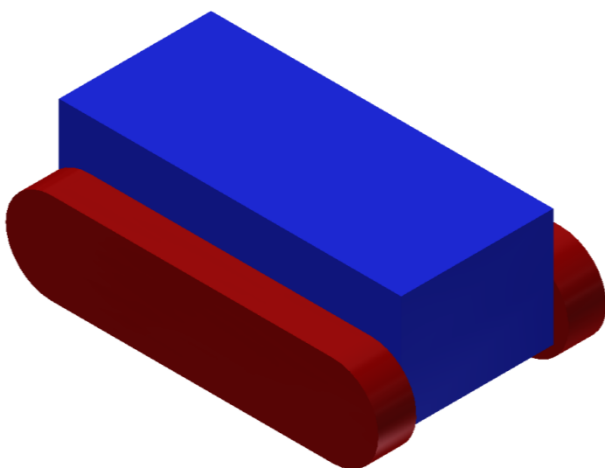


Figure 33: Option 1- Simplest Drivetrain Design

<b>Mobility</b>	Low
<b>Complexity</b>	Low
<b>Cost</b>	Low
<b>Description</b>	Single unit per side No flippers

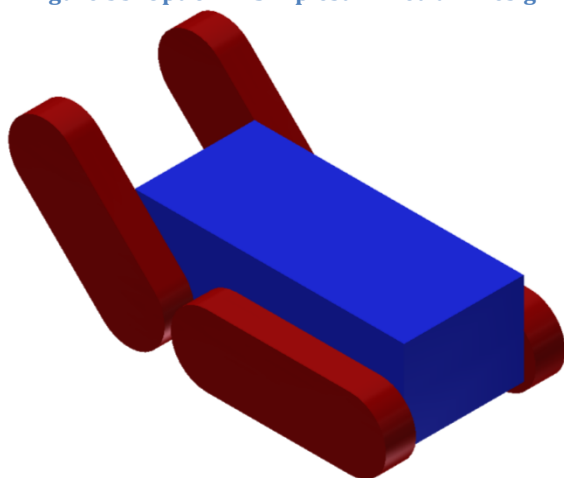
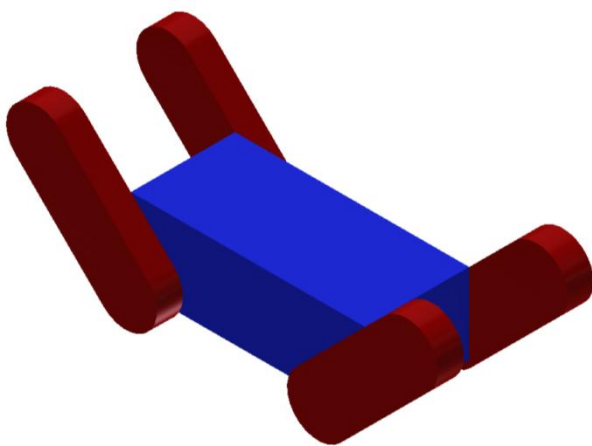


Figure 34: Option 2 - Middle Drivetrain Design

<b>Mobility</b>	Medium
<b>Complexity</b>	Medium
<b>Cost</b>	Medium
<b>Description</b>	Two units per side One set of flippers



<b>Mobility</b>	High
<b>Complexity</b>	High
<b>Cost</b>	High
<b>Description</b>	Two units per side Two sets of flippers

Figure 35: Option 3 - Top Drivetrain Design

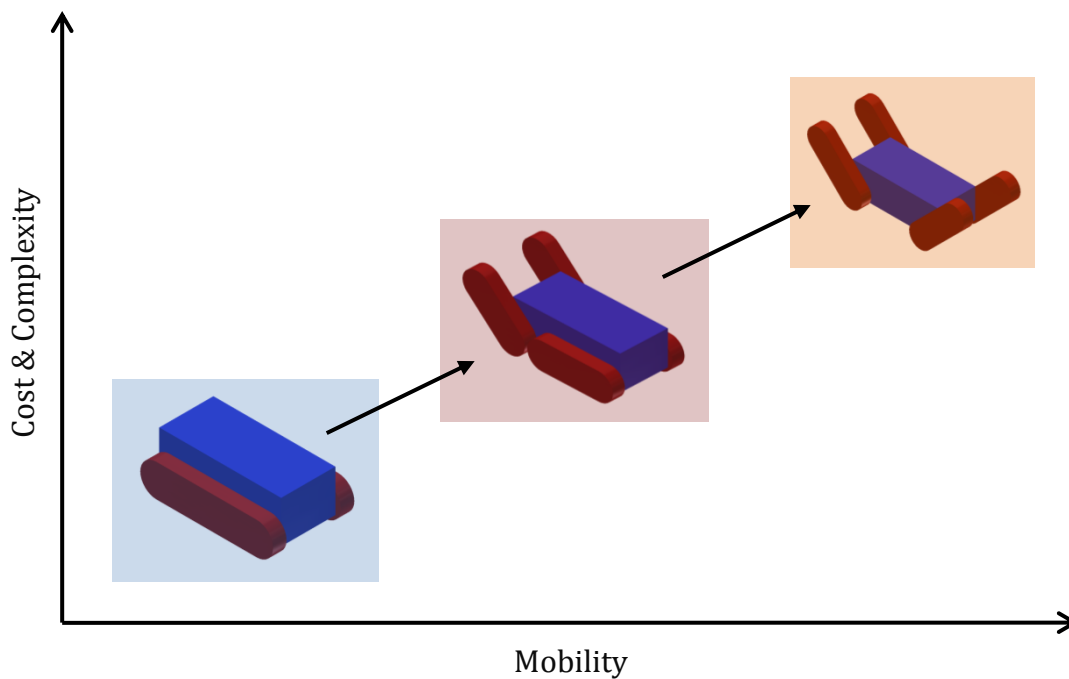


Figure 36: Drivetrain Cost & Complexity vs. Mobility Graph

While option 1 and 2 would be the lowest cost and easiest to implement, the most mobile design, option 3, was chosen as this best meets the specification. This also has the greatest ability to overcome the RoboCup obstacles. Due to the modularity requirement, the design should still allow the track units to be removed and replaced with a single unit as in Option 1 to allow it to be adapted to suit its environment.

### 3.4.3. Dimensions

The robot specification is such that it should fit through a 600mm triangle, and have a turning circle of less than 600mm (Chapter 1.6 and Chapter 2.4.1). This has a direct effect on the size of the track units. Figure 37 illustrates the restricting dimensions of the track units, and their placement on the robot.

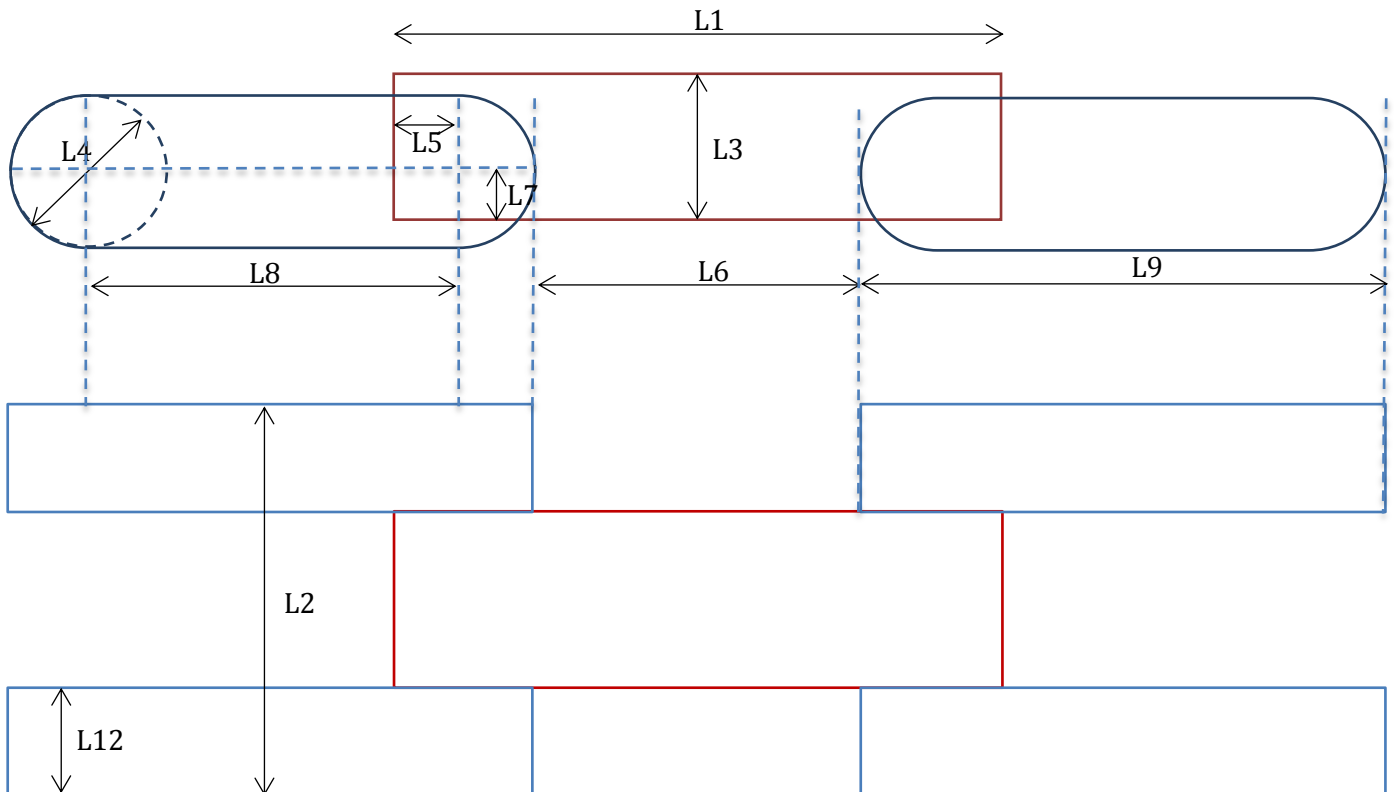


Figure 37: Top view (top) and Side View (bottom) of Restricting Dimensions in the Drivetrain Design

Table 16: Drivetrain Dimension

Dimension	Reference	Value (mm)
Length	L1	450
Width	L2	300
Height	L3	155
Effective diameter	L4	120
Axle from side	L5	60
Gap between tracks	L6	210
Axle from base	L7	30
Track axle separation	L8	205
Track length	L9	325
Track Width	L10	80

The values in Table 16 were calculated in Appendix C.1.

### 3.4.4. Motor Requirements

Using Equation 5 and 6, Table 17 shows what the required torque and rpm for the tracks drive motors are, for given inputs.

Table 17: Track Motor Requirements

	Value	Units
<b>Input Requirements</b>		
Mass	25	[kg]
Number of drive motors	4	
Radius of drive wheel	0.06	[m]
Robot velocity	1	[m/s]
Maximum incline	45	[deg]
Desired acceleration	1	[m/s <sup>2</sup> ]
Total efficiency	65	[%]
<b>Output requirements</b>		
Torque	4.579	[Nm]
Angular velocity	159.24	[rpm]

$$\tau = \left(\frac{100}{e}\right) \frac{(a + g\sin\theta)mr}{n}$$

Equation 5.

Where:

- $\tau$  is torque (N/m)
- $e$  is efficiency of motor/gears/wheels (%)
- $a$  is acceleration (m/s<sup>2</sup>)
- $g$  is acceleration due to gravity (m/s<sup>2</sup>)
- $\theta$  is angle of incline (°)
- $m$  is mass (kg)
- $r$  is radius of effective wheel (m)
- $n$  is number of motors

$$\omega = 60 \frac{v}{2\pi r}$$

Equation 6.

Where:

- $\omega$  is the angular velocity (rpm)
- $v$  is the velocity (m/s)
- $r$  is the radius of effective wheel (m)

See Appendix C.2 for how Equations 5 and 6 were derived.

The requirements for the flipper motors are different, as they need to be able to lift the robot off the floor. Three possible situations are analysed in Appendix C.3, and the motor requirements are recorded in Table 18. The rpm is simply an estimate based upon it taking 10 seconds for a flipper to do a full revolution.

**Table 18: Flipper Motor Requirements**

Variable	Value	Units
Min Torque	40.466	[Nm]
Angular velocity	6	[rpm]

### 3.5. Final Design

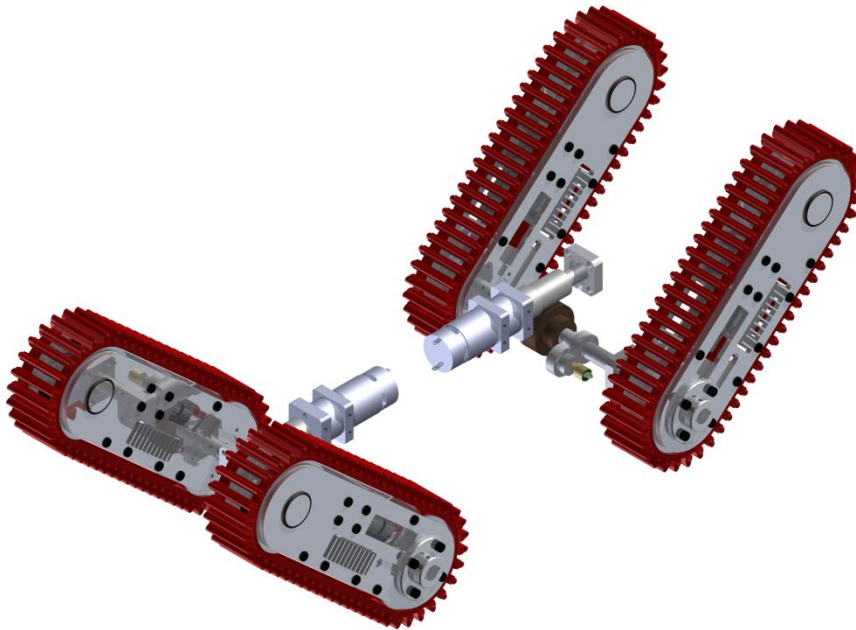
The track units and flipper system were designed and improved in a series of iterations, until the final design shown in Figure 38 was reached. Specifications for the motors and worm gears used can be found in Table 19, including the required values calculated in Chapter 3.4.4. It is clear by comparing what the motors can supply with what is required, that the motors will be able to supply the required torque and rpm. The motors chosen have a very high safety factor, however they are cheap and compact, so finding less powerful motors was deemed unnecessary. The large safety margin also allows for a wide range of possible modifications in future.

**Table 19: Final Drivetrain Motor Specifications**

Section	Name of motor	Torque of motor (Nm)	RPM of motor	Added Gear ratio (X:1)	Torque after gears (Nm)	RPM after gears
<b>Tracks</b>	GR02 gearmotor 18V 24:1	12.1	810	3	36.3	270
	Required:				4.579	159.24
<b>Flippers</b>	GR02 gearmotor 18V 24:1	12.1	810	6	72.6	135
	Required:				40.466	6

See Appendix C.4 for a full design narrative, but in summary; the smallest and simplest solutions were chosen for each design step, using easily sourced and replaceable parts where ever possible. The only complex parts are the side plates. They have had to be designed to fit all

required parts, including wiring, and need a milling machine to make. They are however not expensive, so having a few spares is a very affordable possibility. All other drivetrain parts can be made on a lathe & pillar drill with a little spare material, or bought off the shelf. Each track unit is identical, and can be attached to any corner in any orientation. Figure 38 shows the finished design in CAD.



**Figure 38: Drivetrain Final Design**

### 3.5.1. Manufacture

All of the parts were machined at the University of Warwick, with the exception of some water jet cutting. All technical drawings are included in Appendix C.5. The components were then assembled into the track units (Figure 39).



**Figure 39: Manufactured & Assembled Track Unit (With Tensioning Block)**

Track tensioning blocks were not added to the CAD model due to time constraints; however they were designed and brought the total clearance of the robot to over 45mm. They also direct any impact force away from the sprockets and into the track unit frame.

### 3.6. Testing

#### 3.6.1. Virtual Testing

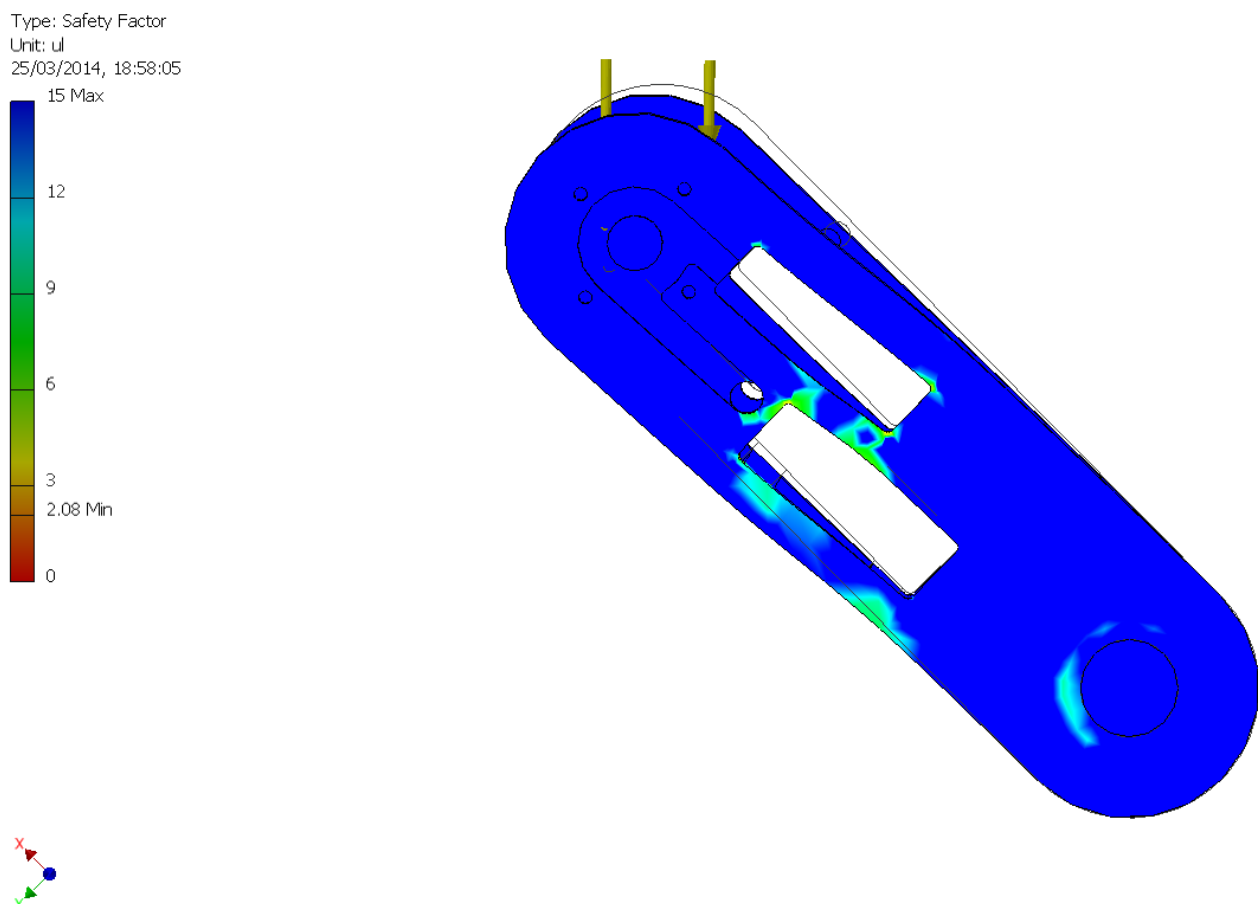
Virtual impact shock testing was conducted to ensure that the robot could withstand large falls within its environment, Table 20 details these calculations.

**Table 20: Impact Shock Calculations**

	<b>Value</b>	<b>Units</b>	<b>Symbol</b>	<b>Formula</b>
<b>Mass</b>	25	kg	m	
<b>Height of fall</b>	0.5	m	s	
<b>Gravity</b>	9.81	ms <sup>-2</sup>	a	
<b>Time to fall</b>	0.319275	s	t	$s = u + 0.5at^2$
<b>Falling velocity</b>	3.132092	ms <sup>-1</sup>	v	$v = at$
<b>Momentum</b>	78.3023	kgms <sup>-1</sup>	M	$M = mv^2$
<b>Time to stop</b>	0.1	s	t*	
<b>Force</b>	783.023	N	F	$F = ma = \frac{M}{t^*}$
<b>Weight</b>	245.25	N		

Two variables affect the force on the robot, the fall height and the stopping time. The higher the fall or shorter the stopping time the larger the force. The robot should not encounter a situation with a drop greater than 0.5m at the competition (Pellenz, 2014). The stopping is an estimate based upon experiments carried out last year with the existing robot (Appendix A.1.1 in Busckstone, et al. (2013)). Using the values calculated in Table 20 the force on the robot is over 780N. As this value was based on estimates, 1000N was used for FEA for the worst case loading scenarios where the entire force is through a single component.

Figure 40 shows the flipper unit under the loading scenario.



**Figure 40: FEA Modelling of the Flipper Unit**

The lowest safety factor of 2.08 (Figure 40) means a force of 2080N could be withstood before the material yields and plastic deformation occurs.



It is standard practice in industry to aim for a safety factor of between 1.5 and 2.5 (Engineering ToolBox, 2014). The rest of the drivetrain's load bearing components were analysed in a similar way and can be found in Appendix C.6.

### 3.6.2. Physical Testing

The treads were originally designed to use easily available off-the-shelf chain, and Araldite to attach the tread sections. Loading testing was performed to determine the strength of the Araldite bond between steel and aluminium (Figure 41, Figure 42 and Figure 43). The results showed the bond's linear strength could withstand  $>88\text{N}$  per link; however at low torsional force the bond broke very easily. Therefore it was decided attachment chain was required, with the fall back of a longer lead time.

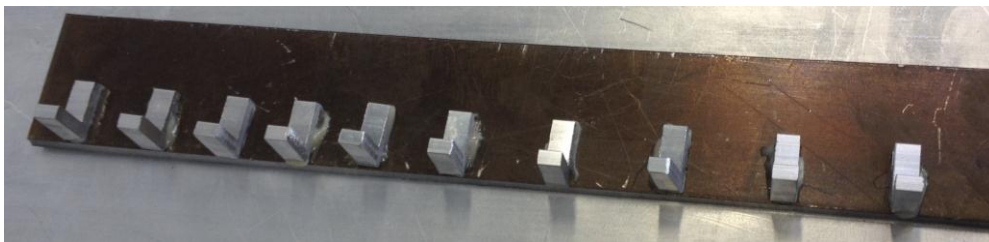


Figure 41: Aluminium L Sections Bonded to Steel with Araldite

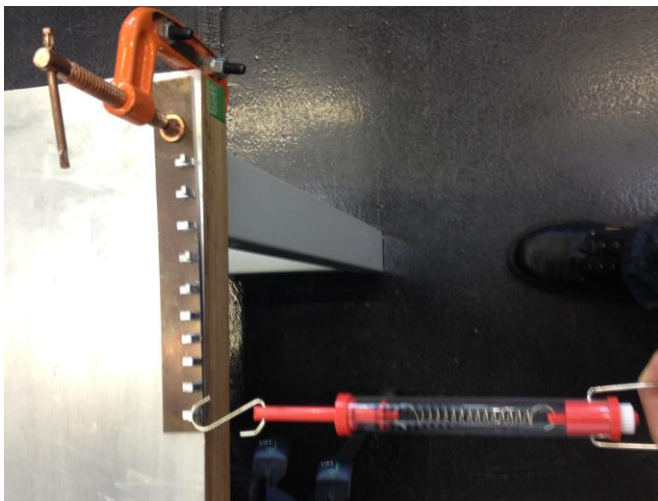


Figure 42: 20N Applied to Bonded Aluminium L Section and Withstood



Figure 43: 88.29N Applied to Bonded Aluminium L Section and Withstood

### 3.7. Critical Review

All parts were manufactured to a level where the drivetrain could be assembled, to see if it would go together as planned, however it is not at a stage where it could be operational. Due to manufacturing delays the tracks were not constructed with time to test physically before the deadline. Future work recommendations can be found in Chapter 6.3.

Table 21 details how well the final design met the specification.

**Table 21: Comparison against Specification**

ID	Constraint	Met?	Explanation
1	Cost	Met	The robot was built within the team's budget.
2	Weight	Not Met	At 17.01kg, it is very heavy. Although the whole robot is under the 25kg limit set there remain significant areas for mass reduction.
3	Modular	Met	The track units house their own motors and control boards
4	Size	Met	The robot's overall dimensions fit within the limits originally set
5	Adaptability	Met	Each track unit can be easily removed and another, different design, put on instead
6	Repair/ Maintenance	Met	The simple and easily accessible design allows for repair & maintenance
7	Complexity	Met	Each track unit is identical reducing complexity
8	Durability	Not Met	The robot has been designed to be durable, however this has not been tested
9	Reliability	Not Met	The robot has been designed to be reliable, however this has not been tested
10	Torque	Met	The motor and gear combinations have the required torque, with a large safety factor
11	Traction	Not Met	The robot has been designed to have the required traction, however this has not been tested
12	Gap/obstacle crossing	Not Met	The design should be able to handle the competition gap's/obstacles, however this has not been tested
13	Clearance	Met	The clearance on the robot is greater than originally specified
14	Mobility	Not Met	The robot has been designed to be mobile, however this has not been tested
15	Power Source	Not Met	The motors are suited to the power source, however this has not been tested
16	Control	Not Met	The robot has been designed to be easily controllable, however this has not been tested
17	Wiring	Not Met	The wiring between the chassis and flippers is undesirable and alternatives should be investigated to allow continuous 360° rotation
18	Environment	Not Met	The design should handle the required environments, however this has not been tested

## Chapter 4. Arm System

The arm system consists of a tele-operated arm, head and gripper. The arm is used to position and orientate the head and gripper. The final design is displayed in Figure 44.

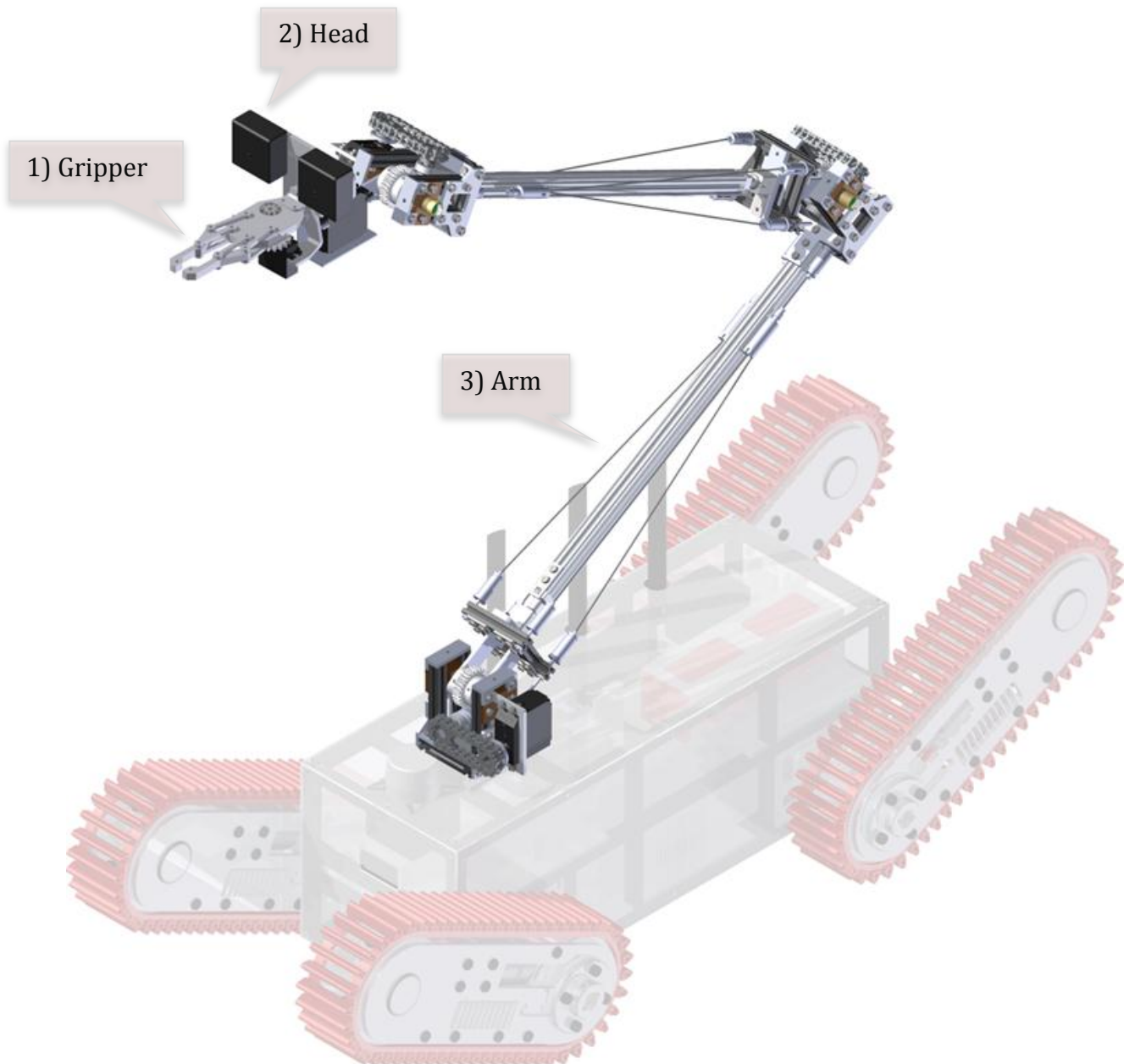


Figure 44: Arm System Overview

### 4.1. Development Strategy

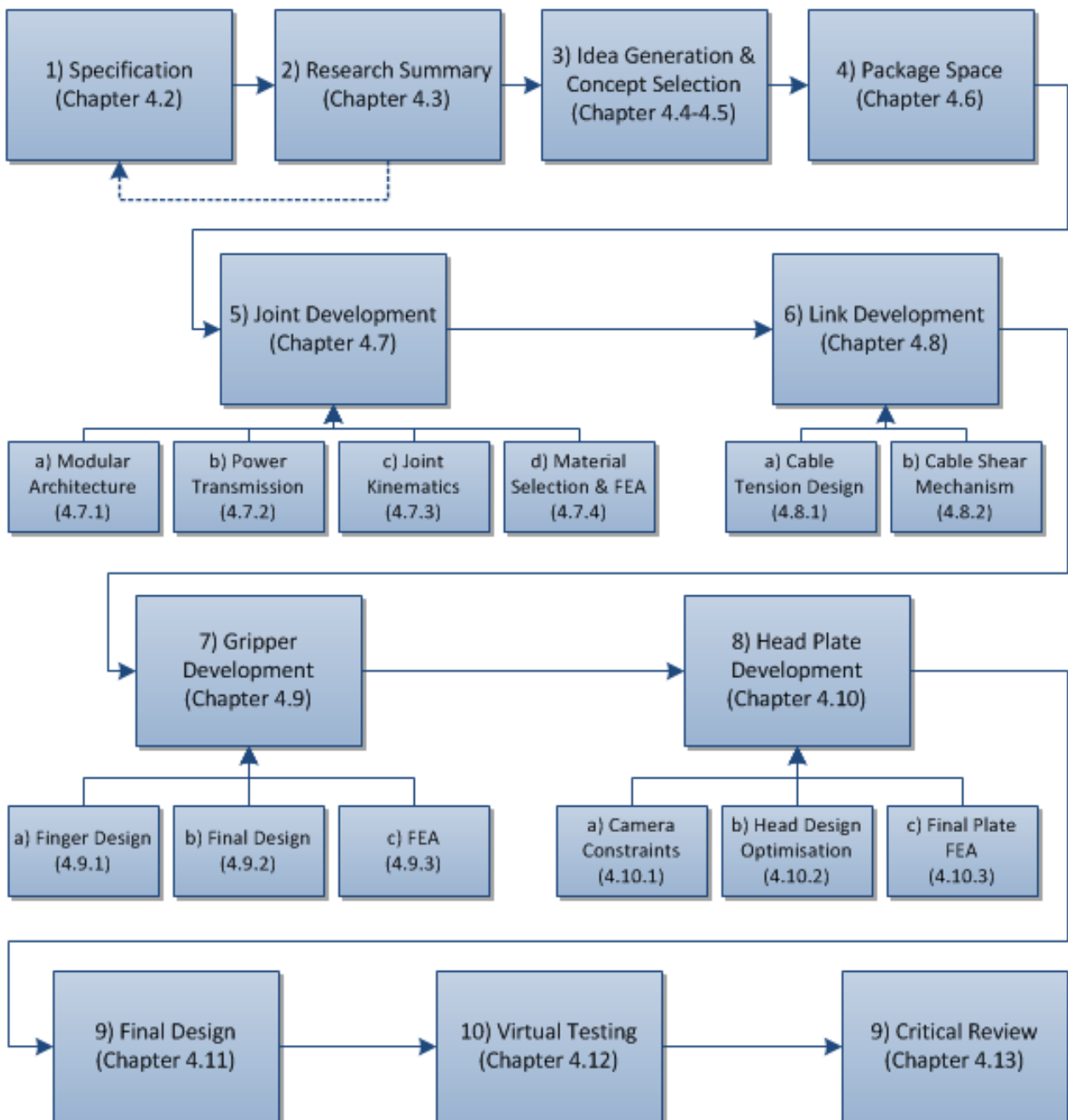


Figure 45: Arm System Development Strategy

## 4.2. Specification

Table 22 details the arm system specification developed from the aims and objectives, original high-level specification (Chapter 1.6), RoboCup Rescue rules and SWOT analysis of the 2012 WMR arm design (Appendix D.1).

Table 22: Arm Specification

ID	Constraint	Description
1	Cost	Arm system to be developed within a material cost budget of £500 Arm is a prototype to be further developed to be commercially viable.
2	Mass	Mass minimised to reduce base joint torque. Head and gripper sub system to be below 0.65kg (2012 design mass).
3	Modular	Develop a core modular architecture allowing the system to be easily modified/ upgraded.
4	Size	Must meet robot max dimensions of 300x450mm. Robot (with arm) must fit through 600mm equilateral triangles in the competition course (cut by first responders) to access shortcuts.
5	Reach	Access victims at a maximum height of 1.6m above ground level
6	Confined spaces	Deployable in confined spaces (500mm roof & 100mm stalactites). Access 150mm diameter holes in multiple orientations. Cannot have sharp edges which could catch on obstacles.
7	Manipulation	Must grip and pull down door handle, then push or pull open door. Have enough DOF required to move/manipulate an object within a 3D workspace, moving around obstacles if required. Objects include 0.5kg water bottles, a hand radio, and shoring blocks (maximum size = 100x100x600mm). Gripper motor should be protected from 'over gripping'.
8	Payload	Deliver payloads to victims with a maximum mass of 1kg.
9	Sensors	Ability to align positions of 3D cameras for the Oculus Rift headset. Gripper must be within focal range of cameras. Flexible attachment of additional sensors.
10	Arm Velocity	Achieving any position and orientation within 8-10 seconds. Arm system should be slow moving in an unstable environment.
11	Power supply	Batteries must power the actuators. Arm system must not collapse when electrical supply is interrupted. Actuators should not consume power when joints are not being used to improve robot operating time.
12	Control	Remotely controlled through inverse kinematics. Must be operated by single person from a laptop or handheld controller. Power/signalling sent along the arm.
13	Repair and Maintenance	Design for ease of repair and maintenance with standard tools.
14	Durability	Robustness required by real-world applications. Avoid failure modes such as overloading and overheating.
15	Head Vibration	Free end movement should not exceed 1cm.
16	Rigidity	High rigidity allows for greater positional accuracy under loading.

### 4.3. Research Summary

A number of competitors arm systems at the 2013 RoboCup Worlds were benchmarked including: R.Rangel & et-al (2013), T.Sittiwanchai & et-al (2013), W.Chaikanta & et-al (2013), A.Mashat & at-el (2013), M.Jenabzadeh & et-al (2013), T.Grabber & et-al (2013), A.Soltanzadeh (2013) and R.Edlinger (2013). Rotary electrical motors were the most common actuation type in the arm and gripper however R.Rangel & et-al (2013) won the ‘Best in class manipulation’ award using linear electric motors in the arm. The most common configuration is illustrated by Figure 46 and described by Table 23.

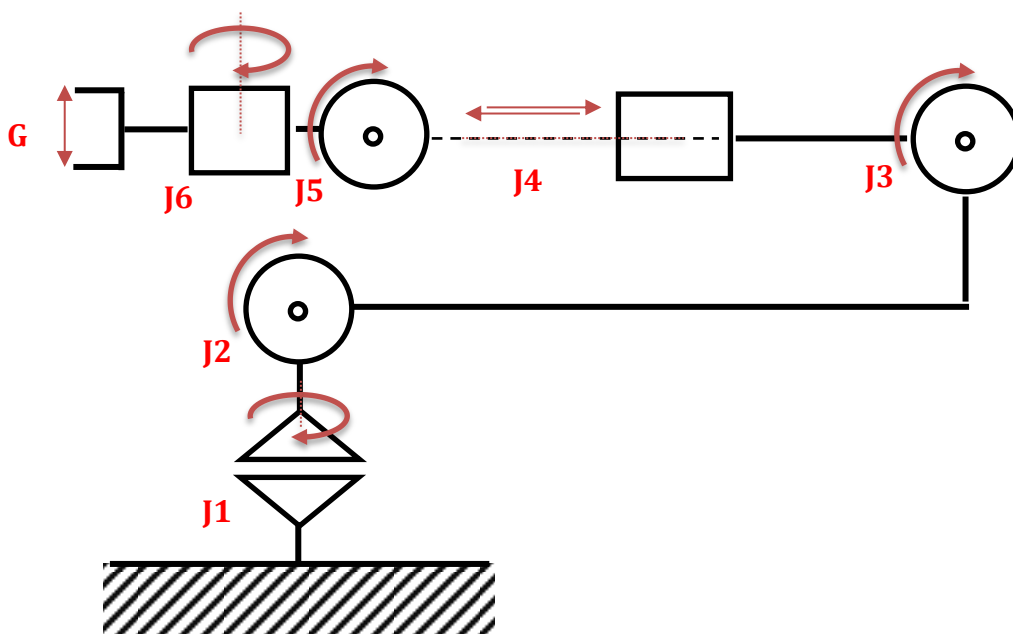


Figure 46: Kinematic Chain of most Common Configuration

Table 23: Joint Description of most Common Configuration

Joint	Joint Description
J1	1DOF $\leq 360$ deg twisting joint, rotating about axis perpendicular to chassis.
J2	1DOF Revolute joint
J3	1DOF Revolute joint (about axis perpendicular to previous link)
J4	1DOF Sliding (prismatic) joint
J5	1DOF Revolute joint (about axis parallel to previous joint) to pitch end effector
J6	1DOF Twisting or revolute joint at wrist, proving head yaw
G	Gripper

#### **4.4. Idea Generation and Concept Selection**

All available actuation and joint configurations were considered for the arm and gripper. Fluid actuation types were discounted as the power source is electrical and there is limited space for such a system in the chassis.

##### **4.4.1. Gripper**

Appendix D.2 concluded that an electric gripper would provide sufficient gripping force to manipulate a wide range of objects.

4.4.2. Arm

From available joint types revolute joints were chosen as the simplest type. Figure 47 details the remaining possible electric motor and transmission configurations. Although the configuration in Figure 46 is desirable, due to time constraints only 4DOF were designed.

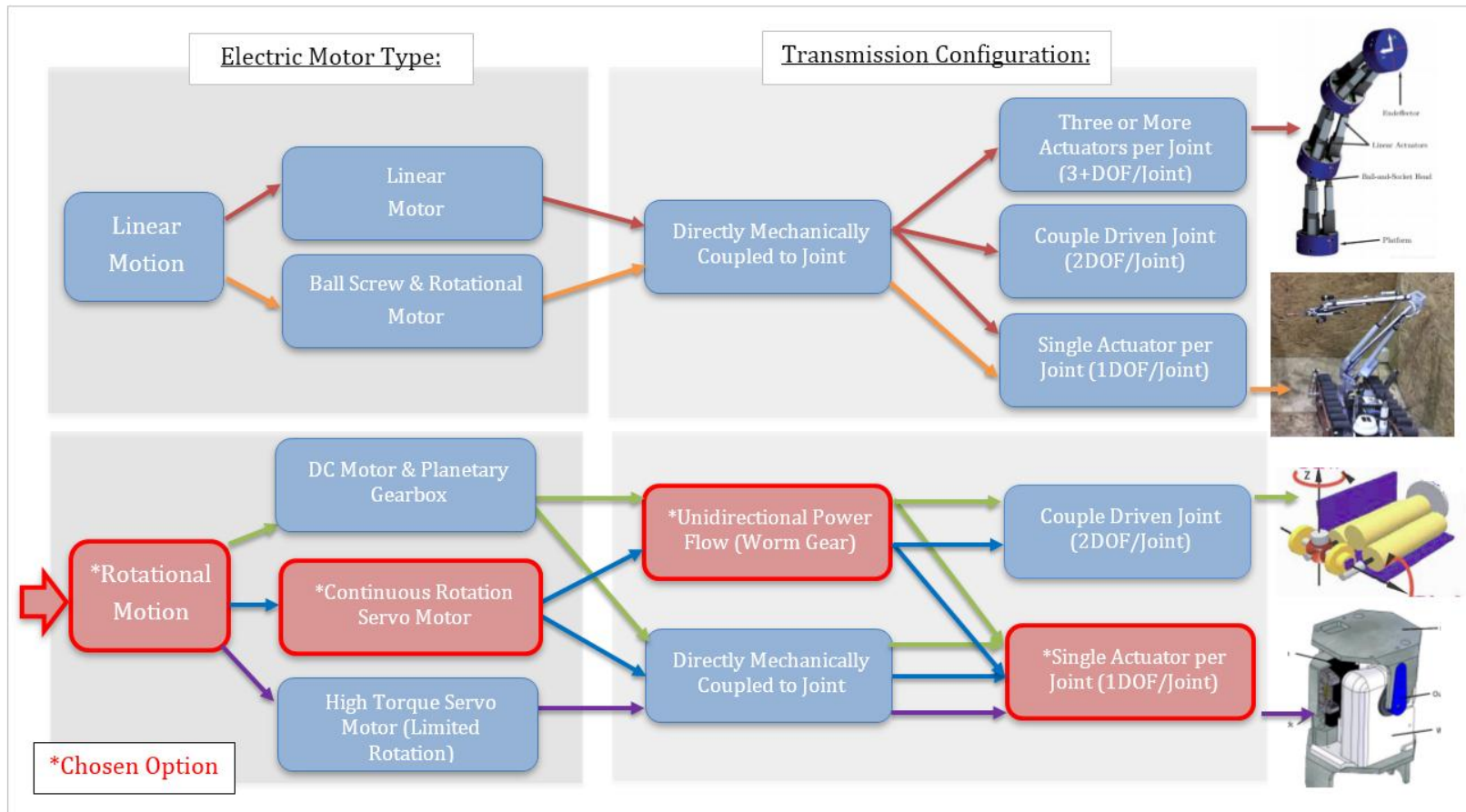


Figure 47: Arm Concept Selection



### 4.5. Chosen Design

The joint configuration chosen is detailed in Figure 48. The methodology used is described by Table 24.

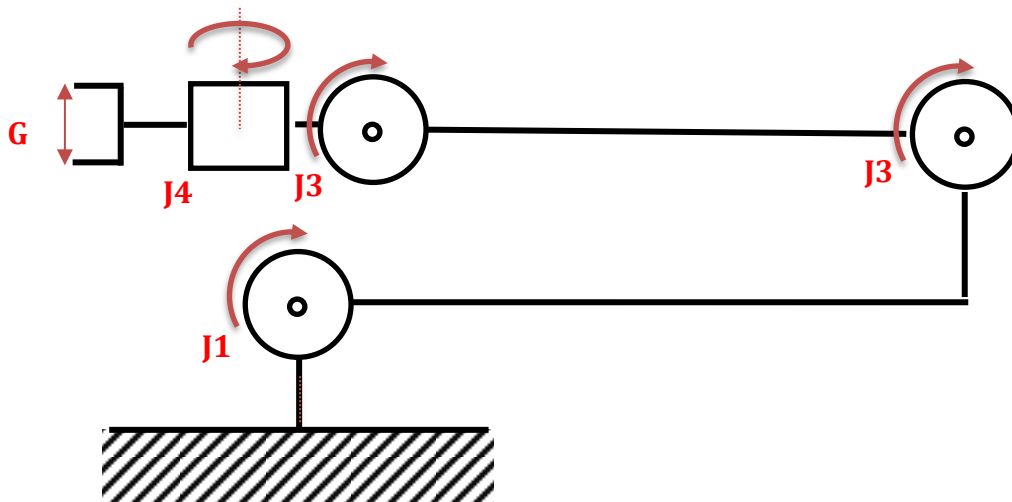


Figure 48: Final Arm Design and Joint Configuration

Table 24: Arm Design Methodology

Methodology	Description
<b>Low cost/Ease of manufacture</b>	Modification of off-the-shelf components and materials reduces cost. Water jet cutting of components from a single thickness of aluminium sheet (where possible) to reduce labour costs. Heavily machined components avoided.
<b>Lightweight Modularity</b>	Highly aluminium intensive design Ability to adapt the arm’s configuration (Figure 49 and Figure 50) allows designs to be optimised to a particular task/ cost to be adjusted for different market price points.
<b>Easy of repair, modification and disassembly</b>	Only M3 bolts were used requiring a single Allen key for maintenance.



Figure 49: Arm with Single Link, Wrist, Head & Griper

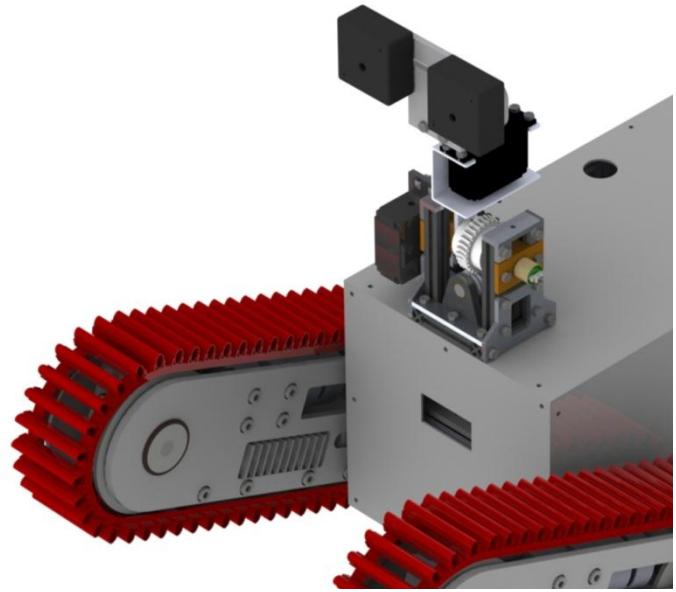


Figure 50: Arm with Wrist and Head

#### 4.6. Arm System Package

The arm system package space (Figure 51) was developed to simultaneously meet the turning circle and height constraints calculated in Chapter 2.4.1.

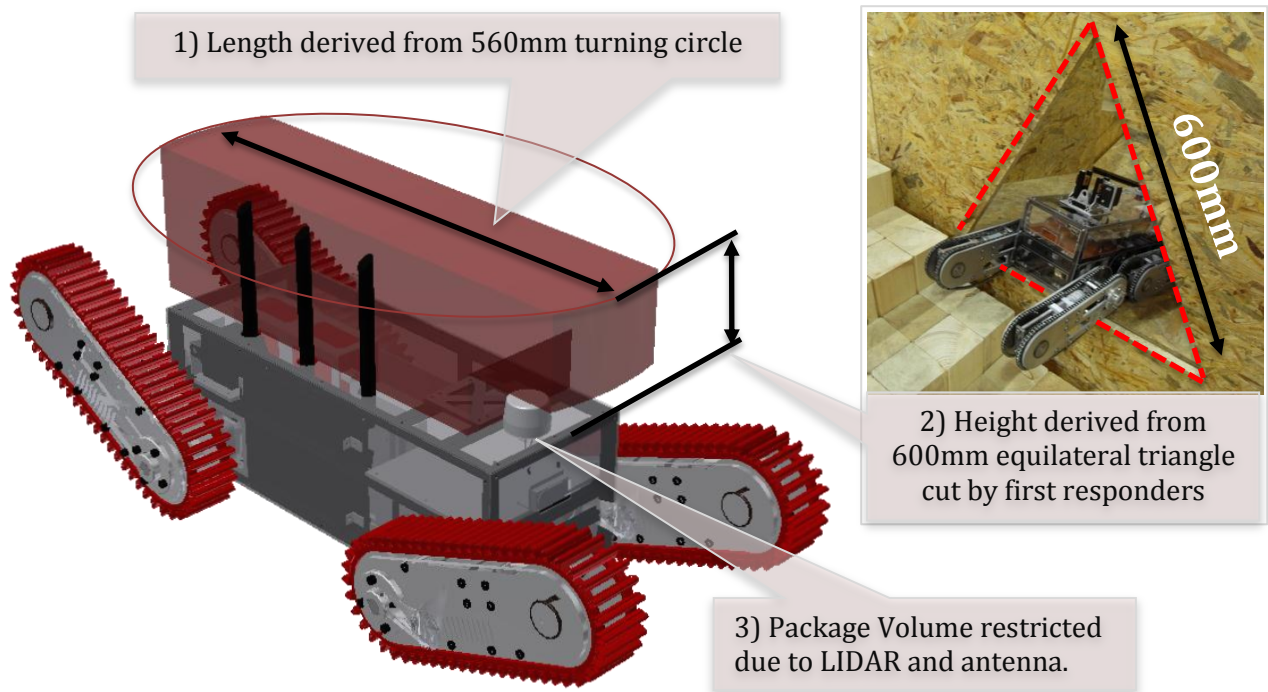


Figure 51: Arm Development Package Constraints

The reach provided by several link configurations was evaluated (Table 25), however it was not possible to meet the reach target within the specified package space (Figure 51). Option 3 was selected even though it does not fit in the desired package space; however it provides the best reach within the development time and can be raised to fit within the turning circle (Figure 52). Future development would allow the reach target to be met by option 4.

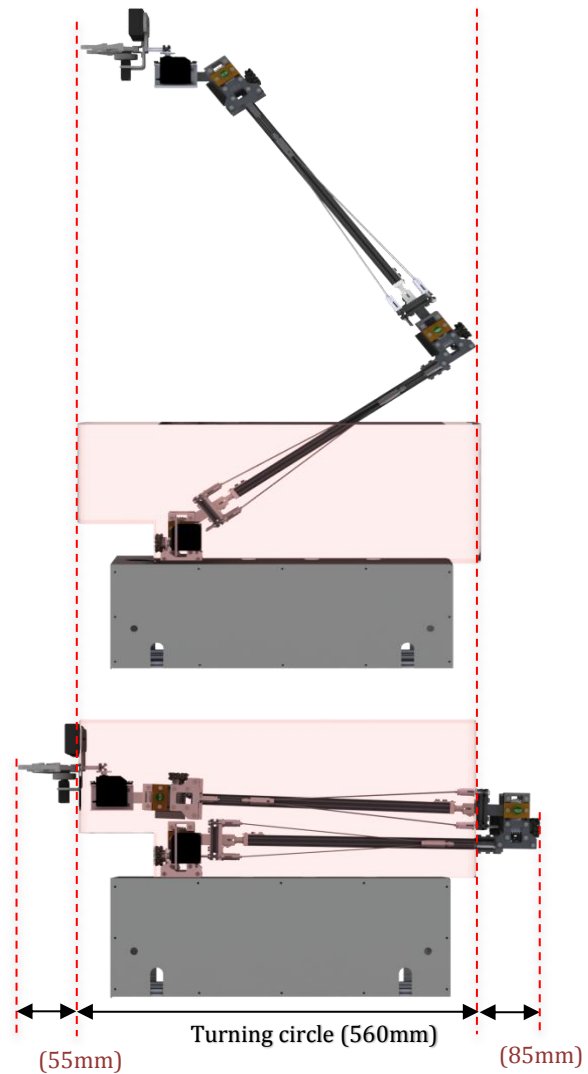


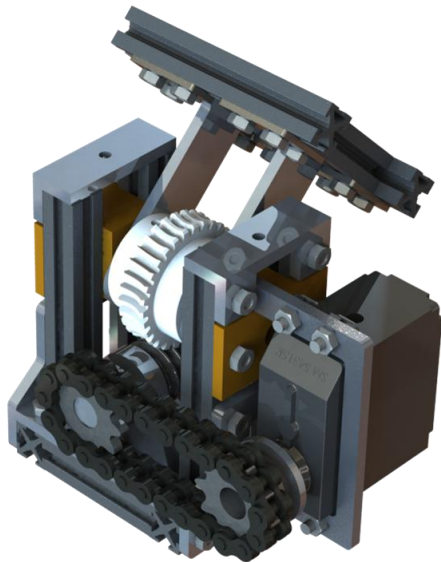
Figure 52: Arm positioned to meet turning circle (Top), and 60cm triangular (bottom)

Table 25: Arm Link Configurations

Configuration	Advantages	Disadvantages
1) 2x0.36m Links	Fits the available package space Built within available development time	Only 1.17m reach (0.43m shortfall)
2) Two 0.36m Links + 0.2m linear Joint	Fits the available package space	Only 1.38m reach (0.22m shortfall) Linear joint cannot be developed within project time scale
3) Two 0.45m Links	Built within available development time	Does not fit the desired package space Only 1.39m reach (0.21m shortfall)
4) Two 0.45m links + 0.2m linear Joint	Only design to meet reach target	Does not fit the desired package space Linear joint cannot be developed within project time scale

### 4.7. Modular Joint

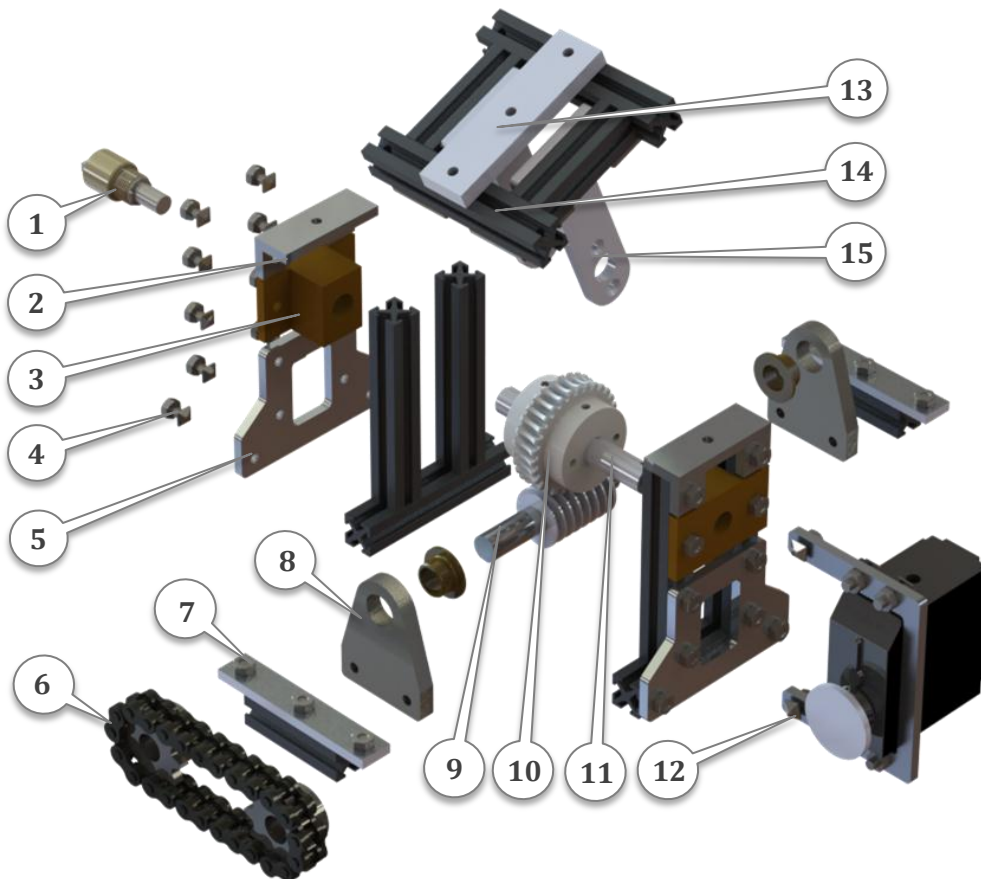
The revolute joint design (Figure 53) is detailed by Figure 54 and Table 26.



**Table 26: Joint Component Index**

No.	Part Name
1	Encoder
2	Mesh Adjuster
3	Slider
4	Fixings - M3 Nut & Bolt
5	Side Reinforcement
6	Sprocket & Chain
7	Base Reinforcement
8	Worm Support & Bush
9	Input Axle
10	Worm and Worm Wheel
11	Output Axel
12	Servo Motor, Bracket & Attachment
13	Link Connector
14	MakerBeam
15	Joint Upper

**Figure 53: Arm Joint**



**Figure 54: Arm Joint Exploded View**

### 4.7.1. Modular Architecture Strategy

The same modular joint is used throughout the arm resulting in fewer unique components. The joint architecture is explained by Figure 55 and Figure 56.

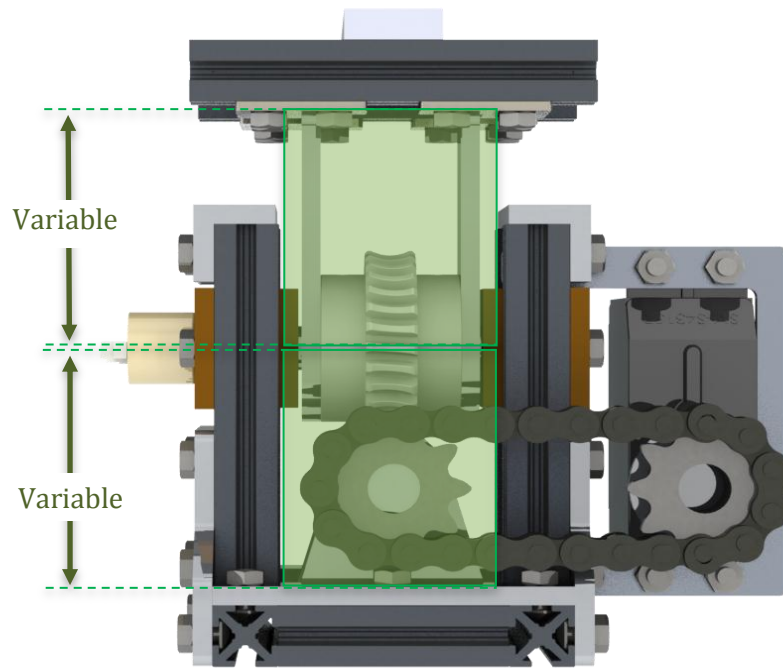


Figure 55: Joint Architecture Variable Dimensions - Front View

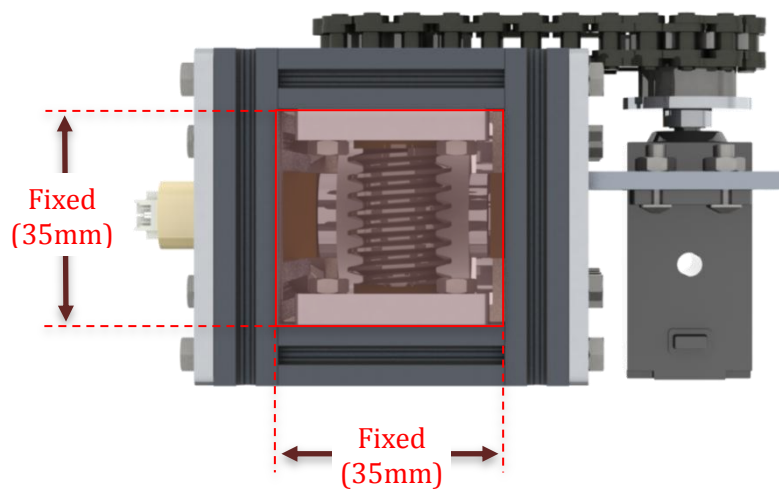


Figure 56: Joint Architecture Fixed Dimensions -Bottom View

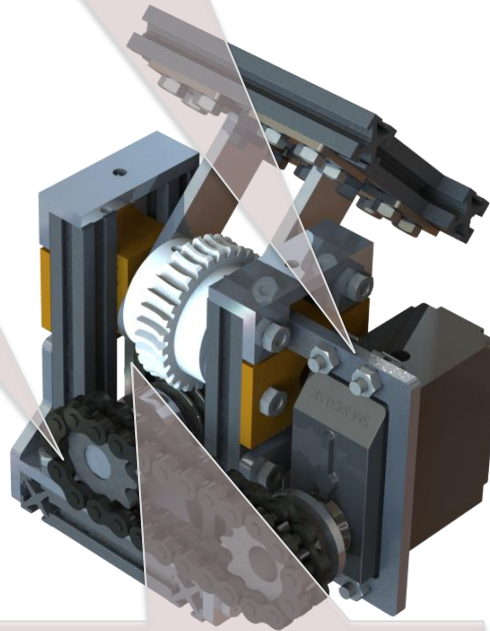
#### 4.7.2. Mechanical & Electrical Power Transmission and Control

Joint power transmission is shown by Figure 57.

1) All joints are powered by a standardised actuator (continuous rotation servo motor).

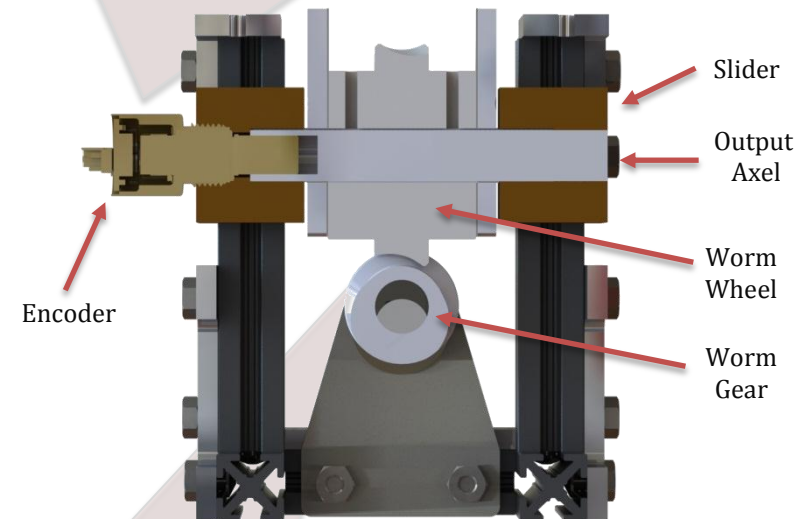
2) Sprocket - chain transmission (1:1 ratio) transfers power from servo to worm gear pair, minimising joint package.

3) The unidirectional mechanical power flow of the worm gear pair (15:1 ratio) prevents arm collapse in an unstable disaster environment (during power loss). This also reduces arm power consumptions increasing operating time.



#### Joint Cross-Section:

4) The Encoder is mechanically coupled to the output rotating shaft, providing accurate positional data required for inverse kinematic control.



5) Worm gear pair mesh is adjusted by adjusting worm wheel height (rather than conventional adjustment of worm). Alternative worm gear pairs can be plugged-and-played (varying torque and speed output) without requiring a joint redesign (as per previous design).

Figure 57: Modular Joint Transmission and Position Control

The joint is powered by a low cost continuous servo. Compared against the existing robot's design this saves £1053 in actuator and transmission cost (Table 27).

**Table 27: Arm Actuation and Transmission Cost Comparison**

	<b>2012 Arm Design</b>	<b>New 2014 Arm Design</b>
<b>Description</b>	Four different DC motors with different planetary gearboxes and worm gear transmissions.	Four identical servo motors with common sprocket-chain and worm gear pair transmission
<b>Cost Difference</b>	<b>£1275-£2222=£1053 (-83%)</b>	

#### 4.7.3. Kinematic Analysis

To design the joint, the arm's four worst-case loading scenarios were considered (Table 28).

**Table 28: Joint Worst Case Loading Scenarios**

<b>No</b>	<b>Description</b>	<b>Defines</b>	<b>Torque</b>
<b>1</b>	<b>Manipulation at edge of workspace:</b> Actuation torque required in base joint ( $J_1$ ) to accelerate the arm from a stationary horizontal position whilst carrying maximum payload (Figure 58).	Actuator torque requirement	16.8 Nm
<b>2</b>	<b>Debris falling on arm at edge of workspace:</b> Torque generated in base joint as a result of incident load on the arm in a horizontal position above which of that required to deliver maximum payload (Figure 60).	Maximum load on joint components (generated by worm gear pair)	32.8 Nm
<b>3</b>	<b>Opening a closed door:</b> Torque required in the elbow joint ( $J_2$ ) to open a door (Appendix D.3)	N/A	15.6 Nm
<b>4</b>	<b>Robot flipping over:</b> Torque generated in base joint ( $J_1$ ) with full maximum mass of robot resting on arm (Appendix D.4)	N/A	245 Nm

The torque generated in  $J_1$  during Scenario 4 is over a magnitude greater than any other loading scenario however this will be mitigated by a cable termination failure mechanism discussed in Chapter 4.8.2. Scenario 2 defines the maximum load on the components and Scenario 1 the maximum joint torque that the actuator will need to overcome (Figure 58). This is required to overcome the moments created by the arm's body (gravity), inertial, Coriolis and centripetal forces (Niku, 2011, p. 165). Assuming that joint speed is near zero (fast or erratic movement is dangerous in an unstable environment), the Coriolis and centripetal forces can be

neglected. Joint acceleration is also assumed minimal under these loading conditions and so this simplifies further to Equation 7.

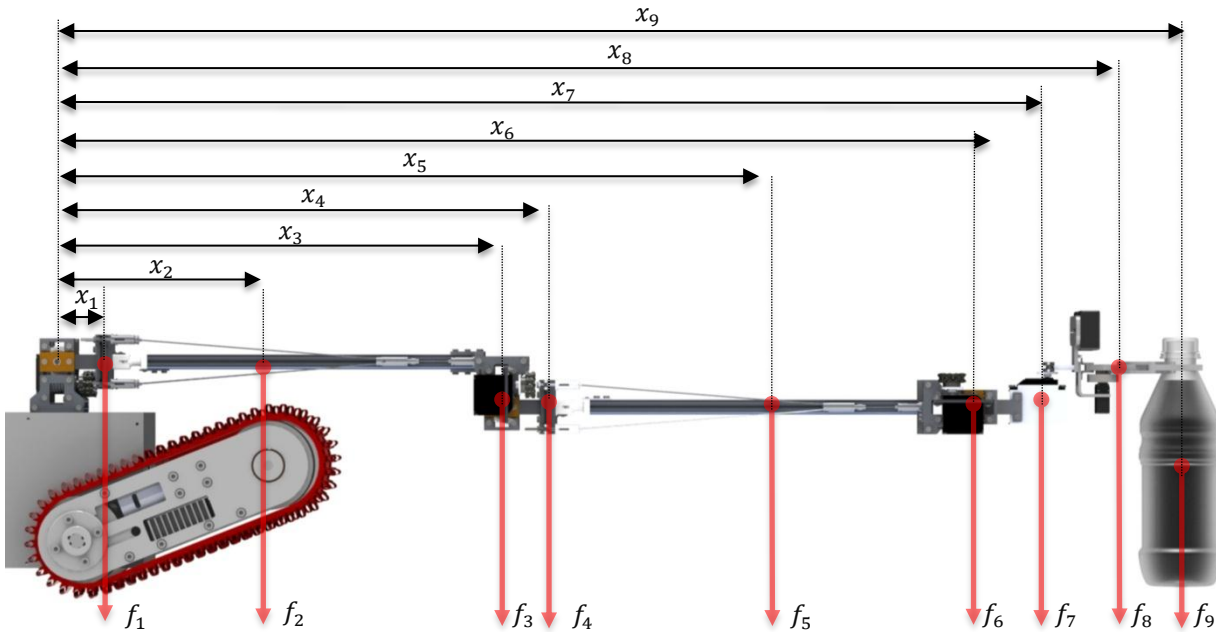


Figure 58: Manipulation of Payload at Edge of Workspace

$$\tau_B = \sum_1^n (F_i \times x_i) \tag{Equation 7.}$$

Where:

- $\tau_B$  is the torque generated at the base (Nm)
- F is the force (N)
- x is the distance from the base joint (m)

Using Equation 7 and the values from Table 29:

$$\tau_B = (F_1 \times x_1 + F_2 \times x_2 + F_3 \times x_3 + F_4 \times x_4 + F_5 \times x_5 + F_6 \times x_6 + F_7 \times x_7 + F_8 \times x_8 + F_9 \times x_9)$$

$$\tau_B = 17.1Nm$$

Table 29: Base Joint Torque Variables

Component Number, $i$	Component Name	Distance from base joint, $x_i/m$	Component Mass, $m_i/kg$	Component Weight, $f_i/N$
1	Joint 1 - Upper	0.05	0.13	1.31
2	Link 1	0.26	0.11	1.10
3	Joint 2	0.45	0.43	4.26



4	Joint 2 - Upper	0.50	0.13	1.31
5	Link 2	0.71	0.15	1.47
6	Joint 3	0.94	0.33	3.21
7	Joint 4	0.98	0.10	1.00
8	Head and Gripper	1.03	0.35	3.43
9	Payload	1.09	0.50	4.91

Figure 59 shows the implications of the future addition of a linear joint to the base joint torque,

$\tau_{B\_Linear}$  (Appendix D.5):

$$\tau_{B\_Linear} = 21.4Nm$$

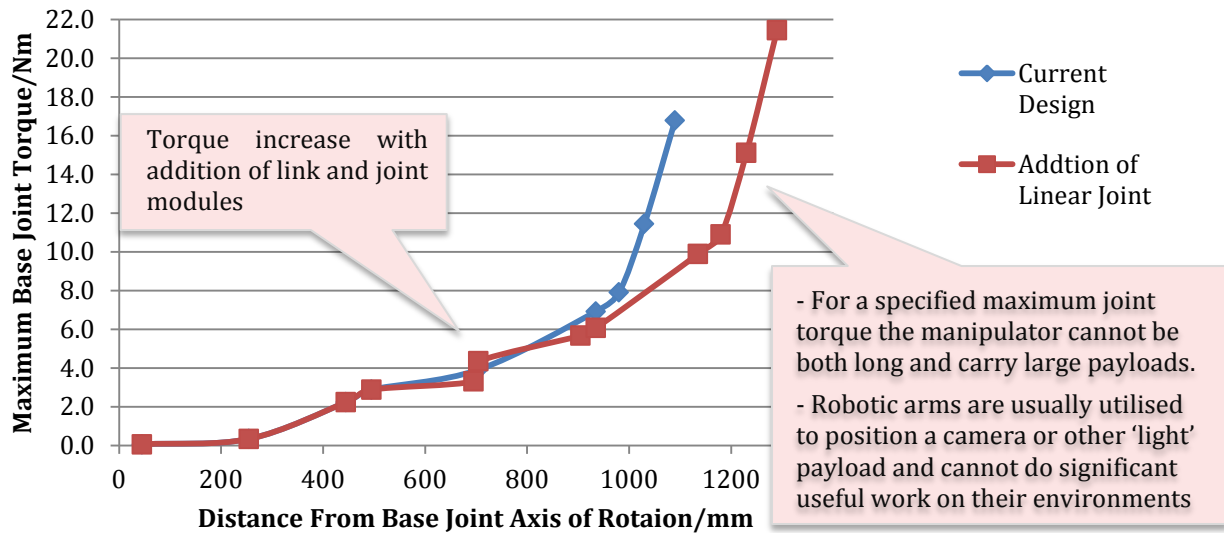


Figure 59: Arm Configuration Base Joint Torque Comparison

For the maximum servomotor torque,  $\tau_{Actuator} = 1.27Nm$ , the required gear reduction is shown by Equation 8.

$$r_g = \frac{\tau_{out}}{\tau_{in}} = \frac{\tau_B}{\tau_{Actuator}} = \frac{16.7 \dots}{1.27} = 13.2 \approx 15:1 \tag{Equation 8.}$$

Where:

$r_g$  is the gear ratio

Although the arm and actuators are designed to lift the maximum payload (loading Scenario 1), the joint components must be designed to withstand the second loading scenario (Figure 60).

This results in a worm wheel input torque of 32.8Nm generating forces in the worm gear pair (Figure 61, Table 30 (Calculated in Appendix B.3)).

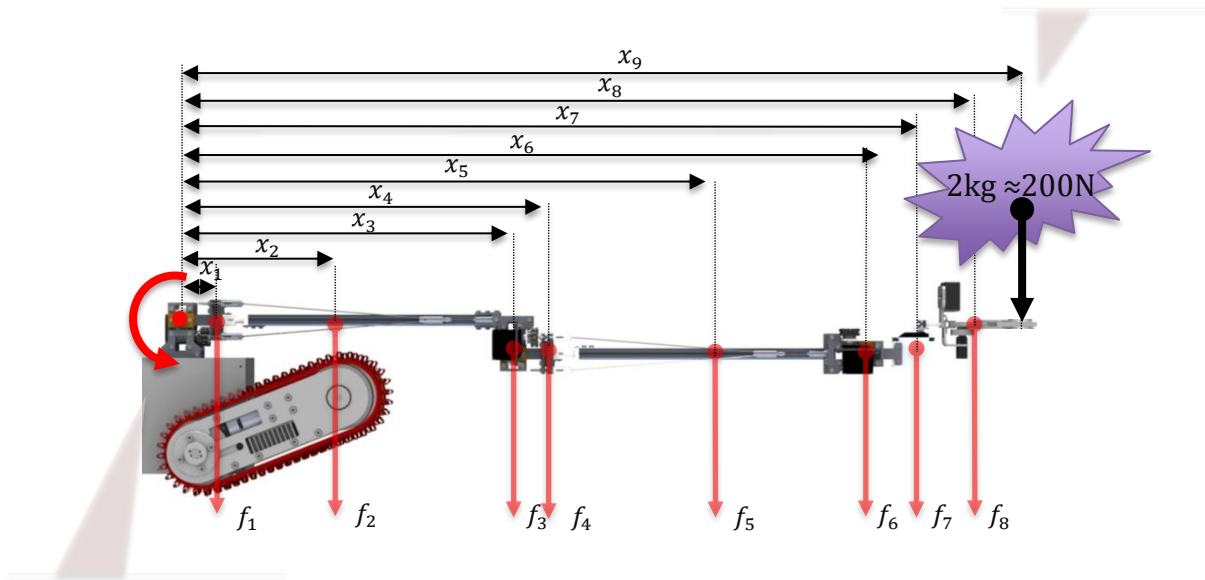


Figure 60: Debris Falling on Arm at Edge of Workspace

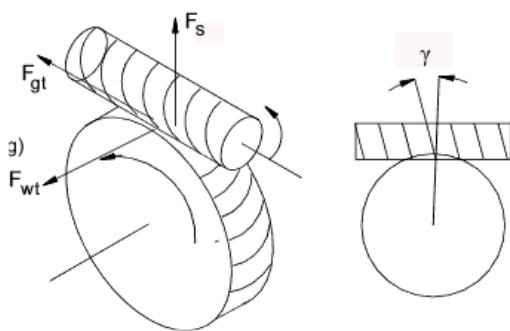


Table 30: Forces Generated in Worm-Gear Pairs

Output Parameter	Symbol	Force (N)
Worm Tangential Force = Worm Gear Axle Force	$F_{wt} = F_{ga}$	284
Worm Axial Force = Worm Gear Tangential Force	$F_{wa} = F_{gt}$	1300
Separating Force	$F_s$	87.2

Figure 61: Forces Generated in Worm-Gear Pairs (R.Beardmore, 2013)

#### 4.7.4. Joint Fine Element Analysis and Material Selection

The kinematic analysis (Chapter 4.7.3) was used with FEA to optimise geometry and component mass. This process is illustrated for the worm gear support (Figure 62) realising a mass reduction of 6.4g (-37.5%) per component. This analysis procedure was repeated for every component in the arm.

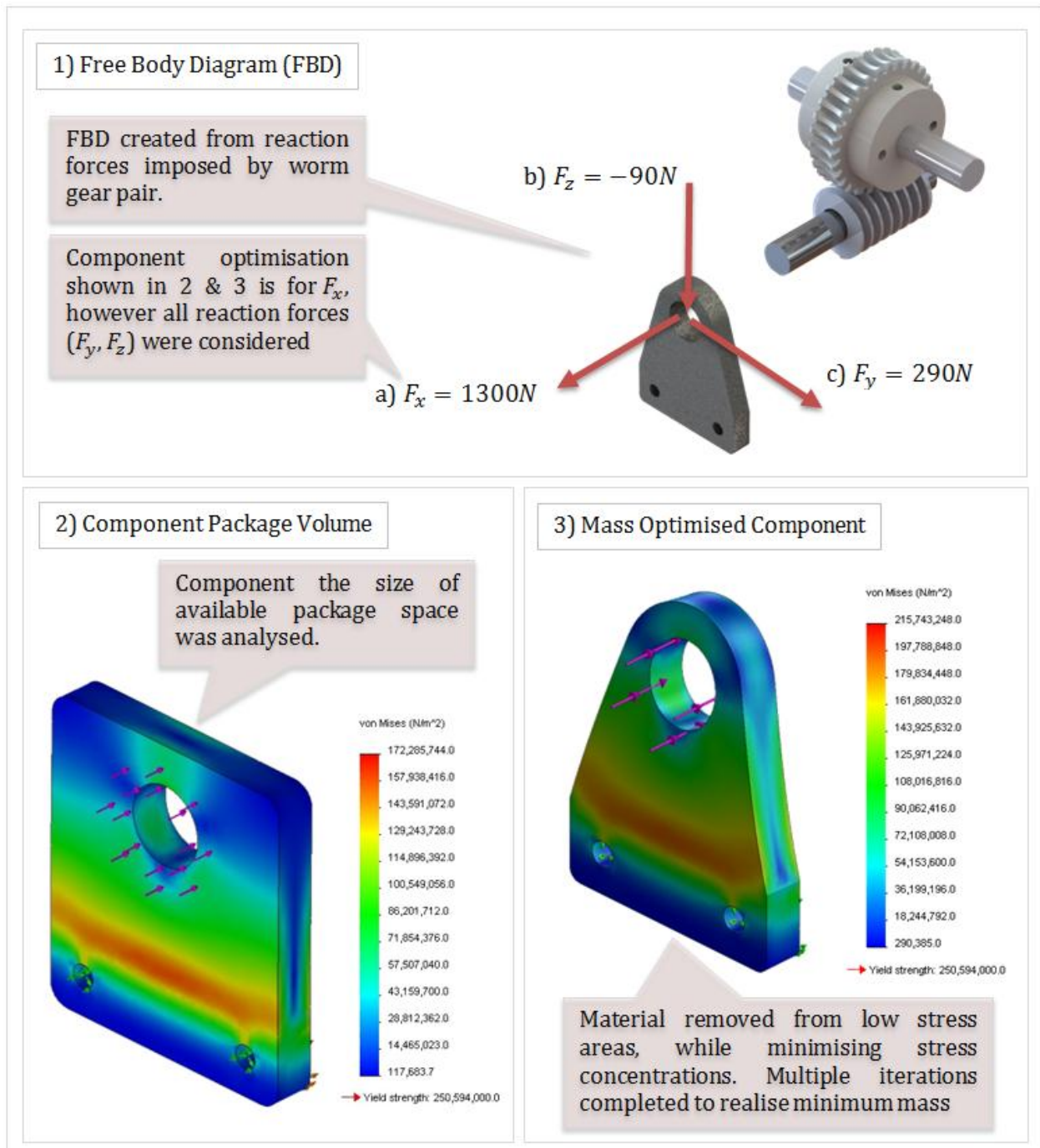


Figure 62: Worm-Gear Support Optimisation Process

The CES EduPack was used to create Figure 63 to analyse materials based on their cost, mass and yield strength. Aluminium 6082T6 was chosen, for most components, due to favourable yield strength, machinability and availability.

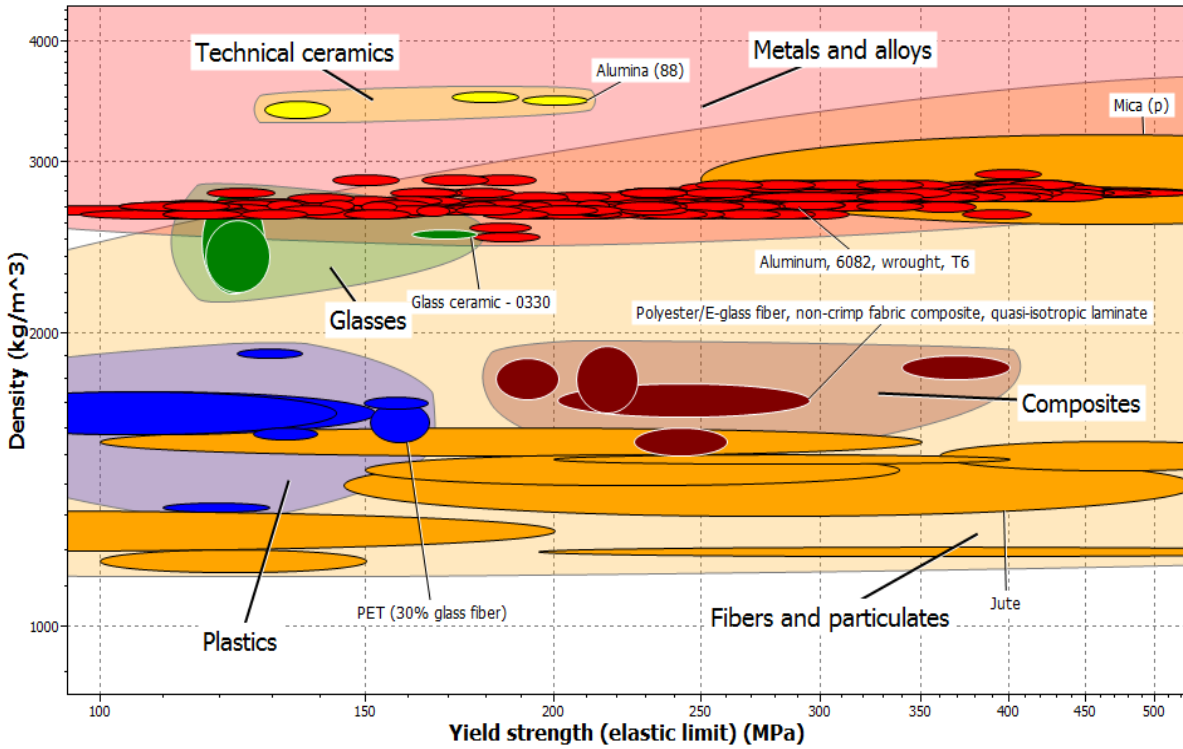


Figure 63: Graph Showing Different Material Density and Yield Strength Properties

The modular design means each joint can support the maximum loading scenario (Chapter 4.7.3) leading to some redundancy in the downstream joints. Material substitution was used to optimise the mass of the wrist transmission where the incident loads are reduced (Figure 64). This results in a 49g (-78.8%) mass reduction and £8.15 (-27.6%) cost saving.

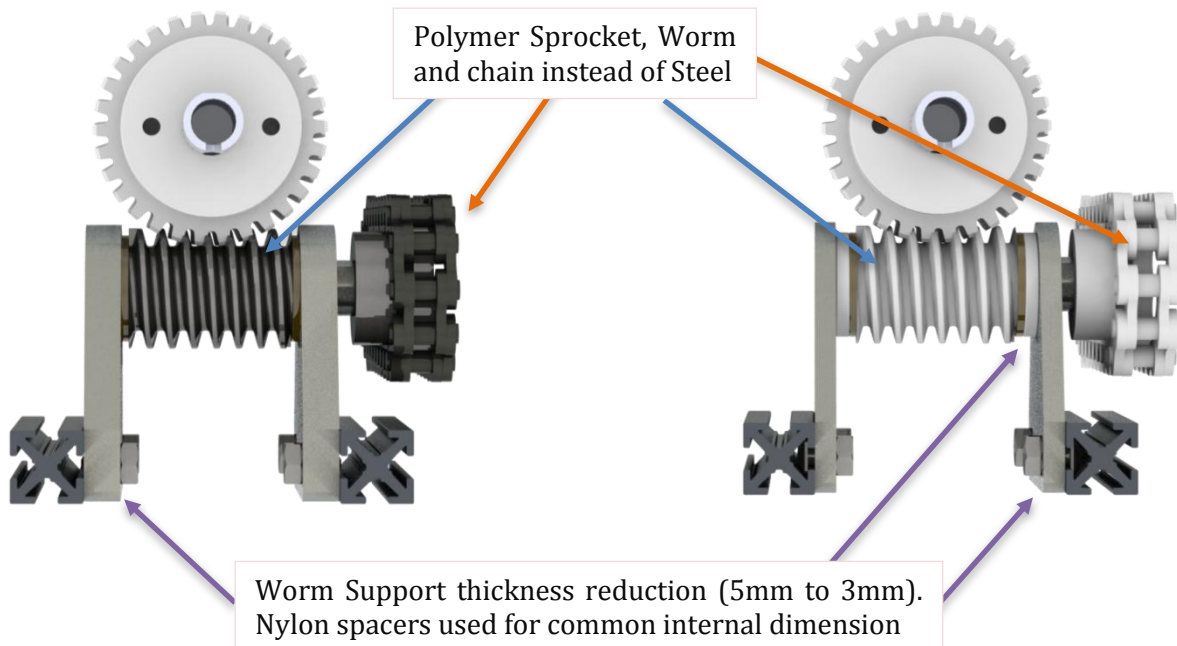


Figure 64: Downstream Joint Transmission Material Optimisation

Table 31: Transmission Weight Reduction Through Material Substitution

Component	Base Joint Mass (g)	Wrist Joint Mass (g)	Mass Difference (g)	Percentage Mass Difference (%)
<b>Chains</b>	18.1	6	-12.1	-66.9%
<b>Sprockets</b>	19.9	2.8	-17.1	-85.9%
<b>Worm</b>	23.8	4.3	-19.5	-81.9%
<b>TOTAL</b>	61.8	13.1	-48.7	-78.8%

Table 32: Transmission Cost Reduction Through Material Substitution

Component	Base Joint Cost (£)	Wrist Joint Cost (£)	Cost Difference (£)	Percentage Cost Difference (%)
<b>Chains</b>	4.92	7.64	2.72	55.3%
<b>Sprockets</b>	7.45	4.76	-2.69	-36.1%
<b>Worm</b>	18.17	9.99	-8.18	-45.0%
<b>TOTAL</b>	30.54	22.39	-8.15	-26.7%

### 4.8. Link Design and Kinematic Analysis

The link uses an innovative lightweight cable tension design (Figure 65), unseen elsewhere in USAR robots. Its ability to quickly change length is shown by Figure 66.

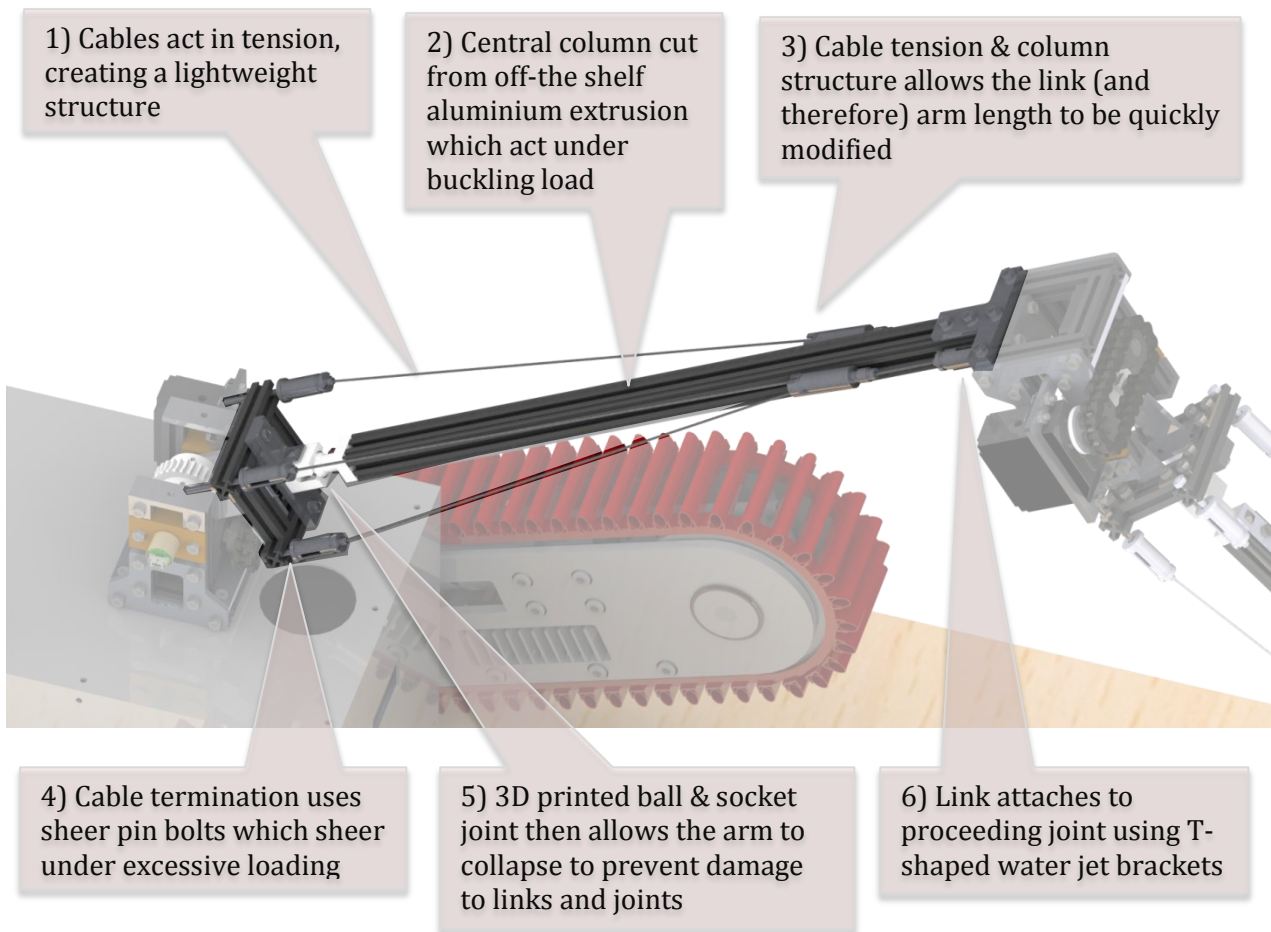


Figure 65: Arm Tension Cable Link Design

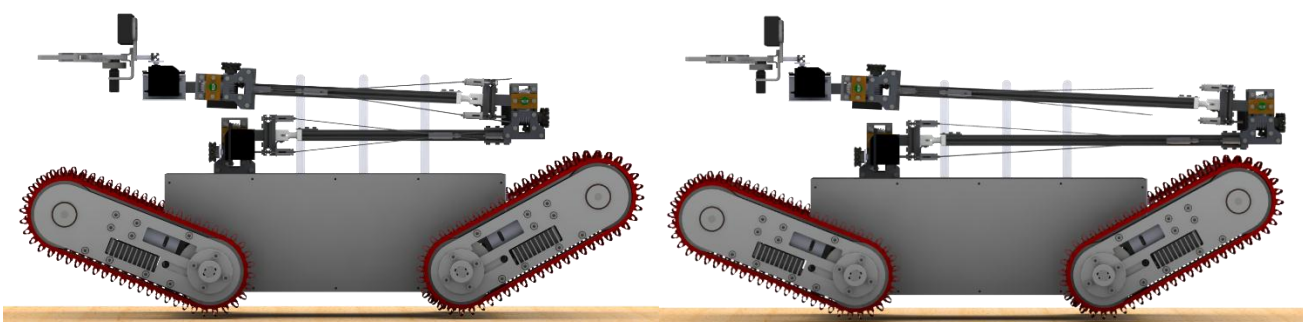


Figure 66: Changeable Link Lengths - Short (left) and Long (right)

To design the link, two loading scenarios were considered (Table 33). The tension generated in the cable by Scenario 2 is almost an order of magnitude greater than Scenario 1. This will be mitigated by the addition of a failure mechanism in the cable termination.

Table 33: Link Loading Scenarios

No.	Scenario Description	Design impact	Tension in cables, $T_c$ (N)
1	<b>Debris falls on arm at edge of workspace:</b> Cable tension required to support the mass of the downstream elements in the arm system and incident debris load of 2kg (Figure 67)	Tension cable diameter and central Column dimensions.	181
2	<b>Robot flipping over:</b> Cable tension required to support the 25kg mass of the robot	N/A	1290

#### 4.8.1. Cable Tension and Buckling Loads

The steel cable diameter was based on the maximum tensions in each cable (Figure 67).

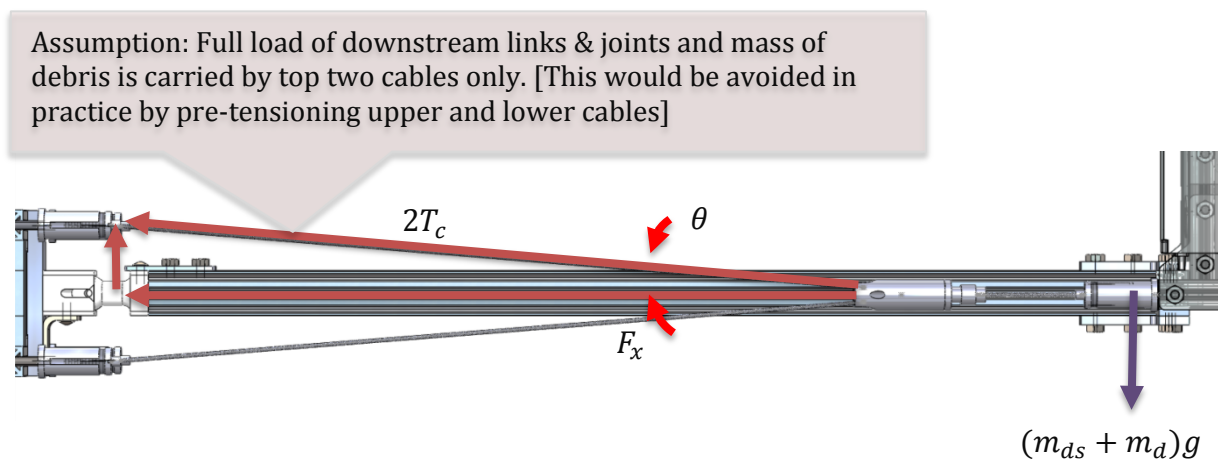


Figure 67: Full arm and payload weight carried by two of the four cables in tension.

The cable tension is found by taking the sum of the vertical forces, Equation 5:

$$2.T_c \sin \theta = (m_{ds} + m_d)g \quad \text{Equation 9.}$$

Where:

- $T_c$  is the cable tension (N)
- $\theta$  is the angle ( $^\circ$ )
- $m_{ds}$  is the mass of the links and joints (mg)
- $m_d$  is the mass of the debris (kg)
- $G$  is acceleration due to gravity ( $\text{ms}^{-2}$ )

Where the angle between the top cable and the horizontal is found using Equation 6:

$$\theta = \tan^{-1} \frac{h}{l} \quad \text{Equation 10.}$$

Where:

h is the height (m)

l is the length (m)

Rearranging this gives Equation 7:

$$T_c = \frac{(m_{ds} + m_d)g}{2 \sin \theta} \quad \text{Equation 11.}$$

Substituting in the values from Table 34 into Equations 6 and 7 gives:

$$\theta = \tan^{-1} \frac{0.025}{0.245} = 5.83^\circ$$

$$T_c = \frac{(1.74 + 2.00) \times 9.81}{2 \times \sin(5.83)} = 181N$$

**Table 34: Cable Tension Parameters**

Parameter	Value
Downstream link and joint mass, $m_{ds}$ (kg)	1.74
Debris mass, $m_d$ (kg)	2.00
Height, h (m)	0.0250
Length, l (m)	0.245

The load required to buckle the central column is given by Equation 12 where the effective length is given by Equation 13 (based on the constraints described by Figure 68).

$$P_{crit} = \frac{\pi^2 E I_{zz}}{L_e^2} \quad \text{Equation 12.}$$

$$L_e = 2L \quad \text{Equation 13.}$$

Where:

$P_{crit}$  is the critical load (N)

E is Young's Modulus (GPa)

I is the second moment of area (m<sup>4</sup>)

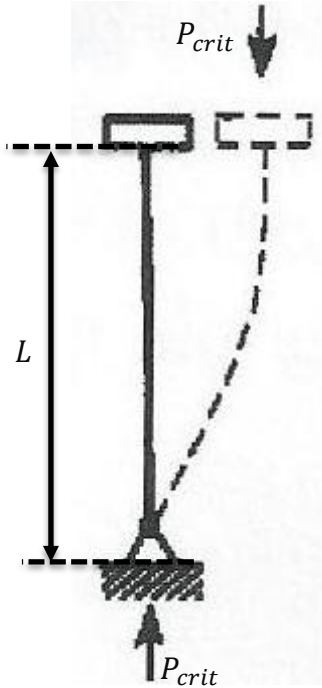
L is the length

The z-axis second moment of area,  $I_{zz}$ , is calculated using Equation 14.



$$I_{zz} = I_{xx} + I_{yy} \tag{Equation 14.}$$

$$I_{xx} = I_{yy} \tag{Equation 15.}$$



**Table 35: Buckling Load Parameters**

Parameter	Value
Youngs modulus, E (Pa)	70.0E+009
X-axis second moment of area, $I_{xx}$ (m <sup>4</sup> )	2.35E-009
Y-axis second moment of area, $I_{yy}$ (m <sup>4</sup> )	2.35E-009
Column Length, L (m)	0.35

**Figure 68: Buckling Load Affected Length**  
(TheCarTech, 2013)

Substituting Equation 12 into Equation 13 and using the values in Table 35,

$$P_{crit} = \frac{\pi^2(70 \times 10^9) \times (2.35 \times 10^{-9})}{(2 \times 0.335)^2} = 16100N$$

Considering the sum of the horizontal forces in Figure 67:

$$\begin{aligned} F_x &= 2 \cdot T_c \cos \theta \\ &= 2 \times 181 \times \cos(5.83) = 360N \end{aligned}$$

This proves that buckling failure will not occur as the buckling load, is over a magnitude greater than the incident load.

4.8.2. Cable Sheer Mechanism

3.9.1.2 Cable Sheer Mechanism

Undercut Nylon M3 bolts (Figure 69) were designed to fail when the cable tension exceeded that of the cable loading in Scenario 1. The diameter of the undercut was calculated using Equation 16 (derived in Appendix D.6), with values found in Table 36.

$$d = \sqrt{\frac{4T_C}{\pi\sigma_{UTS}}} \tag{Equation 16.}$$

$$d = \sqrt{\frac{4 \times 181}{\pi \times 75}} = 1.75mm$$

Where:

d is the diameter (mm)

$\sigma_{UTS}$  is the ultimate tensile strength (Nmm<sup>-2</sup>)

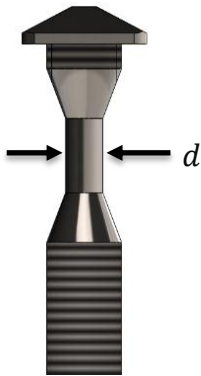


Table 36: Failure Mechanism Parameters

Parameter	Input Value
Cable Tension, $T_C$ (N)	689
Ultimate Tensile Strength, $\sigma_{UTS}$ (N/mm <sup>2</sup> )	410

Figure 69: Bolt Undercut Diameter

When this occurs a ball and socket joint allows the arm to collapse (Figure 70) preventing components from being overloaded.

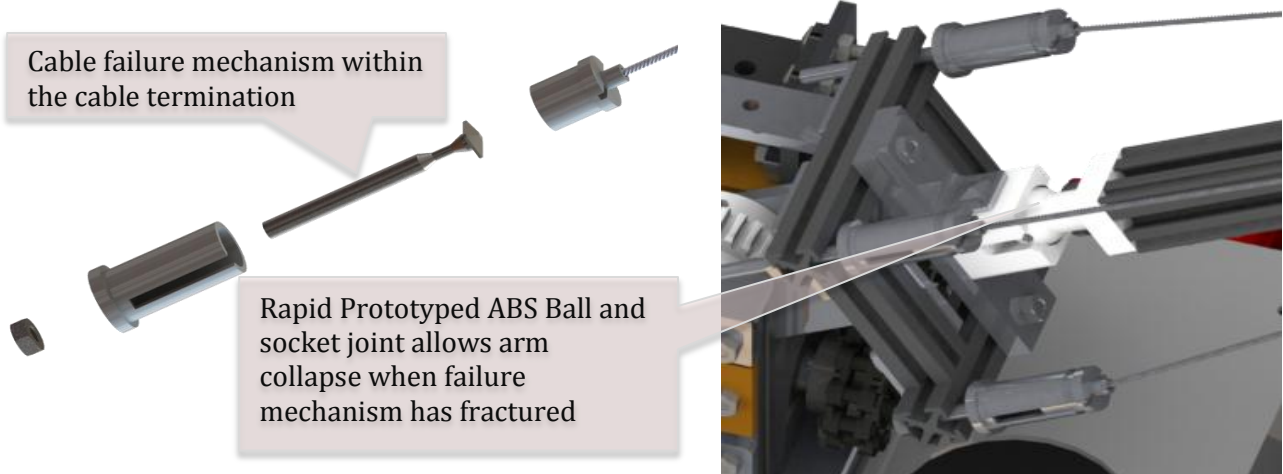


Figure 70: Cable Termination Failure Mechanism with Ball & Socket Joint

## 4.9. Gripper Design

### 4.9.1. Manipulator Design

A low-cost off-the-shelf electrical manipulator design could not be found which gripped all the items specified (Chapter 4.2), therefore a custom design was produced (Figure 71 & Figure 72).

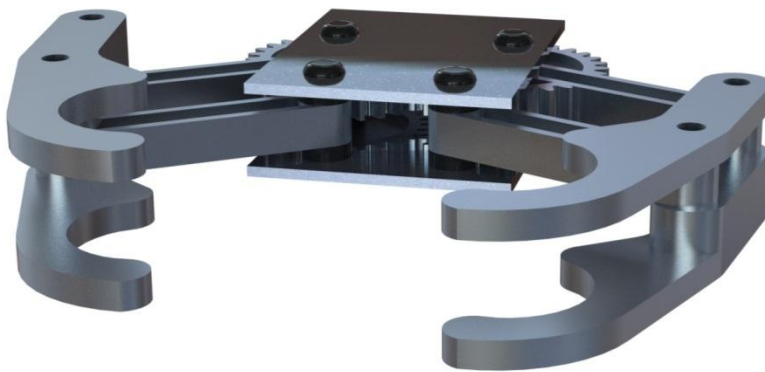


Figure 71: Initial Gripper Concept



Figure 72: Initial Gripper Concept (Transparent)

Several fingers (Figure 73) were designed to allow the gripper to perform different tasks.

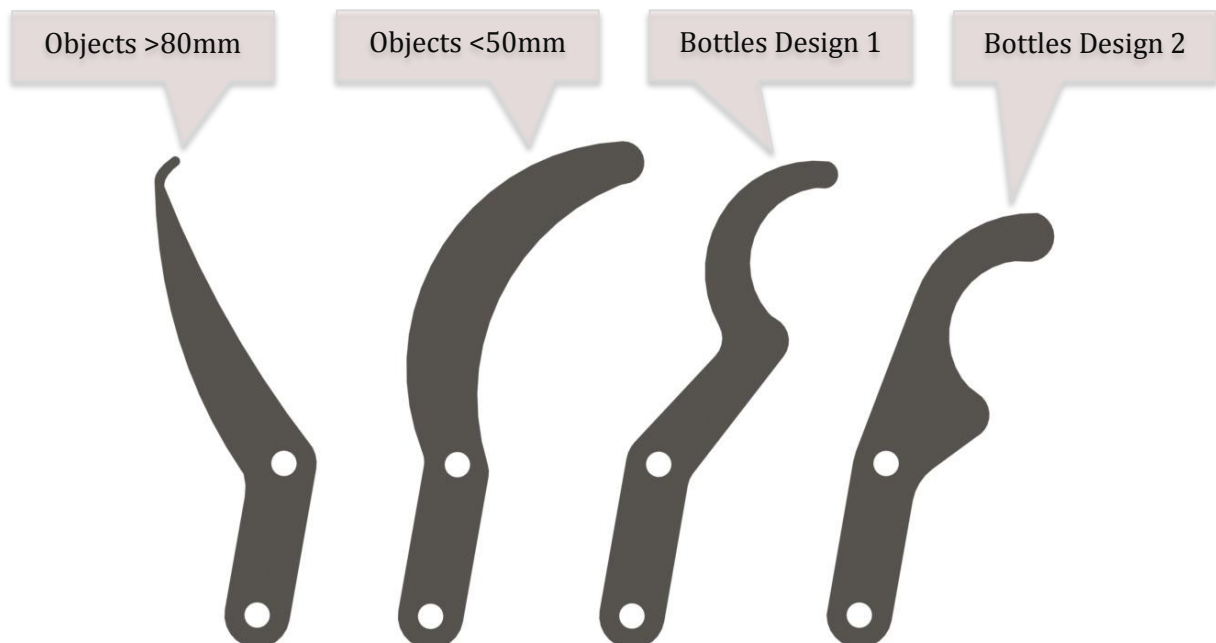


Figure 73: Initial Gripper Finger Designs

#### 4.9.2. Final Design

A cost analysis for material and manufacture (Appendix D.7) indicated a modified off-the-shelf solution would meet the specification and cost ~90% less than a full custom design.

The minimum gripping forces needed to meet the specification (Chapter 4.2– Specification No.7 & No.8) were calculated using Equation 17, summarise in Where:

F is the Force (N)  
 M is the Mass (kg)  
 g is acceleration due to gravity (ms<sup>-2</sup>)  
 μ is the coefficient of friction

Table 37 (full derivation, Appendix D.10).

$$F > 2 \frac{mg}{\mu} \quad \text{Equation 17.}$$

Where:

F is the Force (N)  
 M is the Mass (kg)  
 g is acceleration due to gravity (ms<sup>-2</sup>)  
 μ is the coefficient of friction

**Table 37: Gripping Forces of Various Objects**

<b>Object</b>	<b>Force Required</b>
<b>500ml Water Bottle</b>	49 N
<b>Balsawood Block (10x10x60cm)</b>	78.4 N

The ‘Dagu Mk II Gripper’ (Figure 74) was chosen after analysing available off-the-shelf grippers (Appendix D.7). The gripper servo could use the same controller as the arm servos so could be easily integrated into the arm system. It also contains a spring-loaded clutch, (Figure 75), which limits the load on the motor preventing over gripping. The two-finger arrangement opened to a maximum of 50mm which was insufficient to manipulate all the specified objects. New fingers were designed to overcome this limitation and open 100mm wide as specified. The new finger designs (Figure 76) were designed using calculations in Appendix D.8.



Figure 74: Dagu Gripper

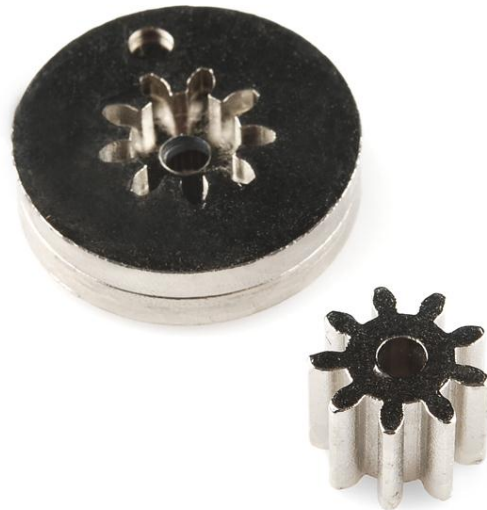


Figure 75: Spring Loaded Clutch

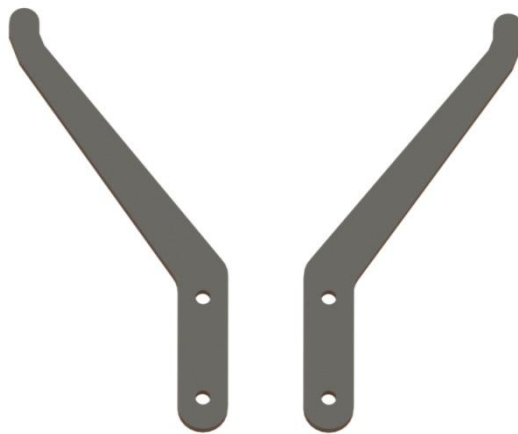


Figure 76: Redesigned Gripper Fingers

Figure 77 and Figure 78 display the new fingers attached to the off-the-shelf gripper.

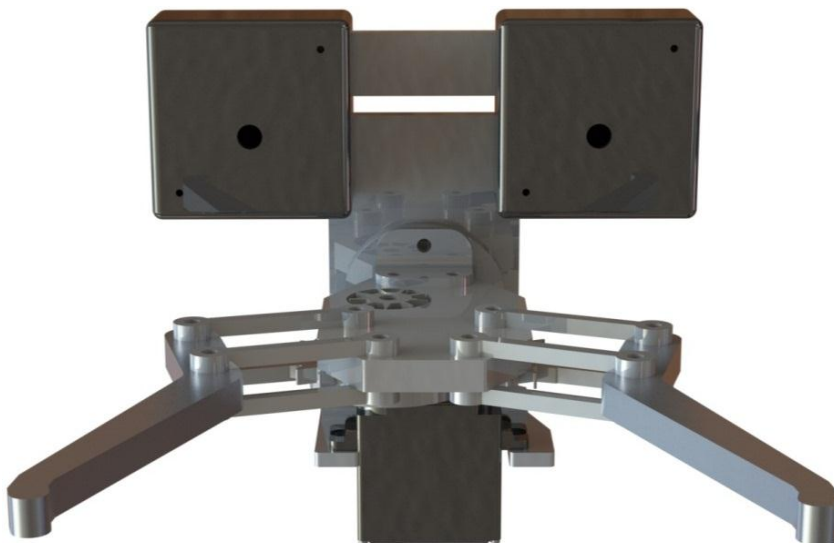


Figure 77: Gripper Assembly with Modified Fingers (Front View)



Figure 78: Gripper Assembly with Modified Fingers (Top View)

To simplify manufacturing, the fingers were made from 3mm thick Aluminium plate, as this was used for other systems in the robot. Two plates would then be bolted together in the final gripper (as used by the original Dagu fingers) giving a total finger thickness of 6mm.

#### 4.9.3. Modified Finger Plates FEA

FEA was performed on the finger plate design to determine how the maximum specified load (1kg) would affect the design when the load is placed on a single finger (Figure 79). Table 38 details the results.

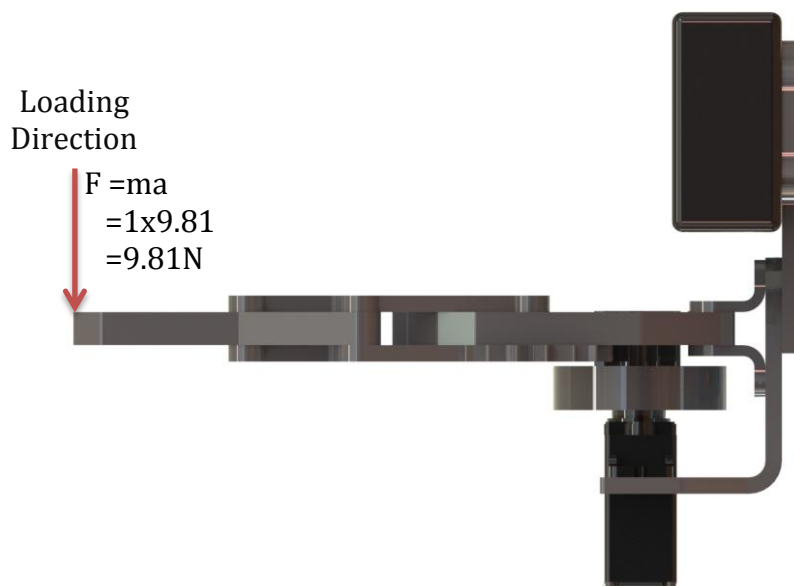


Figure 79: FEA Loading Point on Gripper Finger

Table 38: FEA Results of Gripper Finger

Maximum Von Mises Stress (MPa)	Percentage of Material Yield Strength	Maximum Deflection (mm)
40.8	19.4	0.34

The FEA results show a 0.34mm deflection (Figure 80) with the maximum stress being significantly below the yield strength of the material (Figure 81). This negligible deflection should allow the operator to perform precision manipulation.

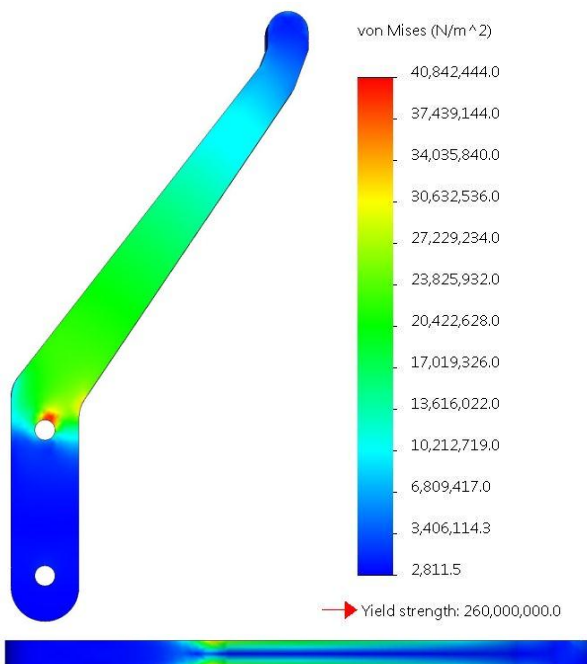


Figure 80: Finger Stress with 1kg loading

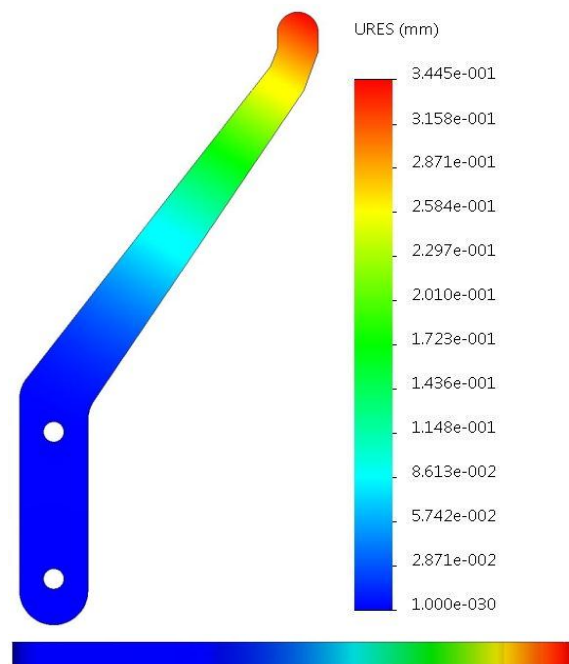


Figure 81: Finger Deflection with 1kg loading

## 4.10. Head Design

The head plate dimensions were based on two critical factors. Confined entry space to victim boxed (150mm diameter holes, Chapter 4.2 Specification No. 6) and secondly the need for dual webcams for integration of the Oculus Rift vision system (Chapter 5.4).

### 4.10.1. Camera Distance Calculations

Calculation of the maximum separation of the cameras based on their focal point allowed the initial head plate to be designed. The maximum camera separation required is the distance between the centres of human eyes, approximately 63mm (Dodgson, 2004).

The cameras also needed to be placed so that the gripper can be viewed in focus to aid in the manipulation of objects. The webcams used (Microsoft HD 3000s) were found to have a fixed focal distance of between 0.1m and 1.5m and viewing angle of  $68.5^\circ$  (Microsoft, 2012). This was used to position the gripper relative to the cameras (Figure 82).

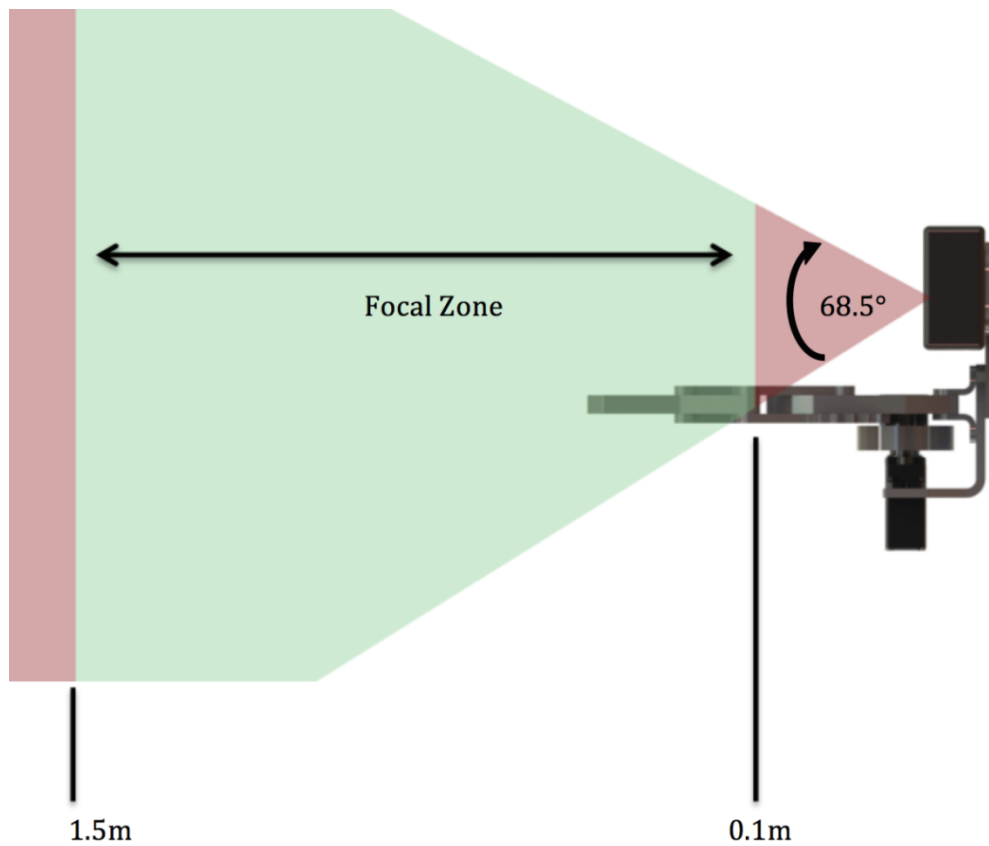


Figure 82: Focal Area of Webcams

#### 4.10.2. Initial Design

The initial design consisted of a main plate, to which the gripper module attached, and two smaller plates mounting the cameras (Figure 83).



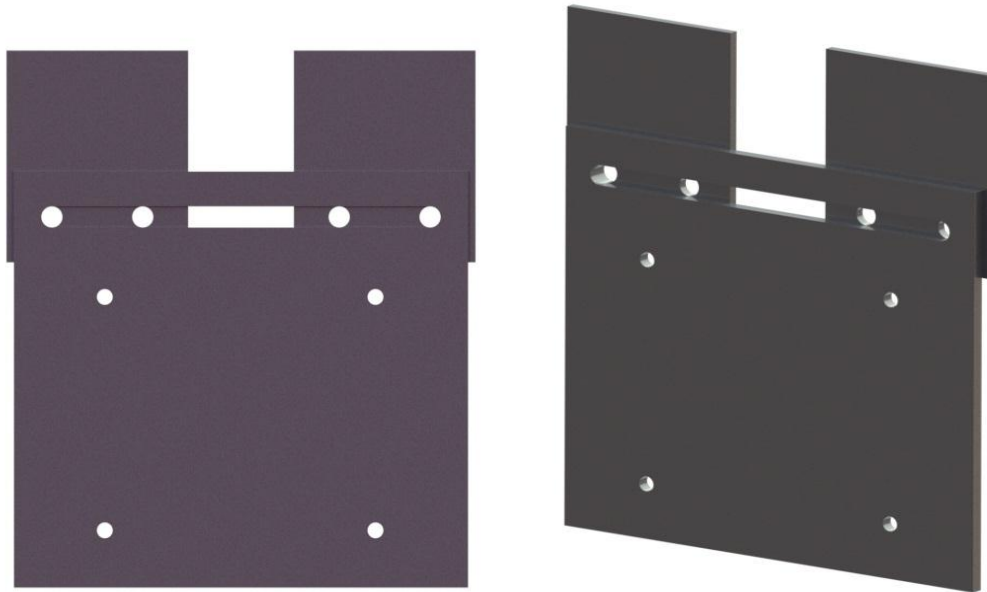


Figure 83: Initial Head Design

This initial design allowed the webcams to be adjusted correctly for use with the Oculus Rift system. However the overall design weighed 0.212kg and could not fit into the 150mm victim holes.

#### 4.10.3. Final Design

The final head plate design (Figure 84, RHS) took into the account the separation between the cameras and the selected gripper.



Figure 84: Evolution of Head Plate Design

A 79% weight saving and a 70% size reduction (Table 39) were achieved with the final design.

Table 39: Weight Comparison of Head Plate

	Initial Design	Final Design
<b>Max Dimensions</b>	150mm x 137.5mm x 4mm	105mm x 60mm x 4mm
<b>Weight</b>	0.211kg	0.042kgg

The camera mounting plates were replaced with ABS enclosures (Figure 85), weighing 68% less (Table 40) and providing more environmental protection for the cameras.

Table 40: Weight Comparison of Webcam Enclosures

	Initial Webcam Mounts	Final Webcam Mounts
<b>Max Dimensions</b>	60mm x 70mm x 3mm	40mm x 40mm x 20mm
<b>Weight</b>	0.033g	0.011g

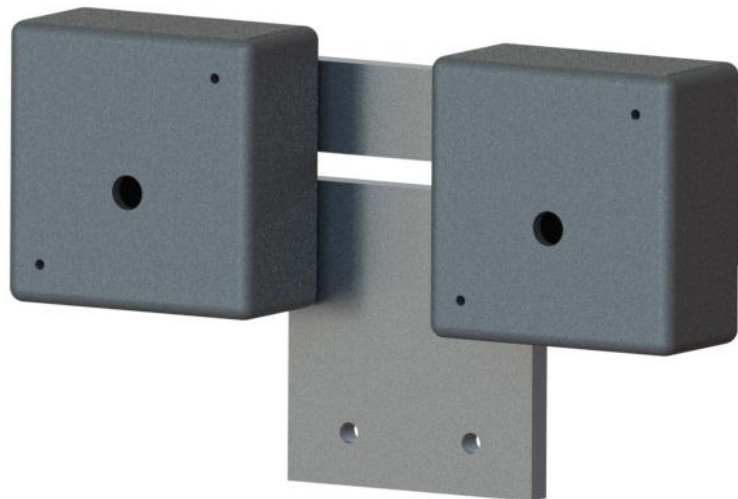


Figure 85: Final Head Design Assembly

#### 4.10.4. Head Plate FEA

Using the maximum estimated speed of the robot,  $1.69 \text{ ms}^{-1}$ , the force experienced by the head plate during a collision with the top edge of the plate was calculated. The acceleration given by Equation 18.

$$a = \frac{v - u}{t} \quad \text{Equation 18.}$$

Where:

- a is acceleration ( $\text{ms}^{-2}$ )
- v is final velocity ( $\text{ms}^{-1}$ )
- u is initial velocity ( $\text{ms}^{-1}$ )
- t is time (s)

From which the force was calculated using Equation 19.

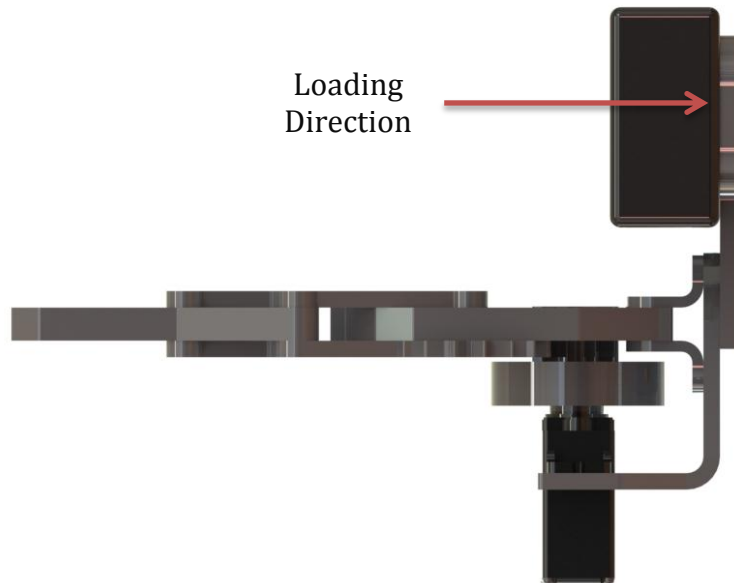
$$F = ma \tag{Equation 19.}$$

The estimated force calculated was 422.5N (Appendix D.12), however due to the several assumptions made in this calculation, a larger 500N force was used for the simulations.

The loading scenarios tested are summarised in Table 41 (calculated Appendix D.12), with the direction of loading shown by Figure 86.

**Table 41: FEA Head Loading Scenarios**

No.	Scenario	Loading Parameters
1	Collision of top edge of head plate at maximum speed of robot (1.69ms <sup>-1</sup> )	500N
2	Collision of top edge of head plate due to a fall or strike by debris	1000N



**Figure 86: FEA Head Loading Scenario**

The results produced by the test are shown in Table 42.

**Table 42: FEA Results for Head Plate in Collision Scenarios**

No.	Maximum Von Mises Stress (MPa)	Maximum Deflection (mm)
1	558.3	3.15
2	1113.9	6.26

In both scenarios, the maximum stress exceeded the yield strength of the material (Figure 87 and Figure 88), causing deformation of the plate. In Scenarios 1 and 2, the 3.15mm and

6.26mm deflection respectively would cause misalignment of the cameras, which would hamper operation of the robot. Although the strength of the plate could be increased, this would add additional mass to the head plate which would have a negative effect on the operation of the arm. It is recommended that whilst driving the robot arm should be in a stowed position reducing the risk of a full speed head collision. In the event of a collision, it is cost effective to replace the head plate with a spare (£1.43, Appendix F.1).

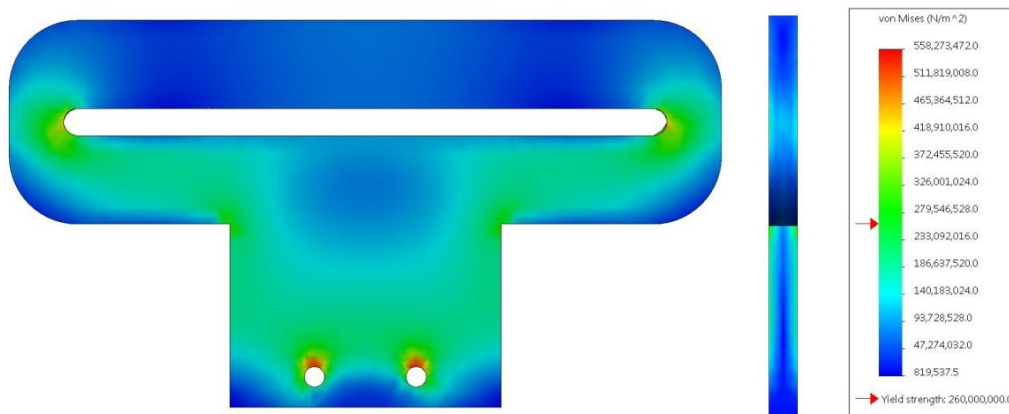


Figure 87: Von Mises Stress Analysis of Final Head Plate (500N)

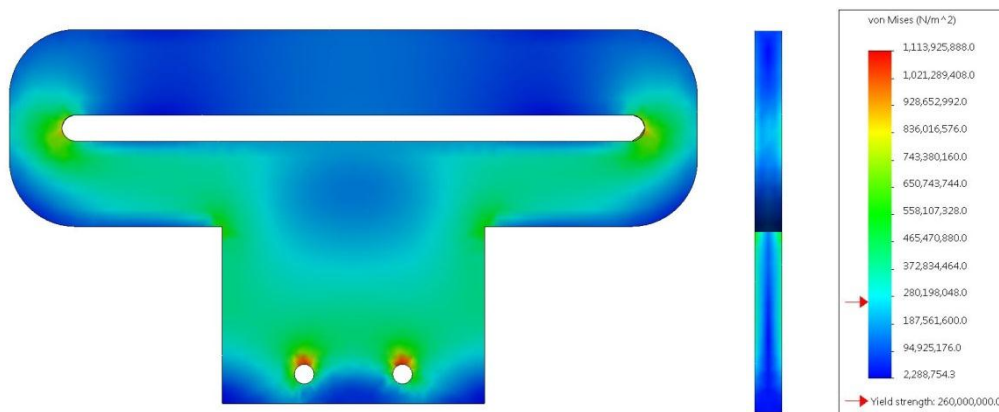


Figure 88: Von Mises Stress Analysis of Final Head Plate (1000N)

## 4.11. Virtual Testing

### 4.11.1. Gripper Testing with Manipulation of Objects

A virtual model of the Dagu gripper was constructed and used to test whether the specified objects could be gripped. This showed it was only possible to grip a 500ml water bottle with the standard fingers (Figure 89). The modified fingers were attached and shown to manipulate all objects including the maximum payload size (100x100x600mm (Figure 90)).



Figure 89: Bottle Manipulation (Original Fingers)

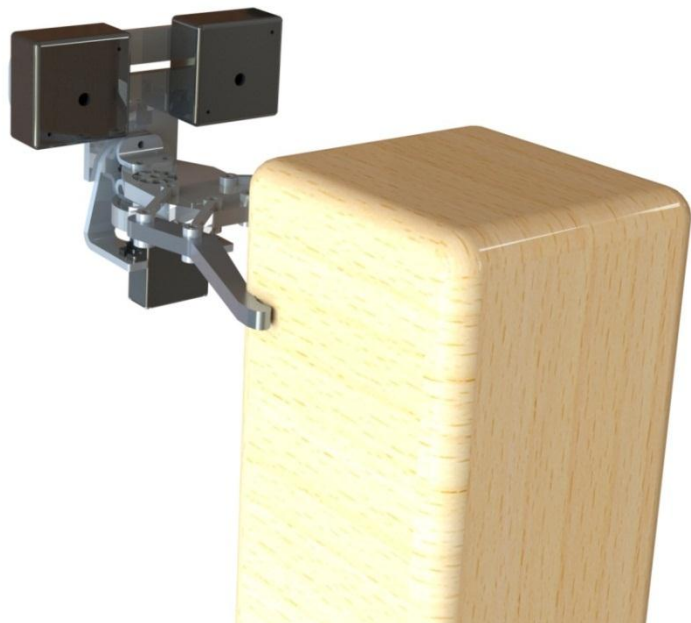


Figure 90: Balsawood Block Manipulation (Modified Fingers)

### 4.11.2. Full Arm System

Figure 91 demonstrate the arm system's capability to reach ground level victims found at the RoboCup competition. Figure 92 and

Figure 93 show the arm system's manipulation capabilities. In the current joint configuration a door can be opened inwards but not outwards and valves cannot be turned. To overcome this limitation a roll DoF is required in the wrist. Further virtual testing of the arm system's reach when combined with the chassis and drivetrain is discussed in Chapter 6.1.2.

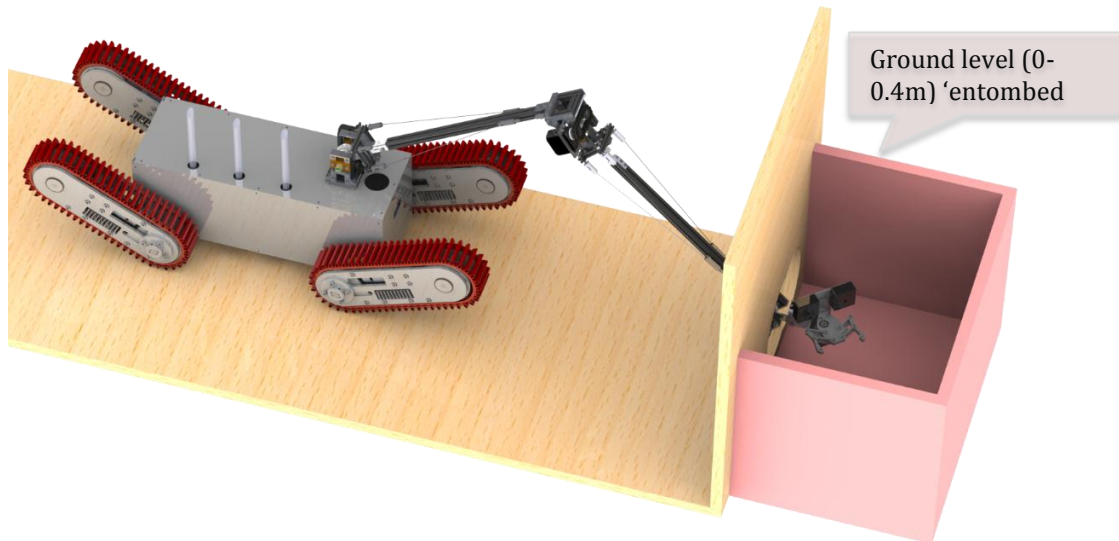


Figure 91: Ground Level Entombed Victim

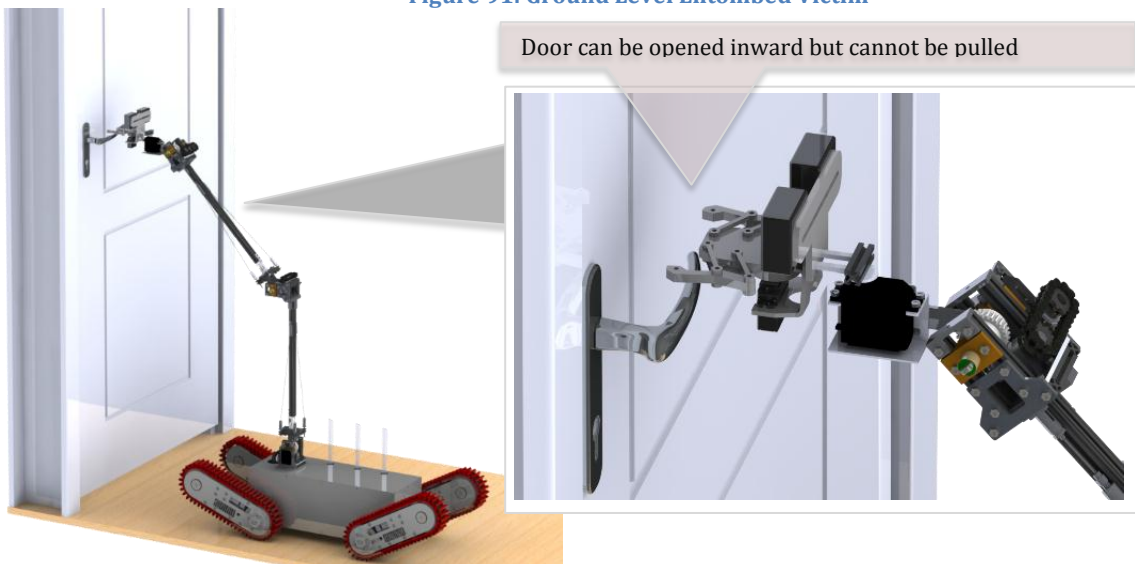


Figure 92: Door Opening Capability

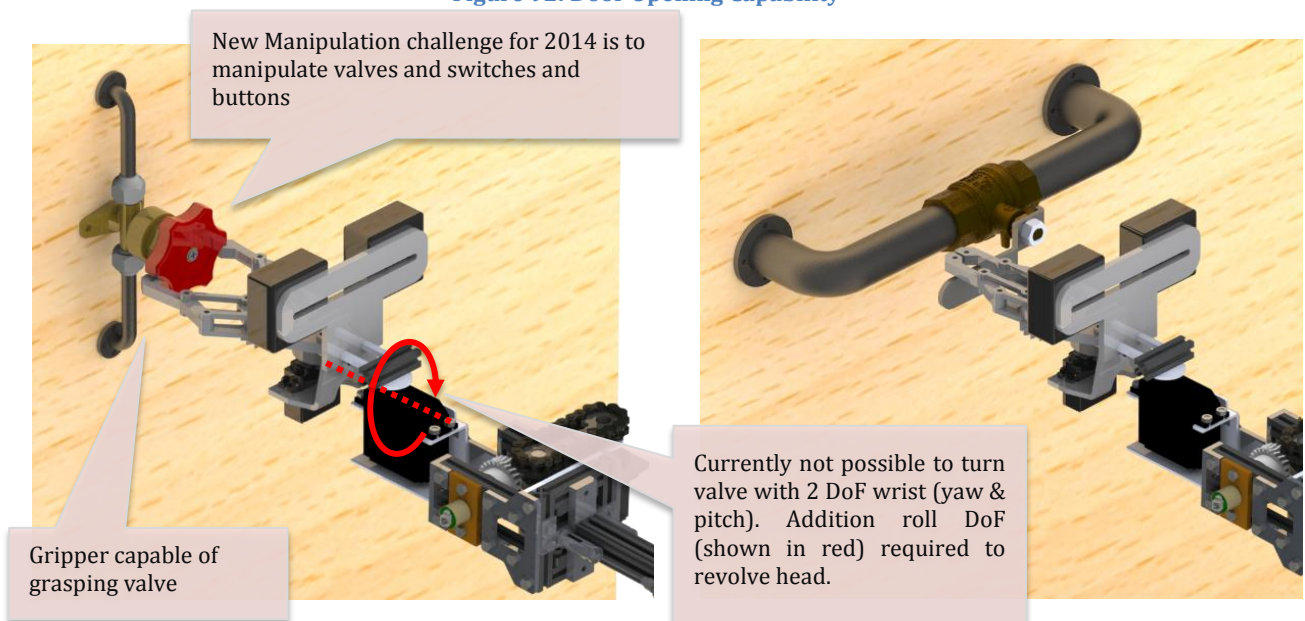


Figure 93: Valve Manipulation Tasks

### 4.12. Critical Review

Figure 94 summarises the final arm system design and compared against the initial specification in Table 43.

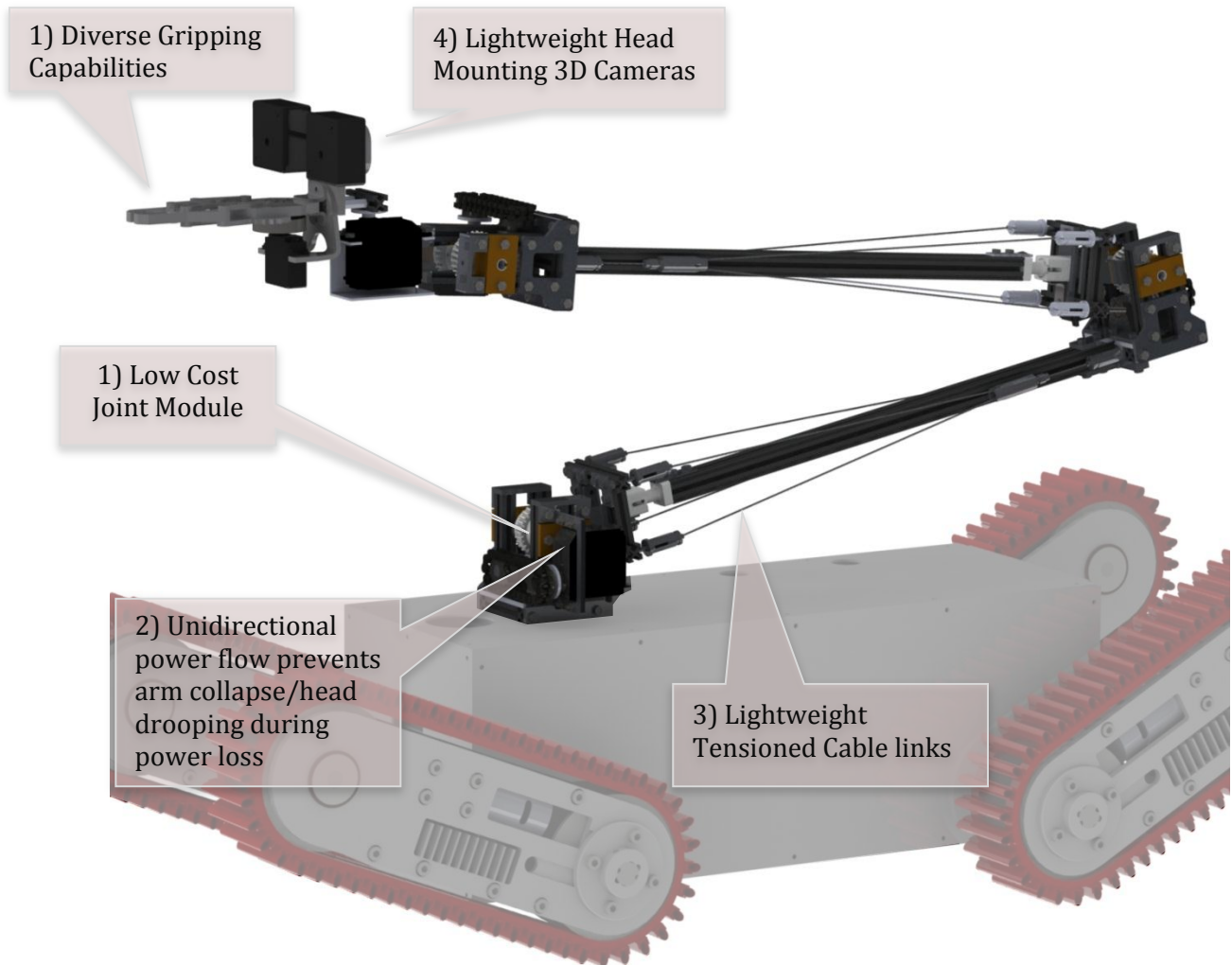


Figure 94: Final Arm System Design

Table 43: Arm System Comparison against Specification

ID	Constraint	Met?	Explanation
1	Low cost		Material cost = £522, within 4% of target
2	Lightweight		Weight =2.06kg (8.2% of maximum robot target weight). Head and gripper sub system weight =0.29kg (44% of target weight).
3	Modular		Arm system’s modularity works well as a research platform but needs to be developed to fixed modules for commercial use.
4	Size		It is possible to meet both turning circle and first responder triangle constraints, however not at the same time.
5	Reach		Reach achieved =1.4m. Reach target (1.6m) could be achieved by developing of a linear joint.

<b>6</b>	Confined spaces	Limited ability to deploy in confined spaces. Although the head can fit through 150mm holes with sufficient clearance to allow detection of victims accessing these would be more easily with a rotary base joint.
<b>7</b>	Manipulation	Current design has exposed edges which could catch on obstacles. Arm system is able to pull down door handle and push open door. End-effector is not currently able to pull open the door. This would require the implementation of a Roll DoF in the wrist. All specified objects could be held (virtually) in the gripper.
<b>8</b>	Payload	Capable of delivering up to 1kg weight within half the extension of the arm. Beyond this, 0.5kg payloads can be manipulated.
<b>9</b>	Sensors	Only horizontal position of cameras can be adjusted to align 3D vision system. Pitch and yaw adjustments cannot. Gripper is positioned within focal range of webcams. Head design allows for future sensor addition
<b>10</b>	Arm Velocity	Physical testing is required to quantify joint velocities.
<b>11</b>	Power supply	Using worm gear pairs in the joint transmission results in unidirectional flow of mechanical power preventing the arm collapsing.
<b>12</b>	Control	Encoders incorporated in the joint design allow accurate positional data to be obtained for inverse kinematic control. The software however was not implemented or tested.
<b>13</b>	Repair and Maintenance	Full arm is made with M3 bolts allowing single Allen-key maintenance.
<b>14</b>	Durability	Arm sub system designed to withstand impacts from light debris preventing damage. Webcams held within ABS enclosures protecting them from the environment.
<b>15</b>	Head Vibration	Physical testing is required to quantify free end deflection.
<b>16</b>	Rigidity	Further testing required to quantify the arm system rigidity

The arm system works well as a research platform allowing quick modification with minimal cost. This should allow future additions to the head such as sensors and new manipulation technologies. To become commercially joints and links need to be developed into self-contained units which end users cannot modify. The magnitude of head deflection from vibrations whilst driving is likely greater than the previous robot design. This was because anti-backlash worm wheels were not used due their high comparative cost. These do however provide uni-directional mechanical power flow, removing power consumption when not in use and retaining their position. The arm system still needs to be constructed and tested to quantify real world performance. Future work recommendations can be found in Chapter 6.3.



## Chapter 5. Electronics & Software

Electronics and custom software are required to power and control the USAR robot’s systems remotely while providing the operator with enough information to do this safely.

### 5.1. Electronics and Software Development Strategy

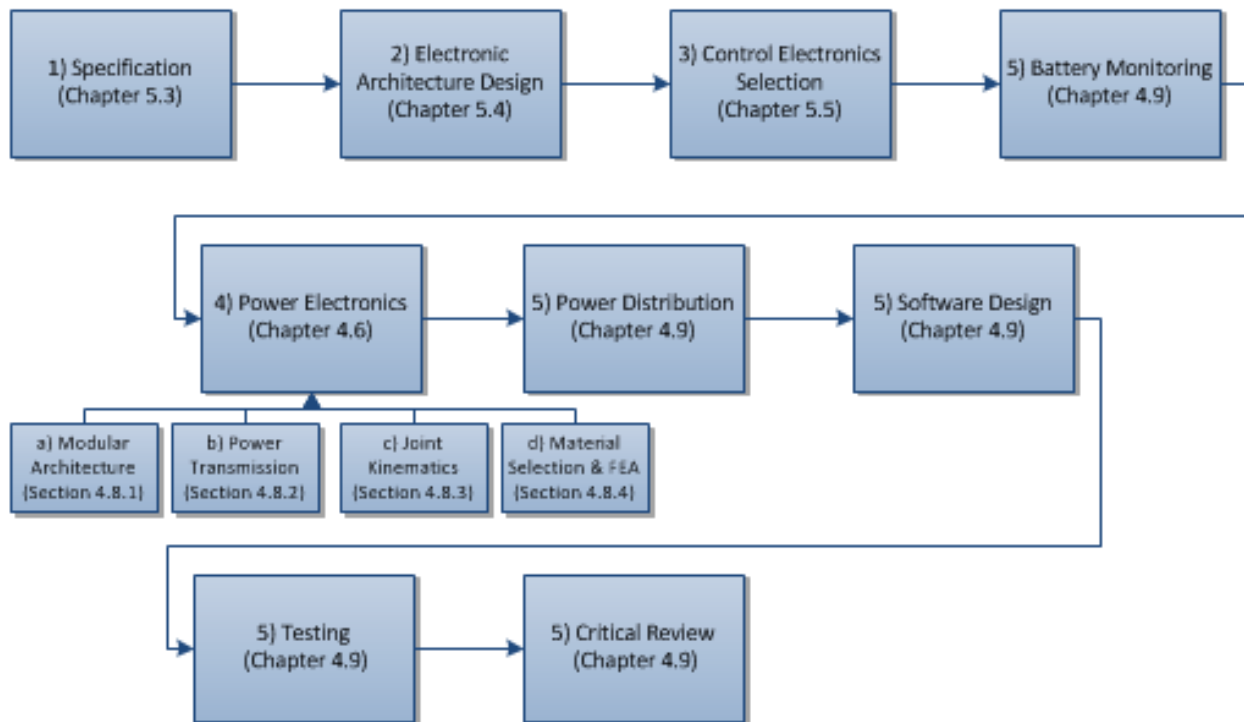


Figure 95: Electronics and Software Development Strategy

## 5.2. Specification

The specification for the new electronics and software system in Table 44 was developed from the aims and objectives, original high-level specification (Chapter 1.6) and RoboCup Rescue rules.

**Table 44: Electrical System Specification**

<b>ID</b>	<b>Parameter</b>	<b>Details</b>
1	Size	Components chosen and electronic designs should be as small as possible in volume but also not exceed dimensions specified by the chassis, drivetrain and arm design parameters to ensure they can fit in the small package space.
2	Mass	Weight must be considered when choosing components and reduced where possible.
3	Modular	Chosen components must have plug and play modularity with connectors for simple removal. Removal of devices should not affect the robots operation of other devices or its reliability.
4	Cost	Electronic components must be low cost
5	Reliability	Low cost should not affect the reliability of the device
6	Communication	Must be able to communicate wirelessly with an operators computer
7	Data	The electronics should be able to control the robot from data supplied by an operator remotely (tracks, flippers, arm) and provide the operator with enough data to control it safely (minimum of 1 camera)
8	Wiring	Simple, tidy and easy to follow wiring Fixed terminal blocks for connections Single point ground connection to prevent ground loops Identify cables with coloured wiring, labels and safety ID pins to physically prevent incorrect wiring of vital devices Produce an accurate wiring diagram for the electrical network
9	Emergency stop	An emergency stop system must be implemented, as good practice with all robotic systems, to remove all power to the drivetrain and arm motors when pressed, but keep the other electronics and communication systems active
10	Fuse Protection	Protect the battery and the robot using fuse protection
11	Protect Battery	Adequate protection from connecting in reverse polarity
12	Monitor Battery	Supply operator with battery charge levels remotely to estimate remaining drive time and prevent over-discharge
13	Improved HMI	A new human machine interface should be investigated to improve operator awareness.

### 5.3. Electronic Architecture Design

A modular electronic architecture was designed to allow a core system to function and provide basic robotic operations (Figure 96). This system could then be expanded to control additional systems; providing additional sensing, manoeuvrability or manipulation capabilities.

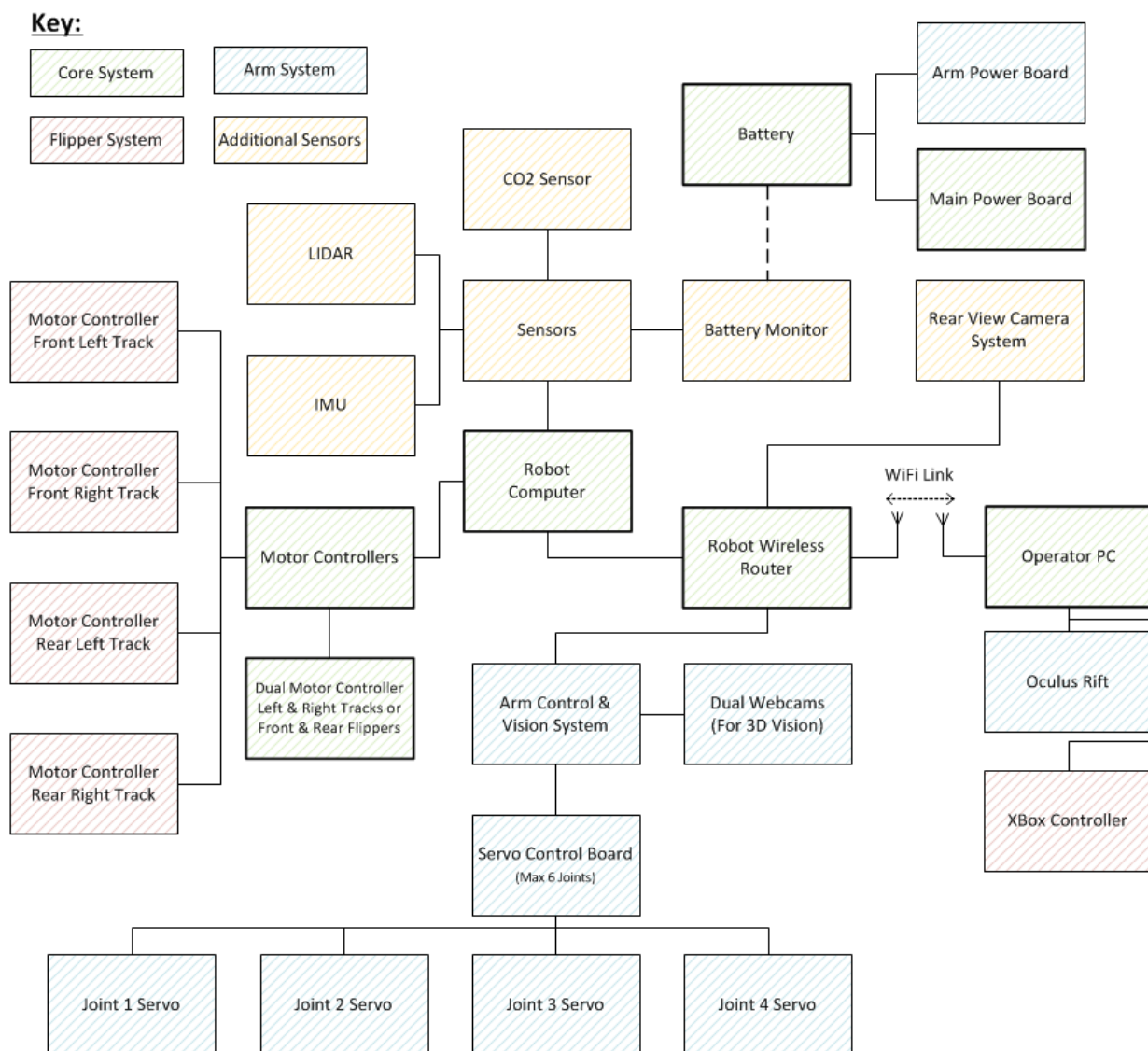


Figure 96: Robot Modular Electronic Architecture

## 5.4. Control Electronics

### 5.4.1. Human Machine Interface

An innovative way of displaying the robot's sensor data and also controlling the arm's wrist was developed. This was achieved using the Oculus Rift virtual reality gaming headset (Figure 97). This novel visual display and control method provides improved situational awareness and more natural operator control. The software is discussed in Chapter 5.7.4.

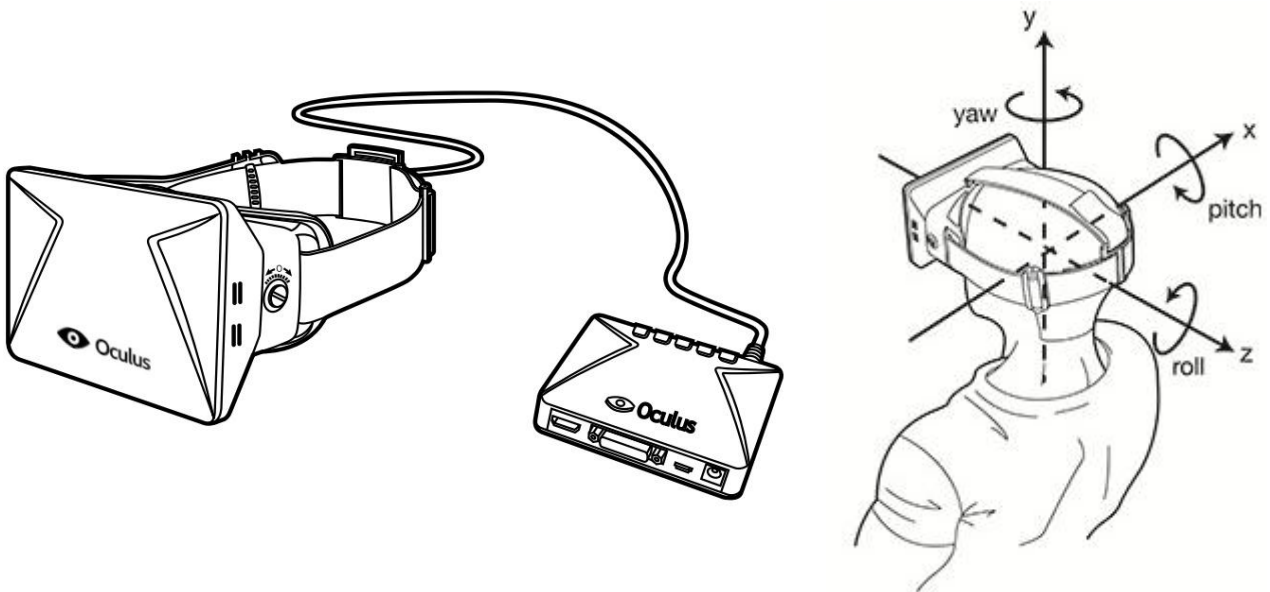


Figure 97: Oculus Rift and RPY Diagram (Oculus VR, 2013)

An Xbox controller was chosen as it had native Windows support and could be configured to vibrate providing terrain feedback from the robot's accelerometers.

### 5.4.2. Communication

Previous WMR teams had '*serious connectivity issues (at the RoboCup Competition) due to hundreds of access points in a very small area*' (Zauls & Winkvist, 2013), demonstrated by Figure 98. Two other problems identified with the current router were being inside a metal 'cage' at the arm's base (Figure 99), and secondly having a low power output (20mW). To improve connectivity the new chassis design allowed the router's antennas to extend out (Figure 100). A review of available routers was conducted and a dual band (2.4GHz and 5GHz)

router was chosen with a power output of 100mW (ASUS, 2013), five times greater than the existing router.

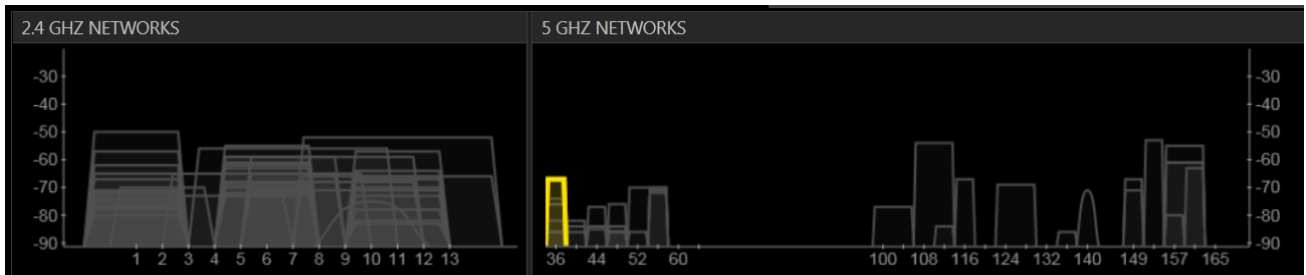


Figure 98: RoboCup 2013 Wireless Spectrum Scan (WMR, 2013)

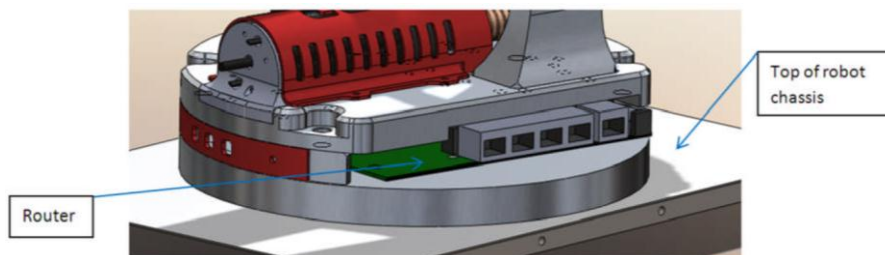


Figure 99: Existing Robot Router Placement

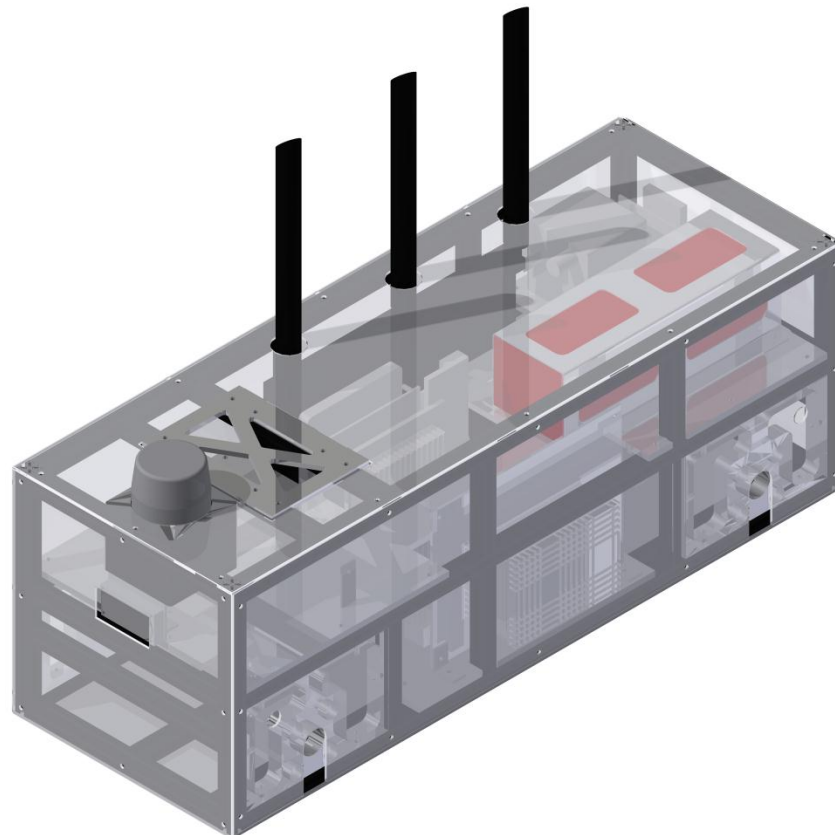
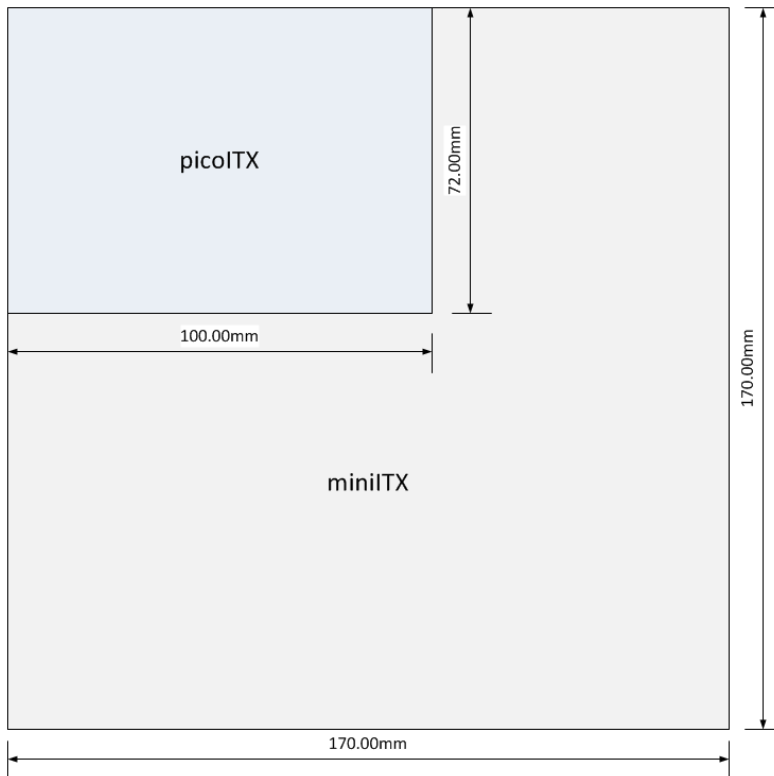


Figure 100: Chassis with the Router's Three Antennas Extruding Out (Black)

### 5.4.3. On-board Computer

Due to limited volume inside the new chassis a 1.86GHz dual core pico-ITX computer was chosen (Figure 102). This was ~60% smaller than the existing robots mini-ITX computer (Figure 101) but has the same processing capabilities.



**Figure 101: pico-ITX vs. mini-ITX Space Savings**

A small computer was required to control the arm system. A raspberry pi was chosen it was low cost and low power. This computer combined with its own power board allowing the arm system to be removed if not required; reducing the robots weight and operational time.

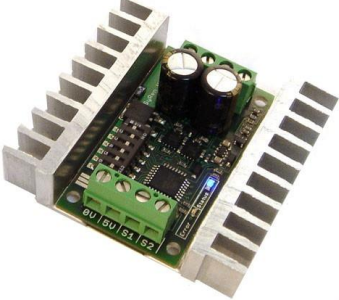
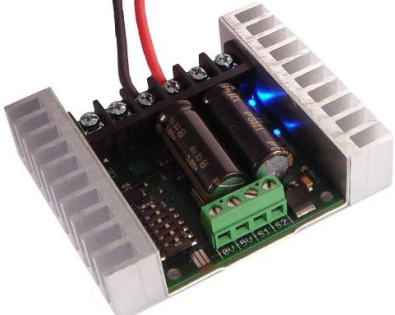



**Figure 102: Axiomtek pico-ITX Computer (Mosuer, 2013)**

5.4.4. Motor Controllers

Two different types of motors were used in the robot’s design, brushed DC motors (Drivetrain) and servo motors (Arm System). The motor controllers chosen are detailed in Table 45.

Table 45: Chosen Motor Controllers (Images and Data from (Active Robots, 2013))

Drive Motor Controller	Flipper Motor Controller	Servo Motor Controller
 <p><b>Figure 103: SyRen 25A Brushed DC Motor Driver</b> The chosen controller (Figure 103) was the only DC motor controller found which supplied the correct power (Voltage &amp; Current) to the drive motors and fitted inside the flippers units.</p>	 <p><b>Figure 104: Sabertooth Dual 25A Brushed DC Motor Drive</b> To drive the flippers two of the Drive Motor Controllers could have been used, however to save space within the chassis a sister product (Figure 104) was found which controlled two motors from the same drive unit.</p>	 <p><b>Figure 105: 1061 - PhidgetServo Controller</b> The chosen servo controller (Figure 105) was the smallest found which supplied enough power to the arm servos simultaneously when trying to move out of the worst-case loading scenario (Chapter 4.7.3)</p>

5.4.5. Sensors

Sensors were required to allow tele-operated control of the robot and obtain the maximum number of points at the RoboCup competition. Table 46 summarises the sensors required, their purpose and the chosen sensor<sup>4</sup>.

Table 46: Sensors Chosen & Why

Sensor & Purpose	Chosen Sensor	Explanation
<p><b>LIDAR:</b> To create map of the USAR robot’s environment and to mark detected victims and QR codes on it.</p>	 <p><b>Figure 106: HOKUYO URG-04LX LIDAR</b></p>	<p>The HOKUYO URG-04LX LIDAR (Figure 106) is small, runs from 5V and was already owned by WMR. (It is also the cheapest LIDAR available – 2013) (Active Robots, 2013)</p>

<sup>4</sup> Each sensor was checked to ensure compatibility with the robot’s on-board computer and software.

**Cameras:**

Required for remote vision. Two cameras for 3D vision on Oculus Rift headset and 1 or more for other locations.



Figure 107: Microsoft HD 3000 Webcam

The cameras chosen for the 3D vision system were light and low-latency HD cameras (Figure 107, (Microsoft, 2012)).

A rear view camera system was also designed and used a Raspberry Pi and dedicated camera (Figure 108), this setup was the same as network camera used in the existing robot but cost less (£45 vs. £311).



Figure 108: Raspberry Pi Camera System

**Microphone:**

Required to transmit audio from the robot to operator

No Standalone Sensor

The Microsoft webcams chosen have built in microphones capable of streaming audio to the operator.

**Inertial Measurement Unit:**

An IMU will measure the robots roll and pitch and feed this information back to the operator to try and prevent flipping the robot or rolling it in difficult terrain. IMU data will also increase the quality of mapping (Chapter 5.8.2)

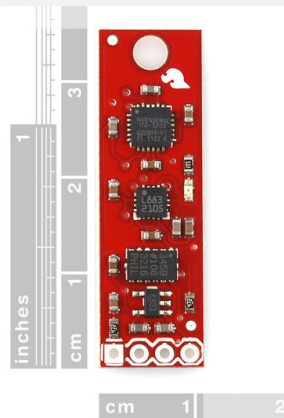


Figure 109: SEN-10724 9-Axis IMU

The SEN-10724 was chosen due to its small size and low cost at £82 (Sparkfun, 2013) in comparison to other available sensors (XSens at ~£1,000 (XSens, 2013))

**Motor Encoders:**

To control the drivetrain flipper angles and the arm joints a small absolute rotary shaft encoder was required.

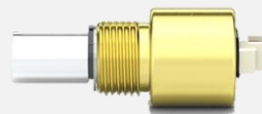


Figure 110: MA3 Miniature Absolute Shaft Encoders

The MA3 was the only miniature **absolute** shaft encoder found, all other encoders compared were either too large or required additional control electronics (Quadrature encoders). Meeting the lightweight objective each encoder was 13grams (US Digital, 2013).

**CO<sub>2</sub> Sensor:**

A CO<sub>2</sub> sensor is used in the competition to detect simulated victims and gains valuable points



Figure 111: SEN0159 CO2 Sensor

Affordable and easily accessible CO<sub>2</sub> sensors were difficult to obtain. The SEN0159 was the only sensor found to meet the specification and cost £33.50 (DFRobot, 2014).



## 5.5. Power Electronics

### 5.5.1. Research Summary

A SWOT analysis was performed on previous robot's power distribution networks (Appendix E.2) summarised in Table 47.

**Table 47: Analysis of the existing USAR power board**

<b>Section</b>	<b>Good/Bad</b>	<b>Analysis &amp; Recommendation</b>
<b>DC-DC Converters</b>	Good	The Traco DC-DC converters are small and have been used without issue by previous WMR teams
<b>Harwin Connectors</b>	Good	Connectors are small and are protected from connecting in reverse polarity. Harwin are also a team sponsor providing the required connectors for free.
<b>nFET/pFET Switches</b>	Good	These switching ICs are used to control the voltage outputs. They are small and can deliver appropriate power to the load. Switchable outputs will conserve battery power when devices are not required.
<b>4 Layer PCB</b>	Bad	A four layer PCB was expensive to manufacture externally
<b>Battery Monitoring</b>	Bad	Previous circuits did not function. Monitoring the battery voltage will give an indication of remaining drive time.
<b>Little Fuses</b>	Good	These fuses are small, surface mount fuses with proven reliability on the USAR robot
<b>Connector Access</b>	Bad	Previous design has issue with access to connections when installed in the chassis. This should be considered in the design process.

To meet the modularity aims (Chapter 1.6 – 2.a) and modular electronic architecture (Chapter 5.4) two PCBs (Printed Circuit Boards) were required. A main power board and an arm power board to allow the arm system to be removed when not required. This first delivers power to the core control electronics and the second to the robotic arm and head electronics.

### 5.5.2. Power Board Requirements

Individual output power requirements for the main power board and the arm power board were dictated by the control electronics chosen in Chapter 5.4 resulting in the output requirements in Table 48 and Table 49.

**Table 48: Required Outputs for the main power board**

Name	Voltage (V)	Current (A)	Power (W)	Fuse (A)	Notes
<b>Router</b>	15	1.6	24	2	19V router will be run off 15V.
<b>Total 15V Power:</b>			<b>24</b>		
<b>pico-ITX</b>	5	3.5	17.5	5	Usually 3A but additional 0.5A due to more RAM
<b>Rear Camera</b>	5	2	10	3	
<b>IMU</b>	5	6.6m	33m	2	
<b>LIDAR</b>	5	0.8	4	2	
<b>CO<sub>2</sub> Sensor</b>	5	<0.5	2.5	2	
<b>Total 5V Power:</b>			<b>34</b>		

**Table 49: Required Outputs from the Arm Power Board**

Name	Voltage (V)	Current (A)	Power (W)	Fuse (A)	Notes
<b>Arm Servos</b>	12	5	60	no	Use 60W Traco (12V at 5A)
<b>Total 12V Power:</b>			<b>60</b>		
<b>Raspberry Pi</b>	5	2	10	no	
<b>ATTiny</b>	5	~1	5	no	Based on full load
<b>Spare Output</b>	5	~1	5	no	Not used, for future use.
<b>Total 5V Power:</b>			<b>20</b>		

The total power requirement of the control electronics was 138W (This included all arm servos running at full load). This equated to a maximum current draw of 6.21A from the battery, calculated by Equation 19 (Williams, 2005):

$$I = \frac{P_{total}}{V_{Battery}} = \frac{138W}{22.2V} = 6.21A \quad \text{Equation 20.}$$

Where:

I is the current (A)

P is the power (W)

V is the voltage (V)

This is composed of 2.61A & 3.6A from the main power board and arm board respectively. As the arm servos will be used infrequently a running time of the robot was calculated to be 1 hour 34 minutes:

$$Time = \frac{Battery\ Capacity\ (Ah)}{Current\ Draw\ (A)} = \frac{5.5Ah}{\left(\frac{78W}{22.2V}\right)} = \frac{5.5}{3.51} = 1.57hours \quad \text{Equation 21.}$$

### 5.5.3. Trace Widths

The PCBs copper traces were to be designed to handle the appropriate operational current (Table 48 and Table 49). The trace widths were calculated using the IPC 2221 PCB technical design requirements (IPC, 2003) Equation 21.

Imperial units of measurement were used for the design of the PCB trace widths “...as a general rule, use imperial for tracks, pads, spacing’s and grids. Only use mm for mechanical and manufacturing type requirements like hole sizes and board dimensions.” (Jones, 2004). The thickness of the copper trace is fixed at 35µm (1.38 mils) due to the manufacturing process.

$$I = k \times \Delta T^{0.44} \times A^{0.725} \quad (\text{IPC, 2003}) \quad \text{Equation 22.}$$

Where:

I is current (A)

A is the cross sectional area (mils<sup>2</sup>)

ΔT is the temperature rise (°C)

K is a constant = 0.048 for outer layers and 0.024 for inner layers.

Rearranging Equation 21 gives the area in mils for the required current.

$$Area\ (mils^2) = \left( \frac{I}{(k \times \Delta T)} \right)^{0.44 \left( \frac{1}{0.725} \right)}$$

$$Width(mils) = \frac{A}{(Thickness \times 1.378)} \quad (\text{TheCircuitCalculator.com, 2006})$$

### 5.5.4. Switchable Outputs

An ATTiny microcontroller communicates over the Inter-Integrated Circuit (I<sup>2</sup>C) protocol with the main computer to switch an nFET/pFET pair of transistors to control each output (Figure 112). The 5V output from the ATTiny provides a high enough gate voltage (1.8 V from Figure 113) to the nFET allowing it to pull the gate of the pFET to 0V and hence allow the output to be connected to the 5V supply. The 1MΩ resistors are ‘bleed’ resistors designed to discharge the gate capacitance during switching. The resistor value was not crucial so a high resistance was chosen to reduce the current drawn. The Vishay Si4564DY switching Integrated Circuit (IC) was used as it has a maximum current ( $I_{DS}$ ) for transistors of  $\approx 9.2A$  (Vishay Siliconix, 2010) and uses less PCB surface area when compared to external through-hole transistors.

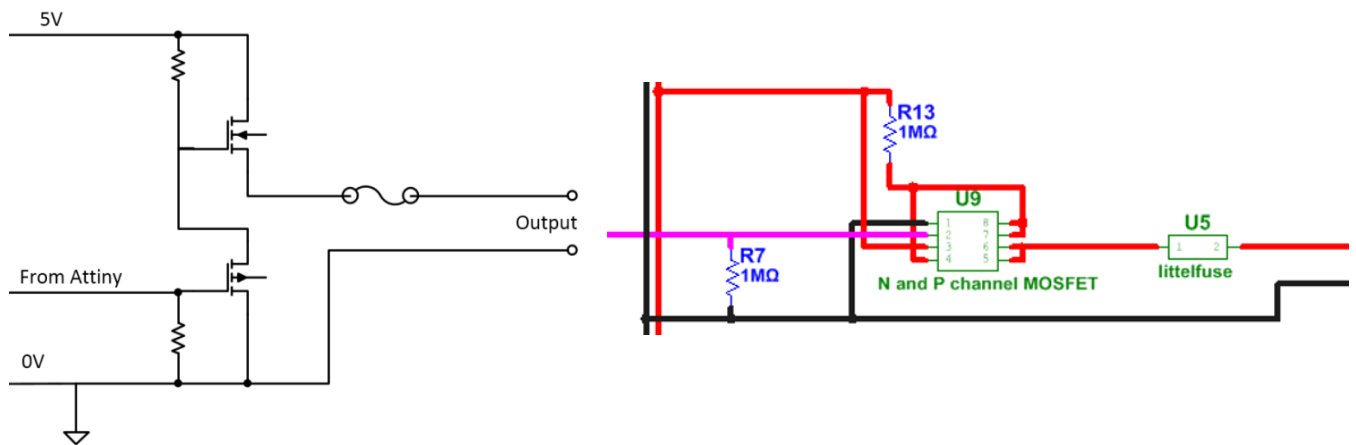


Figure 112: nFET and pFET switching circuit (left) and Multisim layout (right)

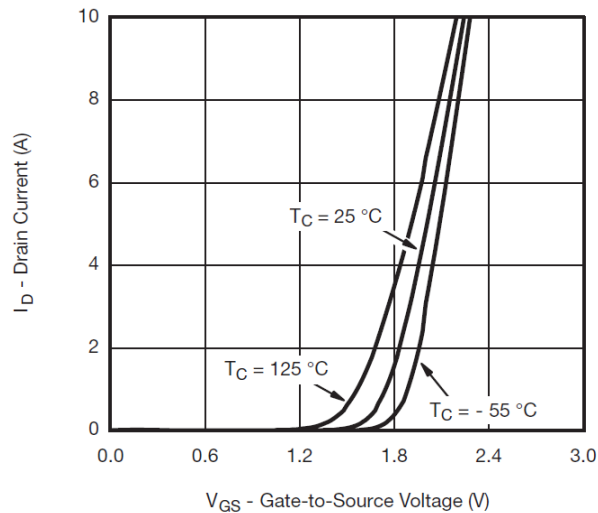


Figure 113: nFET and pFET transfer characteristic (Vishay Siliconix, 2010)

### 5.5.5. Cables Sizing and Fuse Protection

Cable sizing was based on the 17<sup>th</sup> Edition IEEE wiring regulations (Whitfield, 2008). Easy to replace fuses ‘Littelfuse’ were chosen to ensure protection for safety critical circuits. A minimum fuse value of 135% larger than the load current was chosen as recommended in the Optifuse fuse selection guide (OptiFuse, 2010).

### 5.5.6. Final Designs

The circuits were designed using Multisim (Figure 114 and Figure 115) and then transferred to Ultiboard<sup>5</sup> for the PCB design (Figure 116 and Figure 117). The PCBs are both two layer boards with power and ground routed on the bottom (red) and signals on the top (green). The ‘IPC 2221 - A guides to better design the layout of the board’ (IPC, 2003) were followed. To save space inside the chassis the arm power board was also designed to allow direct mechanical and electrical connection to the Raspberry Pi.

<sup>5</sup> Multisim & Ultiboard are software packages by National Instruments which allow circuit schematic layout, wiring and PCB design.

1) Input to Traco power including 47µF capacitor as per Traco power application note.

2) Level translator to convert two wire bus from 3.3V to 5V so that it can integrate with the whole system.

3) Attiny outputs 5V to gate of nFET to switch outputs high.

4) Vishay Switching IC including the nFET/pFET pair. 1MΩ 'bleed' resistors to discharge gate voltage.

5) Harwin connector with 5V supply to Raspberry Pi and 3.3V coming back for the IMU.

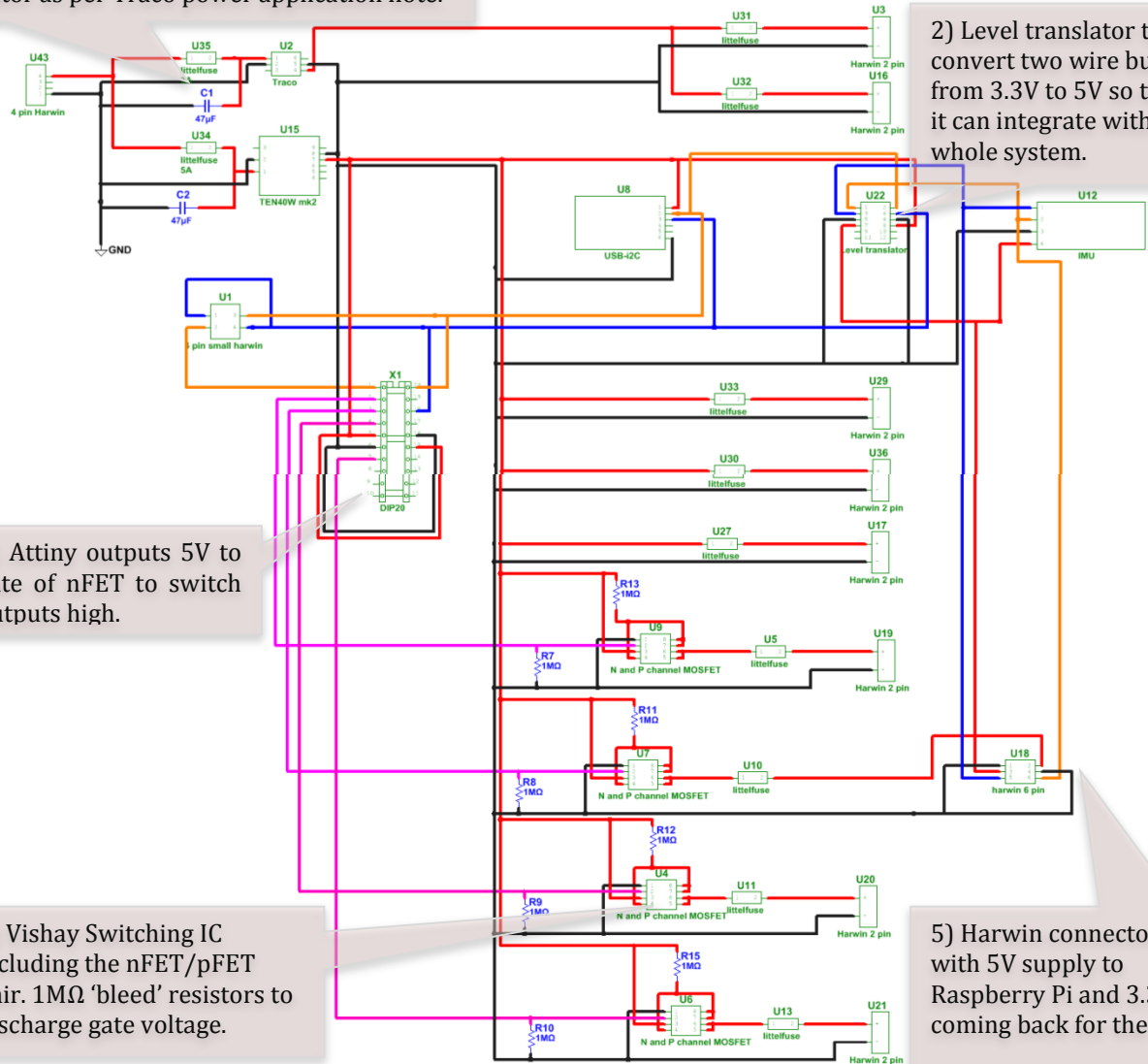


Figure 114: Main Power board Multisim Schematic

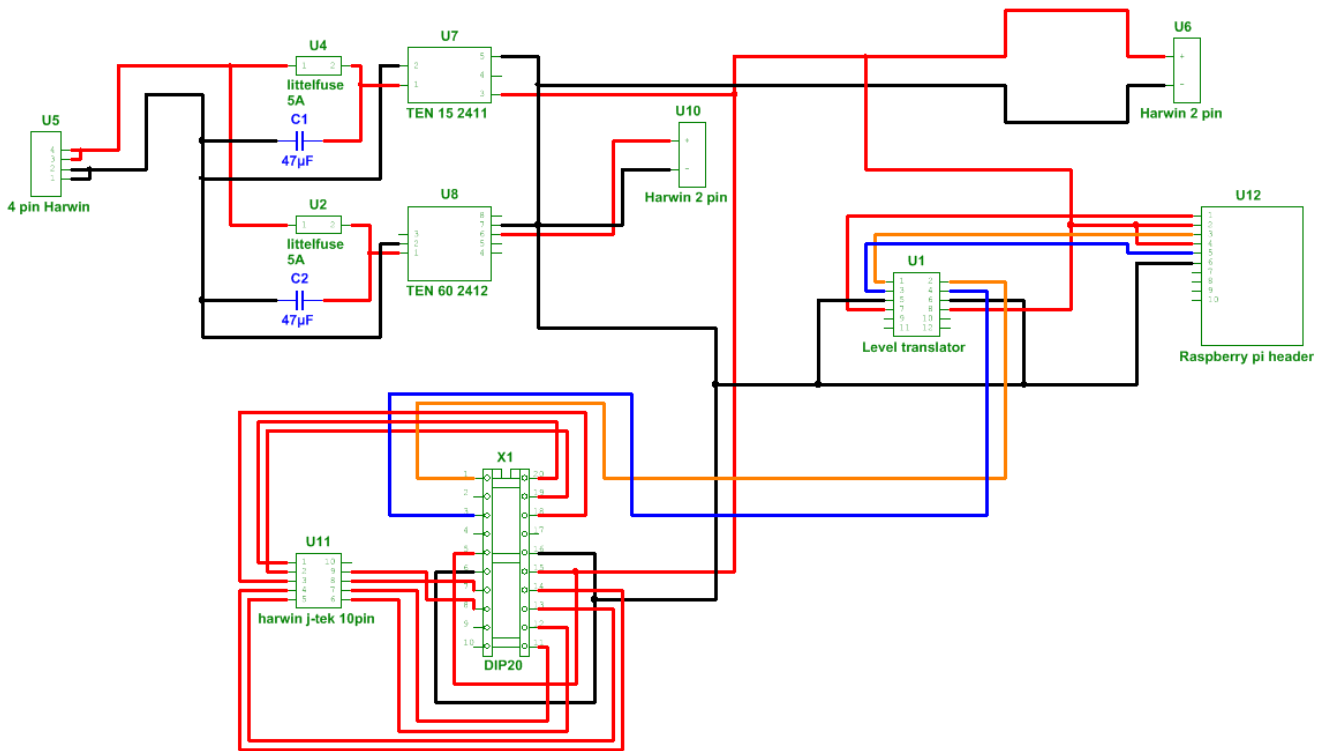


Figure 115: Arm Power board Multisim Schematic

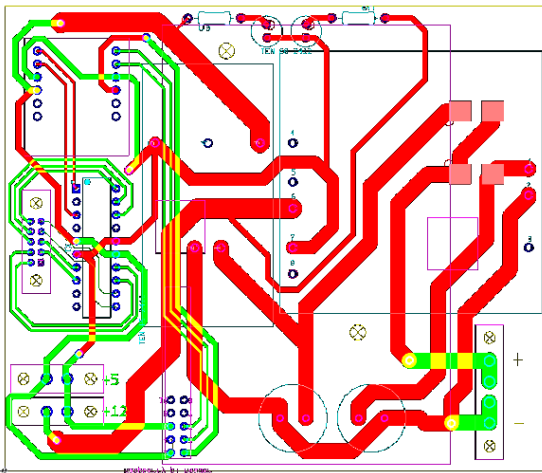


Figure 116: Ultiboard Layout of Arm Powerboard

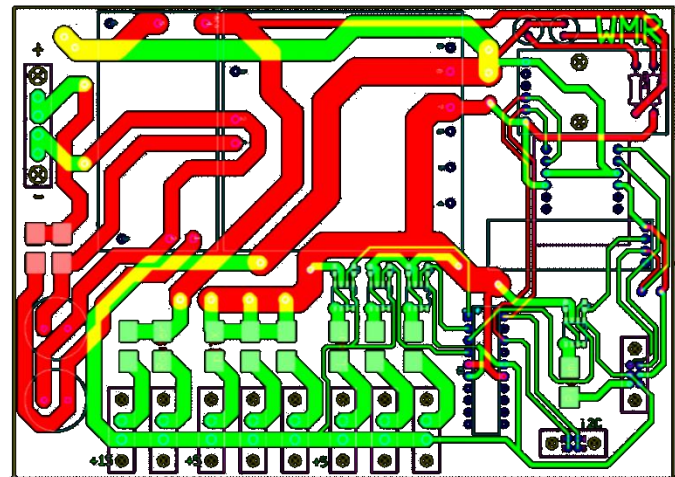


Figure 117: Ultiboard Layout of Main Power board

Figure 118 displays the designed boards in 3D before they were manufactured.

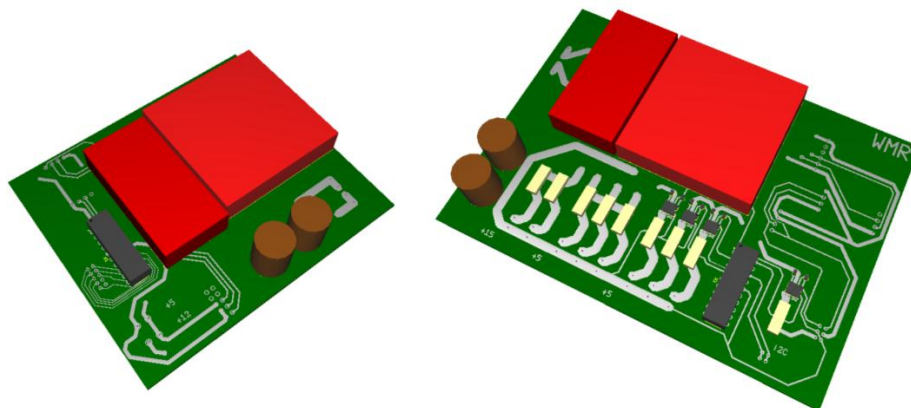


Figure 118: 3D Representation of the boards using Ultiboard 3D preview

### 5.5.7. Manufacture

The PCBs were manufactured by the School of Engineering (Figure 119) using a computer controlled router (~25% cheaper than externally (Quick-tech Ltd, 2013)). Through-hole and surface-mount components were soldered by hand. Spacers were machined using a lathe to give structural strength to the breakout boards and the Raspberry Pi.

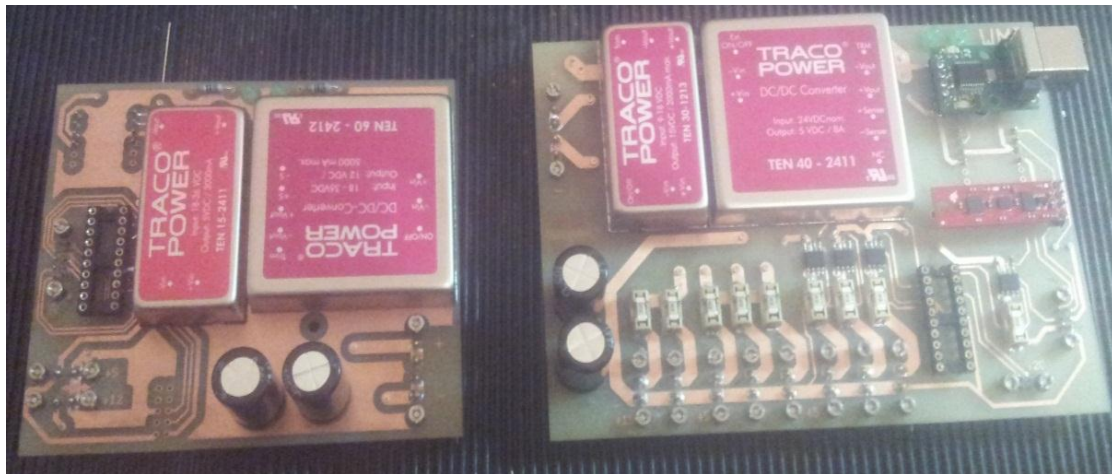


Figure 119: The PCBs after component soldering



### 5.6. Power Distribution

#### 5.6.1. Battery Monitoring

A number of designs were considered and simulated using Multisim (Table 50). However the simulated designs did not meet the specification within the project’s timescale.

Table 50: Battery Monitoring Design

Design	Explanation
<p>Vbatposin Vbatneg Vbatposout Vmonitortoplus Vok Vlow Vcrit Vmonitorgnd</p> <p>R4 91kΩ 1% X1.4 R5 10kΩ R6 91kΩ 1% X1.5 R7 10kΩ R8 75kΩ 1% X1.6 R9 10kΩ</p> <p>U1 LM311H U2 LM311H U3 LM311H</p> <p>R1 1kΩ 5 R2 1kΩ 4 R3 1kΩ 3</p> <p>U4A 74LS04 U4B 74LS04 U4C 74LS04</p> <p>LED1 X1.10 680Ω LED2 X1.11 680Ω LED3 X1.13 680Ω</p> <p>D1 BZX84-A2V4</p> <p>Vbat 25.2v OK: Green LED lit and 'Vok' '1' Vbat 22.5v Low: Orange LED Lit, Green unlit and 'Vlow' '1' Vbat 20.1v Critical: Orange and Red Lit, Green unlit, 'Vcrit' '1' and 'Vlow' '1'</p> <p><b>Figure 120: Battery Monitor Design 1</b></p>	<p>X2 X1 X3 2.5 V 2.5 V 2.5 V X2 X1 X3 2.5 V 2.5 V 2.5 V X2 X1 X3 2.5 V 2.5 V 2.5 V</p> <p>The circuit in Figure 120 changed three output LEDs depending on the voltage level of the battery. However did not pass this information to the operator.</p>
<p>V1 3.4 V V2 3.4 V V3 3.4 V V4 3.4 V V5 3.4 V V6 3.4 V</p> <p>R1 50kΩ 1% R2 5kΩ 1% R3 1kΩ R8 75kΩ 1% R9 10kΩ</p> <p>U3 LM311H U4C 74LS04</p> <p>LED3 X1.13 680Ω D1 BZX84-A2V4</p> <p>R11 470Ω</p> <p>Vbatposout Vmonitorplus analogue Vcrit Vmonitorgnd</p> <p><b>Figure 121: Battery Monitor Design 2</b></p>	<p>This improved circuit (Figure 121) output an analogue voltage from a potential divider which could be read in from a microcontroller to obtain the actual battery voltage. It also included a warning LED for when the battery voltage reached a critical level.</p>

### 5.6.2. Safety System

The robot required an emergency stop button to halt the drivetrain and arm motors when pressed but maintain power to all other control components.

The maximum current the five motor control boards for the drivetrain can draw is 25A (Chapter 5.4.4), however the maximum efficiency current of the motors is 8.5A and should stay within 50% of this under normal loading conditions (Gimson Robotics, 2013). This equated to a maximum current draw of 63.75A from the battery under normal conditions.

$$\begin{aligned} \text{Max Efficient Current} \times \text{Variation} \times \text{No. Motors} &= \\ 8.5A \times 1.5 \times 5 &= 63.75A \end{aligned}$$

A safety factor of 20% was added making the required relay's current rating 80A. An 80A fuse was included, designed to blow if the current exceeded these normal operating conditions, protecting the circuitry and relay.

The arm servo motors operate on 12VDC, with the ability to draw 5A. A separate relay was needed to operate at the different voltage of 12V. The E-stop circuit was first simulated using Multisim to ensure the correct operation and measure current flow through the circuit (Figure 122).

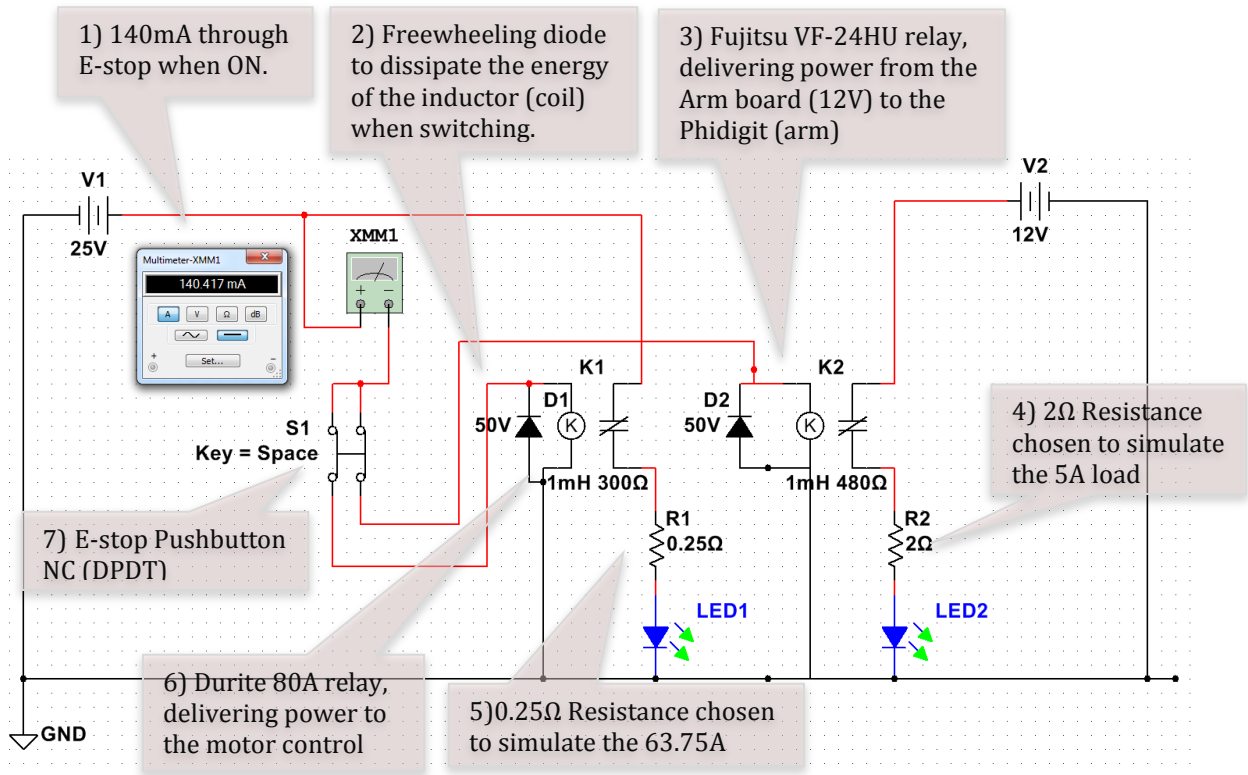


Figure 122: Emergency stop circuit designed using Multisim

### 5.6.3. Wiring Diagrams

Electrical drawings were created to enable simpler wiring of the robot (Figure 123). A full system wiring diagram can be found in Figure 124.

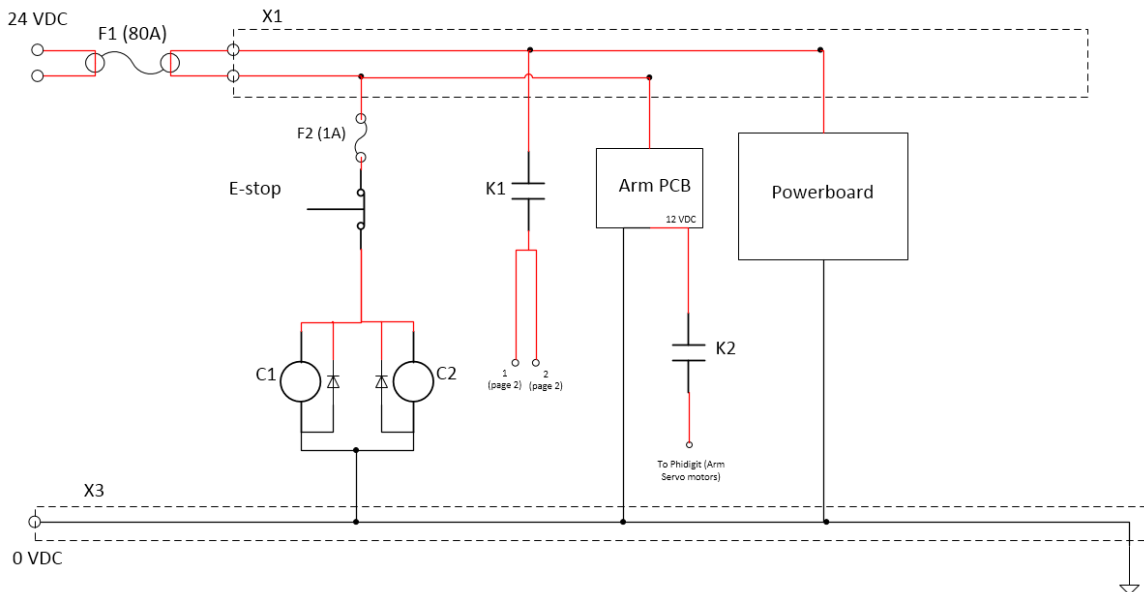


Figure 123: Emergency Stop Electrical Drawing

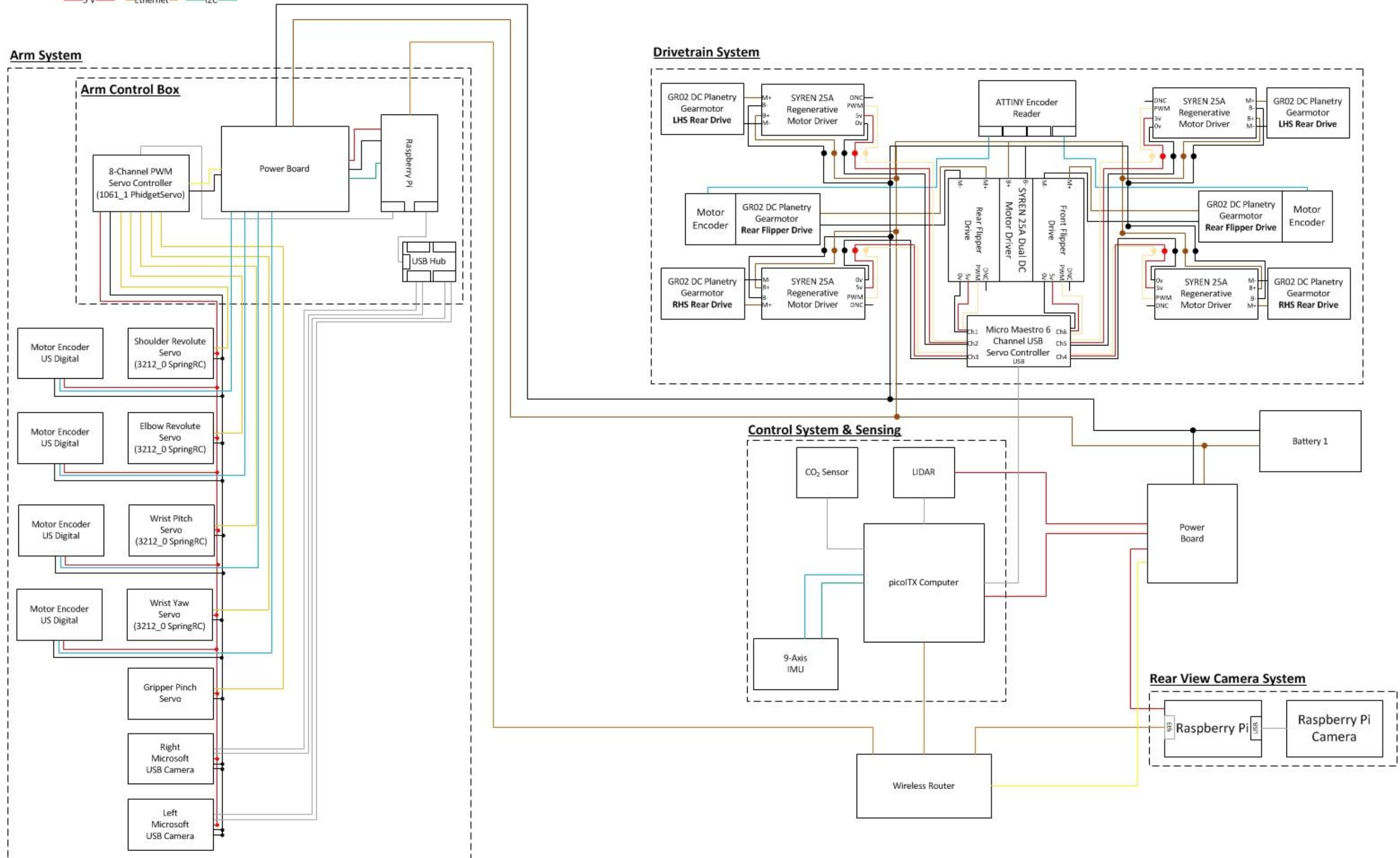
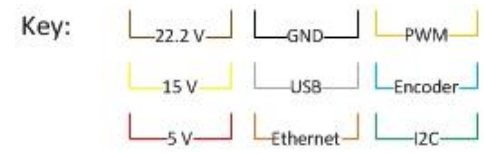


Figure 124: Full System Wiring Diagram

## **5.7. Software Design**

### **5.7.1. ROS**

Ubuntu running Robot Operating System (ROS) was chosen for the new robot. ROS is a flexible framework for writing robot software (ROS, 2014) and allows software to be run as nodes across different devices to allow distributed computing. This allows the modularity and plug and play functionality required. ROS also provides access to a lot of open source software, available to use and modify freely, decreasing development time and increasing functionality. An additional benefit is that although natively written in C++ and Python, nodes can be written in any programming language. This allows future teams to develop in their strongest language.

### **5.7.2. URDF**

ROS uses Unified Robot Description Format (URDF) files to represent and visualise a robot. Each robot section is described with dimensions and connections. The URDF model for the new robot (Appendix E.1) was used to create the node network and visualisation in Figure 126.

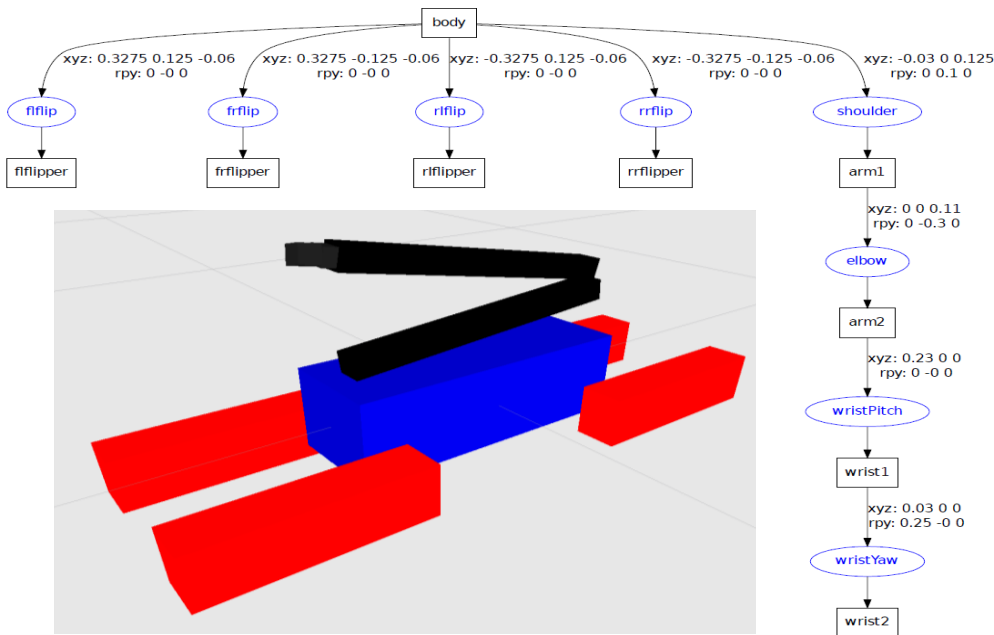


Figure 125: USAR URDF Node Network and Model Visualisation Produced

### 5.7.3. Mapping

2D mapping was implemented using ROS and Hector Slam<sup>6</sup>. A node network (Figure 126) was created for the robot’s URDF model, LIDAR position & data to create the maps. (Testing in Chapter 5.8.2).

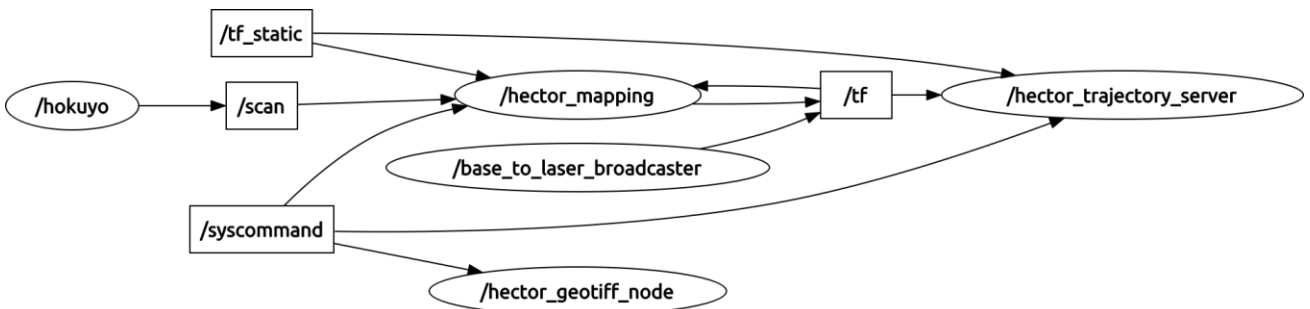


Figure 126: Node Network Created for Mapping

### 5.7.4. 3D Headset Display

Figure 127 shows the designed Head’s Up Display for the Oculus Rift augmented reality display. Each part of the overlay will be fed with data from the robot’s sensors and has been written to dynamically update with this data as shown in Figure 128 and Figure 129.

<sup>6</sup> Hector Slam is an open source mapping framework requiring modification based on the robot’s form & sensors

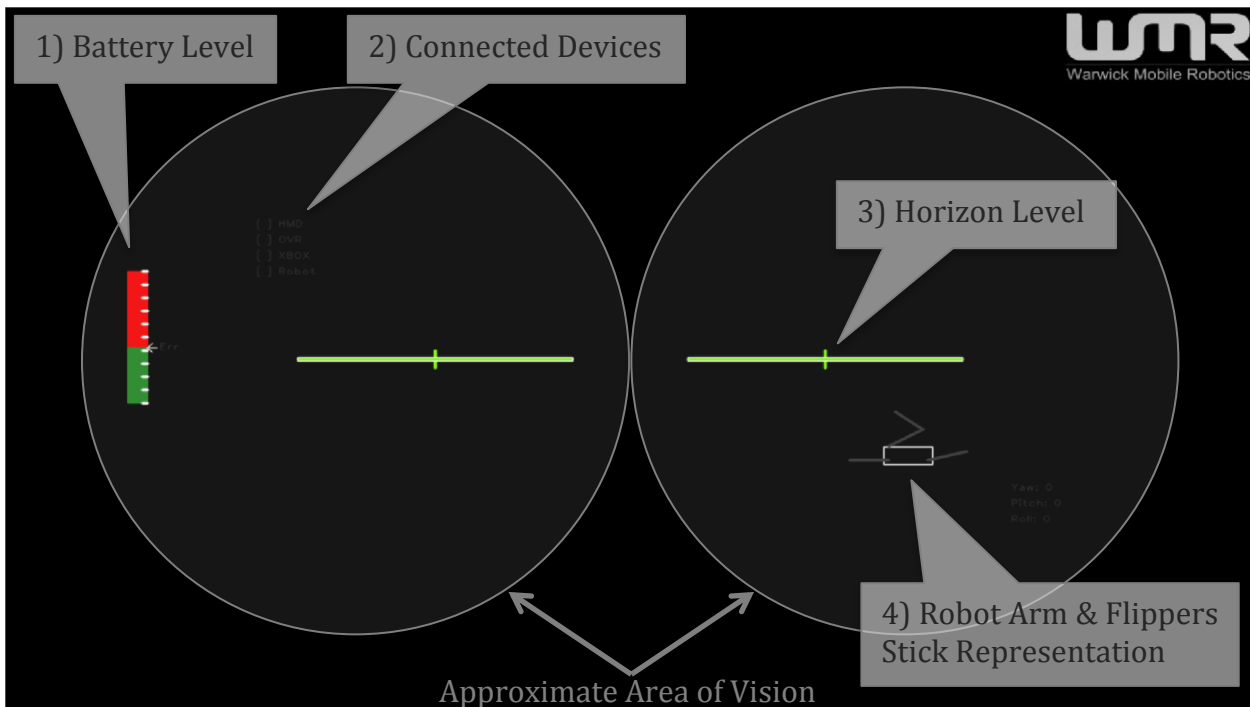


Figure 127: Oculus Rift Headset Display Overview

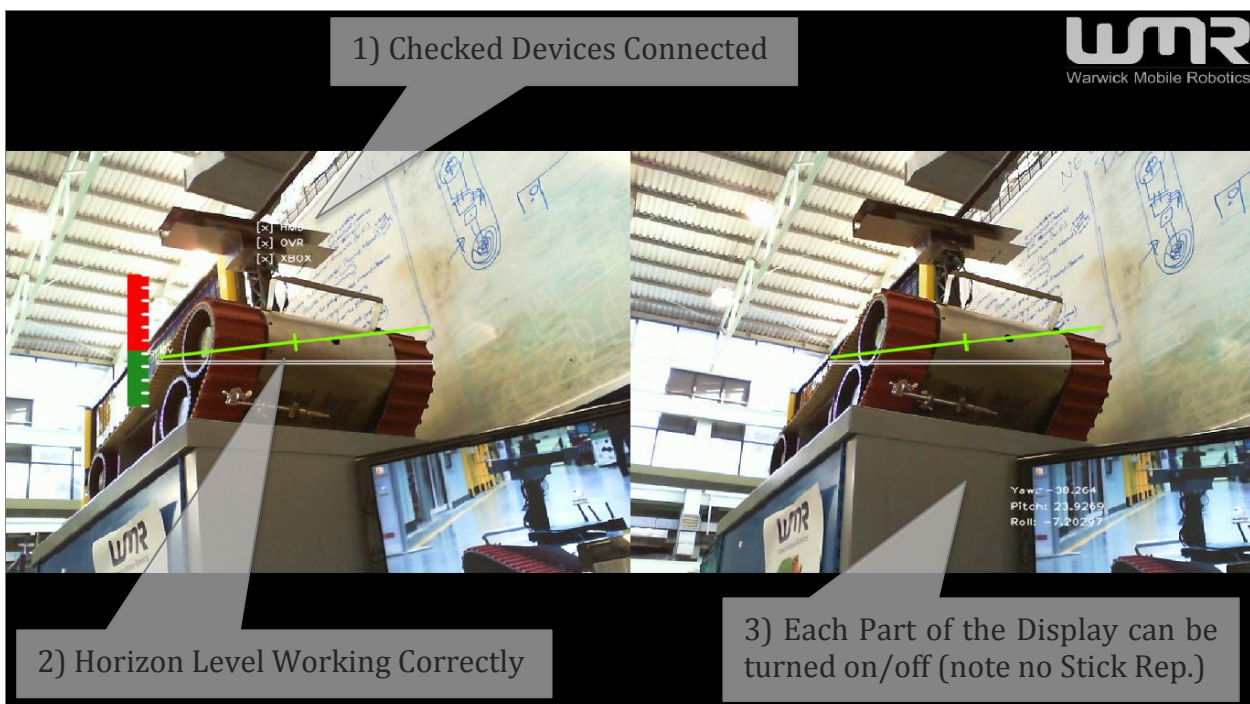


Figure 128: Oculus Rift Displaying Two Different Video Streams & Horizon Level (1)

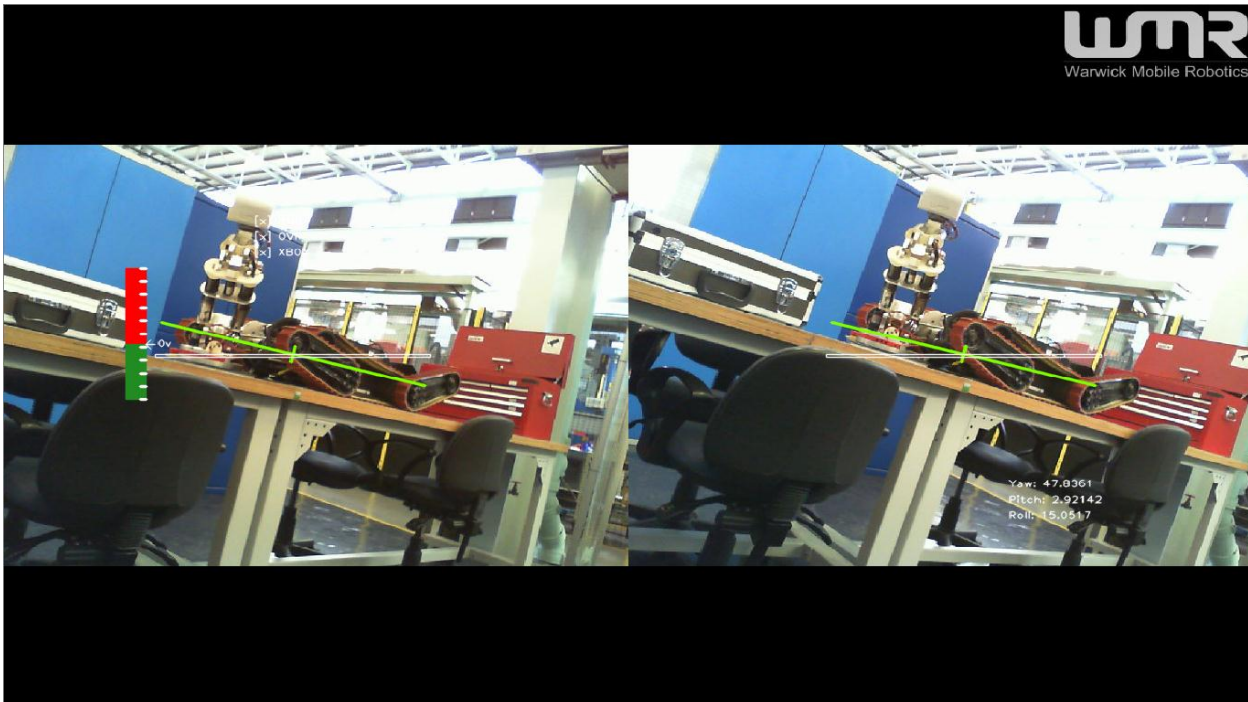


Figure 129: Oculus Rift Displaying Two Different Video Streams & Horizon Level (2)

The Roll, Pitch, Yaw (RPY) angles were also read from the Oculus Rift continuously and fused to the RPY angles of the existing robot's arm's wrist, meaning the operators head movement controlled the wrist movement for intuitive control.

## 5.8. Testing

### 5.8.1. Control Electronics

As the robot design was not complete the control electronics could not be tested. The system has the software installed ready to test once manufacturing is complete.

### 5.8.2. Mapping Software Testing

The mapping software was ported to the existing robot to test at the RoboCup German. Figure 130 shows one of the maps created and explains the key features.



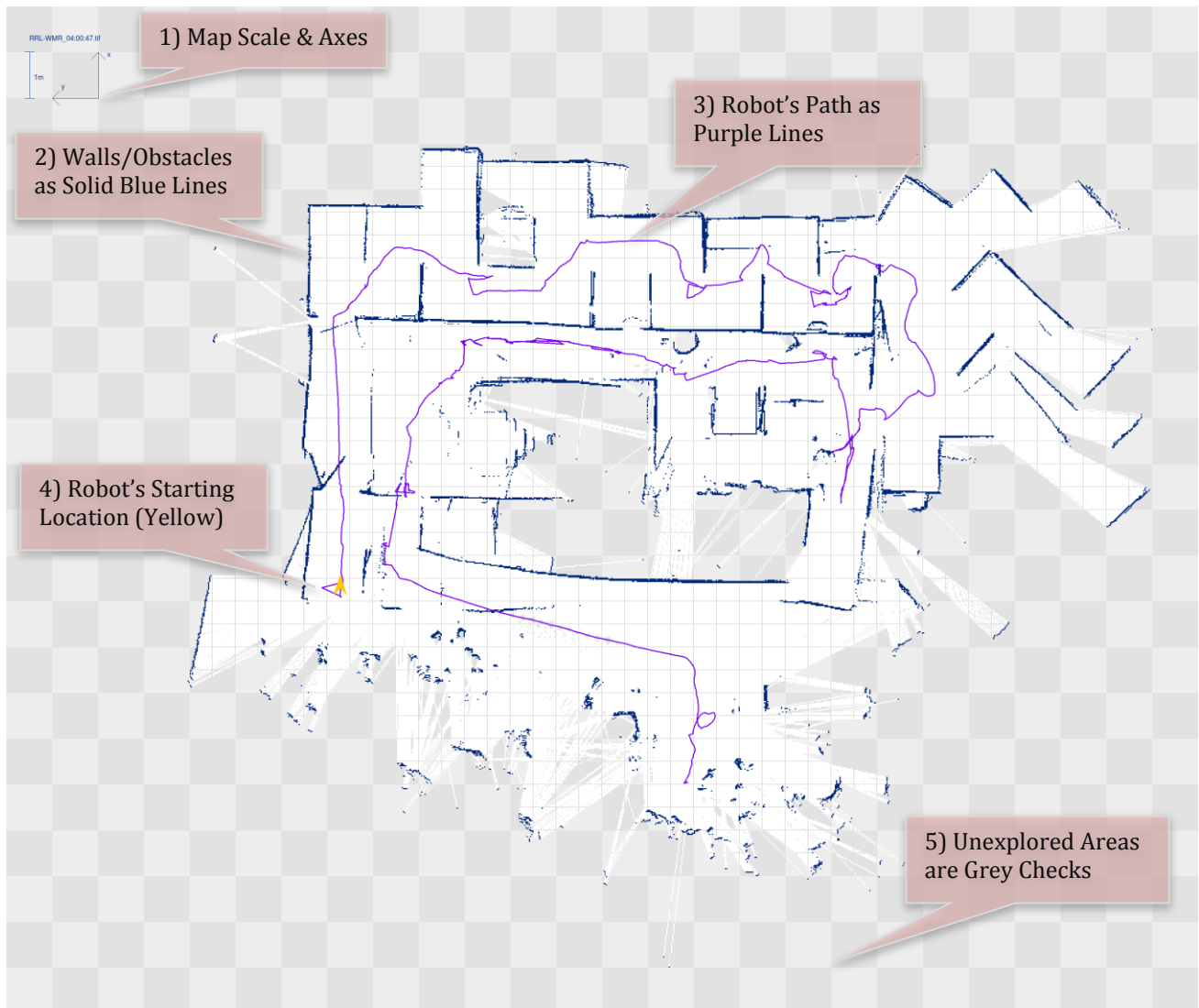
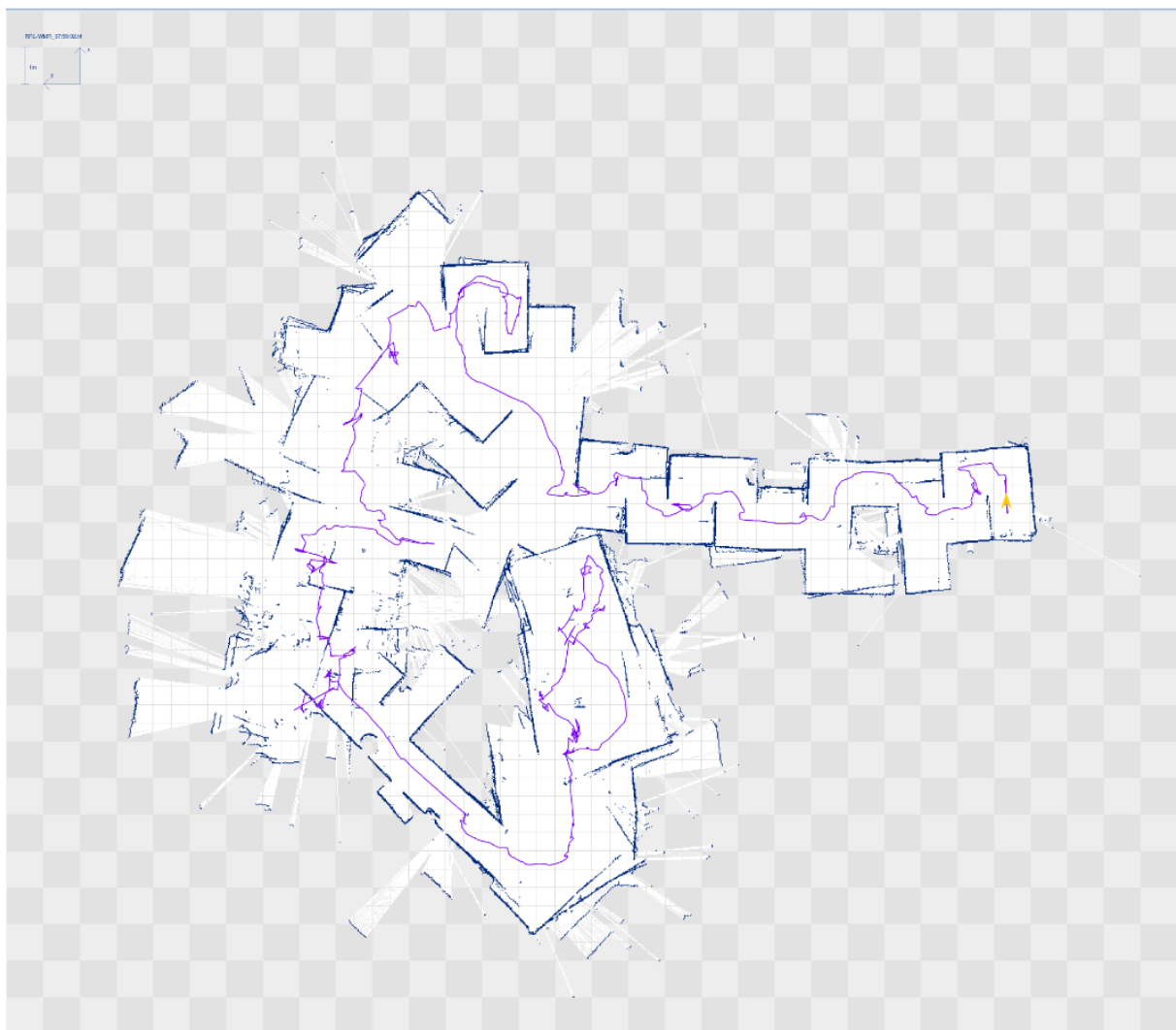


Figure 130: Map 1 Created by the USAR Robot during the RoboCup German Open

Figure 131 shows a map created during a competition run before uneven terrain was encountered, and Figure 132 shows the final map which did not correlate with the arena correctly. This was because the algorithm needs a transformation function to communicate the LIDAR's RPY. Although attempts were made to feed the mapping algorithm with IMU data (Figure 133) this was not successful during the competition.



**Figure 131: Map 2 created by the WMR robot (Part 1/2)**



**Figure 132: Map 2 created by the WMR robot (Part 2/2)**

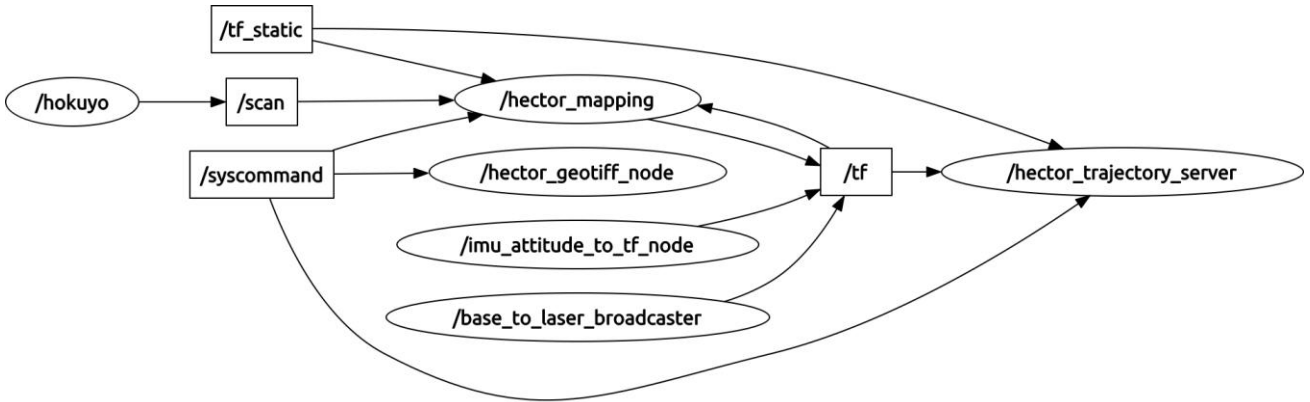


Figure 133: Updated Node Network to Include IMU Attitude Transformation

### 5.8.3. HMI Software Testing

The HMI code and head tracking was modified to control the existing USAR robot design with minimum modification. The arm vision system was moved onto the existing robot and plugged into its router. This allowed the webcams to be seen on the Oculus Rift headset with the software new robot software without modification. Figure 134 explains the head tracking.

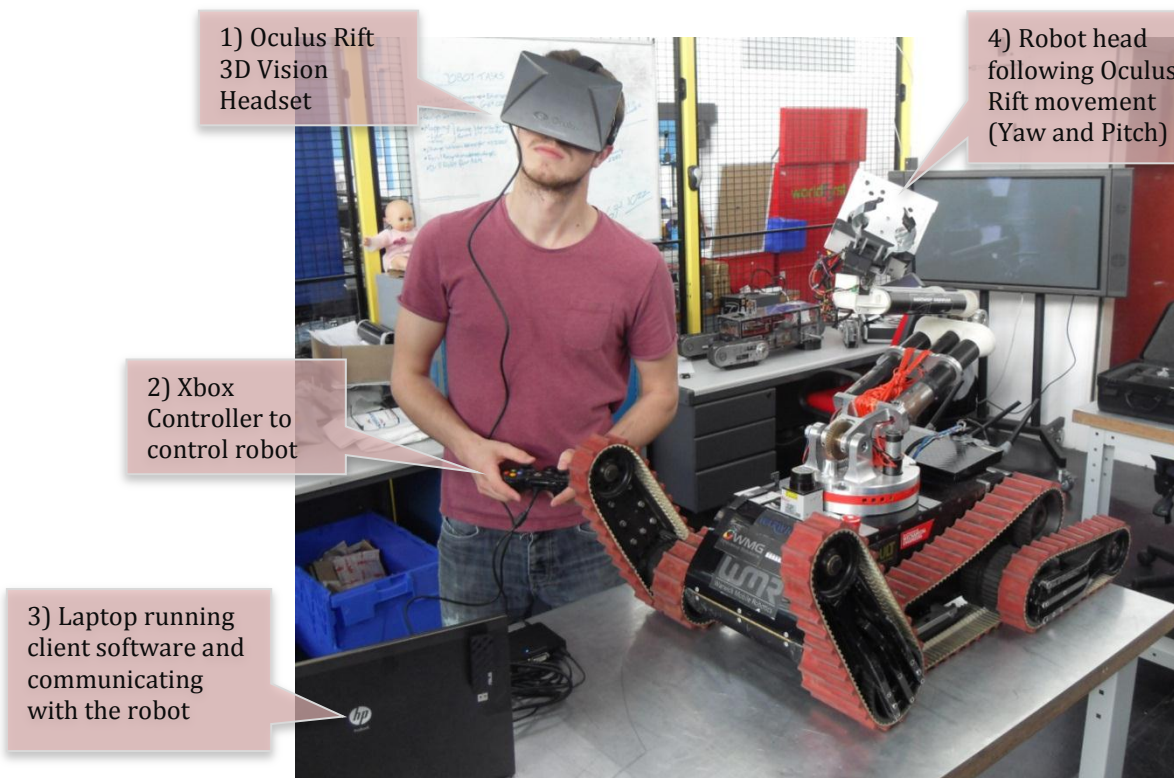


Figure 134: Client Software Program Modified to Control Existing Robot's Head

Figure 135 to Figure 138 demonstrate how the operators head movement directly changes the yaw and pitch angles in the wrist. Although the new HMI improved operator situational awareness and provided intuitive control, the low resolution could not display the same amount of information as the existing setup. Therefore for the competition the existing operator interface was chosen.

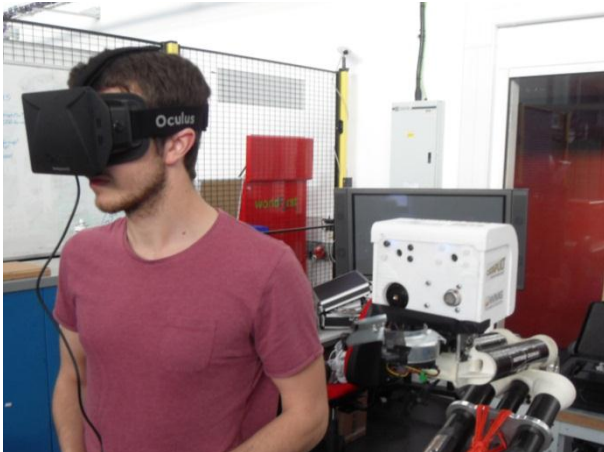


Figure 135: Head Tracking - Looking Forward



Figure 136: Head Tracking - Looking Right



Figure 137: Head Tracking - Looking Left



Figure 138: Head Tracking - Looking Down

#### 5.8.4. Power Board

The testing procedure including continuity testing for both PCBs as described in (Appendix E.3). Figure 139 demonstrate the voltage measurements made with a multimeter for the main power board, once complete the boards were mounted in the chassis (Figure 140). The arm control electronics are shown connected together in Figure 141.

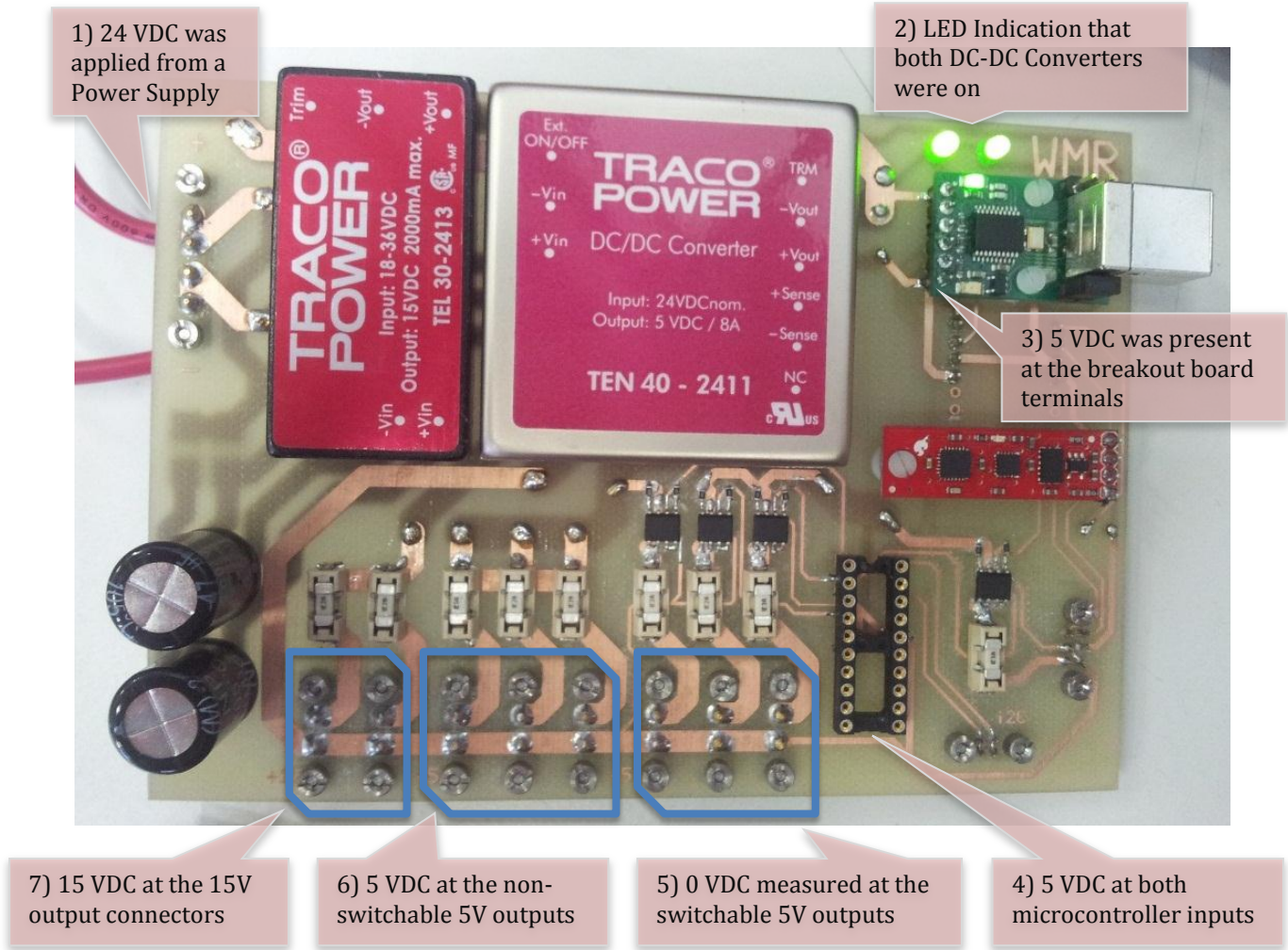


Figure 139: Testing of the Main Power board

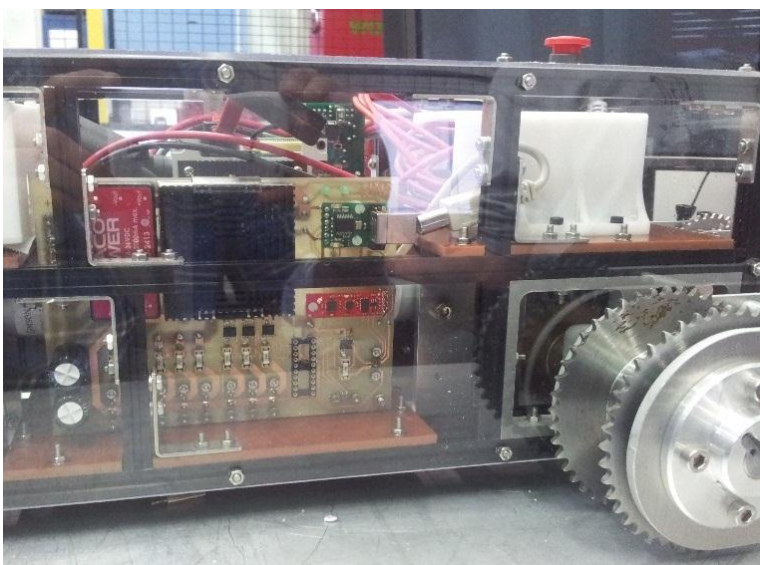


Figure 140: Main Power board mounted inside the robot chassis



Figure 141: Arm Power Board Mounted to Raspberry Pi

## 5.9. Critical Review

Table 51 compares the final design against the original electronic and software specification.

**Table 51: Electronic and Software Results against Specification**

ID	Parameter	Met?	Details
1	Size		Components chosen were small and final power board designs were 90x100mm and 130x100mm for the arm and main power boards respectively. This is x smaller than the existing robot's power board (200x100mm).
2	Mass		Small lightweight components were used when available
3	Modular		The entire electronic, software and power system is modular as demonstrated by the system architecture (Chapter 5.3) and wiring diagram (Chapter 5.6.3).
4	Cost		Electronic components were one of the most expensive parts of the robots full design however costs were kept to a minimum and are in line with previous WMR robot designs.
5	Reliability		The new software and electronics tested on the old robot at the RoboCup competition performed reliably and did not experience any errors or dropouts. However the full system has not been tested so reliability of the final system is not known.
6	Communication		Communication with the existing robot and new router did not experience any problems at the RoboCup Rescue 2014.
7	Data		The robot was not constructed or wired up fully to test this functionality however subsystems were proven to work.
8	Wiring		The robot was not wired up however due to the final location of the boards within the chassis means that cable wiring may be inefficient.
9	Emergency stop		An emergency stop system was designed and simulated to specification however was not tested physically.
10	Fuse Protection		Fuse protection has been designed into the system.
11	Protect Battery		The battery connectors chosen only allow single polarity connection.
12	Monitor Battery		Several battery monitoring circuits were simulated however were not proven to work reliably or to the accuracy level require so were therefore not manufactured or tested
13	Improved HMI		A new HMI was designed and tested successfully, the resolution is not yet at a desirable level but the software will scale up to higher resolutions as the technology matures.

A full modular electronic architecture has been developed and sections tested. The ability to move the 3D vision system to the old robot with no modifications shows that this system is not just modular within the new robot but within other systems. With minimum modifications to the new client software head tracking was tested on the old robot and proved successful

however the resolution of the oculus rift display (640x480 per eye) is not yet a high enough to give preferential choice over using the existing laptop screen setup. With the release of the new oculus rift headset full High Definition (HD) per eye is expected and should become comparable with the laptop setup.

The size of the system and the requirement for wiring simplicity has deviated slightly from the initial specification. The PCBs (although small) show the difficulty that small scale custom PCB manufacturing brings, mainly the inability to use very small surface mount components which cannot be soldered by hand. Although two power boards were created to allow removal of the arm system, space savings could be achieved within the chassis by designing one board to power all systems.

## Chapter 6. Analysis, Conclusion & Recommendations

### 6.1. System Analysis

#### 6.1.1. Mass and Cost Analysis

A full mass and cost analysis of the final robot was conducted at component level to identify potential areas for optimisation (Appendix F.1).

##### *Chassis*

Table 52 summarises the mass and cost breakdown of the chassis. There is limited scope to reduce the mass of the control electronics; however the two power boards could be merged into one, providing a potential mass saving of 185g. The four axle mounting plates (368g) were identified as the best opportunity for further optimisation.

**Table 52: Chassis Mass & Cost Breakdown**

Category	Mass (kg)	% Sub-System	Cost (£)	% Sub-System
<b>Electronics</b>	2.18	39.30	702.61	63.59
<b>Fixings</b>	0.11	2.02	28.51	2.58
<b>MakerBeam</b>	1.32	23.68	245.88	22.25
<b>Mounting Plates</b>	0.85	15.35	105.42	9.54
<b>Shell</b>	0.75	13.46	22.50	2.04
<b>Total Mass:</b>	<b>5.56</b>	<b>Total Cost:</b>	<b>£ 1,104.93</b>	

##### *Drivetrain*

Table 53 summarises the mass and cost breakdown of the drivetrain. The drivetrain accounts for 69% of the robot's mass and 59% of the cost and was therefore identified as having the largest potential savings. Optimisation of the eight identical track side-plates using FEA would realise the largest mass saving. The electronics offer limited scope for light weighting or cost saving as few components meet the specification. Reducing the number of off-the-shelf components would enable greater mass reduction through bespoke component design however this would increase manufacturing costs.



**Table 53: Drivetrain Mass & Cost Breakdown**

Category	Mass (kg)	% Sub-System	Cost (£)	% Sub-System
<b>Electronics</b>	3.04	17.87	403.78	0.16
<b>Manufactured</b>	4.67	27.47	798.18	0.32
<b>Off-the-shelf mechanical</b>	5.20	30.58	654.40	0.26
<b>Treads</b>	4.10	24.08	639.64	0.26
<b>Total Mass:</b>	<b>17.01</b>	<b>Total Cost:</b>	<b>£ 2,496.00</b>	

### *Arm System*

Table 54 summarises the mass and cost breakdown of the arm system. 44% of the arm system's cost is in the electronics. There is little scope for cost reduction due to the requirement of sensors to detect victims. There is potential scope to remove the Raspberry Pi and control the arm system from the main computer; however this removes the ability to operate the arm independently. The current system design has been mass optimised (Chapter 4.7.4). Further mass reduction would require a new design development approach, potentially incorporating a higher percentage of polymers and composite materials.

**Table 54: Arm System Mass & Cost Breakdown**

Category	Mass (kg)	% Sub-System	Cost (£)	% Sub-System
<b>MakerBeam</b>	0.43	18.93	20.25	0.03
<b>Manufactured</b>	0.42	18.70	25.98	0.04
<b>Motor</b>	0.26	11.54	87.67	0.13
<b>Transmission</b>	0.27	11.95	154.87	0.23
<b>Arm Electronics</b>	0.34	15.11	293.53	0.44
<b>Fixings</b>	0.21	9.22	25.16	0.04
<b>Cable System</b>	0.18	8.11	43.70	0.07
<b>Gripper</b>	0.15	6.43	11.95	0.02
<b>Total Mass:</b>	<b>2.27</b>	<b>Total Cost:</b>	<b>663.11</b>	

### *Complete Robot*

Table 55 summarises the mass breakdown by system and demonstrates that the target mass has been achieved (<25kg). Further mass reduction would improve transportation and allow longer operational periods.

The existing robot design utilises the arm's mass to shift its CoG during complex manoeuvres by extending the arm. The lower mass of the new arm system may have reduced the

effectiveness of this technique. Although the drivetrain has been identified as having the greatest potential for mass reduction this currently acts to reduce the CoG, improving stability. High cost prohibits the use of USAR robots in disaster environments. Where re-use of robotic systems cannot be guaranteed, commercial cost should not exceed £10,000 (Sellafeld, (Winkvist, 2013)). Given that the material cost for a single high-end unit was £4,707, there is scope to develop a commercialised version below the £10,000 ceiling.

Table 55: Full System Mass & Cost Breakdown

System	Mass (kg)	% System	Cost (£)	% System
<b>Chassis</b>	5.56	22.37	1,104.93	23.47
<b>Drivetrain</b>	17.01	68.49	2,496.00	53.02
<b>Arm System</b>	2.27	9.14	1,106.63	23.51
<b>Total Mass:</b>	<b>24.84</b>	<b>Total Cost:</b>	<b>£ 4,707.56</b>	

6.1.2. Full System Virtual Testing

Virtual testing of the whole system was performed showing the system could reach victims at up to 1.4m and entombed victims (Figure 142 and Figure 143).

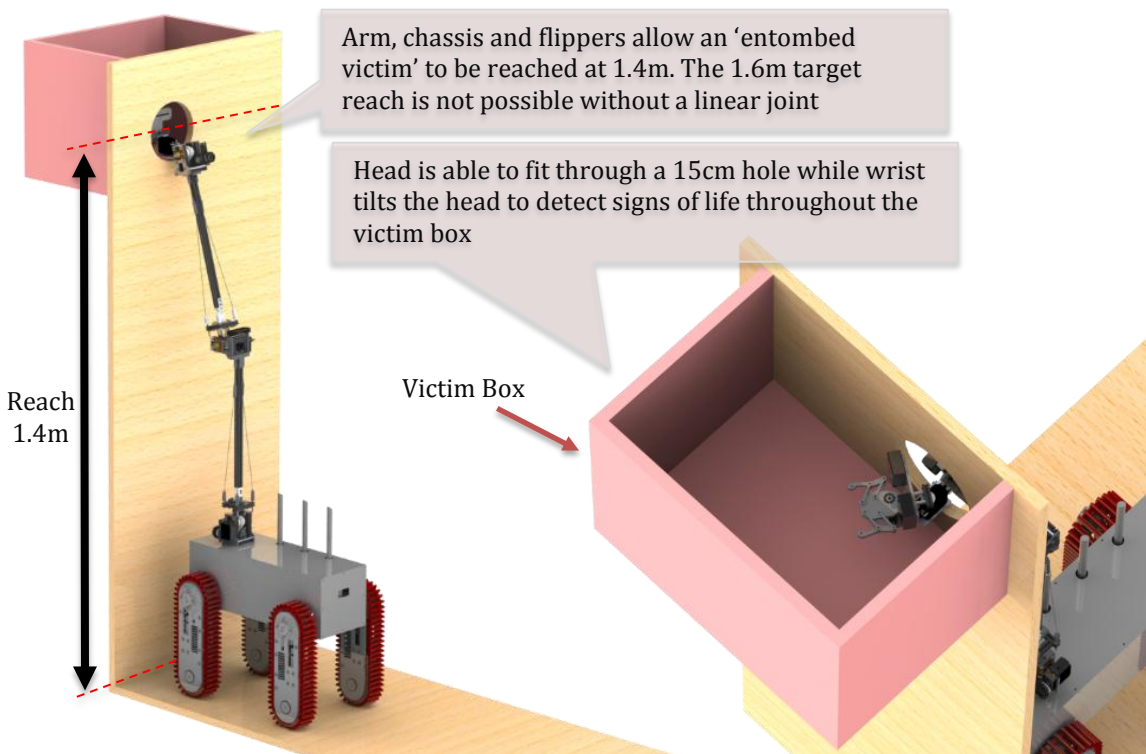


Figure 142: Accessing High Victims and Entombed Victims

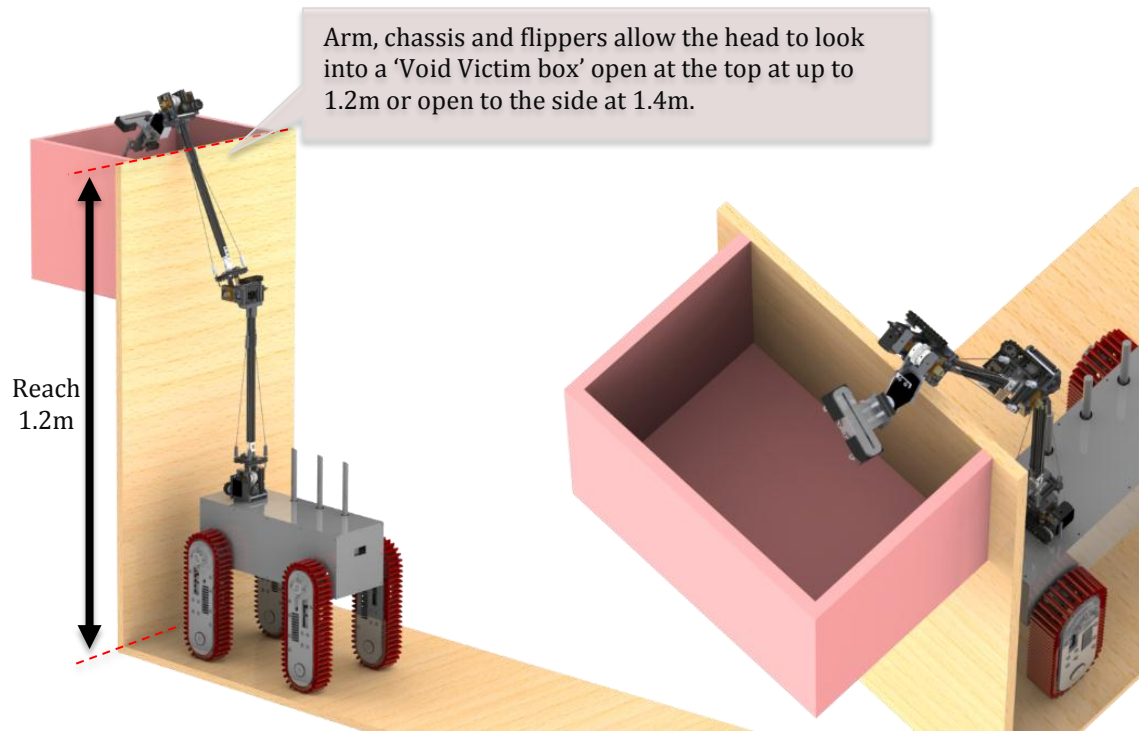


Figure 143: Accessing High 'Void Victim Boxes'

### 6.1.3. Modular Robotic Architecture (MRA)

The MRA developed with MakerBeam works well as a research platform as it allows different prototype and research models to be created quickly with minimal cost. However for a commercial product it is too awkward to adjust or repair.

To become more commercially viable the system's modules (flipper units, arm joints and links) need to be developed into self-contained units which end users cannot modify. These units would then connect together with standardised interfaces to allow the robot to be configured quickly to the user's requirements.

Although the MRA has been demonstrated by developing a small, highly capable USAR robot, the same architecture could be used to develop a range of models from small with low capabilities to large with high capabilities (Figure 144).

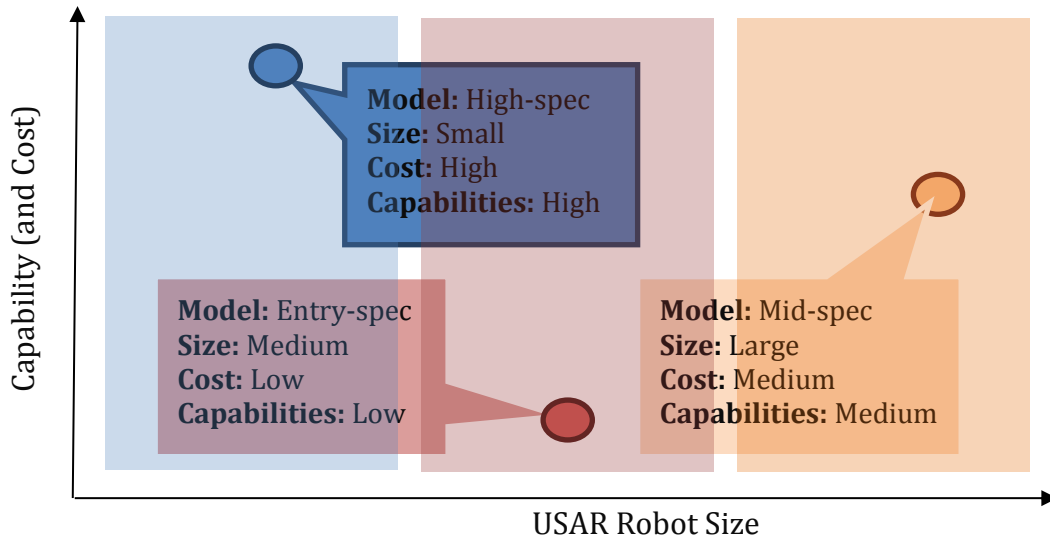


Figure 144: Modular Robotic Architecture Platform Breadth

#### 6.1.4. RoboCup German Open

Although the new USAR robot was not completed in time to compete in the RoboCup German Open 2014, it was taken alongside the existing USAR robot and critically evaluated using the simulated disaster arena which will provide significant benefits to future WMR teams.

Figure 145 illustrates the new robot’s ability to navigate smaller obstacles in the competition arena. This gives the team a competitive advantage over other teams who are yet to have this capability. In this example, the arm is not required, reducing the risk of damage due to the stiff door handle and, in real life applications, will allow to robot to reach survivors faster.

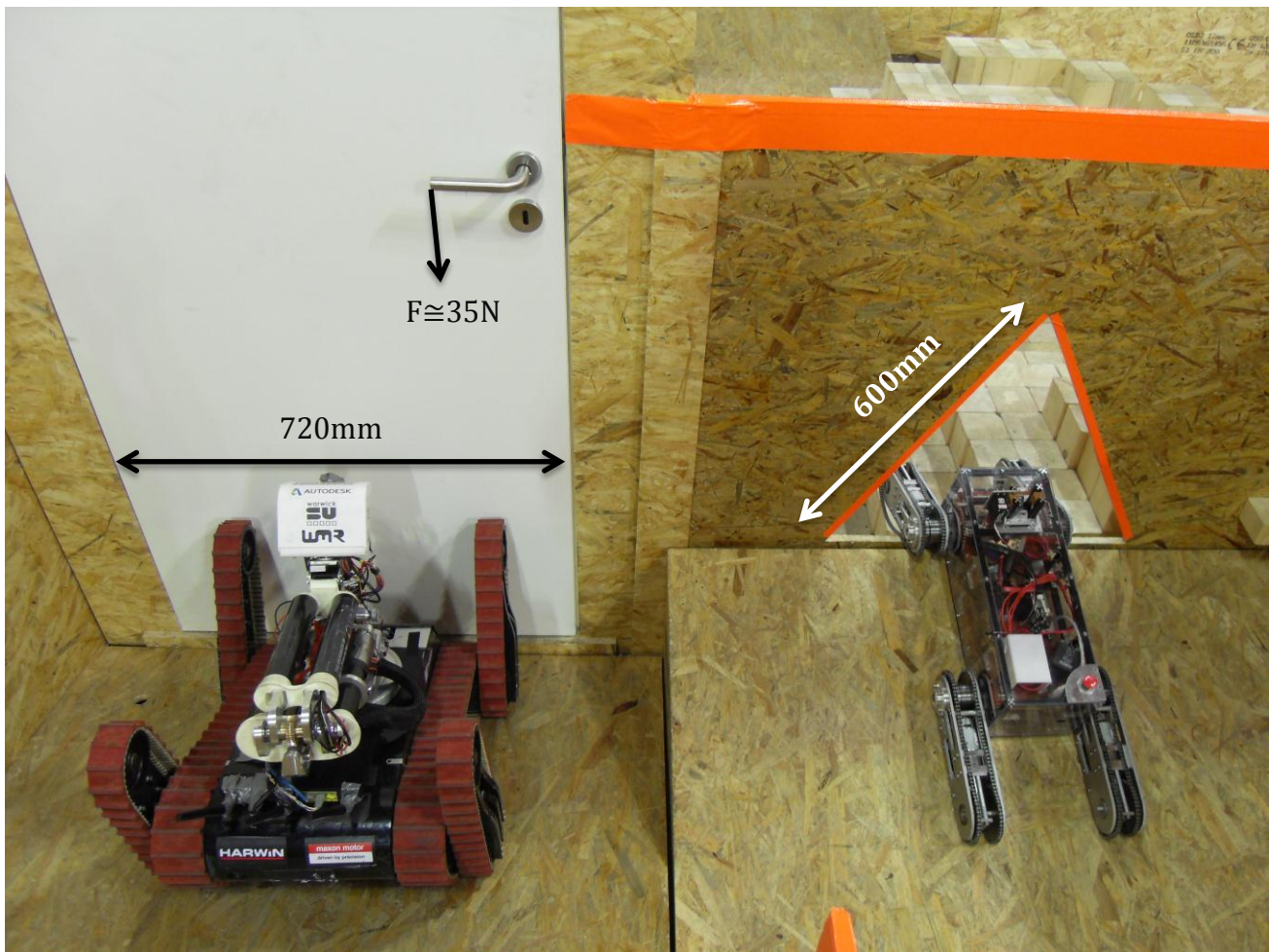


Figure 145: New Robot Entry through First Responder Hole vs. Existing Robot through Door

The robot's low height allows it to move underneath obstacles without removing the debris (Figure 146). The robot is also able to climb slopes where additional survivors may be located (Figure 147). Figure 148 shows that the robot can be carried easily by one person, making it easier to deploy in an emergency. However, as expected, the robot is unable to navigate step fields due to its small size (Figure 149).

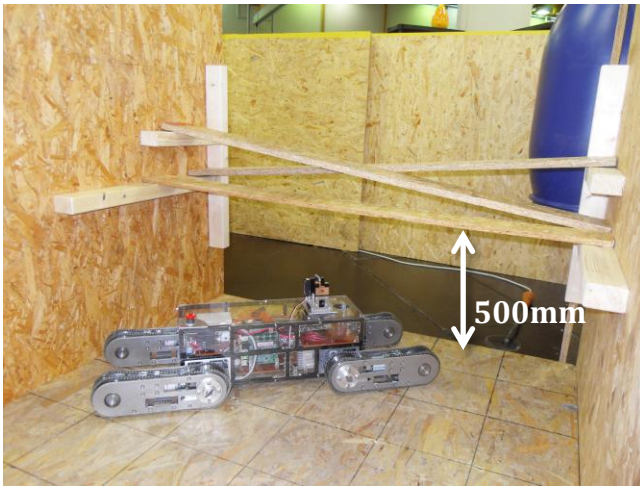


Figure 146: Small Height Avoids Clearing Debris

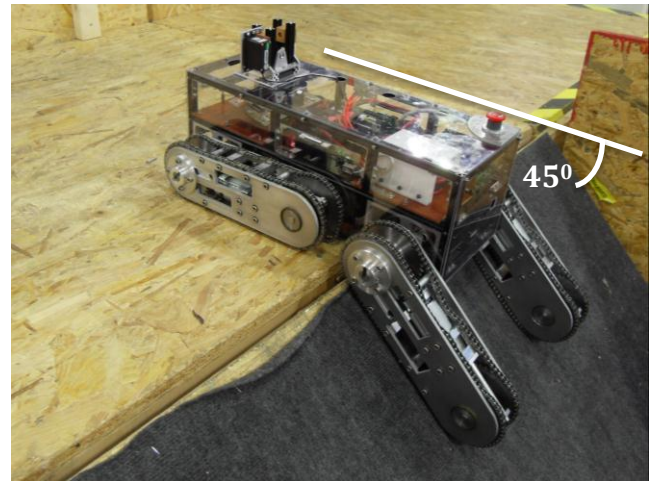


Figure 147: Ability to Climb 45° Slope

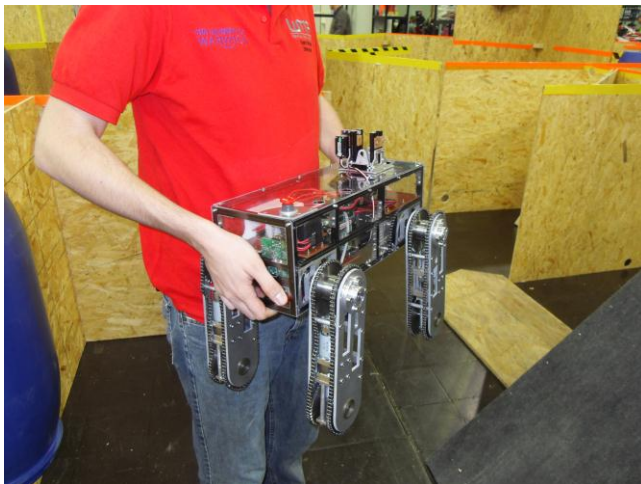


Figure 148: Deployable by 1 Person (<25kg)



Figure 149: Inability to Clear Stepfield due to Small Robot Geometry

### 6.1.5. Comparison against Initial Specification and Aims and Objectives

The competition obstacles were generated in CAD and the robot tested against the original specification. Table 56 details how well the robot designed met the original specification.

Table 56: Original Specification Objectives against Achievements

ID	Objective	Met?	Explanation if not Met
1	15° Ramps	Met	
2	Crossing 15° Ramps	Met	
3	Stairs 45°	Not Met	The robot should be able to climb 45° stairs however not tested
4	Ramps 45°	Not Met	The robot should be able to climb 45° ramps however not tested
5	Confined Spaces	Met	
6	Step field	Not Met	Photos from the RoboCup indicate the chassis would get caught on any step field
7	60x60x60 Triangle	Met	
8	Clear 72cm Door	Met	
9	Arm Stowing	Met	
10	Precision Manipulation	Not Met	Objects can be gripped but valves and doors cannot be opened
11	Object Grasp	Met	
12	Mapping	Met	
13	QR Codes	Met	
14	Two Way Audio	Not Met	Capability exists but has not been implemented
15	CO2 Sensor	Met	
16	Open Victim 'Boxes'	Met	
17	Confined Space Gripper	Met	
18	30 Minutes Power	Met	
19	Wireless Range	Met	
20	Autonomy	Not Met	Autonomy was not attempted as the system was not functional enough to try and implement this
21	Single Operator Control	Not Met	Operator control will be single person however testing needs to be performed
22	Low Vibration in Arm	Not Met	Anti-backlash gears were not used due to cost constraints
23	Withstand 35cm Drop	Not Met	FEA simulations indicate it will however needs to be tested once constructed
24	Low Centre of Mass	Met	
25	Protected Batteries	Met	
26	Easy access & Replace	Not Met	Sides can be removed quickly however this could be improved
27	Battery Monitor	Not Met	A battery monitor still needs to be designed and tested
28	Power Board	Met	
29	Emergency Stop	Met	
30	Single Connection Panel	Not Met	It was found a single connection panel was not required
31	Operator Awareness	Met	

## 6.2. Conclusion

A new urban search and rescue robot specification was compiled after extensive research of existing USAR robots and their intended operating environment. Detailed design work from theoretical principles was performed; balancing between size, mass, capabilities and cost. This work resulted in a modular robotic architecture, allowing the platform to be adapted for specific tasks. However these modules need to be developed into self-contained units which end users cannot modify. These would connect together using standardised interfaces, allowing quick robotic platform re-configuration.

The partially manufactured design was taken to the RoboCup German Open 2014 where the design was assessed against the arena objects. Other teams and competition organisers provided valuable feedback about the new design and highlighted potential areas for improvement, optimisation or redesign.

The robot met the target mass, 24.84kg, 160g less than required. The drivetrain was the highest proportion of the mass at 69%. This provides a low centre of gravity but also presents the greatest opportunity for mass reduction. The chassis was constructed using lightweight aluminium beam giving the robot structural strength and providing a platform to integrate the robot's systems and electronic components. However, problems were recognised regarding the shape which may be susceptible to beaching or catching on obstacles. The MakerBeam system was also not as easy to maintain as first thought. A lightweight modular arm was designed featuring a gripper to allow it to perform manipulation tasks. However, this design was not assembled within the project timescale and therefore has not yet been physically tested.

A modular electronic and software system was designed for the new robot including innovation in 3D vision systems, head tracking, mapping and power saving electronic switching. As the new system was not manufactured in time, the software was tested successfully on the existing robot platform. These software improvements allowed the robot to gain additional points at the competition.



Overall this design and analysis has contributed valuable research towards innovative modular robotic search and rescue solutions which can ultimately be used to save lives.

### 6.3. Recommendations for Further Work

The architecture choices made this year allow future WMR teams to easily adapt and improve this year's design. Analysis of USAR systems in Chapter 1.5 combined with the experience and knowledge gained from designing a new robot and competing at the RoboCup competition has highlighted the following areas for future work with regard to each system:

- Chassis
  - Investigate different shapes to remove the possibility of beaching
  - Develop sliding cover panels to allow easier access to internal components
- Drivetrain
  - Complete mechanical tasks on current design (grub screws in sprockets & gears)
  - Use FEA to identify areas of mass saving in the track side plates
  - Wire the motors, controllers and test physically
- Arm
  - Assemble the manufactured components, wire and test
  - Develop a linear joint to realise the required competition reach (1.6m)
  - Develop a rotary base joint & wrist joint to aid object manipulation
- Electronics
  - Produce a single power board capable of powering all modular systems
  - Complete software and test on robot when mechanically finished
  - Implement 30m LIDAR and RPY compensation with IMU
  - Develop a battery monitoring system

- Continue development of the Oculus Rift head tracking with the new Development Kit 2 – potentially including full inverse kinematic control for height and reach

The WMR team could also collaborate with other RoboCup teams sharing mechanical designs and software to produce search and rescue robots with higher capabilities.

## Chapter 7. Bibliography

A.Mashat & at-el, 2013. *RoboCupRescue 2013 - Robot League Team MRL Rescue Robot (Iran)*, Iran: Mechatronics Research Laboratory.

A.Soltanzadeh, 2013. *RoboCupRescue 2013 - Robot League Team AriAnA (Iran)*, Tehran, Iran : Islamic Azad University of Central Tehran Branch.

Active Robots, 2013. *Dimension Engineering*. [Online]  
Available at: <http://www.active-robots.com/shop-by-brand/dimension-engineering>  
[Accessed 22 March 2014].

Active Robots, 2013. *HOKUYO robotics laser*. [Online]  
Available at: <http://www.active-robots.com/sensors/object-detection/laser-range-finder/hokuyo-robotics-laser.html>  
[Accessed 10 November 2013].

ASM, 2013. *Aluminum 6063-T6*. [Online]  
Available at: <http://asm.matweb.com/search/SpecificMaterial.asp?bassnum=MA6063T6>  
[Accessed 23 December 2013].

ASUS, 2013. *802.11ac Dual-Band Wireless AC1750 Gigabit Router*. [Online]  
Available at: <http://www.asus.com/Networking/RTAC66U/>  
[Accessed 13 March 2014].

Aving, 2006. *A robot of military career in Iraq 'Robhaz DT-5'*. [Online]  
Available at: <http://us.aving.net/news/view.php?articleId=20826>  
[Accessed 25 October 2013].

BBC, 2011. *New Zealand earthquake: 65 dead in Christchurch*. [Online]  
Available at: <http://www.bbc.co.uk/news/world-asia-pacific-12533291>  
[Accessed 8 April 2014].

Brown, H. & et-al, 2003. A Mobile Hyper Redundent Mechanism for Search and Rescue Tasks. *Proceedings of the 2003 IEEE/RSJ Intl. Conferance on Intelligenet Robots and Systems*, pp. 2889-2895.

Buckstone, K. et al., 2013 . *Warwick Mobile Robotics: Urban Search and Rescue Robot - Technical Report*. [Online]  
Available at:  
<http://www2.warwick.ac.uk/fac/sci/eng/meng/wmr/projects/rescue/reports/1213reports/technicalreport.pdf>  
[Accessed 10 January 2014].

Chaikanta, W. et al., 2013. *RoboCupRescue 2013 - Robot League Team STABILIZE (Thailand)*. [Online]  
Available at:  
<https://www.google.co.uk/url?sa=t&rct=j&q=&esrc=s&source=web&cd=1&cad=rja&uact=8&ved=0CC0QFjAA&url=http%3A%2F%2Fstaff.science.uva.nl%2F~arnoud%2Factivities%2Frobo-cup%2FRoboCup2013%2FSymposium%2FTeamDescriptionPapers%2FRescue%2FChamp2013%2FTHAILAND%2FSTABILIZE>  
[Accessed 30 October 2013].

Chavasse, C., 2013. *Warwick Mobile Robotics*. [Online]  
Available at: <http://www2.warwick.ac.uk/fac/sci/eng/meng/wmr/>  
[Accessed 14 April 2014].

- DFRobot, 2014. *CO2 Sensor SKU:SEN0159*. [Online] Available at: [http://www.dfrobot.com/wiki/index.php/CO2 Sensor SKU:SEN0159](http://www.dfrobot.com/wiki/index.php/CO2_Sensor_SKU:SEN0159) [Accessed 18 February 2014].
- Dodgson, N. A., 2004. Variation and extrema of human interpupillary distance. *Sterioscopic Displays and Virtual Reality Systems*, 5291(XI), pp. 36-46.
- Engineering ToolBox, 2014. *Factors of Safety*. [Online] Available at: [http://www.engineeringtoolbox.com/factors-safety-fos-d\\_1624.html](http://www.engineeringtoolbox.com/factors-safety-fos-d_1624.html) [Accessed 26 April 2014].
- Future Robotics Technology Center, 2007. *Quince*. [Online] Available at: <http://furo.org/en/works/quince.html> [Accessed 25 October 2013].
- Gimson Robotics, 2013. *GR02 DC Planetary Gearmotor*. [Online] Available at: [http://www.gimsonrobotics.co.uk/GR02-12V 18V planetary electric gearmotor.html](http://www.gimsonrobotics.co.uk/GR02-12V_18V_planetary_electric_gearmotor.html) [Accessed 20 January 2014].
- Horowitz, P. & Hayes, C. T., 1989. *The Art of Electronics*. s.l.:Cambridge University Press.
- IPC, 2003. *IPC-2221-A Generic Standard on Printed circuit board Design*. s.l.:IPC.
- iRobot, 2013. *iRobot 510 PackBot*. [Online] Available at: <http://www.irobot.com/us/learn/defense/packbot.aspx> [Accessed 25 October 2013].
- Jacoff, A., 2009. *RoboCupRescue Robot League Progress Update and Future Directions*. [Online] Available at: [http://www.isd.mel.nist.gov/projects/USAR/2009/RoboCupRescue Robot League Overview \(2007-2008\).pdf](http://www.isd.mel.nist.gov/projects/USAR/2009/RoboCupRescue_Robot_League_Overview_(2007-2008).pdf) [Accessed 6th March 2012].
- Jacoff, A., 2014. *Robotic Architecture Design [Interview]* (7 April 2014).
- Jones, D., 2004. *PCB Design Tutorial*. [Online] Available at: [http://server.ibfriedrich.com/wiki/ibfwikien/images/d/da/PCB Layout Tutorial e.pdf](http://server.ibfriedrich.com/wiki/ibfwikien/images/d/da/PCB_Layout_Tutorial_e.pdf) [Accessed 8 December 2013].
- K.Blanch & et-al, 2012. *Technical Report - Warwick Mobile Robotics: Urban Search and Rescue Robot 2011/12*, Coventry, UK: Warwick University - School of Engineering - Warwick Mobile Robotics.
- Keiji Nagatani, e.-a., 2013. *Emergency response to the nuclear accident at the Fukushima Daiichi nuclear power plants using mobile rescue robots*, Japan: Journal of Field Robotics Vol.30.
- M.Jenabzadeh & et-al, 2013. *RoboCup Rescue 2013 - Rescue Robot League Team YRA (IRAN)*, YAZD, Iran: Islamic azad university of YAZD.
- MakerBeam, 2013. *MakerBeam Homepage*. [Online] Available at: <http://www.makerbeam.eu/> [Accessed 14 December 2013].
- Microsoft, 2012. *LifeCam HD 3000*. [Online] Available at: <http://www.microsoft.com/hardware/en-gb/p/lifecam-hd-3000#details> [Accessed 20 November 2013].
- Microsoft, 2012. *Microsoft HD300 Product Guide*. [Online] Available at: <http://download.microsoft.com/download/A/E/9/AE96A8F2-B778-44F6-952F->

[6AC466A93FAF/Microsoft%20Product%20Guide.xps](#)

[Accessed 14th Jan 2013].

Mosuer, 2013. *PICO830VGA-N2800*. [Online]

Available at: <http://uk.mouser.com/ProductDetail/Axiomtek/PICO830VGA-N2800/?qs=NaL%252bomqElqtxmRIXQOjV6g==>

[Accessed 27 April 2014].

Niku, S. B., 2011. *Introduction To Robotics: Analysis, Control, Applications 2nd Edition*. s.l.:Pearson Education, Inc.

Oculus VR, 2013. *Building a Sensor for Low Latency VR*. [Online]

Available at: <http://www.oculusvr.com/blog/building-a-sensor-for-low-latency-vr/>

[Accessed 28 November 2013].

OptiFuse, 2010. [Online]

Available at: [http://www.optifuse.com/PDFs/FuseSelectionGuide\\_RevA.pdf](http://www.optifuse.com/PDFs/FuseSelectionGuide_RevA.pdf)

Pellenz, J., 2014. *RoboCupRescue Robot League Rules for 2014*. [Online]

Available at: <http://wiki.ssrrsummerschool.org/doku.php?id=rri-rules-2014>

[Accessed 6 April 2014].

Polymer Technology, 2012. *A GUIDE TO POLYCARBONATE IN GENERAL*. [Online]

Available at: [http://www.ptslc.com/intro/polycarb\\_intro.aspx](http://www.ptslc.com/intro/polycarb_intro.aspx)

[Accessed 20 December 2013].

R.Beardmore, 2013. *Worm Gears*. [Online]

Available at: [http://www.roymech.co.uk/Useful\\_Tables/Drive/Worm\\_Gears.html](http://www.roymech.co.uk/Useful_Tables/Drive/Worm_Gears.html)

R.Bogue, 2011. Robots in the nuclear industry: a review of technologies and applications. *Industrial Robot: An International Journal, Vol 38, Issue 2*, pp. 113-118.

R.Edlinger, 2013. *RoboCupRescue 2013 - Robot League Team RRT-Team FH Wels (Austria)*, Wels, Austria : FH OOE Upper Austria Research & Development.

R.Juvinall, 2012. *Machine Component Design 5th Edition*. Singapore: Wiley.

R.Murphy, 2004. Trial by Fire - Activities of the Rescue Robots at the World Trade Center from 11-21 September 2001. *IEEE Robotics & Automation Magazine*.

R.Murphy & et.al, 2008. *Springer Handbook of Robotics - Search and Rescue Robotics*. s.l.:Springer.

R.Rangel & et-al, 2013. *RoboCup 2013 - Rescue Robot League UP-Robotics (México)*, Aguascalientes, Mexico: Universidad Panamericana.

ROS, 2014. *About ROS*. [Online]

Available at: <http://www.ros.org/about-ros/>

[Accessed 14 March 2014].

Schneider, S. et al., 2007. Assessing key vulnerabilities and the risk from climate change. In: M. Parry, et al. eds. *Impacts, Adaptation and Vulnerability*. Cambridge: Cambridge University Press, pp. 779-810.

Sittiwanchai, T., Blattler, A. & Panas, K., 2013. *Robocup Rescue 2013 - Robot League Team iRAP\_FURIOUS (THAILAND)*. [Online]

Available at:

<https://www.google.co.uk/url?sa=t&rct=j&q=&esrc=s&source=web&cd=1&cad=rja&uact=8&ved=0CC0QFjAA&url=http%3A%2F%2Fstaff.science.uva.nl%2F~arnoud%2Factivities%2Frobo-cup%2FRoboCup2013%2FSymposium%2FTeamDescriptionPapers%2FRescue%2FChamp201>

### 3 THAILAND iRAP FUR

[Accessed 1 November 2013].

Sparkfun, 2013. *9 Degrees of Freedom - Sensor Stick*. [Online] Available at: <https://www.sparkfun.com/products/10724> [Accessed 14 November 2013].

T.Grabner & et-al, 2013. *RoboCupRescue 2013 - Robot League Team Hector Darmstadt (Germany)*, Darmstadt, Germany: Technische Universitat Darmstadt.

T.Sittiwanchai & et-al, 2013. *Robocup Rescue 2013 - Robot League Team iRAP\_FURIOUS (THAILAND)*, Bangkok: King Mongkut's University of Technology North Bangkok.

The Engineering ToolBox, n.d. *Wood Density*. [Online] Available at: [http://www.engineeringtoolbox.com/wood-density-d\\_40.html](http://www.engineeringtoolbox.com/wood-density-d_40.html) [Accessed February 2014].

TheCarTech, 2013. *Long Columns with Central Loading (Buckling)*. [Online] Available at: [http://www.thecartech.com/subjects/machine\\_elements\\_design/Buckling.htm](http://www.thecartech.com/subjects/machine_elements_design/Buckling.htm) [Accessed 22 December 2013].

TheCircuitCalculator.com, 2006. *TheCircuitCalculator.com*. [Online] Available at: <http://circuitcalculator.com/wordpress/2006/01/31/pcb-trace-width-calculator/> [Accessed 5 December 2013].

Tufnol Composites Limited, 2008. *Carp Brand TUFNOL*. [Online] Available at: <http://www.tufnol.com/tufnol/default.asp?id=26> [Accessed 24 December 2014].

US Digital, 2013. *MA3 Miniature Absolute Magnetic Shaft Encoder*. [Online] Available at: <http://www.usdigital.com/products/encoders/absolute/rotary/shaft/ma3> [Accessed 29 November 2013].

Vishay Siliconix, 2010. *N- and P-Channel 40 V (D-S) MOSFET*. s.l.:s.n.

W.Chaikanta & et-al, 2013. *RoboCupRescue 2013 - Robot League Team STABILIZE (Thailand)*, Bangkok: Rajamangala University of Technology Phra Nakhon.

Whitfield, J., 2008. *The Electrician's Guide*. s.l.:IEEE.

Williams, T., 2005. *The Circuit designer's Companion*. 2nd ed. s.l.:Newnes.

Winkvist, S., 2013. *Low Computational SLAM for an Autonomous Indoor Aerial Inspection Vehicle*. [Online] Available at: [http://wrap.warwick.ac.uk/59055/1/WRAP\\_THESIS\\_Winkvist\\_2013.pdf](http://wrap.warwick.ac.uk/59055/1/WRAP_THESIS_Winkvist_2013.pdf) [Accessed 1 November 2013].

WMR, 2013. *RoboCup Rescue 2013 - Eindhoven (Finals) - Photos*. [Online] Available at: <http://www2.warwick.ac.uk/fac/sci/eng/meng/wmr/media/at-the-competitions/robocup2013/photos/> [Accessed 25 April 2014].

XSens, 2013. *MTi-10-IMU-2A8G4-DK*. [Online] Available at: <http://shop.xsens.com/shop/mti-10-series/mti-10-imu/mti-10-imu-2a8g4-dk#!prettyPhoto> [Accessed 1 November 2013].

Zauls, E. & Winkvist, S., 2013. *Handover* [Interview] (October 2013).

## **Appendices**

### **Appendix A – Acronyms**

A-USAR – Autonomous Urban Search and Rescue

CAD – Computer Aided Design

COG – Centre of Gravity

FBD – Free Body Diagram

FEA – Finite Element Analysis

FOC – Factor of Safety

HID – Human Interface Device

HMI – Human Machine Interface

HSI – Human System Interface

IMC – International Manufacturing Centre

MRA – Modular Robotic Architecture

M-USAR – Micro Urban Search and Rescue (Referencing the new USAR robot)

T-USAR – Tele-operated Urban Search and Rescue (Reference to the old, large USAR robot)

USAR – Urban Search and Rescue

WMR – Warwick Mobile Robotics

## Appendix B – Chassis

### B.1 – Analysis of Possible Chassis Materials

Three aluminium based solutions were short-listed for the chassis material from the research undertaken and previous knowledge of materials (Table 57). The seven most relevant factors from the specification were chosen and each material was given a score out of five. Although some factors are more important than others, weighting factors was unnecessary since there was a clear winner across the majority of categories.

**Table 57: Analysis of Possible Chassis Materials**

Material	Ease of manufacture	Ease of assembly	Light-weight	Low cost	Modular	Rigid	Durable	Average
Sheet metal	2	2	4	4	2	1	3	2.57
Aluminium	2	3	1	3	2	5	5	3.00
MakerBeam	4	4	4	4	5	4	4	4.14



## B.2 – Analysis of Possible Shell Materials

A similar process as above was performed for the shell with slightly different factors due to the differing requirements of the shell (Table 58). Here, there was not such a clear choice: aluminium, Tufnol and Polycarbonate all scored relatively highly. Since the shell is merely a protective layer and a major part of the project was to design something low cost and lightweight, these factors were considered more important than the others. For this reason, along with its greater aesthetic appeal, polycarbonate was chosen for the sides, front, back and top of the chassis and where higher impact strength, durability and scratch resistance was required, aluminium sheet metal was chosen for the base plate.

**Table 58: Analysis of Possible Shell Materials**

Material	Ease of manufacture	Low cost	Durable	Modular	Lightweight	Material Availability	Impact Strength	Average
Bamboo Composite	3	1	4	1	3	1	4	2.83
Aluminium	3	3	4	1	2	5	4	3.67
Tufnol	3	2	4	1	3	4	4	3.50
ABS	3	4	2	1	5	4	1	3.33
Polycarbonate	3	3	3	1	4	4	3	3.50
Carbon fibre	1	1	5	1	3	2	5	3.00
Pierced metal sheet	2	2	4	2	2	3	3	3.00

### B.3 – Worm Gear Force Analysis

Worm gears have been used in the arm and powertrain designs, also impacting directly on the chassis design. The following describes the calculations of these forces ().

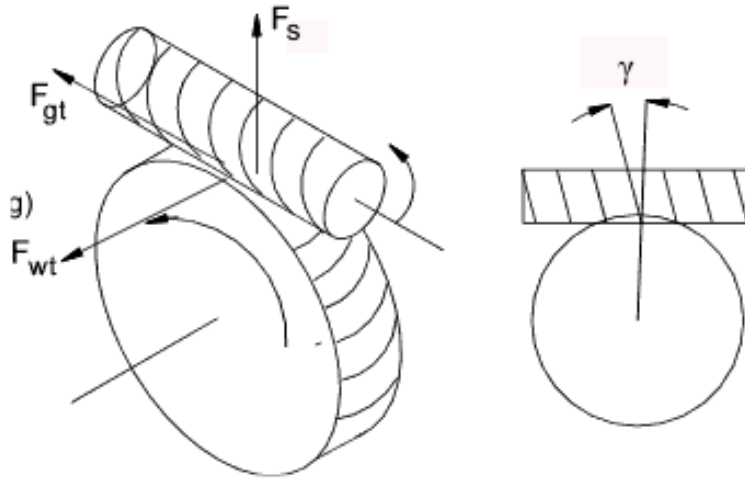


Figure 150: - Forces generated by worm and worm gear pair (R.Beardmore, 2013)

The tangential force on worm equals the axial force on worm wheel, as shown in Equation 23.

$$F_{wt} = F_{ga} = \frac{2 \cdot \tau_1}{d_1} \tag{Equation 23.}$$

All variables are defined in Table 60 and Table 61.

The coefficient of friction varies widely depending upon variables such as the gear material, lubricant, temperature, surfaces finishes, accuracy of mounting and sliding velocity (R.Juvinall, 2012).

The relationship between the coefficient of friction and the sliding velocity is show by Table 59.

Table 59: Slide Velocity- Coefficient of friction relationship (R.Beardmore, 2013)

Sliding velocity, $V_s$ / ms <sup>-1</sup>	Coefficient of friction, $\mu$
0.000	0.145
0.001	0.120
0.050	0.090
0.100	0.080
0.200	0.070

Sliding velocity is calculated in Equation 24.

$$V_s = 0.00005236 \cdot d_1 \cdot n_1 \cdot \sec \gamma \quad \text{Equation 24.}$$

The corresponding coefficient of friction is found from Table 59 using linear interpolation. The axial force on worm equals the tangential force on worm as shown by Equation 25.

$$F_{wa} = F_{gt} = F_{wt} \left( \frac{\cos(\alpha_n) \cdot \cos(\gamma) - \mu \cdot \sin(\gamma)}{\cos(\alpha_n) \cdot \sin(\gamma) + \mu \cdot \cos(\gamma)} \right) \quad \text{Equation 25.}$$

Separating Force on worm-gearwheel is given by Equation 26.

$$F_s = F_{wt} \left( \frac{\sin(\alpha_n)}{\cos(\alpha_n) \cdot \sin(\gamma) + \mu \cdot \cos(\gamma)} \right) \quad \text{Equation 26.}$$

Worm gear efficiency is given by Equation 27.

$$\eta = \left( \frac{\cos(\alpha_n) - \mu \cdot \tan(\gamma)}{\cos(\alpha_n) + \mu \cdot \cot(\gamma)} \right) \quad \text{Equation 27.}$$

Using the input parameters (Table 60) for the worm gear pairs used in the Arm and powertrain with the above equations the resulting forces and efficiencies where found (Table 61).

**Table 60: Input Parameters for Worm Gear Pairs**

Input Parameter	Symb	Arm Base Joint	Flipper orientation motor	Track unit Motor
Normal Pleasure angle/ Deg	$\alpha_n$	20.0	20.0	20.0
Pitch diameter of worm	$d_1$	15.0	48.0	15.0
Modulus	$m$	1.0	2.0	1.3
Number of worm gear teeth	$Z_1$	30.0	24.0	12.0
N.o. of starts on worm	$Z_2$	2.0	4.0	4.0
Worm rotational velocity/ Rpm	$n_1$	60.0	36.0	240.0
Gear reduction	$R_g$	15.0	6.0	3.0
Input torque/N	$M_1$	2.2	5.1	2.7

**Table 61: Output Forces and Efficiencies Generated by Worm Gear Pairs**

Output Parameter	Symb	Arm Base Joint	Flipper orientation motor	Track unit Motor
Worm Tangential Force = Worm Gear Axle Force/N	$F_{wt} = F_{ga}$	284.4	213.5	360.0
Worm Axial Force = Worm Gear Tangential Force/N	$F_{wa} = F_{gt}$	1297.5	1243.9	1032.5
Separating Force/N	$F_s$	87.2	68.0	101.9
Worm Gear Efficiency/%	$\eta$	60.8%	48.5%	76%

#### B.4 – Derivation of Load Value for Arm Chassis Mount FEA

A simplified version of Figure X was used for analysing where the arm attaches to the chassis. The load was modelled as a moment about the arm mounting plate. This was calculated as the sum of the moment produced by the mass of the arm (assumed to be 3kg) acting in middle of the arm, and the mass of the maximum payload (0.5kg) acting at the gripper end of the arm. This is shown by the diagram in Figure X and the total moment:

$$\text{Moment} = (0.6 \times 30) + (1.2 \times 5) = 24Nm$$

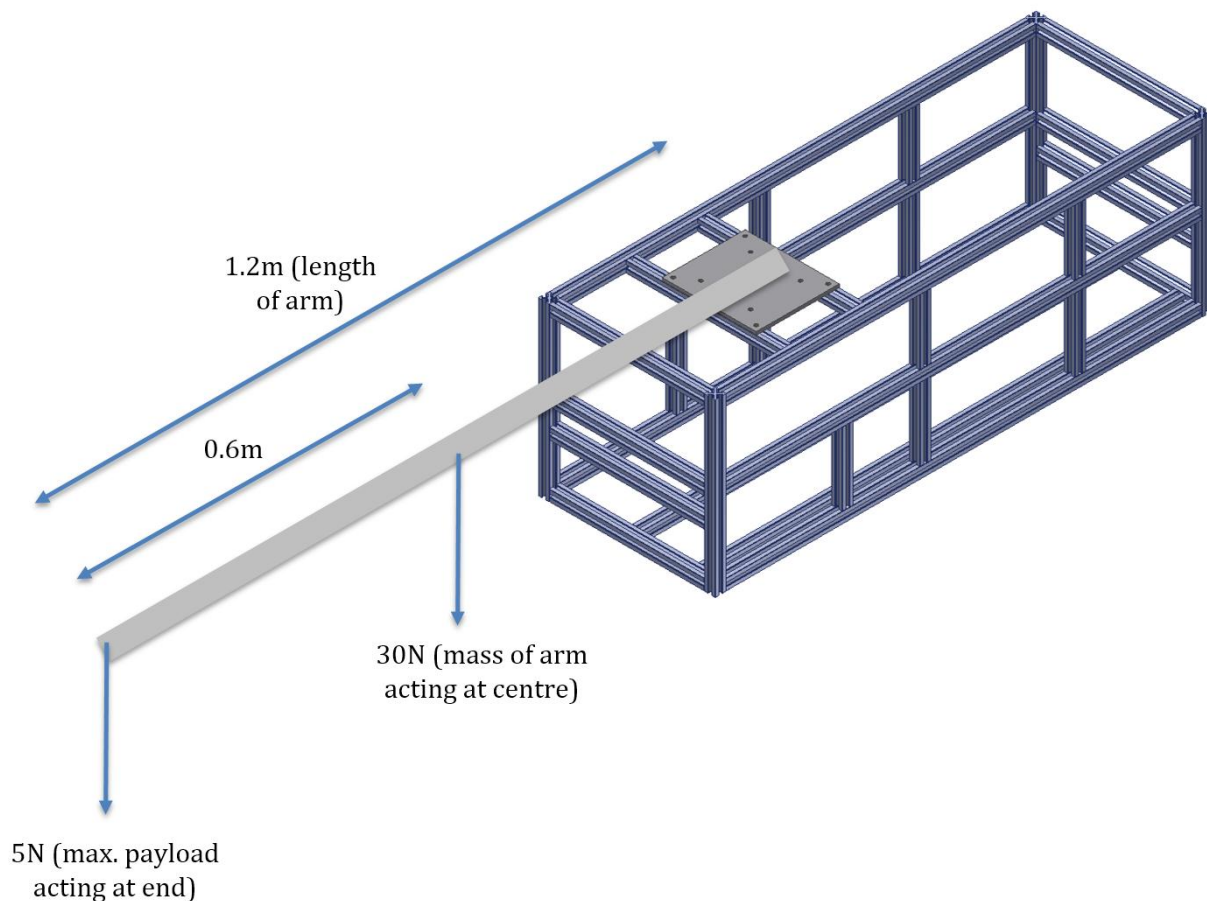


Figure 151: Diagram to Depict the Moment Calculated for the Force of the Arm on the Chassis

### Appendix C – Drivetrain

#### C.1 – Derivation of Drivetrain Dimensions

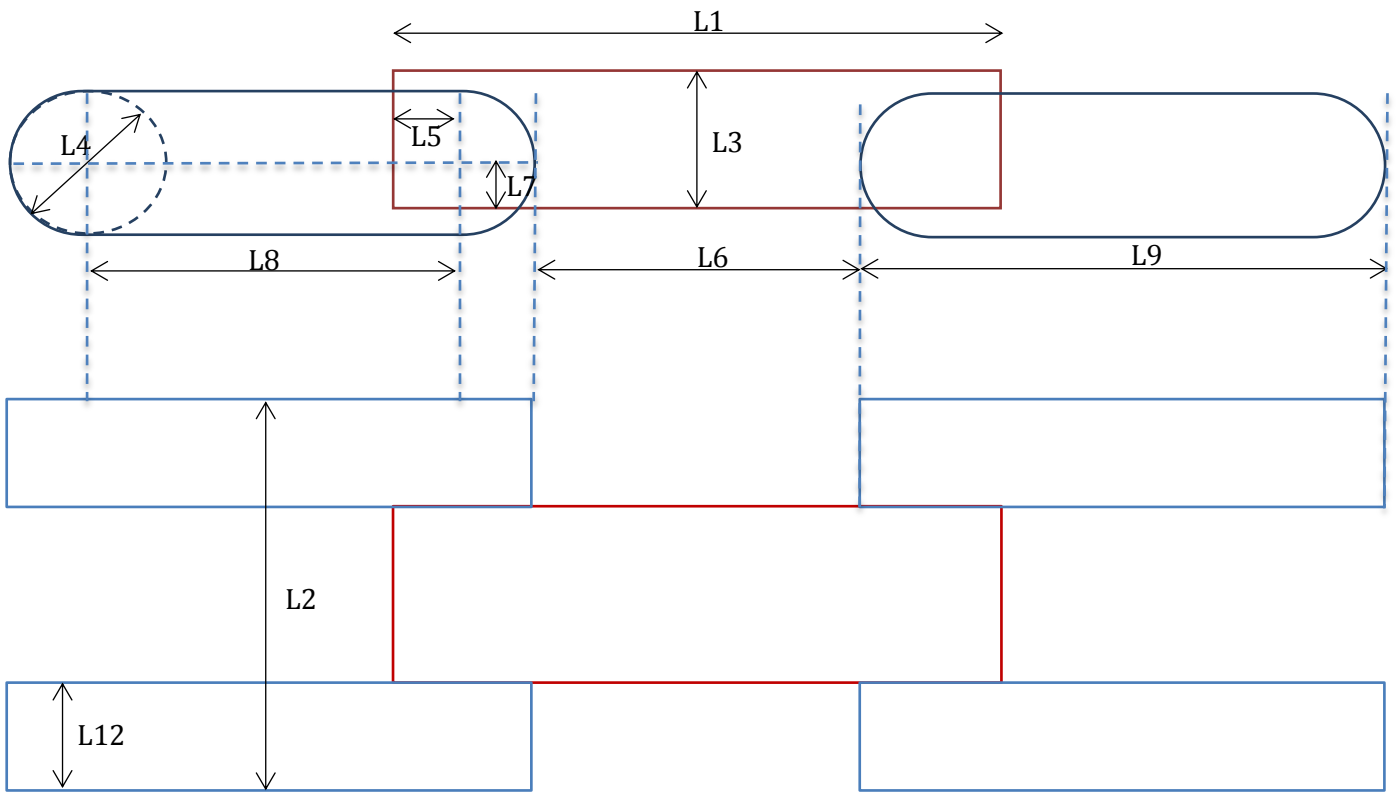


Figure 152: Drivetrain Dimensions

Due to the two primary constraints placed on the design; being able to turn in a 600mm circle and pass through a 600mm triangle, the main dimensions affecting the robot were decided upon (2.4.1, Table 6). This set the values of L1, L2 and L3. L4, the effective diameter/height of the tracks was itself not directly dependent on any other values, but was used in calculating the rest of the values.

L5 is the distance between the flipper axle and the chasis front/back. It needs to be at least half of L4 so that, when positioned vertically, the track units do not protrude out of the L1 constraint.

$$L5 \geq \frac{L4}{2} \tag{Equation 28.}$$

L6 calculates the gap between the tracks, which will affect the length of a track unit (so that it can rotate 360°).

$$L6 = L1 - L4 - 2L5 \quad \text{Equation 29.}$$

L7 is the distance between the flipper axle and the chassis bottom. It is required to be less than half L4, so the tracks go below the chassis. The smaller L7, the greater the clearance of the chassis.

$$L7 < \frac{L4}{2} \quad \text{Equation 30.}$$

L8 is the longest distance possible between a track unit's front and rear axles, while not connecting with the other track unit while rotating 360°.

$$L8 < L6 \quad \text{Equation 31.}$$

L9 is the total length of the track unit, and is just equal to the distance between axles and the effective diameter.

$$L9 = L8 + L4 \quad \text{Equation 32.}$$

Finally, L10 was chosen so that the chassis and both track units, with clearance between, was under the width requirement. Table 62 contains all the values calculated from Equation 28 to Equation 32, and the respective dimensions chosen.

**Table 62 : Drivetrain Dimensions, Calculated and Chosen**

<b>Dimension</b>	<b>Reference</b>	<b>Chosen Value (mm)</b>	<b>Relation</b>	<b>Calculated Value (mm)</b>
<b>Length of robot</b>	L1	450	=	450
<b>Width of robot</b>	L2	300	=	300
<b>Height of robot</b>	L3	155	=	155
<b>Effective diameter</b>	L4	120	=	120
<b>Axle from side</b>	L5	60	≥	60
<b>Gap between tracks</b>	L6	210	=	210
<b>Axle from base</b>	L7	30	<	60
<b>Track axle separation</b>	L8	205	<	210
<b>Track length</b>	L9	325	=	325
<b>Track width</b>	L10	80	=	80

### C.2 – Derivation of Torque and Angular Acceleration Equations

#### Derivation of required torque equation:

For a wheel sitting on a slope, in a no slip situation, a motor (connected to the wheel) needs to produce a torque equal and opposite to the maximum moment friction is applying on the wheel to hold it in place. Equation 33 illustrates the torque required from the motor, and Figure 152 shows an example situation. For units and symbol definitions please see section 1.5.4 (not included is  $f$ , which is friction, and  $F$ , which is force, both with units N).

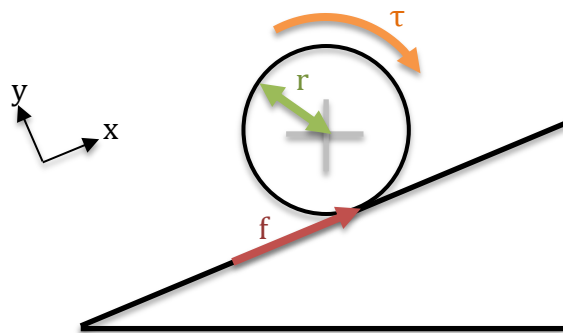


Figure 153: Wheel On a Slope

$$\tau = fr$$

Equation 33.

However, a robot wheel (or track sprocket) needs to not only hold itself in place on the slope, but accelerate up it. Figure 154 shows the wheel accelerating up the slope.

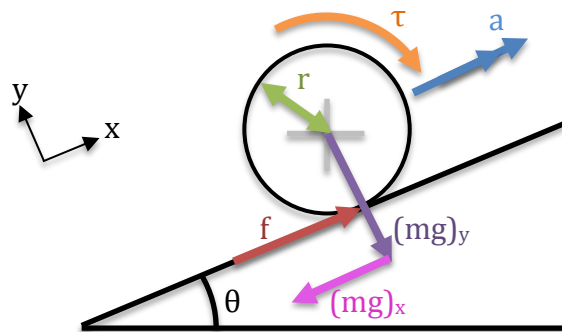


Figure 154: Wheel Accelerating Up a Slope

Balancing the forces in the x direction gives Equation 34.

$$\Sigma F_x = -(mg)_x + f \quad \text{Equation 34.}$$

Where:

$$\Sigma F_x = ma \quad \text{Equation 35.}$$

And:

$$(mg)_x = -mgsin\theta \quad \text{Equation 36.}$$

Substituting Equation 35 and 36 into Equation 34 gives Equation 37.

$$ma = -mgsin\theta + \frac{\tau}{r} \quad \text{Equation 37.}$$

Rearranging Equation 37 to find T gives Equation 38.

$$\tau = (a + gsin\theta)mr \quad \text{Equation 38.}$$

Next to consider is the number of driven wheels (or sprockets). The torque illustrated in Equation 38 is the total torque required, and can be shared between multiple motors.

$$\tau = \frac{(a + gsin\theta)mr}{n} \quad \text{Equation 39.}$$

Finally, motors are not 100% efficient, due to losses from internal friction. There are also energy losses in the gears, and wheels/tracks will slip, all reducing the actual torque applied to the ground. As these losses can only be found by experiment with the finished system, an estimate of the efficiency of the system is needed. Under estimating will also allow a safety margin. For the system talked about in this report, an efficiency of 65% was chosen for the calculations, as the actual efficiency should be considerably higher (estimated at 90% for gears, 90% for grip, and motor values quoted after efficiency was considered illuminating it from our equations, totalling at an estimated 81% efficiency of the system). Equation 40 takes the efficiency into consideration.



$$\tau = \left(\frac{100}{e}\right) \frac{(a + g \sin \theta) m r}{n} \quad \text{Equation 40.}$$

Derivation of required angular velocity equation:

In one revolution, assuming no slip, a wheel at constant velocity travels a distance equal to its circumference. Therefore the number of revolutions required per second is its velocity divided by its circumference, as shown in Equation 41. For units and symbol definitions please see section 1.5.4.

$$\omega = \frac{v}{2\pi r} \quad \text{Equation 41.}$$

However this angular velocity has the units of rps, and most motors are specified with angular velocity measured in rpm. Therefore Equation 42 will give the required angular velocity in rpm.

$$\omega = 60 \frac{v}{2\pi r} \quad \text{Equation 42.}$$

### C.3 – Flipper Torque and Loading Scenarios

#### Situation 1:

Both flipper units are used to lift the robot up while staying level. The force due to the mass of the robot is equally split across the two flipper axles. The moment after the flippers rotate past the horizontal x axis, the force due to mass will act through the only points of contact with the ground; the ends of the flippers, as illustrated in Figure 154.

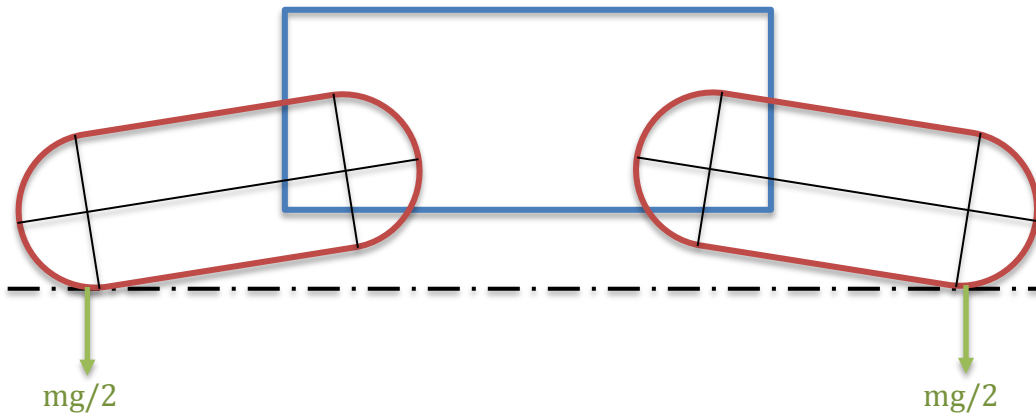


Figure 155: Situation 1.1

To lift the robot, an overall force greater than the weight of the robot is required to be created in the opposing direction. The two flipper motors need to create this force, and it acts at each flipper axle. They create it by applying a torque to the flipper axles. See Figure 155 for an updated diagram with the torque and force from the motors.

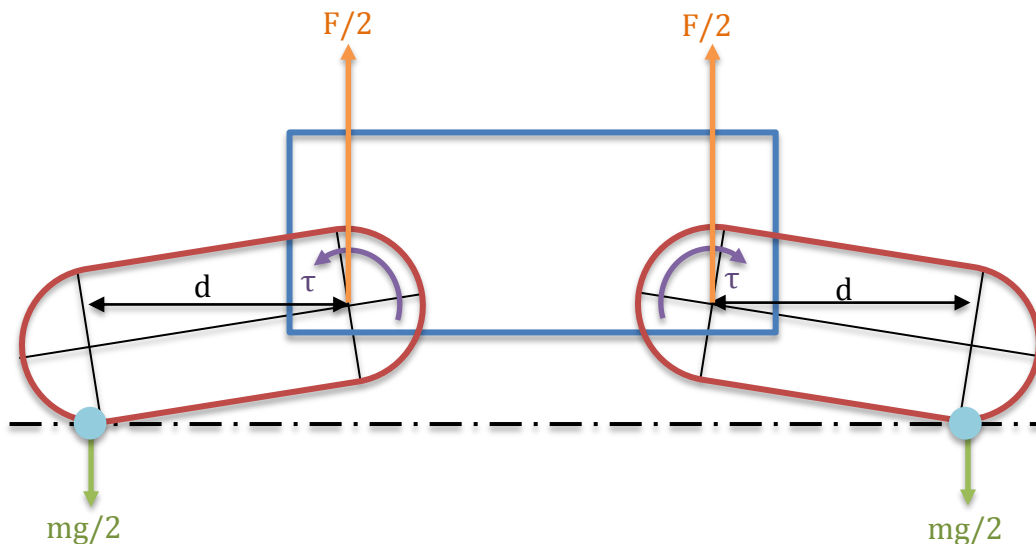


Figure 156: Situation 1.2

Normally, this torque would rotate the flipper units around the flipper axle whilst the axle itself remains stationary. However, the flippers are in contact with the ground, at the points illustrated with blue dots in Figure 155, and cannot be rotated down. For the situation analysed, which is only a stationary moment in time, the blue dots can be considered as fixed.

This means the torque lifts the flipper axles vertically. Equation 43 links the quantities talked about.

$$\tau = \frac{F}{2}d > \frac{mg}{2}d \tag{Equation 43.}$$

Table 63 shows the values for these quantities, and the resulting minimum torque. As the flippers rotate down, the value for 'd', the horizontal distance between the forces, gets smaller, reducing the torque required. We will use the greatest value for 'd' possible, when the flippers are completely horizontal.

Table 63: Situation 1

Input	Value	Units
Mass	25	Kg
Distance	0.205	m
Output		
Min Torque	25.138	Nm

Situation 2:

One flipper unit is used to lift one end of the robot only. The mass of the robot acts from the centre of gravity. This is assumed to be the middle of the robot lengthwise, height is not important for these calculations

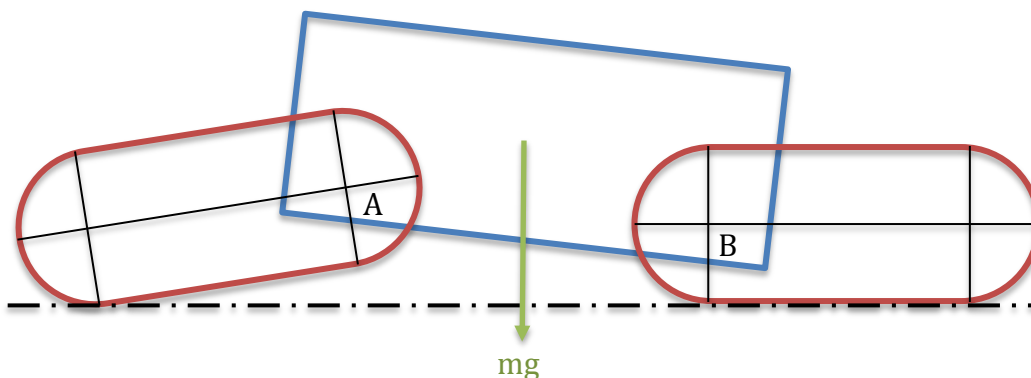


Figure 157: Situation 2.1

The weight of the robot creates a moment around axle B. A force acting upwards at axle A is required, creating a moment to counteract that of the weight. Since the horizontal distance

from A to B is always twice the distance from COG to B, the force required at A has to be half that at COG to hold it in place, or higher to raise A further. Once again, a torque applied onto axle A creates this force. The blue dot and distance 'd' are the same as in situation 1.

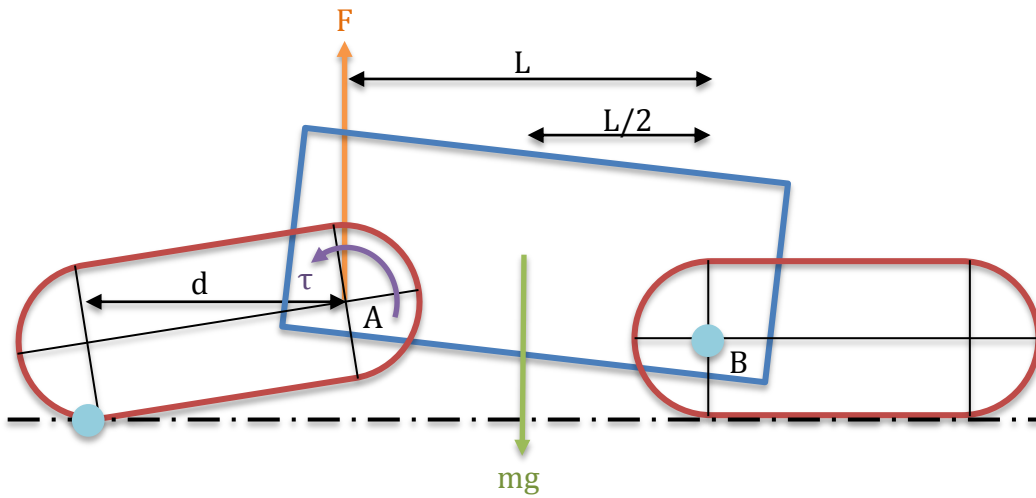


Figure 158: Situation 2.2

In this situation, the vertical force needed at axle A is identical to that which was required in situation 1, i.e. greater than half the weight. This means the torque required is the same when using the same inputs.

$$\tau = Fd > \frac{mg}{2}d \tag{Equation 44.}$$

Table 64: Situation 2

Input	Value	Units
Mass	25	Kg
Distance	0.205	m
<b>Output</b>		
Min Torque	25.138	Nm

**Situation 3:**

Finally, the robot might need to wedge its front flipper in place, i.e. under a stair or boulder, and then use the flipper to lift the rest of the body up. This is illustrated in Figure 158.

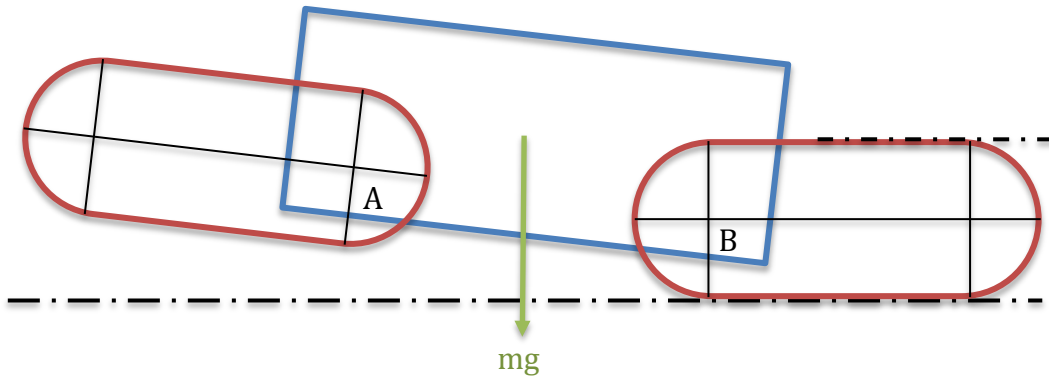


Figure 159: Situation 3.1

The weight of the robot creates a torque anti-clockwise around axle B, and in this situation, the axle needs to produce a clockwise torque greater than the one due to weight.

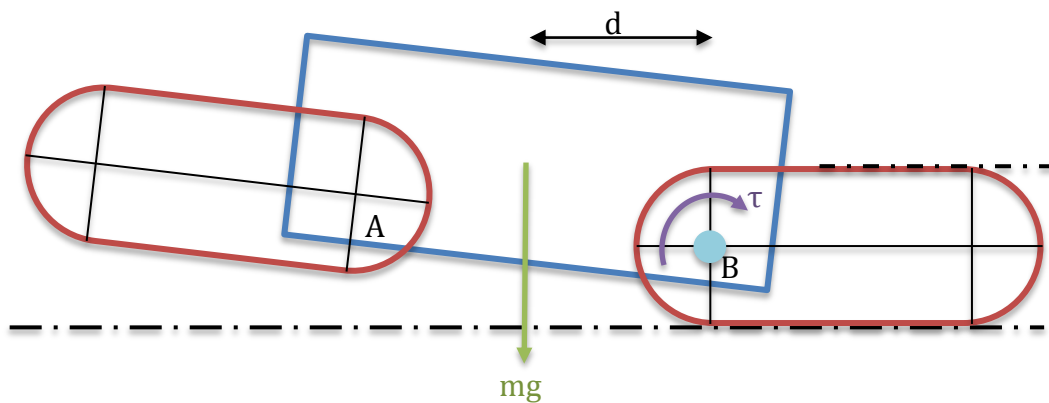


Figure 160: Situation 3.2

$$\tau > mgL$$

Equation 45.

Table 65: Situation 3

Input	Value	Units
Mass	25	Kg
Distance	0.165	m
Output		
Min Torque	40.466	Nm

The torque required for equilibrium is the largest in situation 3, so the motor will need to exceed this value.

### C.4 – Drivetrain Design Narrative

#### Tracks:

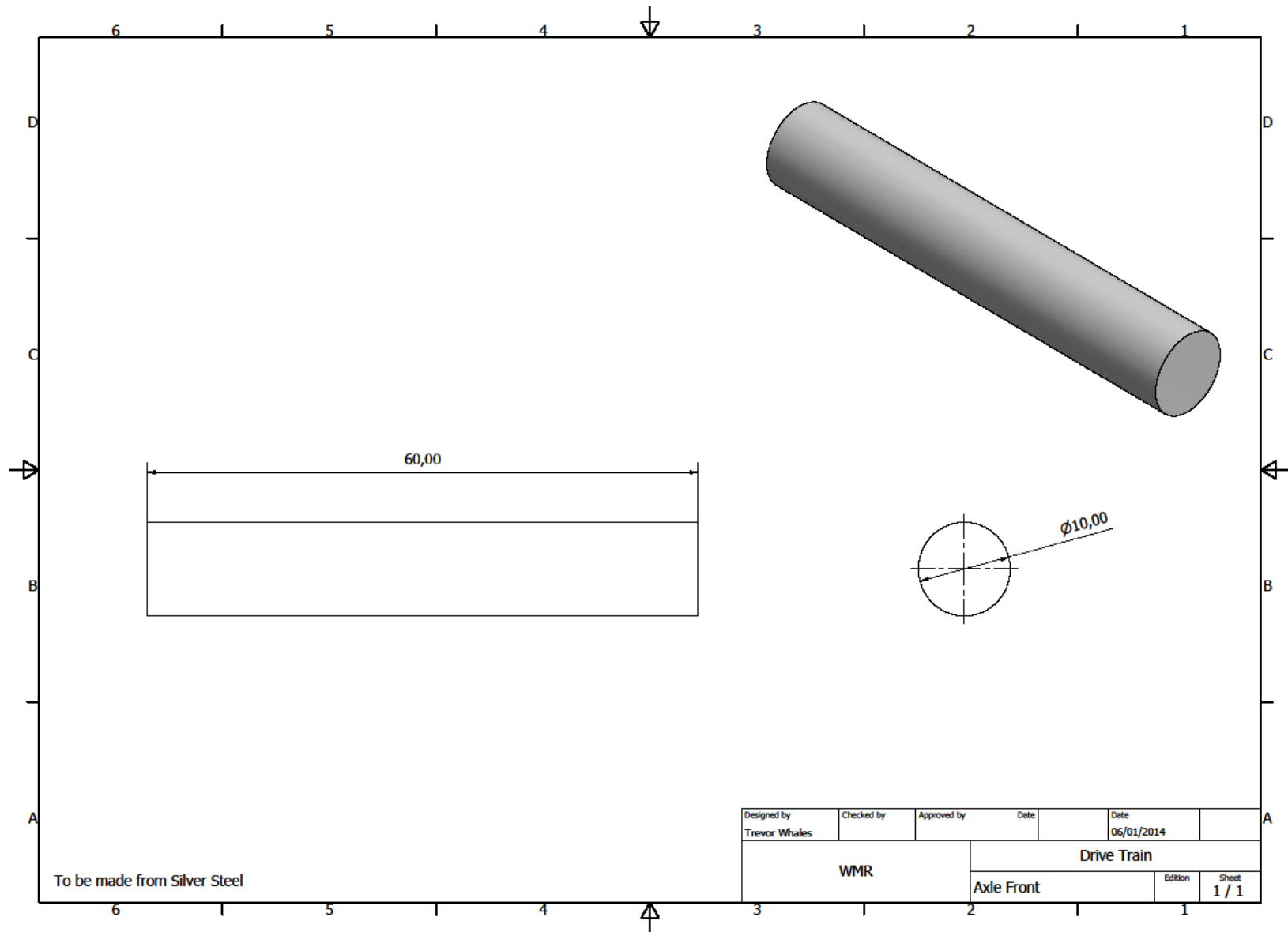
1. Try to get motor inside track unit
2. Motor needs to be lengthwise due to space, so motor axle at  $90^0$  to driven axle
3. As main axle is to be used to actuate flippers
4. Therefore tracks driven by axle at the other end
5. Use bevel gears to make  $90^0$  transition from motor to axle
6. Bevel gears take up too much space so will not work
7. Use ~~bevel~~ worm gears to make  $90^0$  transition from motor to axle
8. Chose worm and wheel gear to have as close to 1:1 ratio as possible, as motor already has required torque
9. Chose to increase torque with close ratio
10. Chose worm and wheel gear to be as small as possible with given requirements
11. Tracks to be two parallel chains, on two sets of sprockets
12. Sprockets on flipper axle need to rotate separately to axle
13. Use IGUS bushes between sprockets and flipper axle
14. Front axle needs to be connected to sprockets, use grub screws
15. Front axle needs to rotate separately to track unit body
16. Use ball bearings to provide low friction turning of front axle
17. Ball bearings + sprocket hubs are too wide
18. Use ~~ball bearings~~ IGUS bushes to provide low friction turning of front axle
19. Turn sprockets around so the hub is inside the IGUS bush and therefore not taking up unnecessary room
20. Length of robot is defined by specification
21. We want track unit to spin  $360^0$  without hitting other unit, so length defined
22. Chose largest sprockets possible for greatest ground clearance based on length, and parts needed to go in between (motor)
23. Create side plates to form base of track unit body
24. Design so both inside and outside are the same in as many ways as possible, as inside on left will be outside on right
25. Bolt motor onto side plates
26. Try to get motor control board inside track unit

27. Will not fit inside
28. Can be placed sideways with gaps in the wall, slightly extruding but acceptable
29. Put in cross bracers between sides where possible
30. Flipper axle needs to be rigidly connected to track unit
31. Design flipper axle hat to attach body to axle
32. Cables need to get from chassis to track unit
33. Design holes/slots/grooves where wires can enter track unit
34. Worm gear needs support at end
35. Design set of plates & poles to support worm gear that attaches to motors face
36. Use another IGUS bush on the end of the worm to allow for low friction rotation
37. Tracks to be made from two chains, with u-channel and rubber tube inside the channel
38. Find chains that have the appropriate attachment and design u-channel sections
39. Tracks need tensioning
40. Design tensioning block for the base of the track unit
41. Tensioning block adds extra ground clearance
42. Tensioning block made out of acetyl resin for low friction

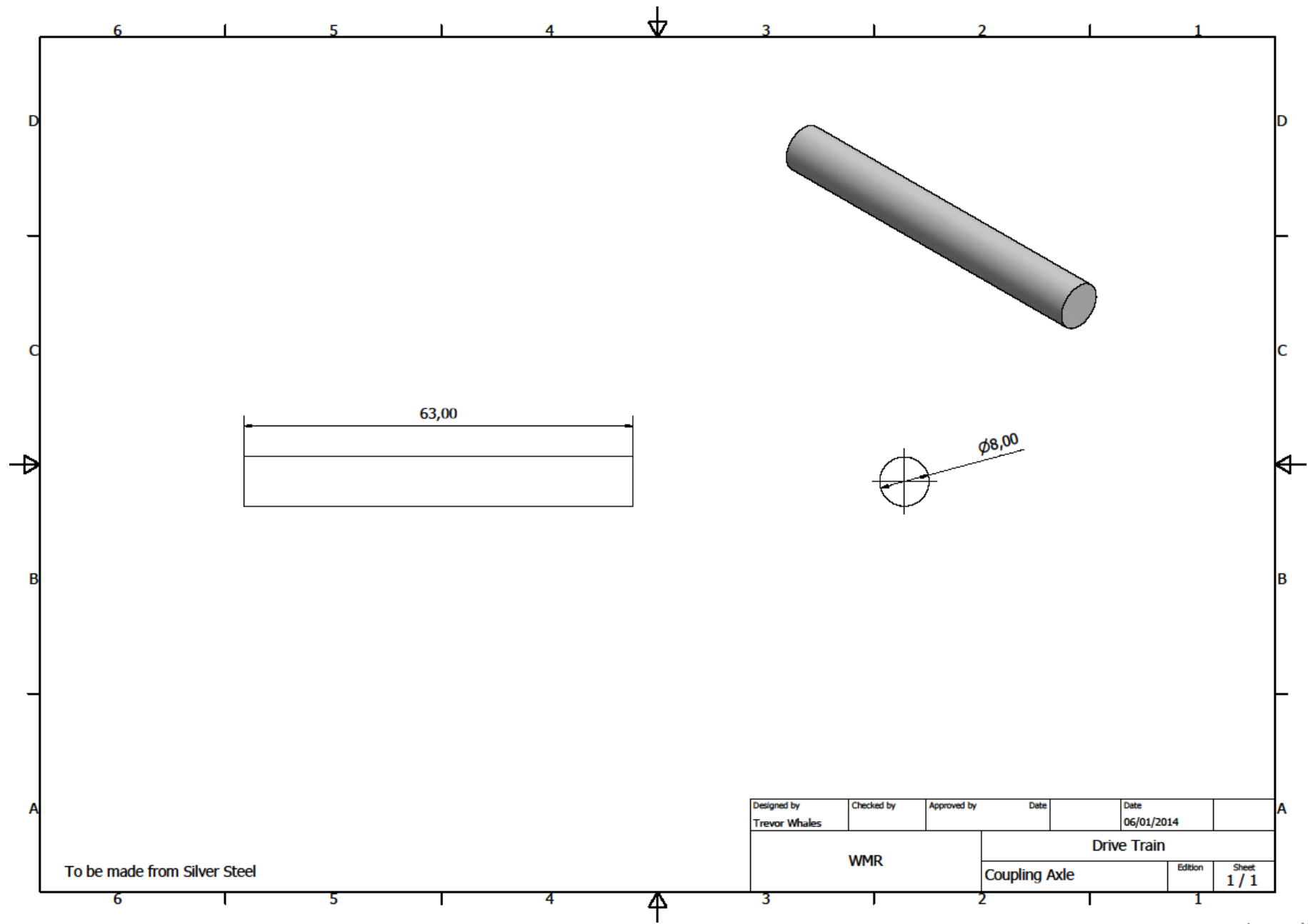
#### Flippers:

1. Use same motor as in tracks for simplicity
2. Use worm and wheel gears to create required torque
3. Therefore motor needs to be at 90° to axle
4. Use Ondrives gearbox to connect motor to flipper axle
5. Chosen gearbox is quite expensive
6. Use ~~Ondrives gearbox~~ individually bought worm and wheel gears to connect motor to flipper axle and save money
7. Flipper axle needs good support and to spin freely
8. Use ball bearings directly mounted to chassis
9. End of worm needs support
10. Use the same ball bearings for simplicity
11. Encoders required to track motion of flippers
12. Use 1:1 Spur gears between axle and encoder to track motion

### C.5 – Drivetrain Technical Drawings

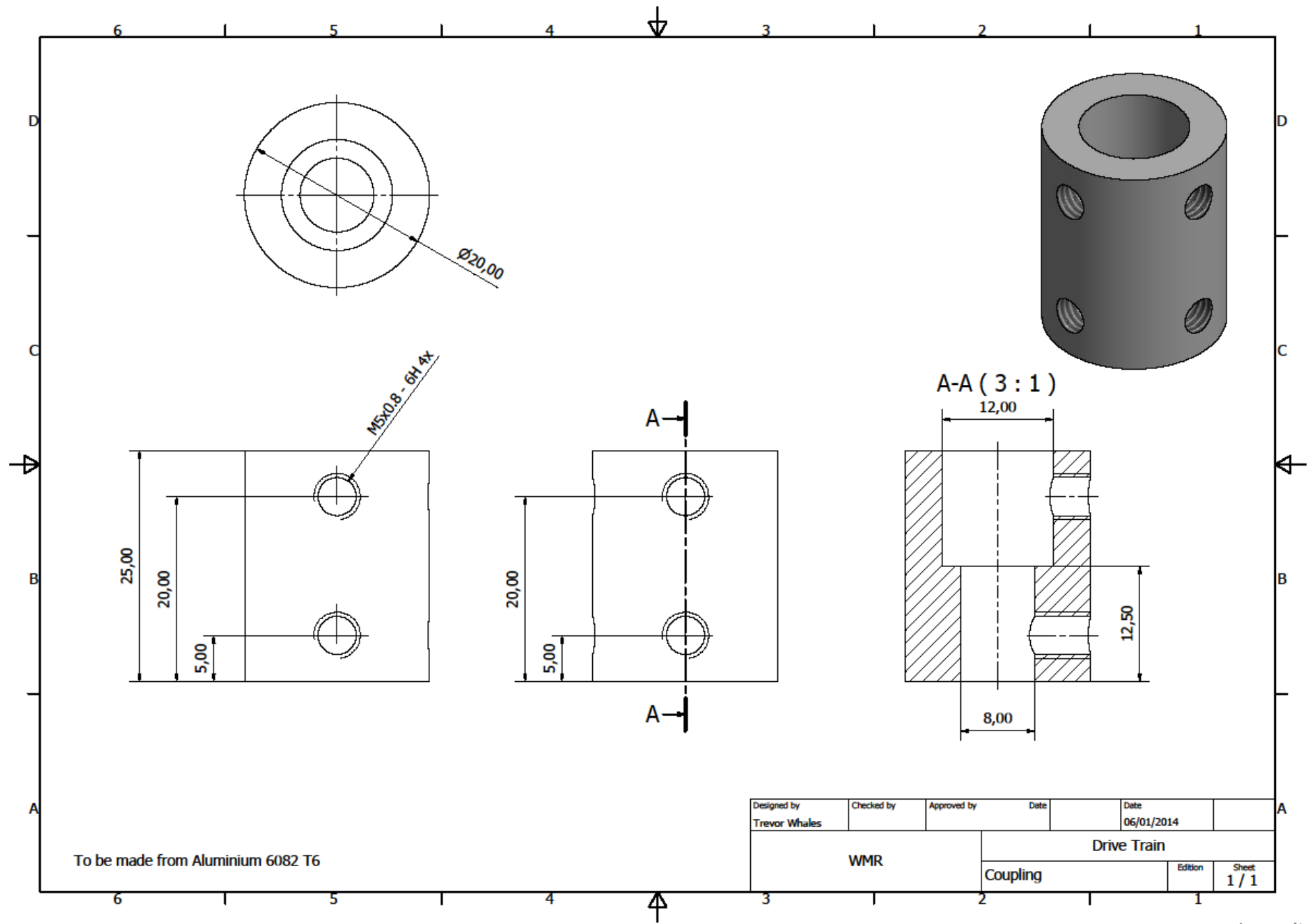






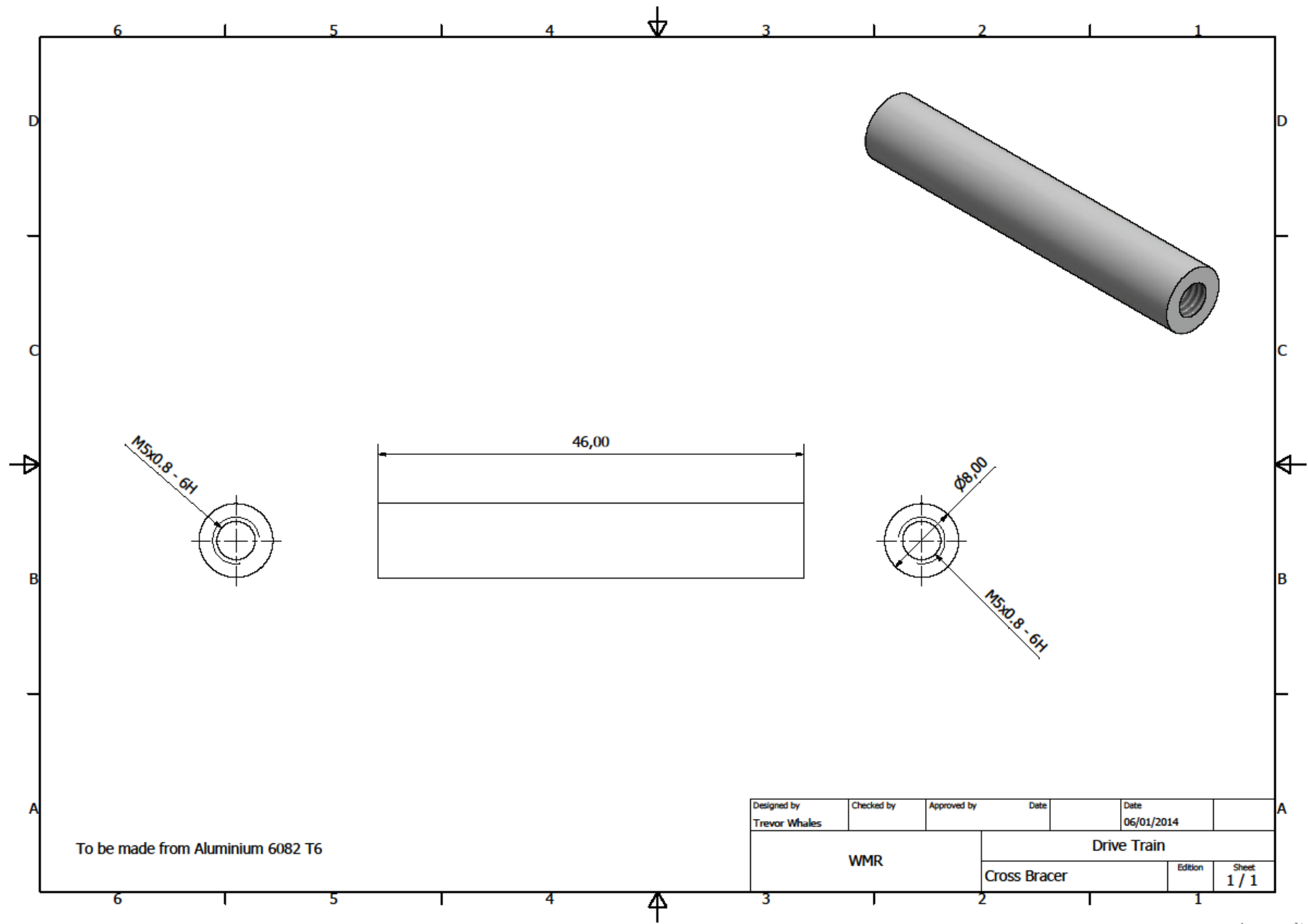
To be made from Silver Steel

Designed by Trevor Whales	Checked by	Approved by	Date	Date 06/01/2014
WMR		Drive Train		
Coupling Axle			Edition	Sheet 1 / 1



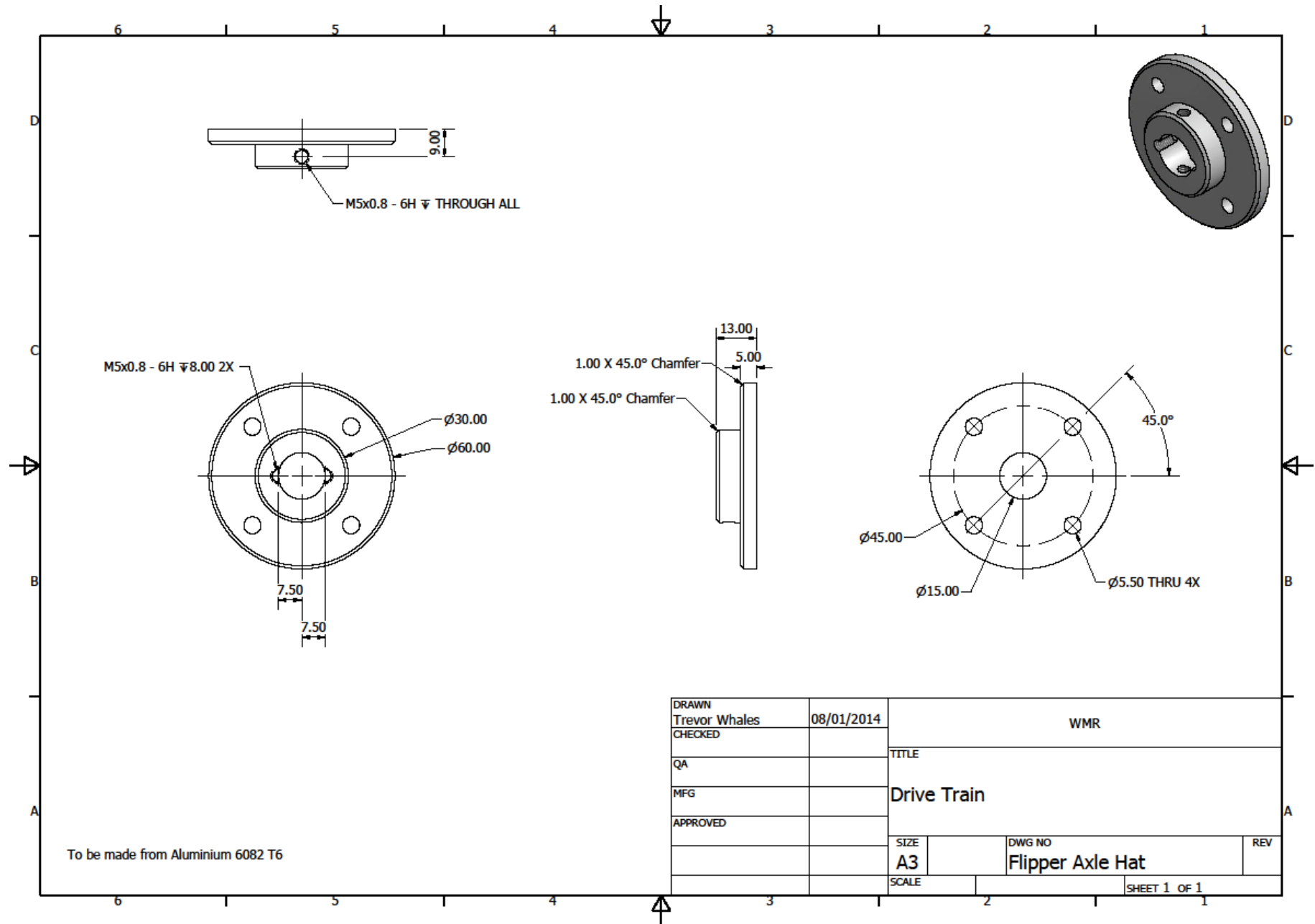
To be made from Aluminium 6082 T6

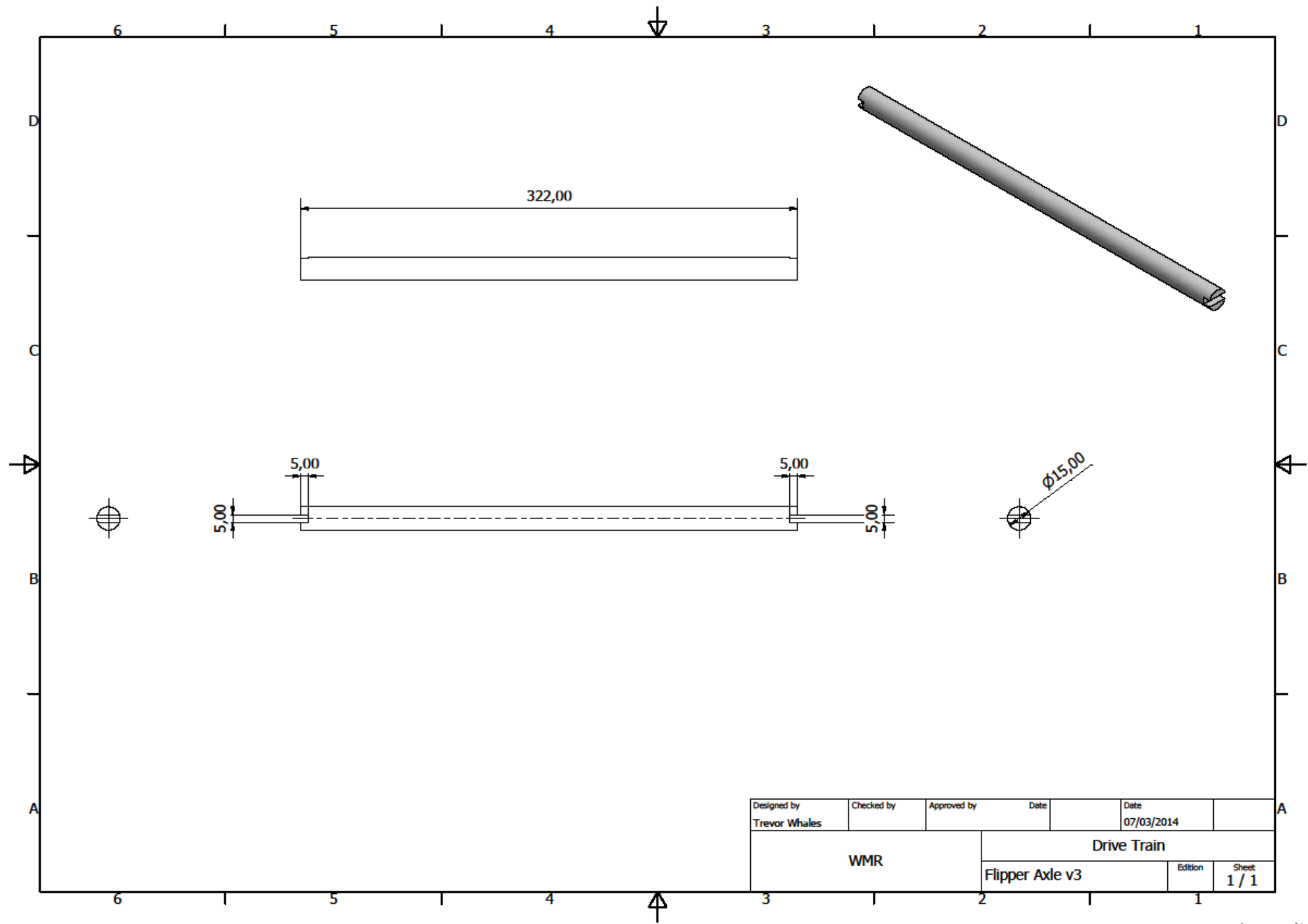
Designed by Trevor Whales	Checked by	Approved by	Date	Date 06/01/2014
WMR		Drive Train		
		Coupling	Edition	Sheet 1 / 1



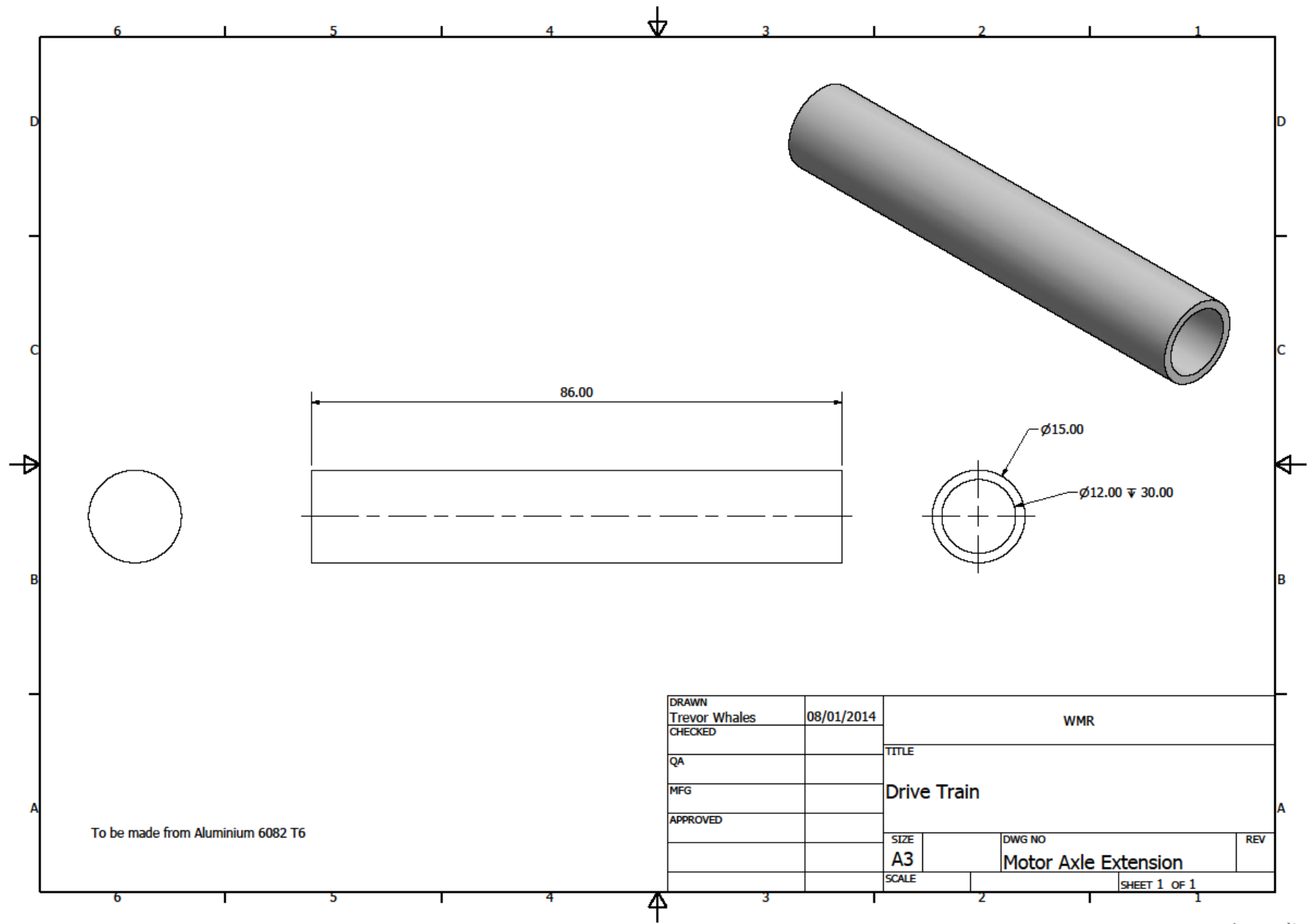
To be made from Aluminium 6082 T6

Designed by Trevor Whales	Checked by	Approved by	Date	Date 06/01/2014
WMR		Drive Train		
		Cross Bracer	Edition	Sheet 1 / 1



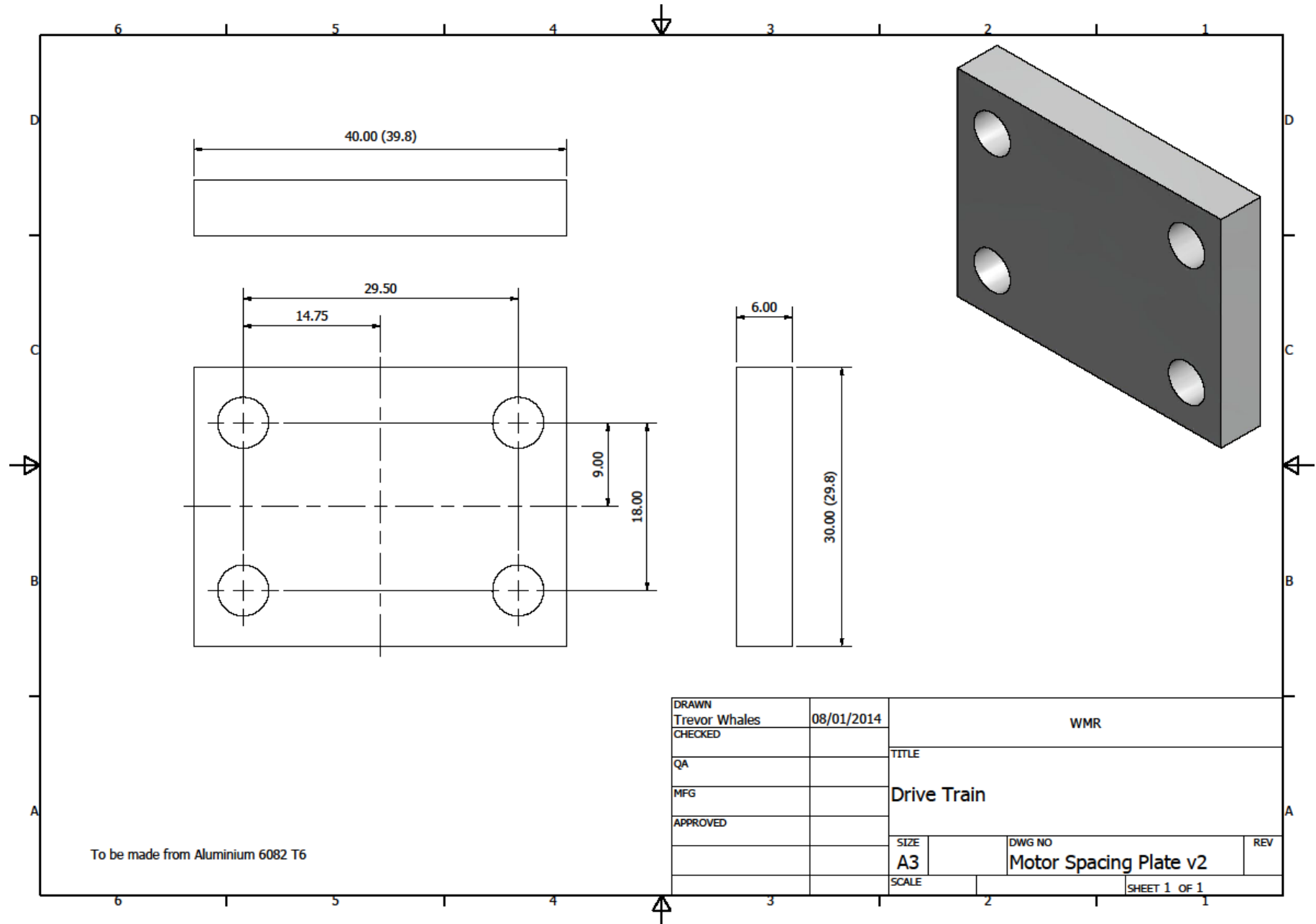


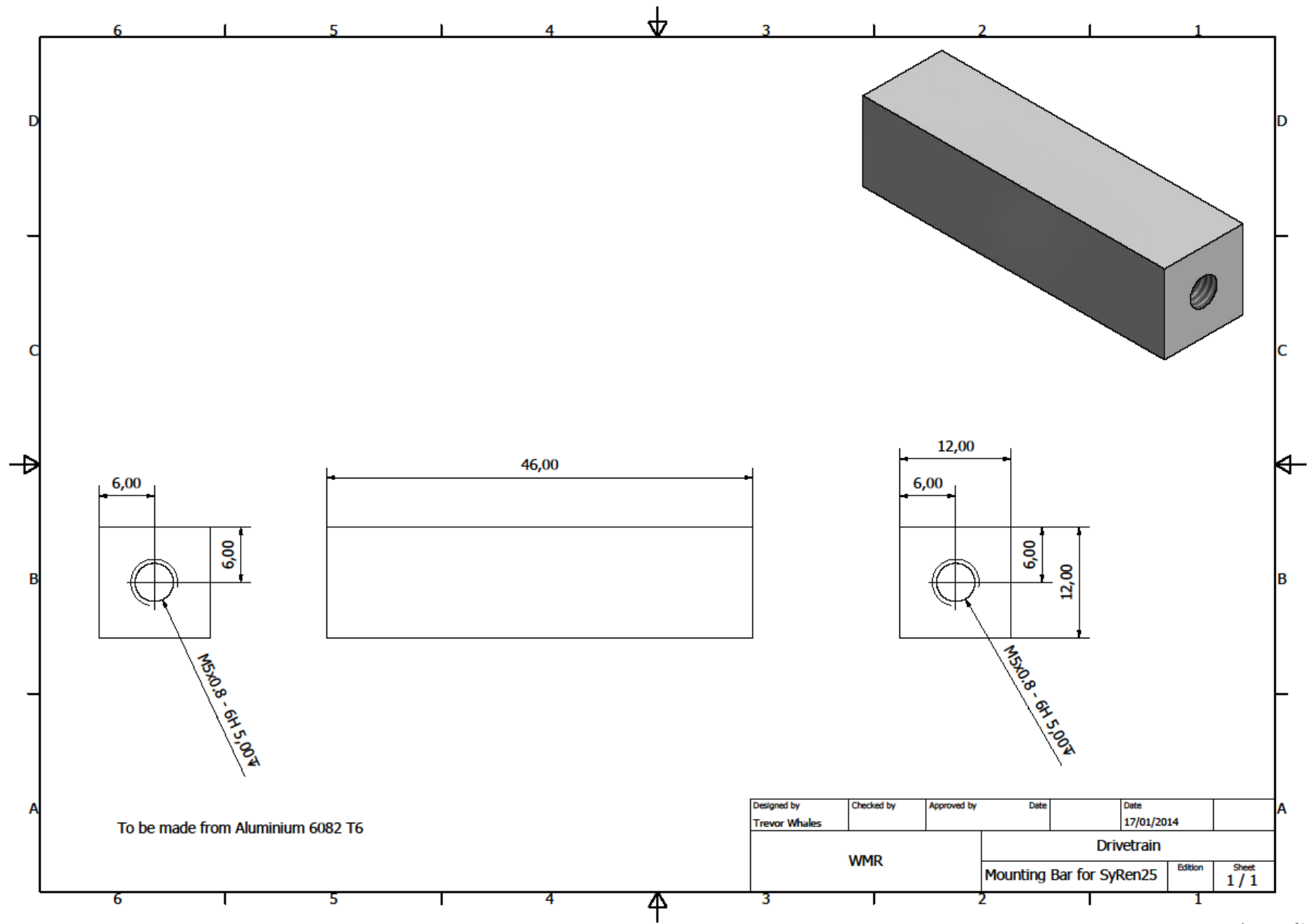
Designed by Trevor Whales	Checked by	Approved by	Date	Date 07/03/2014
WMR		Drive Train		
		Flipper Axle v3		Edition Sheet 1 / 1



To be made from Aluminium 6082 T6

DRAWN	Trevor Whales	08/01/2014	WMR	
CHECKED			TITLE	
QA			Drive Train	
MFG			DWG NO	
APPROVED			Motor Axle Extension	
			SIZE	REV
			A3	
			SCALE	SHEET 1 OF 1

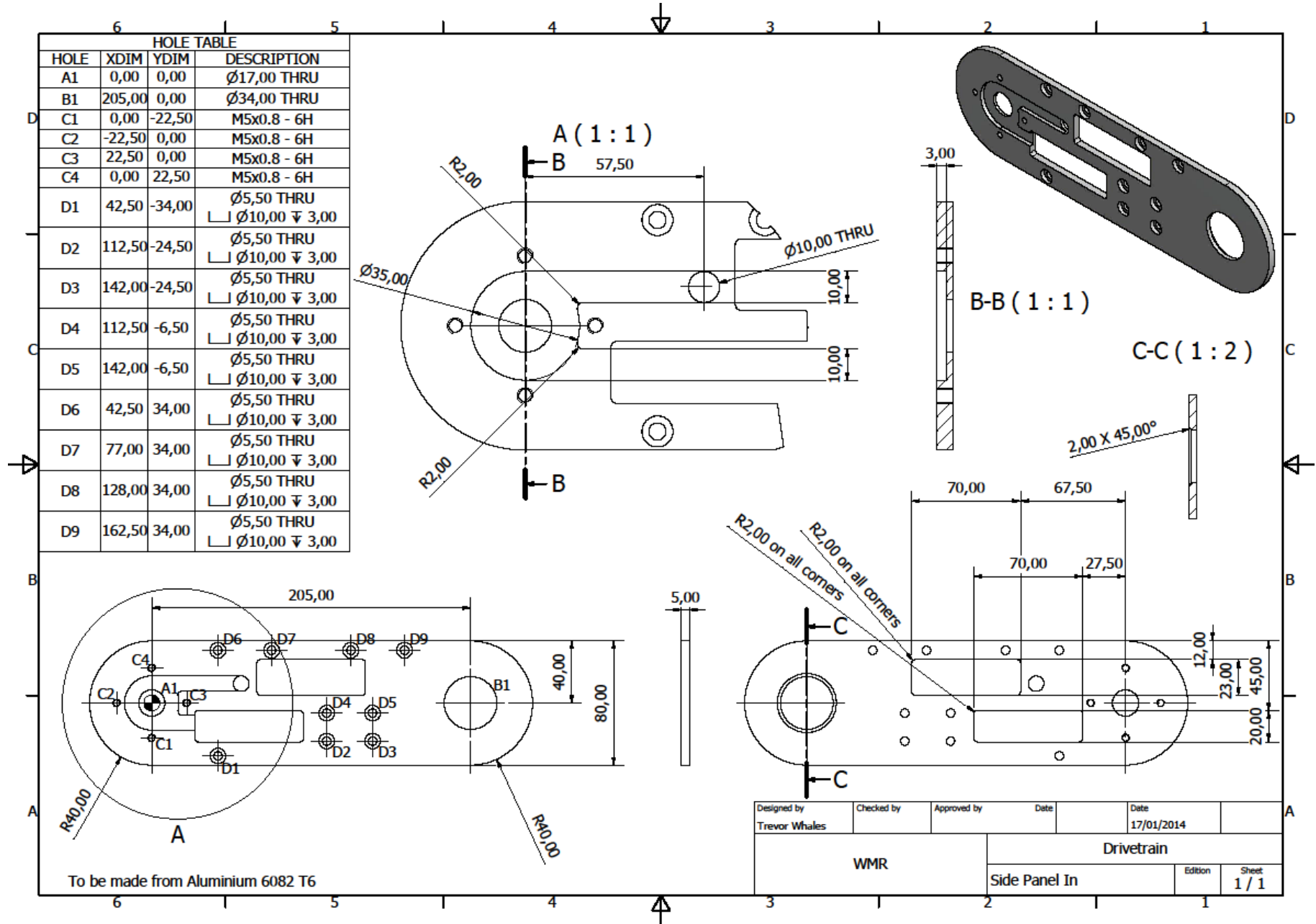


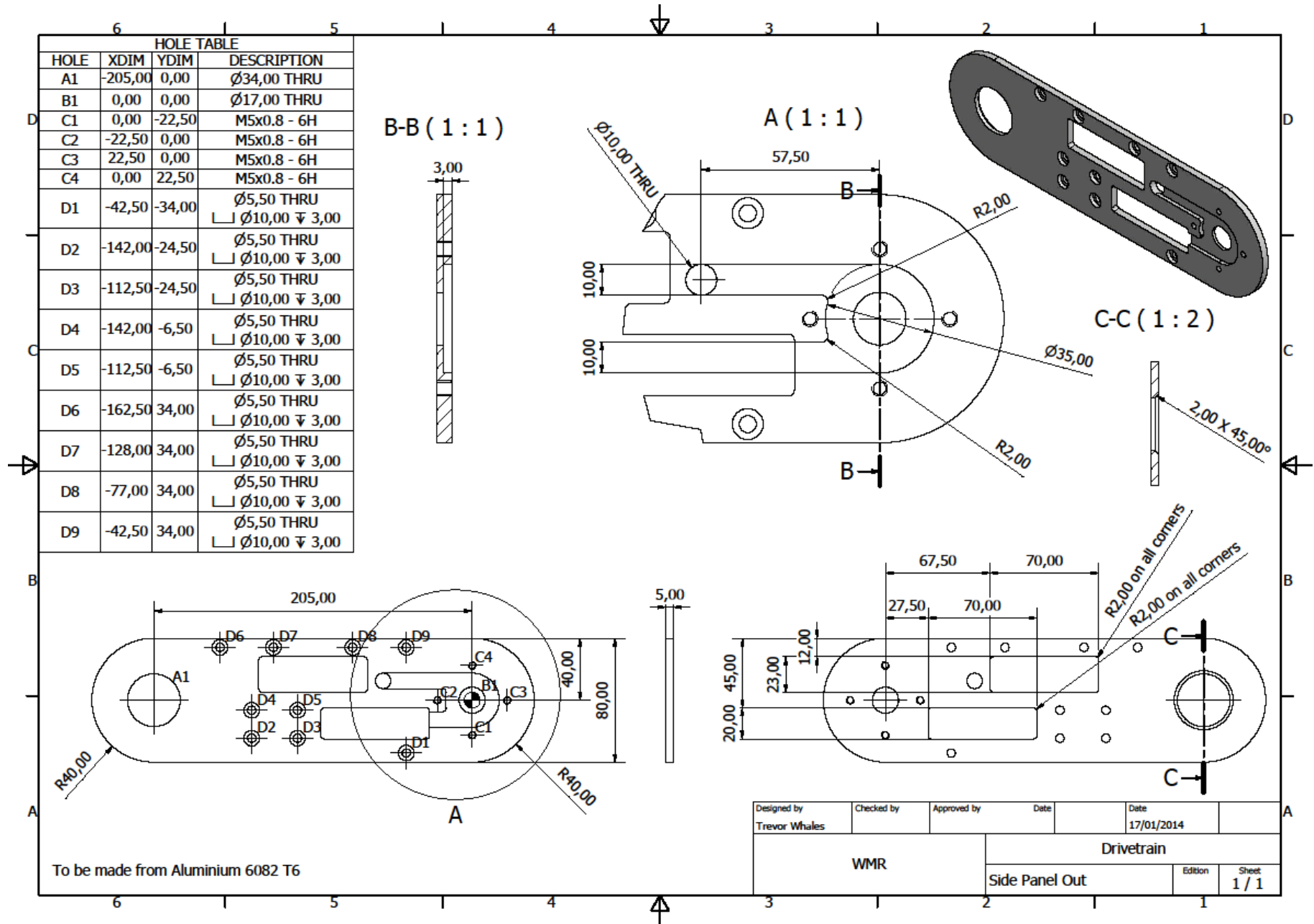


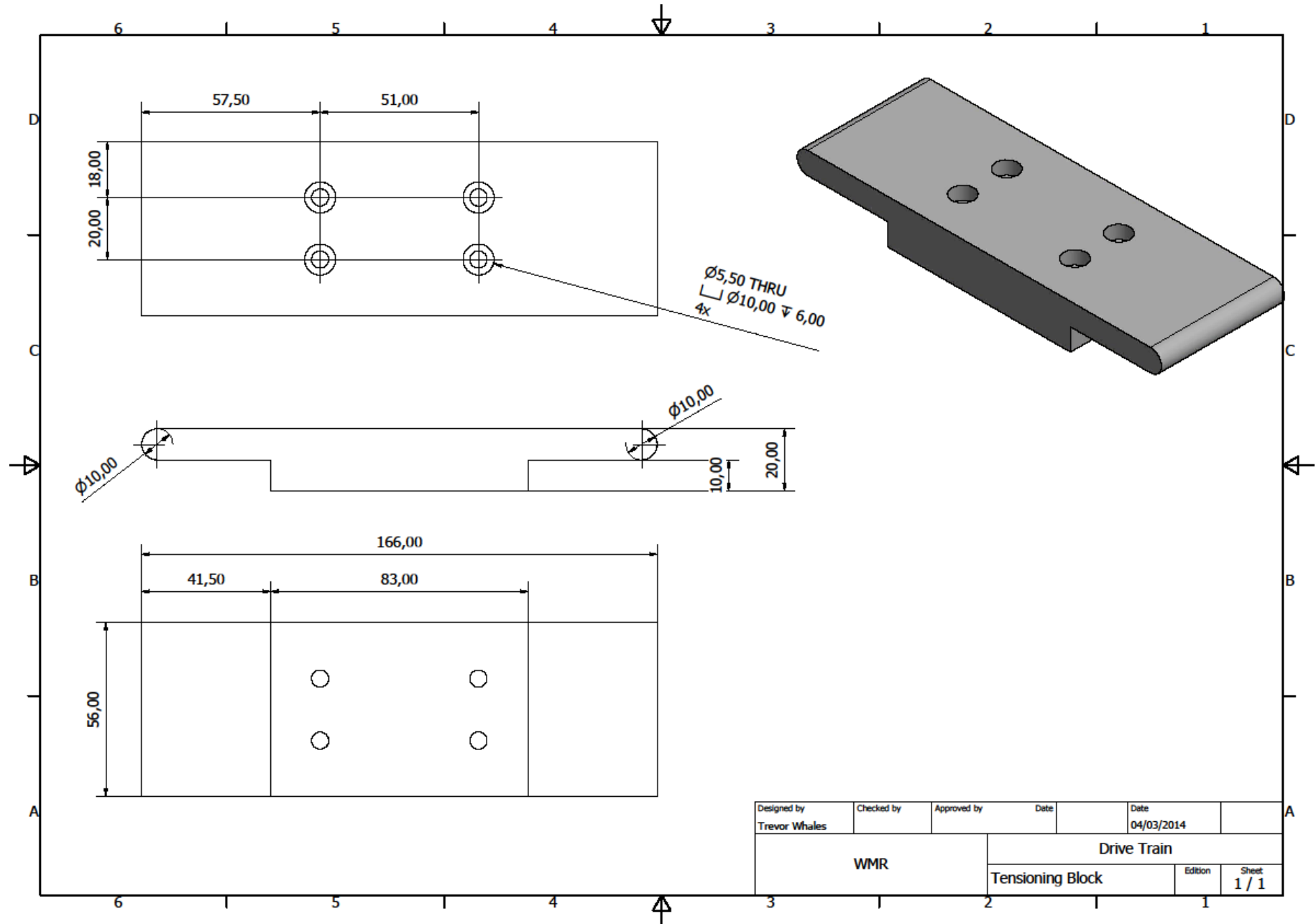
To be made from Aluminium 6082 T6

Designed by Trevor Whales	Checked by	Approved by	Date	Date 17/01/2014
WMR		Drivetrain		
		Mounting Bar for SyRen25	Edition	Sheet 1 / 1

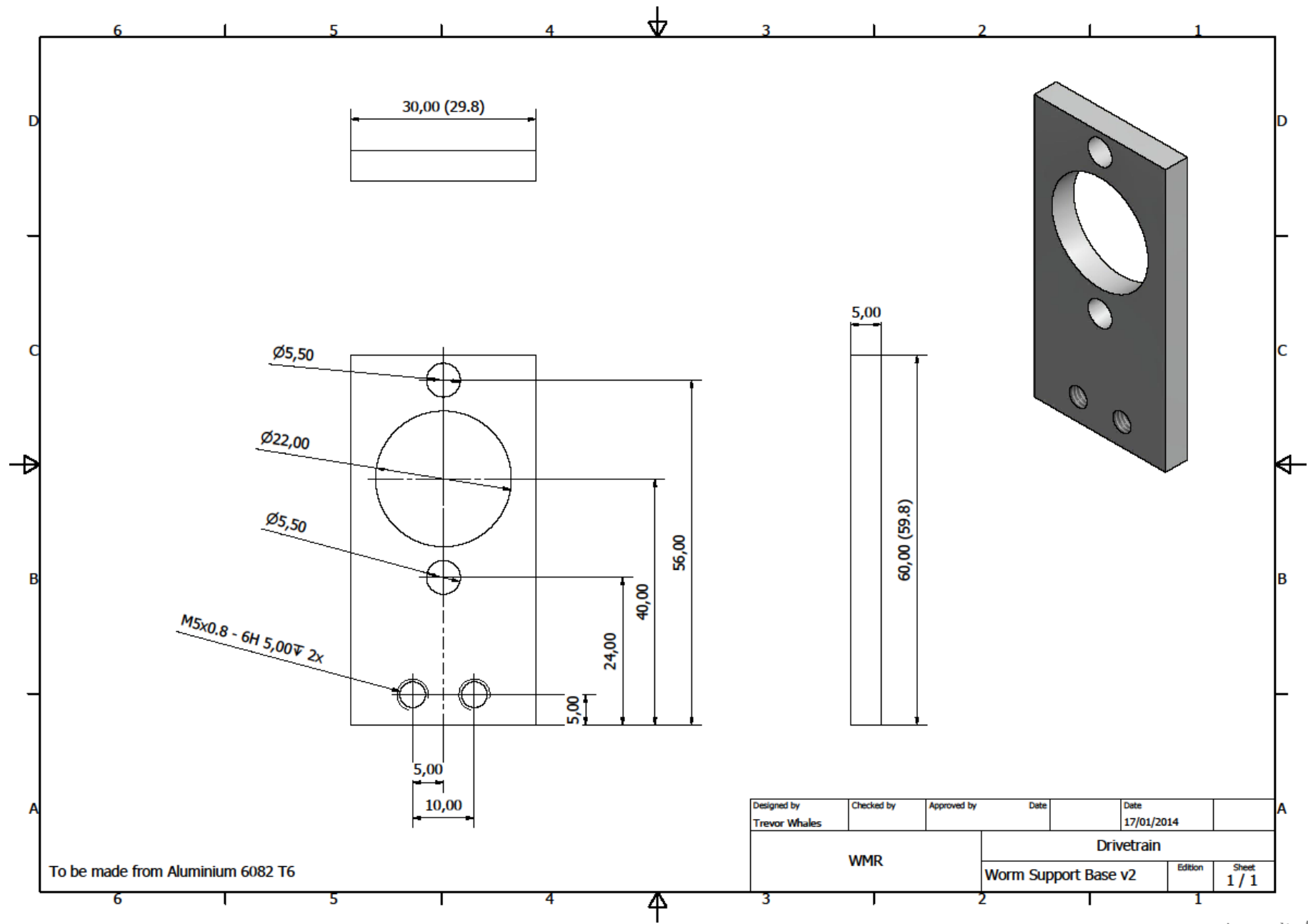


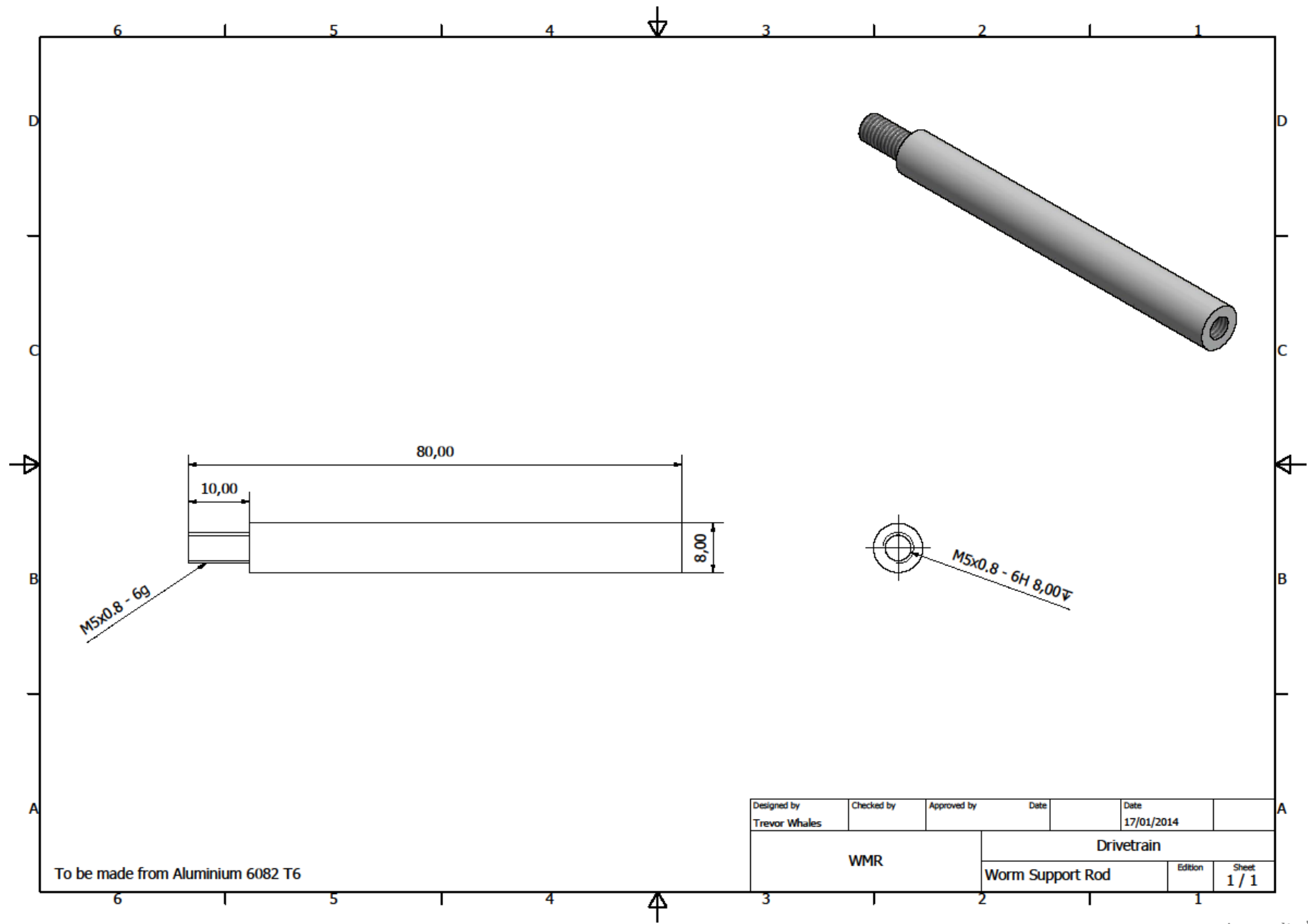






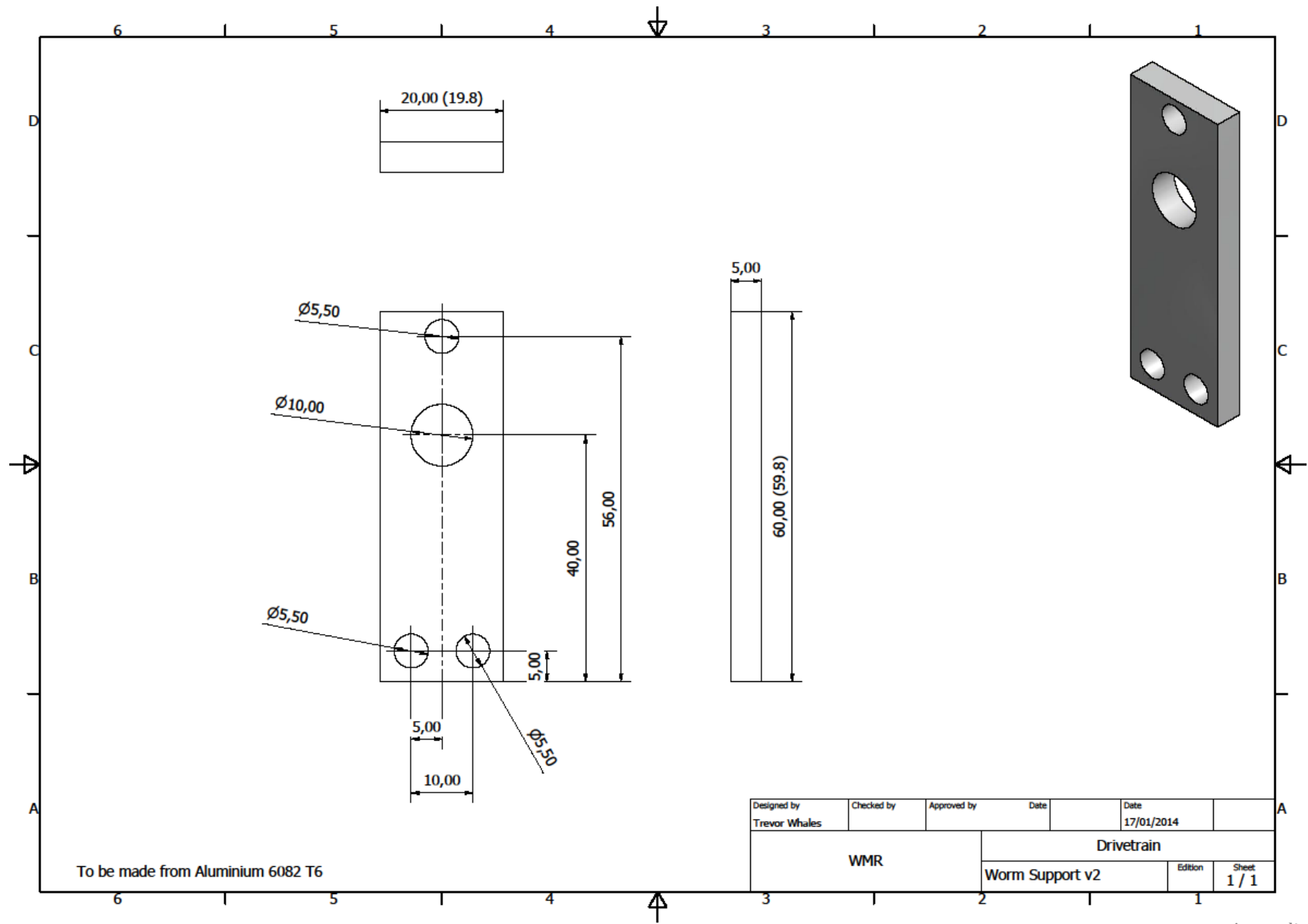
Designed by Trevor Whales	Checked by	Approved by	Date	Date 04/03/2014
WMR		Drive Train		
		Tensioning Block	Edition	Sheet 1 / 1





To be made from Aluminium 6082 T6

Designed by Trevor Whales	Checked by	Approved by	Date	Date 17/01/2014
WMR		Drivetrain		
Worm Support Rod		Edition	Sheet 1 / 1	



To be made from Aluminium 6082 T6

Designed by Trevor Whales	Checked by	Approved by	Date	Date 17/01/2014
WMR		Drivetrain		
		Worm Support v2	Edition	Sheet 1 / 1

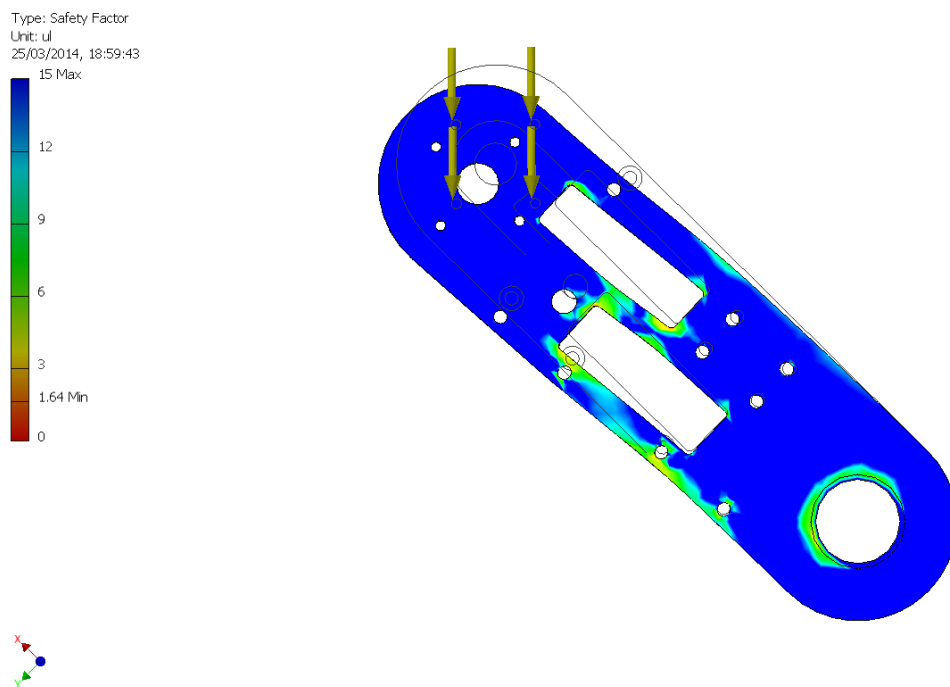
### C.6 – Drivetrain FEA

All the components in the drivetrain have been analysed using FEA on CAD. The impact force experienced was calculated in Chapter 3.6.1 as 1000N. Figure 161 to Figure 164 show the FEA results of several drivetrain components.



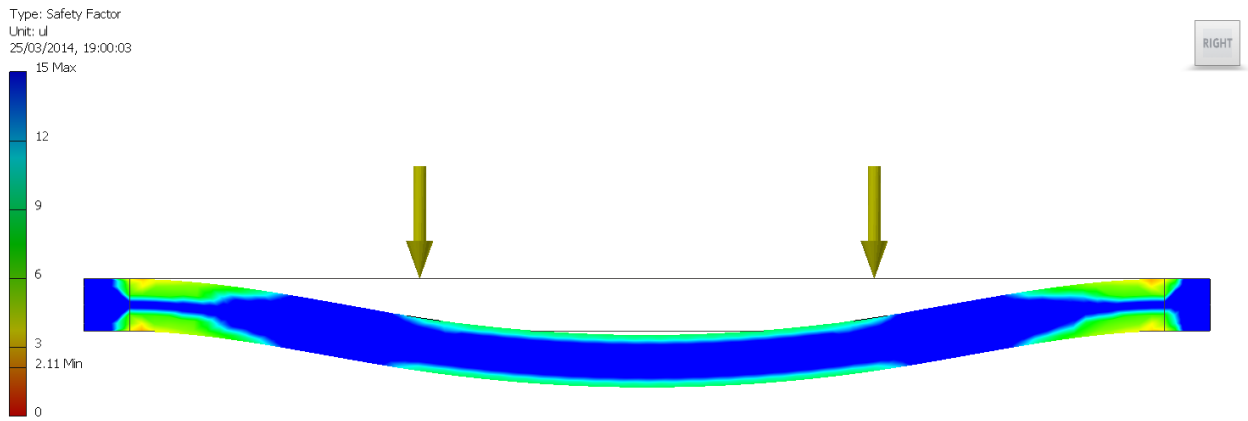
**Figure 161: Front Axle FEA**

Figure 161 shows the safety factor is 3.18 for the front axle.



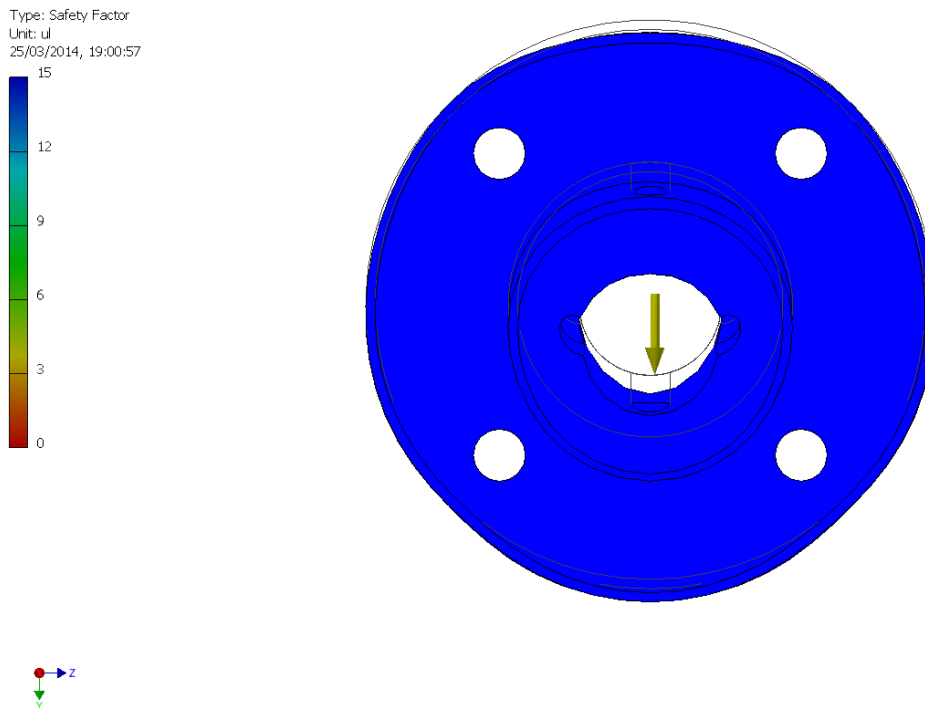
**Figure 162: Track Side Plate FEA**

Figure 162 shows a safety factor is 1.63 for the track side plate.



**Figure 163: Flipper Axle FEA**

Figure 163 shows the safety factor is 2.11 for flipper axle.



**Figure 164: Flipper Axle Hat FEA**

The safety factor for the flipper hats is off the scale in Figure 164, as it is 25.2. This means it can withstand a force of 25200N, so offers lots of room for optimisation.



### Appendix D – Arm, Head and Gripper

#### D.1 – SWOT Analysis of 2013/14 Arm System

SWOT Analysis of Previous Arm (Figure 165) is shown in Table 66.

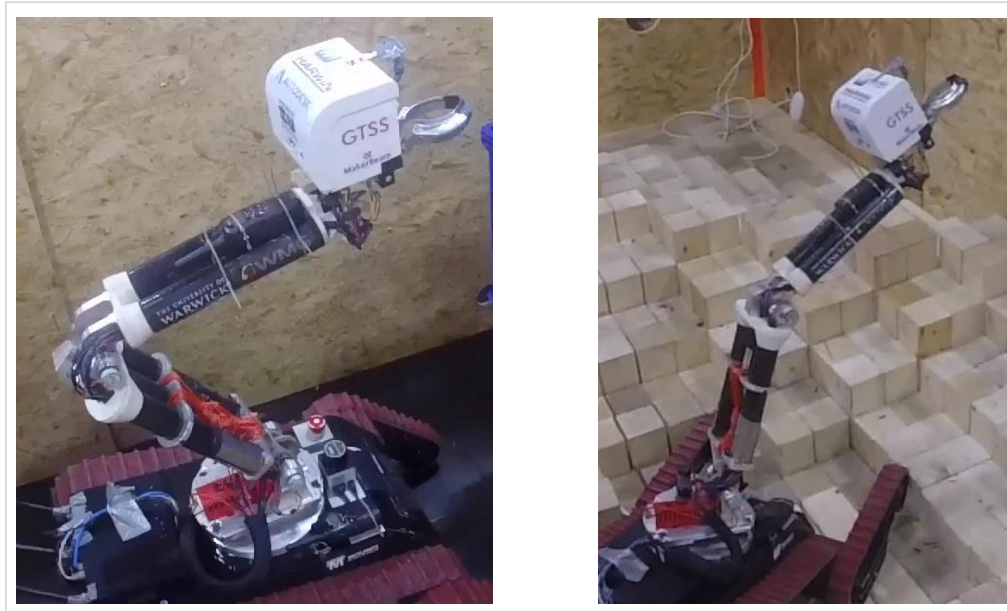


Figure 165: Previous Arm

Table 66: SWOT for Previous Arm

<p><b>Strengths:</b>                  Inverse Kinematics                  Pre-set arm positions</p>	<p><b>Weaknesses:</b>                  Very Heavy &amp; Expensive                  Bespoke Design (Complex components require 5-axis machining)                  Not able to reach highest victims (1.6m)                  CFRP tube links breaks when robot falls over                  Floppy head syndrome                  Continues to try and move through an obstacle when it collides with it</p>
<p><b>Opportunities:</b>                  Lower cost                  Lighter weight                  Linear Joint                  More Robust                  Easier to modify/ repair</p>	<p><b>Threats:</b>                  Unknown rule changes                  Lower cost and lightweight may mean loss or compromise of functionality</p>

SWOT Analysis of Previous Robot Gripper(Figure 166) is shown in Table 67.

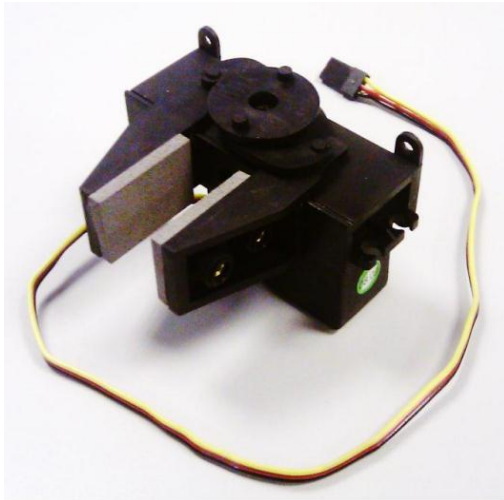


Figure 166: Old Gripper



Figure 167: New Gripper

Table 67: SWOT for Old Gripper

<p style="text-align: center;"><b>Strengths:</b></p> <ul style="list-style-type: none"> <li>• Lightweight</li> <li>• Small</li> <li>• Cheap</li> <li>• Can grip a 500ml bottle</li> </ul>	<p style="text-align: center;"><b>Weaknesses:</b></p> <ul style="list-style-type: none"> <li>• Poor manipulation</li> <li>• Can only grip limited number of items</li> <li>• Small opening of fingers</li> <li>• Weak gripping force</li> <li>• Hard to position around objects</li> <li>• Fragile</li> </ul>
<p style="text-align: center;"><b>Opportunities:</b></p> <ul style="list-style-type: none"> <li>• Better manipulation</li> <li>• Grip a wide variety of objects</li> <li>• Larger opening</li> <li>• Stronger gripping force</li> <li>• Increased robustness</li> </ul>	<p style="text-align: center;"><b>Threats:</b></p> <ul style="list-style-type: none"> <li>• New manipulation challenges including opening and closing switches and valves</li> <li>• Ease of use with Oculus Rift</li> </ul>

SWOT Analysis of Previous Robot Head(Figure 170) is shown in :

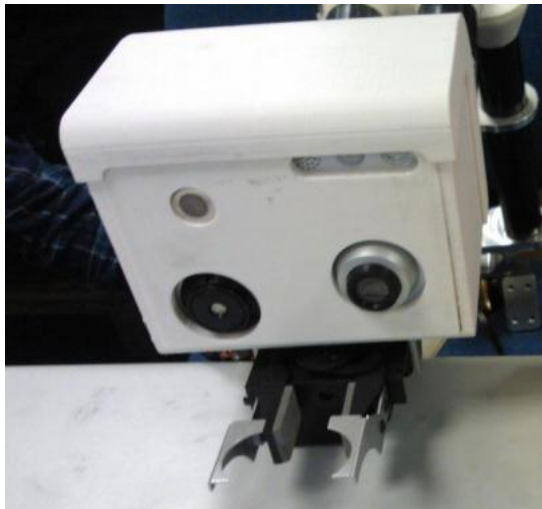


Figure 168: Old Head



Figure 169: New Head & Gripper

Table 68: SWOT for Old Head

<p><b>Strengths:</b></p> <ul style="list-style-type: none"> <li>• Wide Range of Sensors</li> <li>• Well packaged, easy to access components</li> <li>• Space for future expansion</li> </ul>	<p><b>Weaknesses:</b></p> <ul style="list-style-type: none"> <li>• Bespoke Design</li> <li>• Relatively heavy</li> <li>• Cameras exposed to environment</li> <li>• Very large casing limits access to victim boxes</li> <li>• Poor visibility of gripper</li> </ul>
<p><b>Opportunities:</b></p> <ul style="list-style-type: none"> <li>• Lower cost</li> <li>• Lighter weight</li> <li>• Modulus for future changes</li> <li>• Inclusion of multiple cameras for Oculus Rift vision system</li> <li>• Increased visibility of gripper</li> <li>• Smaller for easier access to victim boxes</li> </ul>	<p><b>Threats:</b></p> <ul style="list-style-type: none"> <li>• Small robot means size of head plate is limited</li> <li>• Unknown specification of cameras for Oculus Rift system</li> <li>• Functionality may be lost due to less components and sensors</li> </ul>

## D.2 – Analysis of Actuation Methods

**Table 69: Pneumatic Actuation**

<b>Advantages</b>
High gripping force possible.
Relatively low power consumption.
Improved cycle rates compared to cheaper electric systems
<b>Disadvantages</b>
Air systems prone to leaks.
Air systems require air even when not in use leading to reduced efficiency.
Air canisters have limited number of uses before requiring replacement.
Difficult to control air systems in terms of positioning and level of force.
Air seals wear over time and require replacement and maintenance.
Expensive off-the-shelf solutions.
Requirement for air tubing through robot system.

**Table 70: Electric Actuation**

<b>Advantages</b>
Low cost off-the-shelf options available.
Low energy use.
Does not require power when not in use, therefore more efficient.
Large number of repetitions possible.
Easy integration into systems.
Easier to control and connect to robot electronics.
Easier to repair and modify in comparison to pneumatic actuators.
<b>Disadvantages</b>
Low gripping force from servo motors
Weak motors prone to damage.

Analysis of both pneumatic and electric actuation produced the findings in Table 69 and Table 70. It was decided that the best method of actuation for the gripper would be electric actuation. This is mainly due to the lower-cost associated, the indefinite number of manipulations possible and the simplicity of the integration into the robot system.

Although pneumatic solutions offer greater gripping forces, it was found that a maximum gripping force of 75N was needed to grip the largest object required, which is well within the capabilities of electric actuation.

### D.3 – Maximum Door Handle Torque Calculations

The force required to open a door handle  $F_d=35\text{N}$  (Figure 170), measured experimentally using a newton meter.

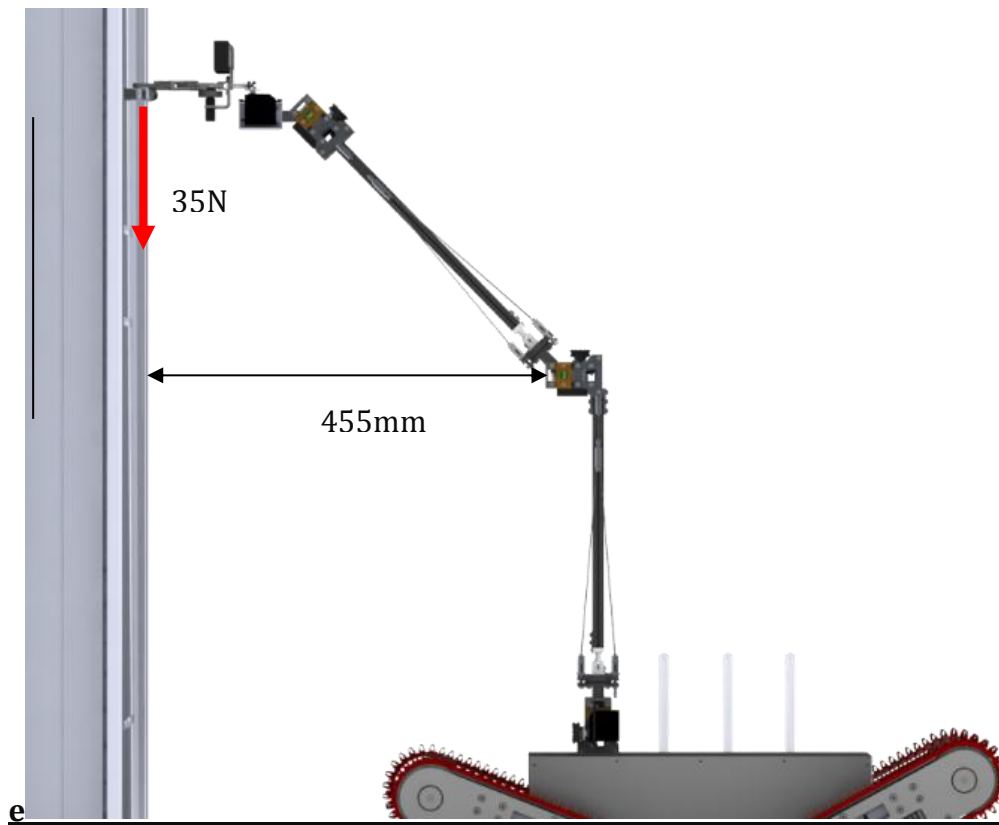


Figure 170: Arm Torque Opening a Door Handle

Torque required in elbow joint,

$$\tau_{Elbow} = (F_d \times x) = 35 \times 0.455 = 15.6\text{Nm}$$

Equation 46.

Where:

$\tau$  is the torque (Nm)

$F$  is the force (N)

$x$  is the distance (m)

#### D.4 – Torque Resulting from Robot Flipping Over

The maximum torque generated by the full weight of the robot resting on the arm (Figure 58,) is calculated using the values from Table 29 (modifying component 9 from 0.5kg to 25kg) with Equation 6. This result in  $\tau_B = 245Nm$

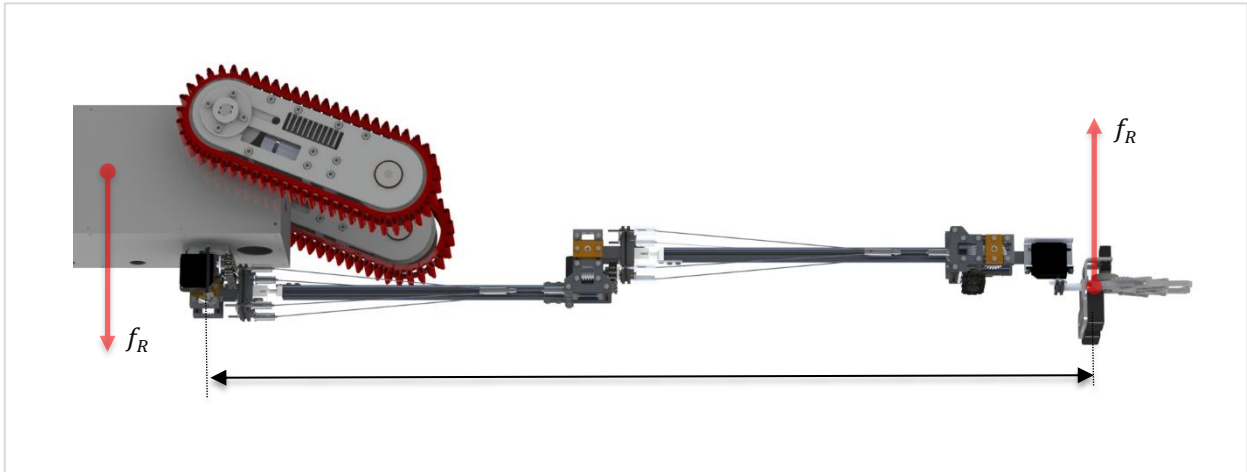


Figure 171: Flipped Robot

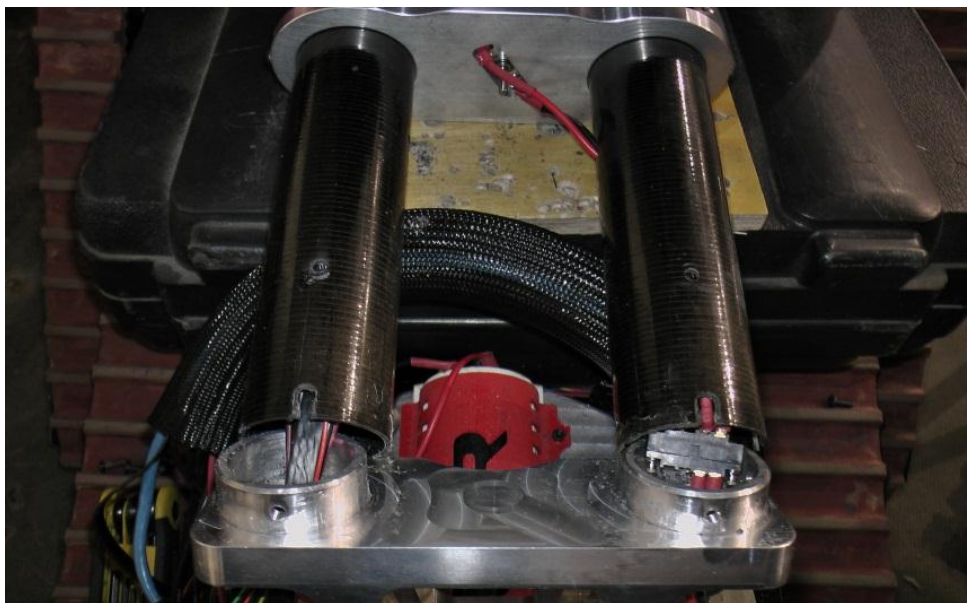


Figure 172: Previous Arm Design Failure

Robot flipping over has previously caused significant damage to the arm (Figure 172).

## D.5 – Base Joint Torque With Linear Joint Addition

$$\tau_{B\_Linear} = \sum_1^n (F_i \times x_i) \quad \text{Equation 47.}$$

$$\tau_{B\_linear} = (F_1 \times x_1 + F_2 \times x_2 + F_3 \times x_3 + F_4 \times x_4 + F_5 \times x_5 + F_6 \times x_6 + F_7 \times x_7 + F_8 \times x_8 + F_9 \times x_9 + F_{10} \times x_{10} + F_{11} \times x_{11} + F_{12} \times x_{12})$$

Using the values from Table 29,  $\tau_{B\_Linear} = 21.4Nm$

**Table 71: Base Joint Torque Variables with Linear**

Component Number, <i>i</i>	Component Name	Distance from base joint, $x_i/m$	Component Mass, $m_i/kg$	Component Weight, $f_i/N$
1	Joint 1 - Upper	0.05	0.13	1.31
2	Link 1	0.26	0.11	1.10
3	Joint 2	0.45	0.43	4.26
4	Joint 2 - Upper	0.50	0.13	1.31
5	Liner Joint -Lower	0.70	0.06	0.62
6	Liner Joint -Middle	0.71	0.15	1.47
7	Liner Joint -Lower	0.91	0.15	1.47
8	Link 3	0.94	0.04	0.42
9	Joint 3	1.14	0.34	3.336
10	Joint 4	1.18	0.09	0.85
11	Head and Gripper	1.23	0.35	3.43
12	Payload	1.29	0.50	4.91

### D.6 – Cable Termination Failure Mechanism

The stress at a point in a rod under a load is given by Equation 45 (shown by Figure 173),

$$\sigma = \frac{P}{A} \quad \text{Equation 48.}$$

$$A = \frac{\pi d^2}{4} \quad \text{Equation 49.}$$

Where:

$\sigma$  is the stress ( $\text{Nm}^{-2}$ )

$P$  is the load (N)

$A$  is the cross sectional area ( $\text{m}^2$ )

Failure occurs beyond where the stress exceeds the ultimate tensile strength of the material,

$$\sigma = \sigma_{UTS} \quad \text{Equation 50.}$$

Substituting the cable tension load and Equation 50 into Equation 48,

$$\sigma_{UTS} = \frac{T_C}{A} \quad \text{Equation 51.}$$

Where:

$T_C$  is the cable tension (N)

Substituting in Equation 49 and rearranging,

$$\frac{\pi d^2}{4} = \frac{T_C}{\sigma_{UTS}} \quad \text{Equation 52.}$$

Where:

$D$  is the diameter (m)

Then rearranging the above,

$$d = \sqrt{\frac{4T_C}{\pi\sigma_{UTS}}} \quad \text{Equation 53.}$$

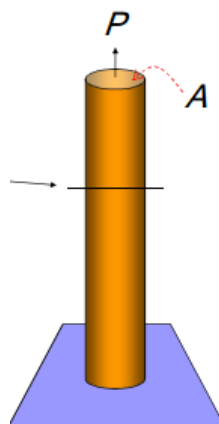


Figure 173: Load Applied to Rod



### D.7 – Comparison of Off-the-shelf Grippers

A comparison of currently available off-the-shelf gripper solutions can be found in Table 72. This comparison was used as a basis for the design of a new gripper and for a cost-benefit analysis to be carried out, comparing the purchase of an off-the-shelf solution with manufacturing a bespoke gripper.

**Table 72: Off-the-shelf Gripper Comparison**

*Little Gripper Kit (Used on Current Robot)*



Cost	£30 - £40
Weight	75.5g
Movement	Can open and close and rotate
Manipulation	2 Finger Gripper with max opening of 3.3cm
Motors	2 x HS-422 Servo Operating Voltage 6V Standby Current 8.8mA

*AX-12 Dual Gripper*



Cost	£174.52
Weight	N.A.
Movement	Dependent on mounting
Manipulation	2 Finger Gripper with max opening of 22cm Each gripper section is 10cm
Motors	2 x AX-12A Servo Operating Voltage 12V Standby Current 50mA Max Current 900mA

*Multi-finger Gripper*



Cost	\$40.00
Weight	110g
Movement	Can open and close
Manipulation	Kit can be constructed into a 2-finger or 4-finger gripper dependent on configuration required. Largest opening of 7.6cm
Motors	?

*Dagu Mk II Gripper*



Cost	£18.90
Weight	290g
Movement	Can open and close
Manipulation	13cm in length with 2 fingers. 2" Maximum Opening
Motors	1 x Servos Operating Voltage 4.8-6V Output Torque 3.2 kg/cm

*SMC Double Action Pneumatic Gripper*



Cost	£374.72
Weight	430g
Movement	Can open and close
Manipulation	2 Finger Gripper with max opening stroke 14mm
Pneumatics	45N Gripping Force per finger 0.7 MPa max operating pressure Parallel Operation

*SMC Double Action Angled Pneumatic Gripper*



Cost	£238.74
Weight	150g
Movement	Can open and close
Manipulation	2 Finger Gripper with max opening 180°
Pneumatics	0.54 N.m gripping force 0.6 MPa max operating pressure Angled Operation

*GIMATIC 2 Finger Single Action Pneumatic Gripper*



Cost	£99.36
Weight	45g
Movement	Can open and close
Manipulation	2 Finger Gripper with max stroke 15°
Pneumatics	80 N.cm gripping force 8 bar max operating pressure Angled Operation

The majority of grippers available consist of a two finger design, that is powered from a servos. From this comparison, it was decided that the most viable gripping option was the Dagu Mk II gripper, due to the cost, ease of modification and overall manipulation abilities.

### D.8 – Gripper Finger Design Calculations

To design finger plates that can be opened to a maximum stroke of 10cm, the angle of the fingers needs to be calculated. This is done in two steps:

The first step was to calculate the angle at which the gripper fingers are from on the Dagu gripper (Figure 164, 175).

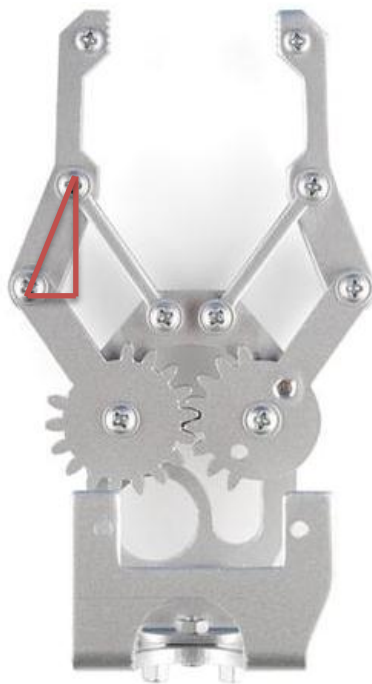


Figure 174: Dagu Gripper Layout

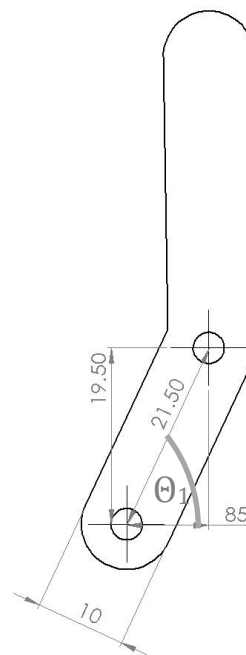


Figure 175: Dagu Gripper Dimensions

Taking the dimensions given in Figure X, the angle from the vertical could be calculated as follow:

$$\sin \theta_1 = \frac{85}{215} \quad \text{Equation 54.}$$

Rearranging this gives:

$$\theta_1 = \sin^{-1} \frac{85}{215} = 23.2^\circ \quad \text{Equation 55.}$$

The distance between the gripper fingers when the gripper was opened to its maximum stroke was then measure as 60mm. From this the modified fingers could be designed.

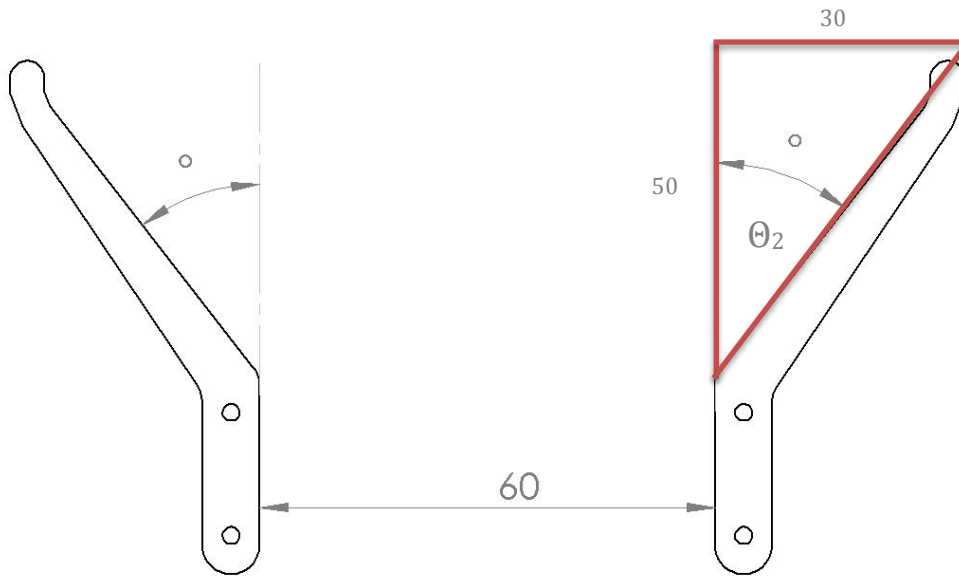


Figure 176: Modified Finger Dimensions

Taking the distance between the end of the finger plates and the gripper as 50mm when fully opened, the angle required for a separation of 120mm when the fingers are vertically aligned was calculated as follows:

$$\tan \theta_2 = \frac{30}{50} \tag{Equation 56.}$$

Rearranging this gives:

$$\theta_2 = \tan^{-1} \frac{30}{50} = 30.9^\circ \tag{Equation 57.}$$

The total angle of the finger plates (Figure 176) was then calculated by adding both the calculated angles together:

$$\theta_1 + \theta_2 = 23.2 + 30.9 = 54.2^\circ$$

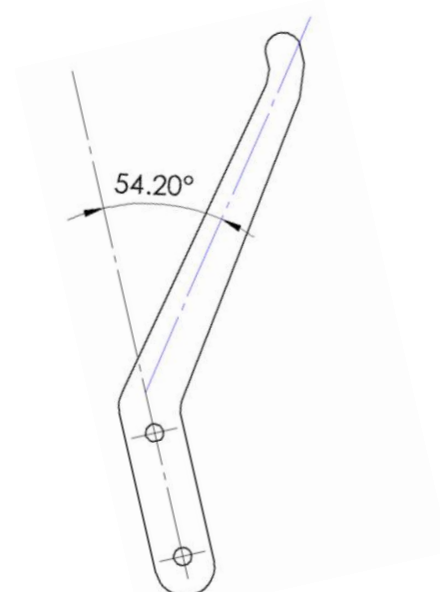


Figure 177: Total Angle  
Appendix XIV

### D.9 – Cost Benefit Analysis of Bespoke vs. Off-the-shelf Gripper

Off-the-Shelf Gripper Costing is shown in Table 73.

**Table 73: Off-the-shelf Gripper Costs**

<b>Part</b>	<b>Manufacturing Required</b>	<b>Total Cost</b>
<b>Dagu MkII Gripper</b>	N/A	£9.95
<b>Medium Servo Motor</b>	N/A	£8.95
<b>New Finger Plates</b>	Waterjet Cutting	£5.00
<b>M3 Bolts</b>	N/A	£0.48
<b>M3 Nuts</b>	N/A	£0.36
	<b>Total</b>	<b>£24.74</b>

Bespoke Gripper Costing is shown in Table 74.

**Table 74: Bespoke Gripper Costs**

<b>Part</b>	<b>Manufacturing Required</b>	<b>Total Cost</b>
<b>Gripper Base</b>	Waterjet Cutting	£5.00
<b>Medium Servo Motor</b>	N/A	£8.95
<b>Finger Plates</b>	Waterjet Cutting	£5.00
<b>Gears</b>	Machining on Lathe (5 Hours Est.)	£150.00
<b>Spokes</b>	Machining on Lathe (2 Hours Est.)	£60.00
<b>Pinion Gear</b>	Machining on Lathe (2 Hours Est.)	£60.00
<b>M3 Bolts</b>	N/A	£0.48
<b>M3 Nuts</b>	N/A	£0.36
	<b>Total</b>	<b>£289.79</b>

At a cost of £30 per hour for technician working time, it was estimated that a bespoke gripper would cost an estimated £289.79. This is significantly higher than buying an off-the-shelf gripper and modifying it. Adding to this the constraint on manufacturing time, made buying an off-the-shelf gripper a more cost-effective option.

### D.10 – Gripper Force Calculations

The gripping force required to lift an object is calculated using:

$$F > \frac{mg}{\mu} \quad \text{Equation 58.}$$

Where:

- F is the Force (N)
- M is the Mass (kg)
- g is acceleration due to gravity ( $\text{ms}^{-2}$ )
- $\mu$  is the coefficient of friction

This is then doubled to include a factor of safety of 2, giving:

$$F > 2 \frac{mg}{\mu} \quad \text{Equation 59.}$$

The maximum weight that needs to be lifted is a 10cm x 10cm x 60cm block made from balsawood. The weight of this block of balsawood can be calculated from the following:

$$m = \rho V \quad \text{Equation 60.}$$

Where:

- $\rho$  is density ( $\text{kgm}^{-3}$ ) given as 160 (The Engineering ToolBox, n.d.)
- V is the volume ( $\text{m}^3$ )

This gives the mass of the block to be:

$$m = 160 \times (0.1 \times 0.1 \times 0.6) = 0.96 \text{ kg}$$

Taking the weight of the balsawood block as 1kg and the coefficient of friction as 0.25-0.6 between clean wood and metal, the gripping force required is given by:

$$F > 2 \left( \frac{1 \times 9.8}{0.25} \right) = 78.4 \text{ N}$$

The same calculation for a 500ml PET water bottle, where the mass is 500g and the coefficient of friction is 0.2-0.4, gives:

$$F > 2 \left( \frac{0.5 \times 9.8}{0.2} \right) = 49 \text{ N}$$

### D.11 – Gripper Finger Deflection Calculations

Taking a simplified design of the gripper fingers as a straight flat piece of Aluminium 6082 T6, with the same thickness and profile as the real gripper fingers. The maximum deflection of two lengths of finger were calculated with the following:

$$y_{max} = \frac{WL^3}{3EI} \quad \text{Equation 61.}$$

Where:

$y_{max}$  is the maximum deflection (m)

W is the weight (N)

L is the length (m)

E is the Young's Modulus (GPa)

I is the Second Moment of Area (m<sup>4</sup>)

#### For finger 1:

Length: 0.062m

Weight: 1kg

Young Modulus, E: 70 GPa

The second moment of area of the cross section is calculated as follows:

$$I = bh \frac{h^2}{12} = 0.01 \times 0.002 \times \frac{0.002^2}{12} = 6.67 \times 10^{-12}$$

This gives a maximum deflection as follows:

$$y_{max} = \frac{1 \times 0.062^3}{3 \times 70 \times 10^9 \times 6.67 \times 10^{-12}} = 1.70 \times 10^{-4} \text{ m} = 0.17 \text{ mm}$$

#### The same calculations were applied to finger 2:

Length: 0.09m

Weight: 1kg

Young Modulus, E: 70 GPa

The second moment of area of the cross section is calculated as follows:

$$I = bh \frac{h^2}{12} = 0.01 \times 0.002 \times \frac{0.002^2}{12} = 6.67 \times 10^{-12}$$

This gives a maximum deflection as follows:

$$y_{max} = \frac{1 \times 0.09^3}{3 \times 70 \times 10^9 \times 6.67 \times 10^{-12}} = 5.2 \times 10^{-4} \text{ m} = 0.52 \text{ mm}$$

#### D.12 – Crash Scenario Calculations for FEA

Using the assumed top speed and maximum design weight of the robot, the forces involved in a crash can be calculated.

This calculation is used to estimate the force experienced by the head plate if it was to collide with something at the top speed of the robot.

Maximum design speed:  $1.69 \text{ ms}^{-1}$

Maximum design weight of robot: 25 kg

Time taken to stop in a crash: 0.1 seconds

Using SUVAT equations:

$$a = \frac{v - u}{t} \quad \text{Equation 62.}$$

Where  $a$  is the acceleration,  $v$  is the final velocity,  $u$  is the initial velocity and  $t$  is time.

This gives an acceleration of:

$$a = \frac{0 - 1.69}{0.1} = 16.9 \text{ ms}^{-1}$$

The force can then be calculated using:

$$F = ma \quad \text{Equation 63.}$$

Where  $F$  is the force,  $m$  represents the mass and  $a$  is the acceleration. This gives a force of:

$$F = 25 \times 16.9 = 422.5 \text{ N}$$



## Appendix E – Electronics & Software

### E.1 - New Robot ROS UDRF File

```

<?xml version="1.0"?>
<robot name="donatello">
  <link name="body">
    <visual>
      <geometry>
        <box size="0.45 .16 .155"/>
      </geometry>
      <material name="blue">
        <color rgba="0 0 .8 1"/>
      </material>
    </visual>
  </link>

  <link name="flflipper">
    <visual>
      <geometry>
        <box size="0.325 .07 .10"/>
      </geometry>
    </visual>
  </link>

  <link name="frflipper">
    <visual>
      <geometry>
        <box size="0.325 .07 .10"/>
      </geometry>
    </visual>
  </link>

  <link name="rlflipper">
    <visual>
      <geometry>
        <box size="0.325 .07 .10"/>
      </geometry>
    </visual>
  </link>

  <link name="rrflipper">
    <visual>
      <geometry>
        <box size="0.325 .07 .10"/>
      </geometry>
    </visual>
  </link>

  <link name="arm1">
    <visual>
      <geometry>
        <box size="0.45 .04 .04"/>
      </geometry>
      <material name="black">
        <color rgba="0 0 0 1"/>
      </material>
    </visual>
  </link>

  <link name="arm2">
    <visual>
      <geometry>
        <box size="0.45 .04 .04"/>
      </geometry>
      <material name="black">
        <color rgba="0 0 0 1"/>
      </material>
    </visual>
  </link>

  <link name="wrist1">
    <visual>
      <geometry>
        <box size="0.03 .03 .03"/>
      </geometry>
      <material name="grey">
        <color rgba="0.1 0.1 0.1 1"/>
      </material>
    </visual>
  </link>

  <link name="wrist2">
    <visual>
      <geometry>
        <box size="0.03 .03 .03"/>
      </geometry>
      <material name="grey">
        <color rgba="0.1 0.1 0.1 1"/>
      </material>
    </visual>
  </link>

  <joint name="flflip"
type="continuous">
    <parent link="body"/>
    <child link="flflipper"/>
    <origin xyz="0.3275 0.125 -0.06"
rpy="0 0 0" />
    <axis xyz="0 0 1" />
  </joint>

  <joint name="frflip"
type="continuous">
    <parent link="body"/>
    <child link="frflipper"/>
    <origin xyz="0.3275 -0.125 -0.06"
rpy="0 0 0" />
    <axis xyz="0 0 1" />
  </joint>

  <joint name="rlflip"
type="continuous">
    <parent link="body"/>
    <child link="rlflipper"/>
    <origin xyz="-0.3275 0.125 -0.06"
rpy="0 0 0" />
  </joint>

```

```

    <joint name="rrflip"
type="continuous">
    <parent link="body"/>
    <child link="rrflipper"/>
    <origin xyz="-0.3275 -0.125 -
0.06" rpy="0 0 0" />
    </joint>

    <joint name="shoulder"
type="continuous">
    <parent link="body"/>
    <child link="arm1"/>
    <origin xyz="-0.03 0 0.125"
rpy="0 0.1 0" />
    </joint>

    <joint name="elbow"
type="continuous">
    <parent link="arm1"/>
    <child link="arm2"/>

        <origin xyz="0 0 0.11" rpy="0 -
0.3 0" />
    </joint>

    <joint name="wristPitch"
type="continuous">
    <parent link="arm2"/>
    <child link="wrist1"/>
    <origin xyz="0.23 0 0" rpy="0 0
0" />
    </joint>

    <joint name="wristYaw"
type="continuous">
    <parent link="wrist1"/>
    <child link="wrist2"/>
    <origin xyz="0.032 0 0" rpy="0 0
0" />
    </joint>
</robot>

```

## E.2 – SWOT Analysis of Electrical System Architecture

Table 75: SWOT for Electrical Architecture

<b>Strengths</b>	<b>Weaknesses</b>
<ul style="list-style-type: none"> <li>• Adequate cable sizing</li> <li>• Fuse protection</li> <li>• Functioning E-stop circuitry</li> </ul>	<ul style="list-style-type: none"> <li>• Messy internal wiring</li> <li>• Terminal blocks loose in the chassis</li> </ul>
<b>Opportunities</b>	<b>Threats</b>
<ul style="list-style-type: none"> <li>• Size reduction for the whole electrical network, using fewer, smaller cables routed in a logical manner.</li> <li>• Reduction in fault finding time in future.</li> </ul>	<ul style="list-style-type: none"> <li>• Over run of timescale</li> <li>• Lack of funds for new electrical system</li> </ul>

### E.3 – Testing Procedure of PCB

The testing procedure is described as follows:

1. Continuity tests were carried out to ensure that adequate electrical connections were made and there were no shorts between differing circuits. The following measurements were made using the multimeter:
  - Between the positive and negative input terminal.
  - The positive and negative output from each Traco Power individually.
  - Ground and power was connected on each component and connector.
  - Between the pins of the surface mount IC's and resistors.
  - Surface mount resistors measured to ensure resistance of 1MΩ.
2. 24 VDC was applied to the boards input directly from a power supply (1) (Figure 1)
  - The LED's are powered by the output from each Traco Power and these gave an initial indication that both Traco Power converters were functioning. (2)
3. Measurements were made using a Mutlimeter of:
  - 15VDC output at the relevant 15V output connectors. (3)
  - 5VDC measured at the pins of the three un-switchable 5V outputs. (4)
  - 0 VDC measured at the pins of the four switchable 5V outputs (5). They require a 5V input from the microcontroller to turn on.
  - 5 VDC and 0 VDC present at both of the power inputs to the microcontroller. (6)
  - 5 VDC and 0 VDC present at the terminals of the USB-i2C interface board, the sensor stick and the logic level converter board. (7)

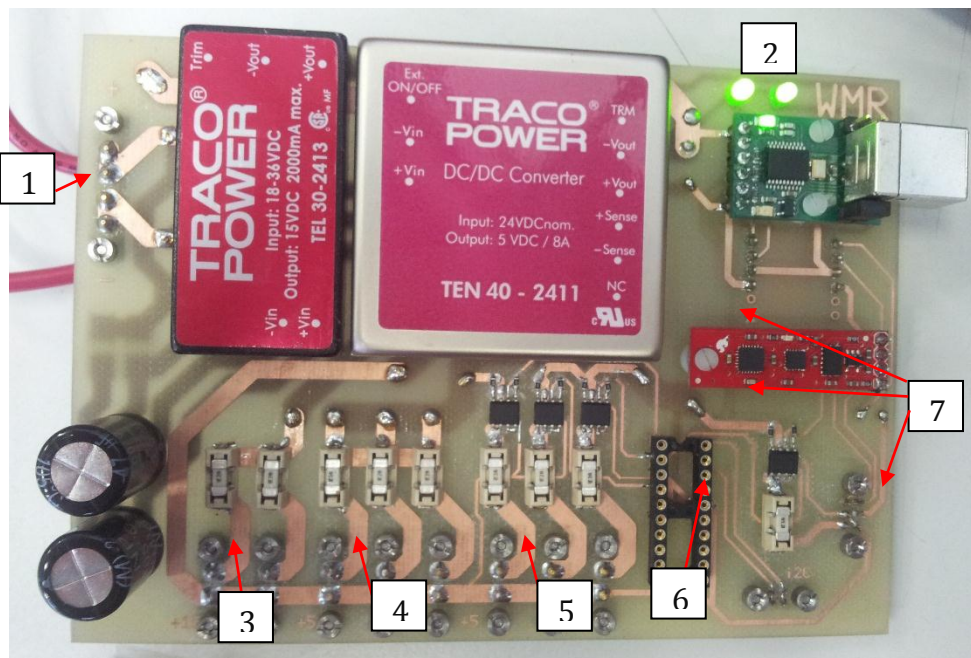


Figure 178: Main Power Board

## Arm Board Testing

The testing procedure for the Arm PCB was similar to the testing procedure for the main power board described in detail in section 8.3 therefore only the key differences in testing will be described.

1. Measurements were made using a Mutlimeter of:

- 12VDC output at the relevant 12V output connectors. (1)
- 5VDC measured at the pins of the 5V outputs. (2)
- 5 VDC and 0 VDC present at both of the power inputs to the microcontroller. (3)
- 5 VDC and 0 VDC present at the terminals of the raspberry pi interface and the logic level converter board. (4)

## Appendix F – Full Testing & Analysis

### F.1 – Mass and Cost Distribution Analysis

Table 76: Mass and Cost Distribution Analysis

Assembly	Sub-Assembly	Categories	Component	Qty.	Material	Mass (kg)	% Robot	Cost (£)	% Robot
Chassis	Chassis	Mounting Plates	Tufnol Base	1	Tufnol	0.104	0.42%	10.00	0.27%
Chassis	Chassis	Mounting Plates	Tufnol Middle Rear	1	Tufnol	0.112	0.45%	17.50	0.47%
Chassis	Chassis	Mounting Plates	Tufnol Middle Front	1	Tufnol	0.128	0.52%	17.50	0.47%
Chassis	Chassis	Mounting Plates	Arm Chassis Mount	1	Aluminium 6083-T5	0.051	0.21%	3.80	0.10%
Chassis	Chassis	Mounting Plates	Axle Mounting Plate 1	2	Aluminium 6083-T5	0.184	0.74%	10.00	0.27%
Chassis	Chassis	Mounting Plates	Axle Mounting Plate 2	2	Aluminium 6083-T5	0.184	0.74%	6.00	0.16%
Chassis	Chassis	Mounting Plates	Encoder Mounting Plate	2	Aluminium 6063-T6	0.014	0.06%	22.48	0.60%
Chassis	Chassis	Shell	Bottom Plate	1	Aluminium 6083-T5	0.298	1.20%	0.00	0.00%
Chassis	Chassis	Mounting Plates	Motor Mounting Plate	4	Aluminium 6083-T5	0.228	0.92%	8.00	0.21%
Chassis	Chassis	Mounting Plates	Emergency Stop Plate	1	Aluminium 6083-T5	0.026	0.10%	3.50	0.09%
Chassis	Chassis	Mounting Plates	Battery Housing	1	ABS	0.051	0.21%	2.04	0.05%
Chassis	Chassis	Mounting Plates	Arm Control Box	1	ABS	0.115	0.46%	4.60	0.12%
Chassis	Chassis	Shell	Shell Top Plate	1	Polycarbonate	0.115	0.46%	4.00	0.11%
Chassis	Chassis	Shell	Shell Side Plate	2	Polycarbonate	0.246	0.99%	8.00	0.21%
Chassis	Chassis	Shell	Shell Front Plate	1	Polycarbonate	0.044	0.18%	7.50	0.20%
Chassis	Chassis	Shell	Shell Back Plate	1	Polycarbonate	0.045	0.18%	3.00	0.08%
Chassis	Chassis	MakerBeam	Makerbeam 430mm	8	Aluminium 6063-T5	0.447	1.80%	25.88	0.69%
Chassis	Chassis	MakerBeam	Makerbeam 140mm	10	Aluminium 6063-T5	0.182	0.73%	10.53	0.28%
Chassis	Chassis	MakerBeam	Makerbeam 65mm	2	Aluminium 6063-T5	0.017	0.07%	0.98	0.03%
Chassis	Chassis	MakerBeam	Makerbeam 66mm	6	Aluminium 6063-T5	0.051	0.21%	2.98	0.08%
Chassis	Chassis	MakerBeam	Makerbeam 59mm	4	Aluminium 6063-T5	0.031	0.12%	1.78	0.05%
Chassis	Chassis	MakerBeam	Makerbeam 155mm	4	Aluminium 6063-T5	0.081	0.32%	4.66	0.12%
Chassis	Chassis	MakerBeam	90 Degree Brackets	6	Stainless Steel	0.024	0.10%	63.34	1.69%
Chassis	Chassis	MakerBeam	Corner Brackets	45	Stainless Steel	0.315	1.27%	49.76	1.33%
Chassis	Chassis	MakerBeam	Angle Bracket	4	Stainless Steel	0.020	0.08%	9.05	0.24%
Chassis	Chassis	MakerBeam	M3 Square Head 12mm Bolts	71	Stainless Steel	0.036	0.14%	22.68	0.61%
Chassis	Chassis	MakerBeam	M3 Square Head 6mm Bolts	261	Stainless Steel	0.112	0.45%	54.25	1.45%
Chassis	Chassis	Fixings	M3 Bolts	22	Stainless Steel	0.017	0.07%	7.15	0.19%
Chassis	Chassis	Fixings	M3 Nuts	243	Stainless Steel	0.075	0.30%	8.80	0.24%
Chassis	Chassis	Fixings	M3 Nyloc Nuts	40	Stainless Steel/ Nylon	0.019	0.08%	3.76	0.10%

Chassis	Chassis	Fixings	Nylon Spacers	4	Nylon	0.001	0.00%	8.80	0.24%
Chassis	Chassis	Electronics	Pico ITX board	1	n/a	0.300	1.21%	278.51	7.44%
Chassis	Chassis	Electronics	Hard drive	1	n/a	0.092	0.37%	43.38	1.16%
Chassis	Chassis	Electronics	Raspberry Pi camera (with mount)	1	n/a	0.006	0.02%	16.56	0.44%
Chassis	Chassis	Electronics	Raspberry Pi (camera)	1	n/a	0.045	0.18%	27.48	0.73%
Chassis	Chassis	Electronics	Router	1	n/a	0.401	1.61%	162.61	4.35%
Chassis	Chassis	Electronics	PCB	1	n/a	0.200	0.81%	42.00	1.12%
Chassis	Chassis	Electronics	Emergency stop button	1	n/a	0.041	0.17%	0.00	0.00%
Chassis	Chassis	Electronics	Relay	1	n/a	0.133	0.54%	7.54	0.20%
Chassis	Chassis	Electronics	Relay (arm)	1	n/a	0.056	0.23%	102.12	2.73%
Chassis	Chassis	Electronics	Battery	1	n/a	0.754	3.04%	0.00	0.00%
Chassis	Chassis	Electronics	LIDAR	1	n/a	0.146	0.59%	17.09	0.46%
Chassis	Chassis	Electronics	Speaker (with mount)	1	n/a	0.010	0.04%	5.32	0.14%
					<b>Total System:</b>	<b>5.557</b>	<b>22.37%</b>	<b>£ 1,104.93</b>	<b>29.53%</b>
<b>Assembly</b>	<b>Sub-Assembly</b>	<b>Categories</b>	<b>Component</b>	<b>Qty.</b>	<b>Material</b>	<b>Mass (kg)</b>	<b>% Robot</b>	<b>Cost (£)</b>	<b>% Robot</b>
Drivetrain	Track units	Electronics	Motor	4	n/a	1.800	7.25%	121.60	3.25%
Drivetrain	Track units	Manufactured	Side Panel	8	Aluminium	1.744	7.02%	115.60	3.09%
Drivetrain	Track units	Manufactured	Motor Spacing Plate	4	Aluminium	0.072	0.29%	24.00	0.64%
Drivetrain	Track units	Manufactured	Cross Bracer	12	Aluminium	0.072	0.29%	101.40	2.71%
Drivetrain	Track units	Manufactured	Mounting Bar	8	Aluminium	0.136	0.55%	121.60	3.25%
Drivetrain	Track units	Electronics	SyRen 25	4	n/a	0.224	0.90%	238.56	6.38%
Drivetrain	Track units	Manufactured	Worm Support Base	4	Aluminium	0.072	0.29%	0.00	0.00%
Drivetrain	Track units	Manufactured	Coupling	4	Aluminium	0.060	0.24%	57.80	1.54%
Drivetrain	Track units	Manufactured	Coupling Axle	4	Silver Steel	0.104	0.42%	0.00	0.00%
Drivetrain	Track units	Off-the-shelf mechanical	Worm Gear	4	Steel	0.208	0.84%	0.00	0.00%
Drivetrain	Track units	Manufactured	Axle Front	4	Silver Steel	0.152	0.61%	121.20	3.24%
Drivetrain	Track units	Off-the-shelf mechanical	Wheel Gear	4	Phosphor Bronze	0.084	0.34%	0.00	0.00%
Drivetrain	Track units	Off-the-shelf mechanical	Sprocket Front	8	Mild Steel	1.416	5.70%	108.18	2.89%
Drivetrain	Track units	Off-the-shelf mechanical	Sprocket Bush Front	8	n/a	0.032	0.13%	260.20	6.95%
Drivetrain	Track units	Off-the-shelf mechanical	Worm Bush	4	n/a	0.004	0.02%	102.52	2.74%
Drivetrain	Track units	Manufactured	Worm Support	4	Aluminium	0.056	0.23%	167.64	4.48%
Drivetrain	Track units	Manufactured	Worm Support Rod	12	Aluminium	0.120	0.48%	0.00	0.00%
Drivetrain	Track units	Manufactured	Flipper Axle Hat	4	Aluminium	0.180	0.72%	12.00	0.32%
Drivetrain	Track units	Off-the-shelf mechanical	Sprocket Back	8	Mild Steel	2.168	8.73%	0.00	0.00%
Drivetrain	Track units	Off-the-shelf mechanical	Sprocket Bush Back	8	n/a	0.008	0.03%	0.00	0.00%
Drivetrain	Track units	Manufactured	Tensioning Block	4	Acetal Resin	0.800	3.22%	60.00	1.60%

Drivetrain	Track units	Treads	Chain	8	Steel	0.848	3.41%	460.48	12.31%
Drivetrain	Track units	Treads	U channel	4	Aluminium	1.568	6.31%	114.16	3.05%
Drivetrain	Track units	Treads	Tube	4	Rubber	1.344	5.41%	65.00	1.74%
Drivetrain	Track units	Treads	Track fastenings	4	Steel	0.336	1.35%	0.00	0.00%
Drivetrain	Track units	Off-the-shelf mechanical	M5 Bolt	26	Stainless Steel	0.078	0.31%	2.08	0.06%
Drivetrain	Flipper system	Electronics	Motor	2	n/a	0.900	3.62%	4.00	0.11%
Drivetrain	Flipper system	Off-the-shelf mechanical	Worm Gear	2	Steel	0.278	1.12%	4.00	0.11%
Drivetrain	Flipper system	Off-the-shelf mechanical	Wheel Gear	2	Phosphor Bronze	0.692	2.79%	0.00	0.00%
Drivetrain	Flipper system	Manufactured	Motor Axle Extension	2	Silver Steel	0.188	0.76%	4.00	0.11%
Drivetrain	Flipper system	Off-the-shelf mechanical	Spur Gear Axle	2	Delrin	0.014	0.06%	96.48	2.58%
Drivetrain	Flipper system	Off-the-shelf mechanical	Spur Gear Encoder	2	Delrin	0.022	0.09%	43.26	1.16%
Drivetrain	Flipper system	Manufactured	Flipper Axle	2	Silver Steel	0.916	3.69%	12.94	0.35%
Drivetrain	Flipper system	Electronics	Encoder	2	n/a	0.026	0.10%	12.94	0.35%
Drivetrain	Flipper system	Off-the-shelf mechanical	Bearing	6	n/a	0.198	0.80%	37.68	1.01%
Drivetrain	Flipper system	Electronics	Motor control board (flippers)	1	n/a	0.090	0.36%	26.68	0.71%
					<b>Total System:</b>	<b>17.010</b>	<b>68.49%</b>	<b>£1973.44</b>	<b>52.74%</b>
Assembly	Sub-Assembly	Categories	Component	Qty.	Material	Mass (kg)	% Robot	Cost (£)	% Robot
Arm System	Joint 1	MakerBeam	MakerBeam - 35mm	2	Aluminium 6082 T6	0.009	0.04%	0.53	0.01%
Arm System	Joint 1	MakerBeam	MakerBeam - 55mm	2	Aluminium 6082 T6	0.015	0.06%	0.83	0.02%
Arm System	Joint 1	MakerBeam	MakerBeam - 62mm	4	Aluminium 6082 T6	0.033	0.13%	1.87	0.05%
Arm System	Joint 1	Other manufactured components	Side Reinforcement	2	Aluminium 6082 T6	0.022	0.09%	0.28	0.01%
Arm System	Joint 1	Other manufactured components	Base Reinforcement	2	Aluminium 6082 T6	0.009	0.03%	0.05	0.00%
Arm System	Joint 1	Motor	RC Servo	1	n/a	0.060	0.24%	19.68	0.53%
Arm System	Joint 1	Other manufactured components	Servo Motor Bracket	1	Aluminium 6082 T6	0.006	0.03%	0.12	0.00%
Arm System	Joint 1	Transmission	Attachment	1	n/a	0.001	0.00%	0.00	0.00%
Arm System	Joint 1	Transmission	Sprocket metal	2	Mild Steel	0.040	0.16%	14.90	0.40%
Arm System	Joint 1	Transmission	Sprocket plastic	0	Derlin	0.000	0.00%	0.00	0.00%
Arm System	Joint 1	Transmission	Chain metal	1	Mild Steel	0.018	0.07%	4.92	0.13%
Arm System	Joint 1	Transmission	Chain plastic	0	Derlin	0.000	0.00%	0.00	0.00%
Arm System	Joint 1	Transmission	Axle 55mm	1	Aluminium 6082 T6	0.007	0.03%	0.26	0.01%
Arm System	Joint 1	Transmission	Worm Metal	1	Unharded Mild Steel	0.024	0.10%	18.17	0.49%
Arm System	Joint 1	Transmission	Worm Plastic	0	Derlin	0.000	0.00%	0.00	0.00%
Arm System	Joint 1	Other manufactured components	Worm Support 5mm	2	Aluminium 5083 T6	0.021	0.09%	0.59	0.02%
Arm System	Joint 1	Other manufactured components	Worm Support 3mm	0	Aluminium 6082 T6	0.000	0.00%	0.00	0.00%
Arm System	Joint 1	Transmission	IGUS bearing - hat	2	Unknown	0.001	0.00%	1.72	0.05%



Arm System	Joint 1	Other manufactured components	Tufnol Slider	2	Carp Brand Tufnol	0.014	0.06%	3.50	0.09%
Arm System	Joint 1	Transmission	Axle 47mm	1	Aluminium 6082 T6	0.006	0.03%	0.26	0.01%
Arm System	Joint 1	Arm Electronics	Encoder	1	n/a	0.016	0.06%	25.43	0.68%
Arm System	Joint 1	Transmission	Worm Gear plastic	1	Derlin	0.016	0.06%	13.39	0.36%
Arm System	Joint 1	Other manufactured components	Mesh Adjuster	2	Aluminium 6082 T6	0.011	0.04%	0.26	0.01%
Arm System	Joint 1	Transmission	IGUS bearing - flat	2	Unknown	0.000	0.00%	1.62	0.04%
Arm System	Joint 1	Fixings	M3 bolt-6mm (8mm total) & Nut	38	Steel	0.027	0.11%	2.98	0.08%
Arm System	Joint 1	Other manufactured components	Upper Joint	2	Aluminium 6082 T6	0.016	0.06%	0.19	0.01%
Arm System	Joint 1	MakerBeam	MakerBeam - 35mm	2	Aluminium 6082 T6	0.009	0.04%	0.53	0.01%
Arm System	Joint 1	MakerBeam	MakerBeam - 62mm	2	Aluminium 6082 T6	0.017	0.07%	0.93	0.02%
Arm System	Joint 1	Fixings	Corner bracket (mod L)	4	Mild Steel	0.012	0.05%	2.60	0.07%
Arm System	Link 1	Other manufactured components	Wrist connector	1	Aluminium 5083 T6	0.011	0.04%	0.14	0.00%
Arm System	Link 1	Other manufactured components	Socket	1	ABS	0.003	0.01%	0.00	0.00%
Arm System	Link 1	Other manufactured components	Ball	1	ABS	0.003	0.01%	0.00	0.00%
Arm System	Link 1	Fixings	Lower ball and socket fixing	1	Mild Steel	0.004	0.02%	0.73	0.02%
Arm System	Link 1	Fixings	Upper ball and socket fixing	1	Mild Steel	0.003	0.01%	0.65	0.02%
Arm System	Link 1	Cable System	35mm M3 nut and bolt	4	Mild Steel	0.010	0.04%	0.31	0.01%
Arm System	Link 1	Cable System	Cable termination upper	4	Mild Steel	0.012	0.05%	11.44	0.31%
Arm System	Link 1	Cable System	Cable termination Lower	4	Mild Steel	0.019	0.08%	5.20	0.14%
Arm System	Link 1	Fixings	M3 bolt-6mm (8mm total)& Nut	6	Mild Steel	0.004	0.02%	0.47	0.01%
Arm System	Link 1	MakerBeam	Open Beam	1	Aluminium 5083 T6	0.099	0.40%	3.23	0.09%
Arm System	Link 1	Cable System	Cable 250mm	4	Steel	0.009	0.04%	0.88	0.02%
Arm System	Link 1	Other manufactured components	Base Reinforcement	1	Aluminium 5083 T6	0.004	0.02%	0.03	0.00%
Arm System	Link 1	Other manufactured components	Elbow T Braket	2	Aluminium 5083 T6	0.015	0.06%	0.24	0.01%
Arm System	Link 1	Cable System	Top end cable termination	2	Mild Steel	0.032	0.13%	6.56	0.18%
Arm System	Link 1	Cable System	Cable termination upper	2	Mild Steel	0.006	0.02%	5.72	0.15%
Arm System	Link 1	Cable System	Cable termination lower	2	Mild Steel	0.009	0.04%	2.60	0.07%
Arm System	Link 1	Cable System	Cable 35mm	2	Steel	0.001	0.00%	0.07	0.00%
Arm System	Joint 2	MakerBeam	MakerBeam - 35mm	2	Aluminium 6082 T6	0.009	0.04%	0.53	0.01%
Arm System	Joint 2	MakerBeam	MakerBeam - 55mm	2	Aluminium 6082 T6	0.015	0.06%	0.83	0.02%
Arm System	Joint 2	MakerBeam	MakerBeam - 62mm	4	Aluminium 6082 T6	0.033	0.13%	1.87	0.05%
Arm System	Joint 2	Other manufactured components	Side Reinforcement	2	Aluminium 6082 T6	0.022	0.09%	0.28	0.01%
Arm System	Joint 2	Other manufactured components	Base Reinforcement	2	Aluminium 6082 T6	0.009	0.03%	0.05	0.00%
Arm System	Joint 2	Motor	RC Servo	1	n/a	0.060	0.24%	19.68	0.53%
Arm System	Joint 2	Other manufactured components	Servo Motor Bracket	1	Aluminium 6082 T6	0.006	0.03%	0.12	0.00%

Arm System	Joint 2	Transmission	Attachment	1	n/a	0.001	0.00%	0.00	0.00%
Arm System	Joint 2	Transmission	Sprocket metal	2	Mild Steel	0.040	0.16%	14.90	0.40%
Arm System	Joint 2	Transmission	Sprocket plastic	0	Derlin	0.000	0.00%	0.00	0.00%
Arm System	Joint 2	Transmission	Chain Metal	1	Mild Steel	0.018	0.07%	4.92	0.13%
Arm System	Joint 2	Transmission	Chain plastic	0	Derlin	0.000	0.00%	0.00	0.00%
Arm System	Joint 2	Transmission	Axle 55mm	1	Aluminium 6082 T6	0.007	0.03%	0.26	0.01%
Arm System	Joint 2	Transmission	Worm Metal	1	Unharded Mild Steel	0.024	0.10%	18.17	0.49%
Arm System	Joint 2	Transmission	Worm Plastic	0	Derlin	0.000	0.00%	0.00	0.00%
Arm System	Joint 2	Other manufactured components	Worm Support 5mm	2	Aluminium 5083 T6	0.021	0.09%	0.58	0.02%
Arm System	Joint 2	Other manufactured components	Worm Support 3mm	0	Aluminium 6082 T6	0.000	0.00%	0.00	0.00%
Arm System	Joint 2	Transmission	IGUS bearing - Hat	2	Unknown	0.001	0.00%	1.72	0.05%
Arm System	Joint 2	Other manufactured components	Tufnol Slider	2	Carp Brand Tufnol	0.014	0.06%	3.50	0.09%
Arm System	Joint 2	Transmission	Axle 47mm	1	Aluminium 6082 T6	0.006	0.03%	0.26	0.01%
Arm System	Joint 2	Arm Electronics	Encoder	1	n/a	0.016	0.06%	25.43	0.68%
Arm System	Joint 2	Transmission	Worm Gear plastic	1	Derlin	0.016	0.06%	13.39	0.36%
Arm System	Joint 2	Other manufactured components	Mesh Adjuster	2	Aluminium 6082 T6	0.011	0.04%	0.26	0.01%
Arm System	Joint 2	Transmission	IGUS bearing - flat	2	Unknown	0.000	0.00%	1.62	0.04%
Arm System	Joint 2	Fixings	M3 bolt-6mm (8mm total) & Nut	56	Steel	0.039	0.16%	4.48	0.12%
Arm System	Joint 2	Other manufactured components	Upper Joint	2	Aluminium 6082 T6	0.016	0.06%	0.19	0.01%
Arm System	Joint 2	MakerBeam	MakerBeam - 35mm	2	Aluminium 6082 T6	0.009	0.04%	0.53	0.01%
Arm System	Joint 2	MakerBeam	MakerBeam - 62mm	2	Aluminium 6082 T6	0.017	0.07%	1.62	0.04%
Arm System	Joint 2	Fixings	Corner bracket (mod L)	4	Mild Steel	0.012	0.05%	2.60	0.07%
Arm System	Link 2	Other manufactured components	Wrist connector	1	Aluminium 5083 T6	0.011	0.04%	0.14	0.00%
Arm System	Link 2	Other manufactured components	Socket	1	ABS	0.003	0.01%	0.00	0.00%
Arm System	Link 2	Other manufactured components	Ball	1	ABS	0.003	0.01%	0.00	0.00%
Arm System	Link 2	Cable System	Cable termination upper	4	Mild Steel	0.012	0.05%	0.00	0.00%
Arm System	Link 2	Cable System	Cable termination lower	4	Mild Steel	0.019	0.08%	2.92	0.08%
Arm System	Link 2	Fixings	Lower ball and socket fixing	1	Mild Steel	0.004	0.02%	0.73	0.02%
Arm System	Link 2	Fixings	Upper ball and socket fixing	1	Mild Steel	0.003	0.01%	0.65	0.02%
Arm System	Link 2	Fixings	35mm M3 nut and bolt	4	Mild Steel	0.010	0.04%	0.30	0.01%
Arm System	Link 2	MakerBeam	Open Beam	1	Aluminium 6082 T6	0.099	0.40%	3.23	0.09%
Arm System	Link 2	Cable System	Cable 250mm	4	Steel	0.009	0.04%	0.88	0.02%
Arm System	Link 2	Cable System	Top end cable termination	2	Mild Steel	0.032	0.13%	6.56	0.18%
Arm System	Link 2	Fixings	M3 bolt-6mm (8mm total) & Nut	14	Mild Steel	0.010	0.04%	1.12	0.03%
Arm System	Link 2	Cable System	Cable termination upper	2	Mild Steel	0.006	0.02%	0.44	0.01%

Arm System	Link 2	Cable System	Cable termination lower	2	Mild Steel	0.009	0.04%	0.05	0.00%
Arm System	Link 2	Cable System	Cable 35mm	2	Steel	0.001	0.00%	0.07	0.00%
Arm System	Link 2	Other manufactured components	Wrist connector	1	Aluminium 5083 T6	0.011	0.04%	0.14	0.00%
Arm System	Link 2	MakerBeam	MakerBeam - 35mm	1	Aluminium 6082 T6	0.005	0.02%	0.26	0.01%
Arm System	Link 2	Fixings	Corner bracket (mod L)	4	Mild Steel	0.012	0.05%	2.60	0.07%
Arm System	Joint 3	MakerBeam	MakerBeam - 35mm	2	Aluminium 6082 T6	0.009	0.04%	0.53	0.01%
Arm System	Joint 3	MakerBeam	MakerBeam - 55mm	2	Aluminium 6082 T6	0.015	0.06%	0.83	0.02%
Arm System	Joint 3	MakerBeam	MakerBeam - 62mm	4	Aluminium 6082 T6	0.033	0.13%	1.87	0.05%
Arm System	Joint 3	Other manufactured components	Side Reinforcement	2	Aluminium 6082 T6	0.022	0.09%	0.28	0.01%
Arm System	Joint 3	Other manufactured components	Base Reinforcement	2	Aluminium 6082 T6	0.009	0.03%	0.05	0.00%
Arm System	Joint 3	Motor	RC Servo	1	n/a	0.060	0.24%	19.68	0.53%
Arm System	Joint 3	Other manufactured components	Servo Motor Bracket	1	Aluminium 6082 T6	0.006	0.03%	0.12	0.00%
Arm System	Joint 3	Transmission	Attachment	1	n/a	0.001	0.00%	0.00	0.00%
Arm System	Joint 3	Transmission	Sprocket metal	0	Mild Steel	0.000	0.00%	0.00	0.00%
Arm System	Joint 3	Transmission	Sprocket plastic	2	Derlin	0.006	0.02%	9.52	0.25%
Arm System	Joint 3	Transmission	Chain Metal	0	Mild Steel	0.000	0.00%	0.00	0.00%
Arm System	Joint 3	Transmission	Chain plastic	1	Derlin	0.006	0.02%	7.64	0.20%
Arm System	Joint 3	Transmission	Axle 55mm	1	Aluminium 6082 T6	0.007	0.03%	0.26	0.01%
Arm System	Joint 3	Transmission	Worm Metal	0	Unharded Mild Steel	0.000	0.00%	0.00	0.00%
Arm System	Joint 3	Transmission	Worm Plastic	1	Derlin	0.004	0.02%	9.99	0.27%
Arm System	Joint 3	Other manufactured components	Worm Support 5mm	0	Aluminium 5083 T6	0.000	0.00%	0.00	0.00%
Arm System	Joint 3	Other manufactured components	Worm Support 3mm	2	Aluminium 6082 T6	0.013	0.05%	0.16	0.00%
Arm System	Joint 3	Transmission	IGUS bearing - Hat	2	Unknown	0.001	0.00%	1.72	0.05%
Arm System	Joint 3	Other manufactured components	Tufnol Slider	2	Carp Brand Tufnol	0.014	0.06%	3.50	0.09%
Arm System	Joint 3	Transmission	Axle 47mm	1	Aluminium 6082 T6	0.006	0.03%	0.26	0.01%
Arm System	Joint 3	Arm Electronics	Encoder	1	n/a	0.016	0.06%	25.43	0.68%
Arm System	Joint 3	Transmission	Worm Gear plastic	1	Derlin	0.016	0.06%	13.39	0.36%
Arm System	Joint 3	Other manufactured components	Mesh Adjuster	2	Aluminium 6082 T6	0.011	0.04%	0.26	0.01%
Arm System	Joint 3	Transmission	IGUS bearing - flat	2	Unknown	0.000	0.00%	1.62	0.04%
Arm System	Joint 3	Fixings	M3 bolt-6mm (8mm total)& Nut	44	Steel	0.031	0.12%	3.52	0.09%
Arm System	Joint 3	Other manufactured components	Upper Joint	2	Aluminium 6082 T6	0.016	0.06%	0.19	0.01%
Arm System	Joint 4	Other manufactured components	Servo Holder	1	Aluminium 6082 T6	0.011	0.04%	6.48	0.17%
Arm System	Joint 4	Motor	RC Servo	1	n/a	0.060	0.24%	19.68	0.53%
Arm System	Joint 4	MakerBeam	MakerBeam - 35mm	1	Aluminium 6082 T6	0.005	0.02%	0.26	0.01%
Arm System	Joint 4	Transmission	Attachment	1	n/a	0.001	0.00%	0.00	0.00%

Arm System	Joint 4	Fixings	M3 bolt-6mm (8mm total)& Nut	7	Mild Steel	0.005	0.02%	0.56	0.01%
Arm System	Electronics	Arm Electronics	Raspberry Pi (arm)	1	n/a	0.045	0.18%	27.48	0.73%
Arm System	Electronics	Arm Electronics	Servo motor controller (arm)	1	n/a	0.026	0.10%	86.83	2.32%
Arm System	Electronics	Arm Electronics	PCB (arm)	1	n/a	0.185	0.74%	32.00	0.86%
Arm System	Head	Other manufactured components	Main Plate	1	Aluminium 6082 T6	0.042	0.17%	1.43	0.04%
Arm System	Head	Other manufactured components	Camera Enclosures	2	ABS	0.022	0.09%	2.82	0.08%
Arm System	Head	Arm Electronics	Webcam	2	n/a	0.012	0.05%	35.96	0.96%
Arm System	Head	Arm Electronics	CO2 Sensor	1	n/a	0.027	0.11%	34.97	0.93%
Arm System	Head	Fixings	Enclosure Case Screws	4	Stainless Steel	0.002	0.01%	0.00	0.00%
Arm System	Head	Fixings	M5 Bolts	4	Stainless Steel	0.012	0.05%	0.32	0.01%
Arm System	Gripper	Gripper	Main Gripper with Mounts	1	Aluminium	0.090	0.36%	9.95	0.27%
Arm System	Gripper	Gripper	Pinion Gear	1	n/a	0.008	0.03%	0.00	0.00%
Arm System	Gripper	Gripper	Clutch	1	n/a	0.027	0.11%	0.00	0.00%
Arm System	Gripper	Gripper	Fastner for Clutch and Gear	1	Stainless Steel	0.003	0.01%	0.00	0.00%
Arm System	Gripper	Motor	Medium Servo	1	n/a	0.021	0.08%	8.95	0.24%
Arm System	Gripper	Fixings	Servo Fastner	1	Stainless Steel	0.008	0.03%	0.00	0.00%
Arm System	Gripper	Fixings	M3 Bolts	12	Stainless Steel	0.009	0.04%	0.48	0.01%
Arm System	Gripper	Fixings	M3 Nut	12	Stainless Steel	0.004	0.01%	0.36	0.01%
Arm System	Gripper	Gripper	New Fingers	4	Aluminium 6082 T6	0.017	0.07%	2.00	0.05%
					<b>Total System:</b>	<b>2.269</b>	<b>9.14%</b>	<b>£663.11</b>	<b>17.72%</b>
					<b>Total Mass (kg):</b>	<b>24.836</b>	<b>Cost (£):</b>	<b>£3,741.48</b>	